JOURNAL OF LIQUID CHROMATOGRAPHY

VOLUME 17 NUMBERS 14 & 15 1994

Special Issue on
POLYMER SEPARATION BY
NON-EXCLUSION LIQUID
CHROMATOGRAPHY

Edited by SADAO MORI
Department of Industrial Chemistry
Mie University
Tsu, Mie 514, Japan

JOURNAL OF LIQUID CHROMATOGRAPHY

August/September 1994

Aims and Scope. The journal publishes papers involving the applications of liquid chromatography to the solution of problems in all areas of science and technology, both analytical and preparative, as well as papers that deal specifically with liquid chromatography as a science within itself. Included will be thin-layer chromatography and all models of liquid chromatography.

Identification Statement. *Journal of Liquid Chromatography* (ISSN: 0148-3919) is published semimonthly except monthly in May, July, October, and December for the institutional rate of $1,350.00 and the individual rate of $675.00 by Marcel Dekker, Inc., P.O. Box 5005, Monticello, NY 12701-5185. Second Class postage paid at Monticello, NY. POSTMASTER: Send address changes to *Journal of Liquid Chromatography*, P.O. Box 5005, Monticello, NY 12701-5185.

			Individual Professionals'	Foreign Postage		
Volume	Issues	Institutional Rate	and Student Rate	Surface	Airmail to Europe	Airmail to Asia
17	20	$1,350.00	$675.00	$75.00	$110.00	$130.00

Individual professionals' and student orders must be prepaid by personal check or may be charged to MasterCard, VISA, or American Express. Please mail payment with your order to: Marcel Dekker Journals, P.O. Box 5017, Monticello, New York 12701-5176.

CODEN: JLCHD8 17(14&15) i–viii, 2991–3322 (1994)
ISSN: 0148-3919

Printed in the U.S.A.

JOURNAL OF LIQUID CHROMATOGRAPHY

JOURNAL OF LIQUID CHROMATOGRAPHY

JOURNAL OF LIQUID CHROMATOGRAPHY

Indexing and Abstracting Services. Articles published in *Journal of Liquid Chromatography* are selectively indexed or abstracted in:

■ Analytical Abstracts ■ ASCA ■ Berichte Pathologie ■ BioSciences Information Service of Biological Abstracts (BIOSIS) ■ CAB International ■ Cambridge Scientific Abstracts ■ Chemical Abstracts ■ Chemical Reactions Documentation Service ■ Current Awareness in Biological Sciences ■ Current Contents/Life Sciences ■ Current Contents/Physical and Chemical Sciences ■ Engineering Index ■ Excerpta Medica ■ Journal of Abstracts of the All-Union Institute of Scientific and Technical Information of the USSR ■ Physikalische Berichte ■ Reference Update ■ Saltykov-Shchedrin State Public Library ■ Science Citation Index

Manuscript Preparation and Submission. See end of issue.

This journal is also available on CD-ROM through ADONIS™ beginning with the 1991 volume year. For information contact: ADONIS, Marketing Services, P.O. Box 839, Molenwerf 1, 1000 AV Amsterdam, The Netherlands, Tel: +31-20-6842206, Fax: +31-20-6880241.

The Journals of Marcel Dekker, Inc. are available in microform form: RESEARCH PUBLICATIONS, 12 Lunar Drive, Drawer AB, Woodbridge, Connecticut, 06525, (203) 397-2600 or Toll Free 1-800-REACH-RP(732-2477). Outside North and South America: P.O. Box 45, Reading, RG1 8HF, England, 0734-583247.

Contributions to this journal are published free of charge.

Effective with Volume 6, Number 11, this journal is printed on acid-free paper.

POLYMER SEPARATION BY NON-EXCLUSION LIQUID CHROMATOGRAPHY

Edited by

Sadao Mori
Department of Industrial Chemistry
Mie University
Tsu, Mie 514, Japan

This is a special issue of *Journal of Liquid Chromatography,*
Volume 17, Numbers 14 & 15, 1994.

MARCEL DEKKER, INC. New York, Basel, Hong Kong

JOURNAL OF LIQUID CHROMATOGRAPHY, 17(14&15), vii-viii (1994)

PREFACE

Most synthetic polymers have a molecular weight distribution (MWD) which can be measured by size exclusion chromatography (SEC) rapidly and precisely. Copolymers have a chemical composition distribution (CCD) in addition to MWD, and CCD of the copolymers has mostly been measured by SEC - a dual detector system or SEC-IR. Although size exclusion chromatography has established itself as an indispensable analytical method for measuring molecular weight averages and MWD of polymers, accurate information on both MWD and CCD of copolymers cannot be obtained by SEC alone.

Because separation in SEC is considered, in principle, to be achieved according to the effective sizes of molecules in solution, and because molecular weights of copolymers are not proportional to molecular size unless compositional variation is negligible and the chemical structure is constant across the whole range of molecular weights.

There are other parameters which control the properties of polymers besides MWD and CCD. A functionality distribution of end groups of polymers influences the properties of polymers, especially low-molecular-weight-polymers and oligomers. Blending of polymers of different structures frequently occurs as a technique of polymer reforming. Degree of branching of polymers affects the crystallization of polymers. Characterization of such complex structures of polymers cannot be achieved only by SEC or by hyphenated techniques such as SEC-IR and SEC-NMR. Non-exclusion liquid chromatography (NELC), e.g., liquid adsorption chromatography (LAC), precipitation liquid chromatography, normal- and reversed-phase liquid chromatography, LAC at critical condition, orthogonal chromatography, field-flow fractionation (FFF), temperature rising elution fractionation (TREF) must be used, either separately or coupled with SEC.

Recent advances in NELC in the past decade for polymer characterization are remarkable and we have entered a phase of consolidation. From this point of view, the special issue on "Polymer Separation by Non-Exclusion Liquid Chromatography" has been planned and edited in this volume. Leading experts in this field have contributed and seventeen papers have been compiled in this issue: three papers dealing with copolymer separation according to composition; one on polymer separation according to functionality; three on the separation of polyethers; four on retention behavior of

homopolymers; one on TREF; two on FFF; and two on the separation of ionic polymers. One paper is a review on alternatives to SEC.

As guest editor of this special issue, I wish to thank all contributors to this issue. I hope this special issue provides significant impact to great development of polymer liquid chromatography.

Tsu (Japan) Sadao Mori

JOURNAL OF LIQUID CHROMATOGRAPHY, 17(14&15), 2991-3023 (1994)

Review

ALTERNATIVES TO SIZE EXCLUSION CHROMATOGRAPHY

A. REVILLON
Centre National de la Recherche Scientifique
Laboratoire des Matériaux Organiques à Propriétés Spécifiques
B.P. 21
69390 Vernaison, France

ABSTRACT

Size Exclusion Chromatography (SEC) is a convenient and powerful method for polymer characterization, but alternatives have appeared to overcome its limitations or improve its responses. These methods are examined, comparing their advantages and disadvantages, with a special attention to Hydrodynamic Chromatography (HDC).

INTRODUCTION

Basic questions in a polymer laboratory are molecular and macromolecular characterization in relation with synthesis and expected properties. A favourite method for molecular weight determination is size exclusion chromatography (SEC), the advantages of which are well-known. But some polymer characteristics may depend not only on molecular weight, but also of particle size, so that analysts are faced to a more general problem, the solutions of which are numerous. Nearly 3 thousand papers have been published on particle size

measurements, as reviewed regularly by Barth et al (1-4) for actualization of a basic book (5). We first examine limitations of SEC, then give an evaluation of other methods and report comparative results in HDC.

SEC AND PERSISTING PROBLEMS

Separation by SEC suffers practical difficulties for : i) very high molecular weights, ii) for complex mixtures, iii) for unsoluble polymers. It suffers also theoretical problems for getting the accurate molecular weight values. Thirty years of practice have lead to improvements of column packings and to appearance of new types of detectors, allowing simultaneously i) rapid analysis, ii) rather high resolution and iii) absolute results, so that this analysis is routinely used in polymer laboratory and has appeared in process control.

Actuality of S.E.C. is continuously proved by its mention in every polymer publication and by a series of papers which appeared at the Fall ACS Meeting 1993 (6), as well as in the 1993 ISPAC Summer Meeting (7). These recent papers are essentially devoted to calibration problems, which may be partially solved with the help of on-line multidetection. Absolute weight average molecular weight (M_W) was obtained first by coupling a concentration detector with a low-angle laser light scattering detector. Moreover, this procedure allows to derive true values, whatever is the separation power of the columns. Radius of gyration or hydrodynamic radius may be measured by using multi-angle or dynamic light scaterring detector, respectively. Complementary information on the macromolecular chain (branching, solvent thermodynamic quality) is obtained by adding a viscometer.

These papers indicate that, despite these improvements, some limitations are remaining : e.g. the difficulty to determine volume correspondance and coupling between detectors signals

of different width and sensitivity (to c, cM, η). Other problems are the absence of ultra-porous packing (with sufficient mechanical properties) for very large molecules, the low amplitude of the working volume Vp of the packing (between V_0 and $2V_0$, what means a capacity factor of 2 only), the decrease of resolution when molecular weight increases, the presence of secondary effects (from enthalpic origine), the high shear rate in pores, the evident necessity to have soluble samples. The aim of this paper is examination of other methods for solving some problems in polymer characterization : molecular weight, composition, number of components, particle diameter, effect of detector type on signal intensity, phase volume effectively available for separation, diffusion effects altering an effective use for samples with a large size distribution.

ADDITIONAL SEPARATION METHODS

To the question, "why and when change a technique?" answer may be : to improve it or overcome its limitations, either without large changes in equipment, keeping chromatography in mind, or using other separation principles. These attempts may be summarized as :

Source of limitations : proposed solution

-high shear rate : greatly increase channel dimensions

-lack of large internal diameter support (limiting sample size or molecular weight) : use of "infinite" one

-limited porosity : work in unlimited domain

-interaction with stationary phase : suppress this phase or use a liquid one

-problem with mobile phase : suppress it and use electric motion

-constant flow-rate : variable with time

-pore size is governing parameter : changing the origin of the driving force

-constant composition of eluent : gradient of elution
-constant temperature : programmed T
-no internal field in the column : add one
-no external field : add one
-resolution decreases when elution time increases : reverse elution order
-sample in solution : sample in dispersion.

Some of these difficulties and some of the above suggestions may be solved by using other types of chromatography : liquid (LC), field-flow fractionation (FFF) normal and steric (SFFF) (8, 9), hydrodynamic (HDC) (10), respectively packed or capillary (CHDC) column, supercritical fluid (SFC) (11, 12), capillary electrophoresis. Countercurrent chromatography (CCC or Centrifugal Partition Chromatography, CPC) is a potential tool to separate copolymers of different structure or nature, but at this time, is poor in exemples (13, 14). These methods correspond to a large variety of separation mechanisms based on kinetics or thermodynamics, where surface, volume, active specific sites of materials, or thermal, gravity, electric, magnetic applied fields, bring their contribution. They are called : "fractionation" and have some similar features with chromatography. Basis may be found in ref. 15 and 16. Their progress is presented in Symposium and accounted recently for instance in ref. 17 and 18. One of the characteristics is the absence of stationary phase, which solves the problems of side phenomena (adsorption, no active and sometimes disruptive interface across which the sample must partition, mass transport, column channeling, degradation, shear rate) and allows a higher variety for eluent choice.

Some other solutions are non-chromatographic methods, working with or without separation, such as mass spectrometry, NMR spectrometry, dynamic light scattering (photocorrelation spectroscopy), centrifugation.

RESULTS

Elution

Figure 1 presents schematically the different elution characteristics of several separation modes, in a semi-log plot. Three observations may be made. i) We first consider the order of elution : increasing volume for decreasing size in classical SEC, also in HDC (with packed or capillary columns) and steric FFF, and the reverse for LC, FFF and SFC. These curves indicate only the tendency for the relation : size-V, and are not true calibration curves. ii) Second, independently of elution order, we see that LC, SFC, FFF (normal and steric SFFF) may have very large elution domain (theoretically unlimited), on the contrary of SEC and HDC, which have limited ones (respectively 2 and about 1.3, as measured by the capacity factor). Wide domain is obtained when enthalpic process makes difference between molecules and when a gradient can increase the effects, either of solvent strength or temperature. iii) Third, depending on the mechanism, the sample size domain varies from nanometer to several microns (or MW from about 10^2 to more than 10^{10} mol/g). LC is concerned by the smaller sizes, whereas SEC is convenient for polymers, but also for oligomers and some low molecular weight compounds, while SFC may also cover this domain. Polymers and larger species, soluble or not, may be analyzed by FFF under different forms. Finally, the number in italic figures indicates approximate ratio of maximum to minimum sizes measured by the considered technique. The numerous possibilities of FFF allow to cover the wider range of sizes.

After this first approach, we may try to better determine the shape of the calibration curve (diameter D or mass M as a function of V), which is a semi-log plot in SEC and HDC, whereas this relation does not hold for certain other modes. Log plot of either M or M square root versus V does not lead to a straight

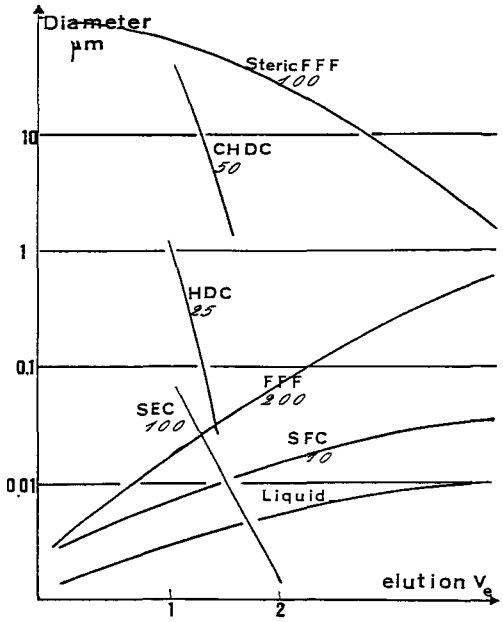

Figure 1. Semi-log plot of sample diameter versus elution volume for different liquid chromatographic modes (italic figures are the ratio of maximum to minimum diameters).

line. Small molecules are eluted on the effect of chemical or physical forces, roughly in increasing order of size, but this order is strongly affected by the choice of the two antagonist phases. In SFC, M is proportional to $V^{0.5}$ (low values), then to V (higher values) (19). In thermal FFF with programmed temperature (TDE), log MW may be proportional to retention time (20), at least in a limited zone (21), but size may vary approximately as the square of V. The calibration difficulty may be partly solved by using a continuous viscosity detector (20). Log of MW increases with retention time, so as the Log of the product "viscosity * MW", but different plots are obtained

for polymers of different nature, instead of the unique calibration curve, which is observed in SEC.

When conditions are drastically changed (high flow-rate and high temperature gradient between the two walls) the order is the reverse : the process is called T hyperlayer FFF (22). Size rather than MW is the fundamental factor governing the retention, as demonstrate by elution of linear and star polymers (23). In (sedimentation) SedFFF, most of the papers show exemples of separation, but do not indicate a calibration curve (24). "The trend of increasing retention with increasing particle size is apparent" (25). In (steric) SFFF, elution time is approximately proportional to particle mass (26).

Resolution

We are now tourning to comparison of resolution (R) in the different processes : we shall examine R value and its variation with elution volume. We suggest to define first, a specific resolution (Rs) = R/ratio of diameter of considered species and second, resolution per unit of time (Rt) = Rs/time of measurement, in order to compare respectively different samples and different elution conditions. To obtain polymer dimensions in solution, molecular mass is converted to diameter, applying the equation : diameter proportional to $M^{0.6}$.

R depends on chemical or physical factors, packing size being one of them. As a general rule in chromatography, resolution increases when packing size decreases (N is inversely proportional to the square of particle diameter). Generally LC has a very high and constant resolution (corresponding to about 100 000 theoretical plates per meter), which is interesting to separate compounds of very similar structure. Polymers are considered to present continuous distribution of species, fitting known theoretical equations and their

representative curves. In spite of its rather low resolution, even with new small sizes packings (particle diameter lower than 5 μm, almost same number of theoretical plates per meter as in LC), SEC is sufficient to obtain this molecular weight distribution. Yet, "high" resolution is specially interesting for separation of oligomers (up to 30-40 mers). This gives information on polymerization mechanism and allows to follow step-condensation process kinetics. In SEC, calibration is not affected by particle size : ratio of elution volumes of two compounds is unchanged; the resolution is increased since peaks are not so broad. Whereas in HDC with packed column, this R_f ratio is increased by using fine packings and resolution is increased (27). Figure 2 illustrates such effects. Pore size and pore volume being the origin of molecules separation, strongly affect elution in SEC, whereas effect of porosity is controversial in HDC, where the main phenomenon takes place essentially between (and not in the porous part of) particles. Combined HDC+SEC action increases separation domain, in terms of sample mass and elution volume (28).

For other separation modes, resolution depends on the applied field. In SFC, peak width decreases when V increases, so that N is greatly increased with V. The resolution is good for polymer standards, but commercial polymers may cover a very large elution domain, so that effective separation seems difficult (19). Excellent resolution for oligostyrenes (29, 30) has been obtained with packed columns (silica, 5 μm, pressure, flow rate and composition gradients) and 200 000 plates have been claimed, but exemples concern only small species (31).

In thermal FFF, peak width increases (factor 1.5) with V, but N may stay constant or even increases (from 18 to 70), since V is greatly increased : three times in this separation of three polystyrene standards (21, 32). Even for these narrow molecular weight distribution samples, plate number is low (about 70), so as Rt : 0.009 (21). Yet, separation of 3 PS may be obtained in 2 min (by high speed thermal FFF) as well as in 2

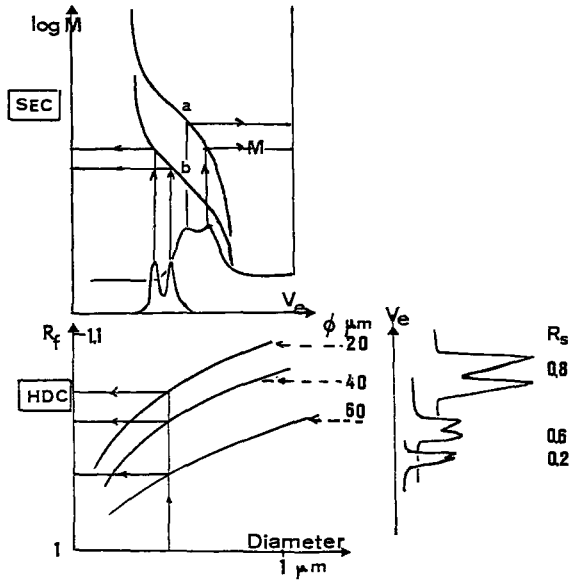

Figure 2. Particle size effects on elution volume and resolution in SEC (same calibration curves for a and b, b being fine particles) and HDC (particle size, R_S and R_f as indicated).

hrs (33). Plate numbers in both cases are of the same order (about 50), so as resolution : 0.8, but Rt is equal respectively to 0.21 and 0.013. For SEC, HDC, SFC, TFFF, theoretical plate height generally increases with flow rate according to van Demter law, so that resolution decreases, but sometimes Rt may increase, particularly by a proper use of gradient or when mass transfer does not play a role.

For all separations, it is possible to obtain an accurate molecular weight by using deconvolution to remove system dispersion (34).

Table 1 indicates meaningful values of R, Rs, Rt and analysis time.

TABLE 1
Resolution of Various Fractionation Modes

mode / Param.	CHDC	HDC	DCP	TFFF	SFFF	SFC
Rs	0.15	0.15	1.5	0.7-2	2.2	1.2
Rt	0.025	0.025	0.15	0.2-0.02	0.07	0.03
t (min)	6	6	10	45-120	30	20-60
ϕ µm	>1	<1	<60	<1	<2	0.05

Separation mode

Classical chromatographic separation occurs from the difference in partition of a soluble compound between mobile and stationary phases. More generally, separation is the result of local differences in distribution of the sample compounds in the mobile phase. The partition coefficient is related to the thermodynamic process : $LnK = \Delta G°/RT$, relation which indicates the possible effects of three factors : enthalpy (ΔH) or entropy (ΔS) changes and temperature T. Practically, separation is achieved under the effect of two forces (or fields) in one phase or two phases. One phase is necessary for transport and may have a physical or chemical role in the separation. It is to be noted that in capillary electrophoresis, motion is due to an internal electric field, and not to the liquid phase.

LC is governed by an enthalpic process between two active phases, the internal field having only a transport role. SEC is governed by an entropic process between two phases : a stationary inert one, and a mobile one, which creates an hydrodynamic field. Nature of phases is chemically and physically indifferent. HDC is acting under the effect of one hydrodynamic field moving one mobile phase; even if a packing is present, its only role is to decrease the capillary size. The separation is due to the existence of a flow velocity profile

in the channel, in which small particles tend to be closer of the external wall, where the flow is stagnant. The nature of mobile phase is theoretically indifferent, but differences between solvents have been observed.

In FFF, separation is result of one phase under two fields : one hydrodynamic internal field, one other external, perpendicular to the flow. Examination of the various subtechniques is out of the scope of this presentation and may be found in 15, 16, 35, but two exemples will be cited. This field may be a thermal one (TFFF), which drives species to one wall (accumulation wall). Brownian diffusion acts slightly in the opposite direction. Larger species are located in a region of low velocity, so that retention increases with size. This soft process has been shown to be valuable with ultrahigh molecular weight polymers, since there is no shear degradation. Moreover band broadening is low, so that true molecular weight distribution may be obtained (36).

At high flow rates, deformation of long polymer chains leads to entropy decrease, so that an entropy gradient gives rise to a driving force, opposite to the field-driven motion. The result is an equilibrium of species at some distance from the wall. This distance increases with MW, so that large molecules are in a high velocity domain and elute first. This is called hyperlayer TFFF (22) or focusing FFF (36, 37). Elution time is greatly reduced : some minutes are sufficient for elution of 3 to 20 10^6 mol/g polystyrenes. Peak width is rather broad and increases for lower MW (22).

A second source of field is provided by centrifugation. Larger species tend to accumulate at the external wall, where flow velocity is low : again, elution is in the order of increasing size. Yet, for particles larger than 1 μm, Brownian motion becomes negligible and their bulk becomes the efficient parameter, so that largest particles, far from the wall, are carried faster than the smaller ones : consequently, they are eluted first. A mixture of glass beads is nicely separated in

components (10 to 32 μm diameter) in a few minutes (26), the same for a mixture of polystyrene lattices (2 to 45 μm diameter) (32).

The existence of an external field allows the possibility to monitor the elution, by changing it with time, for instance programming the temperature gradient. This can be done rapidly and easily. Three effects may be obtained : i) increasing rapidity of analysis, ii) decreasing peak width, leading to better detection sensitivity and constant resolution with retention volume and iii) changing retention mechanism, from normal to inverse mode. For instance, first and second features are obtained by decreasing the temperature according to an exponential decay program (constant τ) after a given time, τ (21) : "time-delayed exponential-decay (TDE)". Number of plates is increased, capacity factor is decreased from 9 to 5, resolution is maintained and Rt is increased from 0.009 to 0.025. The peak capacity is increased from 3 to 6 in the same analysis time. The same profile is applied for centrifugational field decrease (39). It appears to be more beneficial than simple linear or parabolic or simple exponential field-programmed.

HYDRODYNAMIC CHROMATOGRAPHY

Hydrodynamic chromatography (HDC) is a technique for separating solutes or particulates, at high dilution, in the micron range and according to decreasing sizes (10). Separation mechanisms are taking into account hydrodynamic and electrostatic effects. Larger particles are located preferentially in the axis of capillaries where the flow-rate is maximum (parabolic profile), whereas smaller ones are close to the walls, where the rate is minimum. Ratio of their respective elution volume is called separation factor $R_f>1$. Classical capillary

(CHDC) columns are operating in the range from 1 to 30 μm. Voids between beads in packed columns play the role of small channels - of continuously changing diameter - similar to a capillary. Packed columns are effective for diameter 30 to 1000 nm. New capillary columns allow also separation in the sub-micron range (40). It is a rapid and convenient method to obtain a finger-print of size distribution with an instrument similar to those of liquid chromatography, easy to operate. There is no limitation of solvent nature. Difficulties are low plate number N, so that generally the number of peaks (peak capacity n) in a chromatogram is low. Quantitative interpretation needs calibration (in elution volume and signal intensity).

Since its introduction by H. Small (10), studies have been mainly devoted to packed columns. It has been shown (10) that resolution is increased by packing with small monodisperse spheres. Nevertheless, the elution domain is very limited, defined by a maximum ratio R_f of 1.15 in most papers. By using 2 μm non-porous silica gel packings, a value of 1.21 is obtained for R_f, but the chromatogram has only 5 PS peaks (41). Additives, either surfactants or electrolytes may vary this limiting value. A recent work indicates that at high ionic strength, elution is opposite of "normal" mode. The raison could be that very strong van der Waals interactions dominate over the hydrodynamic effect (42). Moreover, the chemical composition could play a role, so that mixture of latex (PS and PMMA) of identical size can be separated.

Large porous particles are still used (at low flow rate) to take profit of the pores as capillaries, with a R_f value of 1.16 (43). But, combining HDC and SEC, by using porous particles, the R_f ratio may be increased to 2.11 (44). Moreover small size packing allows to obtain a high plate number, so that expected peak number is 66. Considering resolution is unity and constant with V, it is easy to express this capacity as :

$$n = 1 + (R_f-1)\ N^{0.5}\ /4\ R_f.$$

This corresponds to 37 in this case, and the obtained number is approximatively 15, which is an excellent value. These autors are also using non-porous monodisperse particles, leading to the theoretical plate height minimum value, with a low dependence of flow rate (45, 46).

With normal open capillary tube, the resolution is poorer, but the R_f may be as high as 1.45, so that the peak capacity is the same that with packed columns. (Figure 3). The choice of tube or beads diameter corresponds to the different ranges of sizes to be separated (47). Table 2 (40, 48-62) summarizes conditions of separation by CHDC and typical results (N, R_f). It can be seen that capillary diameter varies considerably, from 1 to 1000 (or even 15000) µm. Most of the initial work has been done with 250-500 µm diameter. To reduce extra-column band broadening, an optimization of injection-detection system has been presented with 50-100 µm capillaries with exemples of results by capillary electrophoresis (63). With microcolumns, efficient separation has been obtained for PS 10^3 to 10^6 daltons. The chromatogram is similar to that of SEC, but with a limited R_f of 1.1 (instead of 2) and a low number of plates N = 50 (53). Another work (54, 55) shows a very high number of plates : 10^5/m, but a more limited R_f : 1.05. Increase of N is not accompanied with that of R_f, so that the peak capacity remains low (less than 10). More recent work indicates higher values of R_f : 1.63 and rather good resolution between latex samples (62). Even with 4000 plates, the peak capacity is about 7.

Our effort was mainly devoted to optimize parameters in capillary HDC and determine exact diameter values.

EXPERIMENTAL

The instrument we used is similar to a liquid chromatograph : Waters pump 510 (Milford, Mass.), six-port injection valve

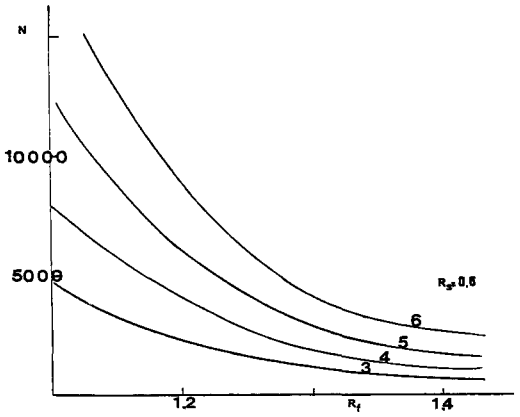

Figure 3. Peak capacity versus N and R_f (resolution assumed to be 0.6).

TABLE 2
Characteristics of Capillary Hydrodynamic Chromatography

Length, m	Int.diam., mm	N/m	Rf max	Ref.
88-201	250-500	?	1.3	48
50	180-450	25	1.5	49
60-200	250-500	10	1.55	50
15	100	25-200	> 1.2	51
0.45-7	1000	6	1.5	52
0.15-0.2	1	250	1.1	53
0.7-3.3	1.2-10	105	1.05	54, 55
91-168	250-500	16-100	1.4	56
12	15000	?	1.15	57
30-120	250-500	16-250	1.5	58
2	4	2000	>1.15	59, 60
2	6.5	?	1.42	61
5	7	600	1.63	62
2.5	10	580	>1.46	40

Rheodyne 712 (Cotati, Cal.) with external loop 20 µl. It may be replaced by a 12-port valve with two injection loops (Valco Europe, Vici, Switz.). This allows the injection of two (identical or different) samples on one or two consecutive columns. One of the advantages is the Rf accurate determination by the help of an internal standard and this avoids peak interfernce. Detector is a UV spectrometer Waters 455. A microcomputer IBM PCXT Model 286 (RAM 640 Ko), equipped with an acquisition card (analogic/digital converter) is directly connected to the output of the spectrometer. An IBM Proprinter x24, with a buffer memory (16 Ko) allows accurate drawing and the rapid transfer of values in a few seconds. Software is written in Turbo Pascal 4.0.

Analysis has been performed either with a packed column (crosslinked polystyrene spheres 20 µm : 50 cm length, 0.78 cm internal diameter), water being the eluent at a flow-rate 1.5 mL/min or with capillary stainless steel columns tested separately (L=30-60-120 m, internal diameters 2R = 0.25 and 0.5 mm). An additional fine metering valve (Vernier Handle, 18/21Y, Hoke, Creskill, N.J.) was placed before the packed column, to divide the main flow into two parts, one entering directly into the column and the other through the injection valve. It plays an important role on peak symetry. Three different eluents were used : H_2O, CH_3OH and THF, in presence of various additives. The reference sample, used as "marker", was $Cr_2O_7K_2$. Other reference materials for calibration were monodisperse polystyrene latexes (0.84 and 4 µm), prepared by emulsion polymerization in our laboratory. A larger (crosslinked) polystyrene was a 10 µm Microstyragel phase for SEC. Other samples were unknown materials (polymers and silica beads). Quantitative measurements on peaks were : height (h), base width (w), half-height width ($w_{1/2}$), skewing factor (sk=a/b, ratio of second to first part of the peak at h/10), absolute (V_e) and relative (R_f) elution volumes. Samples were injected separately and in mixtures.

Diameters were determined also by TEM (An Hitachi HU 12-A transmission electron microscope was used for dried samples deposited on a 200 mesh grid.) and quasi-elastic light scattering (QELS-PCS, photon correlation spectroscopy Brookhaven goniometer and software, a ionized argon laser, Spectraphysics 2020, being the light source). In PCS, diameter is derived from the instantaneous changes in scattered intensity due to Brownian motion. The correlation curve of intensity (correlation time τ) gives access to the translational diffusion constant $D = \tau / q^2$, related to equivalent radius a by the Stokes-Einstein law :

$$D = k_B T / 6 \Pi \eta a$$

For sizes larger than one micron, light diffraction (LD) was achieved with a Malvern Master Particle Sizer (Malvern, UK).

Sedimentation measurements were performed with the Brookhaven (Holtsville, NY) BI-DCP Particle Sizer (Disc Centrifuge Photosedimentometer).

RESULTS

Effect of Additives in Water (Ionic Strength, Surfactant and Viscosifying Agent)

With packed columns, several authors (10, 47) have observed a change of R_f with ionic strength, due to competition mainly between van der Waals (attractive) and double layer (repulsive) strengths. Electrolytes affect the critical micellar concentration (CMC) of the surfactant, the role of which appearing to be more essential. In capillary columns, we did not observed any effect of either $NaNO_3$ (0 to 28.6 g/l) or NaCl (0 to 48.7 g/l) on the shape of peak and elution volume of samples and marker.

Sodium dodecyl sulfate (SDS) from 0 to 4.8 g/l has been added to the water eluent. Its CMC is 2.5 g/l. This agent provides wettability of beads and ensures a low ionic strength (0.01) which favors higher R_f and better elution and resolution. Another work found that non-ionic surfactants lead to higher R_f than ionic ones (61).

A small amount of ethylene glycol (EG) may prevent aggregation. Theoretically, transversal motion must be decreased and R_f increased, when the viscosity is increased. In this respect, polymers have been used with more or less success (64). We did not observed an increase of R_f or a better shape of peaks in the range 0 to 6% EG. The pressure is markedly increased, according to Darcy's law and a permeability K_o coefficient may be derived. For L = 60 m, the value of 2.4 10^{-8} m^2 is far lower than that of filtration membranes (10^{-12} m^2), which indicates the low separating power of a capillary column.

In consequence of these observations, only surfactant - SDS : 3 g/l -was used.

Flow Rate Q and Nature of the Eluent

Different variations of N and R_f with flow-rate Q have been observed. They depend upon the sample size. Some deformation of peaks was observed at low flow-rates. The resolution between 0.84 µm and marker or 4 µm was unchanged, but was decreased for 4 µm and marker. The interpretation may be found in the tubular pinch effect, taking account of the Reynolds number of the particle $R_{e\ p}$. Effectively, the limiting value is 10^{-3}, which corresponds to very different flow-rates : 0.6 and 74 ml/min for 4 and 0.84 µm sample, respectively. For this latter latex, a change in mechanism occurs in the investigated domain - $R_{e\ p}$ from 1.74 to 41.7 10^{-4}- whereas the smaller latex is not concerned by this effect : $R_{e\ p}$ varies from 1.6 to 39 10^{-6}.

It is known that generally, low flow-rates v favor minimum plate height, according to van Demter law ($H = L/N = a + b/v + cv$). Here, this general expression holds with zero as c value, since it represents the mass transfert term. Diffusion is $b = 7$ cm^4/min and $a = 10$ cm for longitudinal and eddy terms, respectively. These values, far higher than in liquid chromatography, mean a high sinuosity coefficient and large equivalent beads size. Number of plates increased with flow rate, but R_f decreases for the 4 μm sample and the resolution is slightly affected, which is shown on Figure 4.

These different results for R_s, N and R_f show that operating conditions must be chosen in function of the analysis and not in an absolute way. It may be interesting to obtain either rapid results in 1.5 min with a medium resolution or higher number of plates, but in 36 min. It is also interesting to note that the highest number of plates is obtained not only for the marker, but for a largest sample.

Practical application must take account of Poiseuille law,

$$\Delta P = 8 \eta L D / \Pi R^4$$

Pressure increases with flow-rate, viscosity and decrease of capillary diameter (Tables 3 & 4).

In methanol, the number of plates was increased (Table 3). Its value was rather constant for 0.84, 4 μm and marker, but reached a maximum for the 10 μm sample, when Q increased. The resolution, so as R_f, decreased when Q is increased.

THF has a low viscosity and a good solvent power. Respectively, this may allow higher flow rates and the study of polymer in solution. In fact, although excellent base line, very high number of plates and fine chromatograms of crosslinked polystyrene were obtained, the upper limit of R_f was decreased (Table 3). With microequipment, separation has been reported with a good efficiency (53, 54).

Water being a more versatile eluent, and offering a good compromise between R_f and N values, will be the main solvent, at a flow-rate $Q = 1$ ml/min. This value also is a compromise

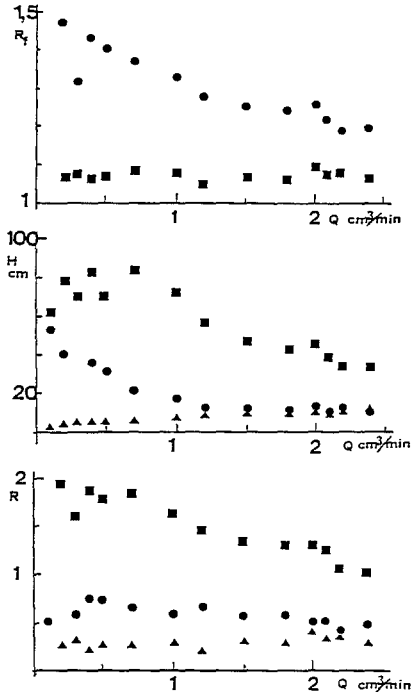

Figure 4. Effect of flow rate on R_f (for ● 4 µm, ■ 0.84 µm, marker M), H (for ● 4 µm, ■ 0.84 µm, ▲ M) and R (■ between 4 µm and M, ● 4 µm and 0.8 µm, ▲ 0.8 µm and M). Capillary column, L = 60 m, R = 125 µm.

between higher R_f and lower resolution at the higher flow rates.

Columns characteristics

Attempts realized with a 30 m column gave insufficient results, so that the essential of the work was done with 60 m

TABLE 3
Results in Hydrodynamic Chromatography

L m	30	60	120	120	60	120	0.5
R mm	0.125	0.125	0.125	0.125	0.250	0.125	3.7
Mode	capillary						packed 20 μm
Eluent	w	w	w	meth	w	THF	w
Pres. bar	45	90	175	120	12	60	35
u cm/s	34						0.1
Shear rate s^{-1}	10^4				1400	10^4	10^8
Rf max	1.4	1.45	1.45	1.45	1.6	1.26	1.15
N max	500	900	1900	7000	2300*	30000	7000
N max/m	16.7	15	15.8	58.3	38.3	250	14000
Range μm	0.8-20						0.05-0.8

TABLE 4
Effects of Operating Parameters on Peaks Characteristics

	L	R	Q	η	I	TA	C	λ
R_f	0	↘	0	0	0	↘	0	0
R_s	↗	↘	0	↘	↘	0	0	↗↘
N	↗	↘	↗	↘	↘	↘	0	
n	↗	↘	0	↘	↘	↘	0	
h	↘	↘	↘	0	↘	↗	↗	↗↘
w	↗	↗	↗↘	0	↗	↗↘	0	
t	↗	↗	↘	0	0	0	0	
ΔP	↗	↘	↗	↗		0	0	
R_e	0	↗	↗	↘	0	0	0	
$\dot{\gamma}$	0	↘	↗	0	0	0	0	

and finally optimized with 120 m length. A basic formula relating R_f and size of sample is :

$$R_f = 1 + 2\,a / R - (2\,g + 1)\,(a / R)^2$$

where g is a coefficient depending on flowing conditions. As expected, R_f must be - and was rather - independent of length L. The coefficients of the law are quite far from the theoretical values : that of a/R is ß =17 and g is 110 (instead of 2 and 2/3 respectively). This expresses that R_f is higher than expected and that particles move not far from the wall, according to ref. 47, 65.

The resolution was far better with 120 m, since w increased as the square root of L and V_e, proportionally to the length, as a general law in chromatography. By going from 60 to 120 m, H was found unchanged and N increased from 380 to 800, for the 4 µm sample. A way to illustrate that increase in resolution is to consider the calibration as represented in SEC. A lesser slope allows a better separation.

The second characteristics of the column is its diameter. The limit in R_f shows that over a certain sample size, no separation occurs. This limit of size may be related to the ratio : average radius of sample a to radius of tube R. A third order law, relating a to R may have a reasonable approximation in a linear one :

$$a = f + k\,R\ (\mu m)$$

with f = -7 and k = 0.1, R being in µm. A column of diameter 500 µm may have a medium domain of separation of 18 instead of 5 µm for the 250 µm one. Taking account on published results (44), ratio R to a is about 100, and for a given diameter of column, the usable a/R range varies roughly from 10^{-3} to 10^{-1}. The interest of large diameter is also the decrease of γ, rate of shear. It is to be noted that the resolution is higher for narrow tubes. The corresponding coefficients of the calibration curve R_f are ß = 10 and g = 25.

Table 3 summarizes the main effects of column and eluent variables on the chromatograms and separation possibilities.

These results are in general agreement with those published elsewhere.

Injection - Detection and Interpretation

Table 4 presents in a synthetic way the effects of all the parameters we varied in this study.

Signal increases linearly with concentration or injected volume (5 to 25 μl), which means that no interaction, adsorption or overloading were occuring. Sensitivity is so high than a few 25 particles in the detector cell give a noticeable signal. Peak characteristics V_e, w, N, R_f, R_s are not affected, but the slope of the corresponding curve varies with sample size. The result is that quantitative interpretation needs preliminary calibration. The reason is that signal depends upon absorption and scattering, which vary with sample diameter at a power a. Taking into account the number of particles in the samples, we found the exponent a being less than 3 for the 4 μm sample.

A general formula in liquid chromatography for the instantaneous detector response at each elution volume V is

$$H = \Sigma N_i\,(V)\; D_i^a\,(V)\; K_i\,(V)$$

where K_i is the extinction coefficient for particles of diameter D_i and a = 2 in the Mie scattering regime for a turbidity detector. In the Rayleigh regime, valid for $\lambda/D < 0.3$, a = 6 for turbidity and 3 for refractometry (66). This explain the effect of λ on signal shape and intensity. Moreover, the intensity decreases when there is no absorption at λ = 630 nm, in agreement with results in (67). Intermediate values of a may correspond to a combination of a and K (V); finally a = 1 holds for refractometry and spectrophotometry of polymers in SEC, so that the range 1 to 6 will be considered.

Assuming the formulas

$$\overline{D_n} = \Sigma ND/\Sigma N$$

$$\overline{D_w} = \Sigma ND^4/\Sigma ND^3$$

for number- and weight- average diameters and the simplified general relationship $H \propto ND^n$, (K and a are independent of V), then

$$\overline{D_n} = \Sigma(H/D^{n-1})/\Sigma(H/D^n) \text{ and}$$
$$\overline{D_w} = \Sigma(H/D^{n-4})/\Sigma(H/D^{n-3}).$$

For all the investigated polystyrene latexes, number and weight average diameters decrease deeply when n is increased (an exemple is given on Figure 5 for a PS standard of 106 nm diameter). The best agreement with TEM is obtained for n = 3-4, which is in agreement with theory since their diameters are in the range of the wavelength of detection (254 nm). Except for n = 2, the polydispersity index P is not affected by n, and is the same for all samples. Nevertheless distributions do not correspond to true ones. These high polydispersity values as compared to that determined by TEM analysis (1.02) clearly show the necessity of band broadening correction.

Dispersion Correction

There are many approaches for solving the dispersion problem. It has been shown (68) that skewed instrumental spreading functions derived from the plug-flow dispersion model (69) fit data for particle separations by HDC, where the spreading function is

$$G(V,y) = \{4(\pi Pe^{-1}(v/y))\}^{-0.5}\exp\{-(v-y)^2/4\ Pe^{-1}(v/y)\}$$

(with the dispersion term as the Peclet number Pe = UL/D'; Superficial velocity U, length of the packed bed L, an empiric dispersion coefficient D', elution volume v and at the maximum of peak y).

Pe = 100 corresponds to no correction of peak. The effect of larger Pe on diameter distribution (latex 106 nm) is shown on Figure 6. The results for the other samples are similar.

Whatever the value of n, Dn increases with Pe, the effect being stronger for higher n. On the contrary, Dw increases or

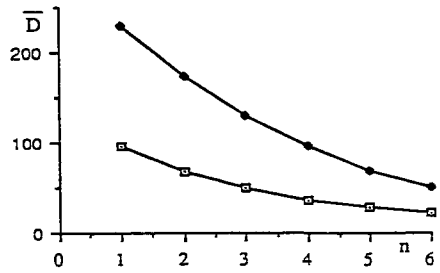

Figure 5. Average diameters versus exponent n for a PS latex standard, 106 nm (by TEM).

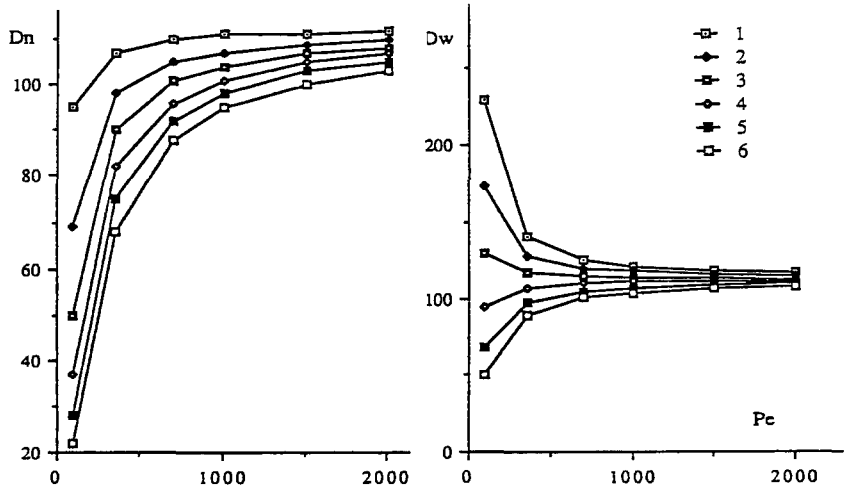

Figure 6. Average diameters versus Pe, for different values of exponent n for a PS latex standard, 106 nm (by TEM).

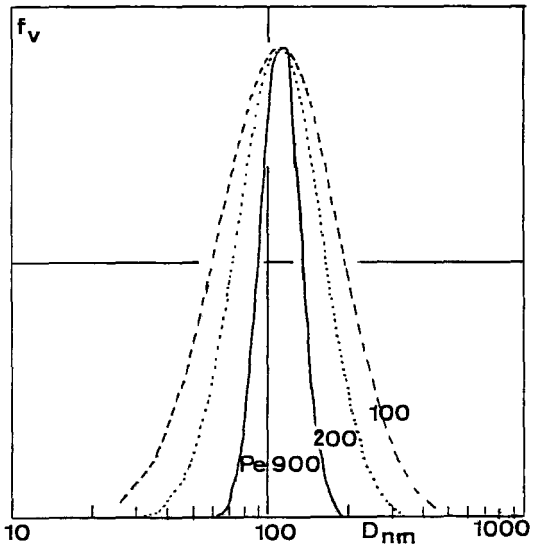

Figure 7. Effect of Pe on diameter frequence distribution for a PS latex standard, 106 nm (by TEM).

decreases with Pe, depending on n. Quasi-constant value corresponds to n = 3-4. More detailed results may be found in (70).

In another representation of results, Dw versus n, for different Pe values, curves for all samples have a common intercept between n = 3 and 4. A rapid change of D is noted up to Pe = 500, then Dn and Dw tend slowly to close values, independent of n.

Practically, considering the whole set of results, n must be chosen as 3-4 and Pe 500, for getting best average and distribution values, as well as narrow peaks, which means enhanced resolution. This effect on diameter distribution is shown on Figure 7.

It is necessary to have a high accuracy in data acquisition, since the useful elution domain is narrow. A frequent calibration procedure is also necessary, with possibility to correct small changes in elution volume (70.

To overcome calibration procedure and use of standards, on-line viscosity has been proposed, but this method "will await the development of improved pressure transducers" (71). Our approach was discontinuous measurements of sample size on eluted fractions. As mentionned earlier, they have been operated by TEM, PCS and sedimentometry. Exemple of these two last methods are given on Figure 8. It shows the high resolution of sedimentometry (time is inversely proportional to diameter squared) for a mixture of four latexes and a reasonable resolution for HDC. PCS, operated with a proper choice of parameters may give an excellent correlation with TEM values and an excellent resolution for a similar mixture of two latexes. For the three methods the analysis time is similar.

CONCLUSION

In capillary HDC, additives effect is low, surfactant being the most useful. The R_f is strongly affected by flow rate in methanol and is rather constant in water. The high number of plates in THF is not accompanied by a high maximum R_f value. This separation factor may be higher with 60 m than with 120 m, but the resolution is not so high. Even with microequipments (small diameter capillaries, short columns) of enhanced resolution, peak capacity is very limited. They are an interesting alternative for packed columns. HDC is rapid and very sensitive, but some conditions must be obeyed to obtain reliable results. First, the need of an accurate calibration, with frequent adjustment of parameters and choice of a column giving a low slope. Second, the need of changing the detector response factor (exponent n) and third, correcting for axial

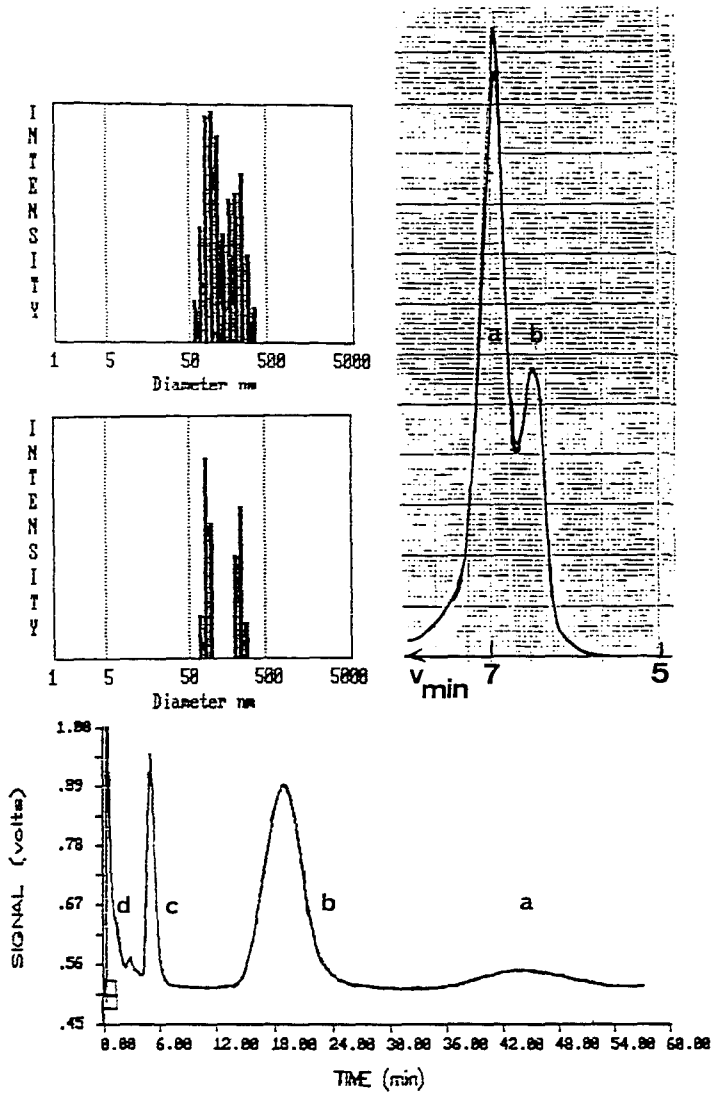

Figure 8. Mixture of PS latexes standards, 88 and 234 nm, by optimizing software parameters (below) in PCS analysis. HD Chromatogram on packed column (20 μm; 50x0.78 cm; water 1.5 ml/min) of PS latexes standards, a-50 and b-234 nm. Sedimentogram of a mixture of PS latexes standards, a-106, b-176, c-357 and d-1130 nm.

dispersion by use of a simple equation. As a consequence of the combined analysis of the effects of n and Pe, the proposed value for exponent n is 3.5 and a Peclet number of 500. Results are compared on eluted fractions with those of direct methods, for instance photon correlation spectroscopy and sedimentometry, this latter being of high resolution. By proper use of interpretation parameters, HDC leads to good results, in a short time, for a low cost and with a simple procedure.

REFERENCES

1. H.G. Barth, S-T Sun, *Anal. Chem.*, **57**, 151R-175R (1985)

2. H.G. Barth, S-T Sun, R.M. Nickol, *Anal. Chem.*, **59**, 142R-162R (1987)

3. H.G. Barth, S-T Sun, *Anal. Chem.*, **61**, 143R-152R (1989)

4. H.G. Barth, S-T Sun, *Anal. Chem.*, **63**, 1R-10R (1991)

5. H.G. Barth ed. *Modern Methods of Particle Size Analysis*, John Wiley & Sons, Inc., New York, 1984

6. *ACS Preprints, PMSE* **69**, Polym. Mater. Sci. and Eng. Chicago, Aug.1993

7. 6th ISPAC, Aghia Pelaghia, Greece, July 1993

8. J.C. Giddings, *Sep. Sci.*, **1**, 123 (1966)

9. J.C. Giddings, *J. Chem. Ed.*, **50**, 667 (1973)

10. H. Small, *J.Colloid Interface Sci.*, **48**, 147 (1974)

11. J.J. Czubryt, M.N. Myers, J.C. Giddings, *J. Phys. Chem.*, **74**, 4260-4266 (1970)

12. R.E. Jentoft, T.H. Gouw, *J. Chromatog. Sci.*, **8**, 138-142 (1970)

13. Y. Ito, M. Weinstein, I. Aoki, R. Harada, E. Kimoura, K. Nunogaki, *Nature*, **212**, 985 (1966)

14. D. Thiébaut and R. Rosset, *LC-GC Intl*, **6** (3), (1993)

15. J. Janca, *Field-Flow Fractionation. Analysis of Macromolecules and Particles*, Chrom. Sci. Ser. **39**, Marcel Dekker inc., New York, 1988

16. J.J. Gunderson and J.C. Giddings, *Comprehensive Polymer Sci*, Vol.1, chap. 14, 279, G. Allen and J.C. Bevington ed., Pergamon Press plc, Oxford, 1989

17. V.T. Remcho, *Intern. Lab.*, 18-21, May 1993

18. M.E. Schimpf, *LC-GC Intl*, **6** (2), 106-108 (1993)

19. F.P. Schmitz, E. Klesper, *Polym. Comm.*, **24**, 142-144 (1983)

20. J.J. Kirkland, S.W. Rementer, and W.W. Yau, *J. Appl. Polym. Sci.*, **38**, 1383-1395 (1989)

21. J.J. Kirkland, W.W. Yau, *Macromol.*, **18**, 2305-2311 (1985)

22. J.C. Giddings, S. Li, P.S. Williams, M.E. Schimpf, *Makromol. Chem., Rapid Comm.*, **9**, 817-823 (1988)

23. M.E. Schimpf and J.C. Giddings, *Macromol.*, **20**, 1561-1563 (1987)

24. G.B. Levy, *Intern. Lab.*, 40-50, October 1987

25. J.C. Giddings, F.J.F. Yang, M.N. Myers, *Anal. Chem.*, **46**, 1917-1924 (1974)

26. J.C. Giddings, M.N. Myers, *Separation Science and Techn.*, **13**, 637-645 (1978)

27. H. Small, *Adv. in Chrom.*, **15**, 113-129 (1977)

28. D.J. Nagy, C.A. Silebi and A.J. McHugh, *J.Appl.Polymer Sci.* **26**, 1555 (1981).

29. F. Vérillon, D. Heems, B. Pichon, K. Coleman, J.-C. Robert, *Intern. Lab.* 29-35, July/Aug. 1992

30. F.P. Schmitz, E. Klesper, *Makromol. Chem., Rapid Comm.*, **2**, 735-739 (1981)

31. T.A. Berger, W.H. Wilson, *Anal. Chem.*, **65**, 1451-1455 (1993)

32. J.C. Giddings, *ACS, C & N*, 34-45, October 10, 1988

33. J.C. Giddings, K.A. Graff, K.D. Caldwell, M.N. Myers, *ACS, Adv. Chem. Ser.*, **203**, 257-269 (1983)

34. M.E. Schimpf, P.S. Williams, J.C. Giddings, *J. Appl. Polym. Sci.*, **37**, 2059-2076 (1989)

35. J.J. Janca, *Mikrochim. Acta*, **111**, 135-162 (1993)

36. Yu S. Gao, K.D. Caldwell, M.N. Myers, J.C. Giddings, *Macromol.*, **18**, 1272-1277 (1985)

37. J.J. Janca, *J. Appl. Polym. Sci. : Appl. Polym. Symp.* **51**, 91-100 (1992)

38. J.J. Janca, *Mikrochim. Acta*, **111**, 163-175 (1993)

39. J.J. Kirkland, S.W. Rementer, and W.W. Yau, *Anal. Chem.*, **53**, 1730-1736 (1981)

40. J.G. Dos Ramos, C.A. Silebi, *Polymer Intern.*, **30**, 445-450 (1993)

41. J.C. Kraak, R. Oostervink, H. Poppe, U. Esser, K.K. Unger, *Chromatographia*, **27**, 585-590 (1989)

42. H. Small, *Acc. Chem. Res.*, **25**, 241-246 (1992)

43. F.J. Molina, A.O. Villa, C. Llacer, M.J. Martos, J.E. Figueruelo, *J. High Resol. Chromatog.*, **14**, 590-592 (1991)

44. G. Stageman, J.C. Kraak, H. Poppe, *J.Chromatogr.*, **550**, 721-739 (1991)

45. G. Stageman, R. Oostervink, J.C. Kraak, H. Poppe, K.K. Unger, *J.Chromatogr.*, **506**, 547-561 (1990)

46. G. Stageman, J.C. Kraak, H. Poppe, *J.Chromatogr.*, **634**, 149-159 (1993)

47. D.C. Prieve and P.M. Hoysan, *J.Colloid Interface Sci.*, **64**, 201-203 (1978).

48. M.E. Mullins and C. Orr, *Int. J. Multiphase Flow*, **5**, 79 (1979).

49. A.W.J. Brough, D.E. Hillman, R.W. Perry, *J.Chromatog.*, **208**, 175 (1981).

50. R.J. Noel, K.M. Gooding, F.E. Regnier, D.M. Ball, C. Orr, M.E. Mullins, *J.Chromatog.* **166**, 373 (1978).

51. F. Zarrin, N.J. Dovichi, *Anal. Chem.*, **57**, 1826 (1985).

52. J.A. Biesenberger, A. Ouano, *J. Appl. Polymer Sci.*, **14**, 471-482 (1970).

53. S. Mori, R.S. Porter, J.F. Johnson, *Anal. Chem.*, **46**, 1599 (1974).

54. R. Tijssen, J. Bos, M.E. van Kreveld, *Anal. Chem.*, **58**,3036 (1986).

55. R.Tijssen, J.P.A. Bleumer, M.E. van Kreveld, *J. Chromatog.*, **260**, 297 (1983).

56. C.D. Shuster, J.R. Shroeder, D. McIntyre, *Rubber Chem. and Techn.*, **54**, 882 (1981).

57. P. Elie, M. Renaud, *Entropie*, **115**, 27 (1984).

58. A. Revillon, P. Boucher, *J. Appl. Polym. Sci., Symp. Ed.*, **43**, 115 (1989).

59. C.A. Silebi, J.G. Dos Ramos, *J. Coll. Interf. Sci.*, **130**, 14 (1989)

60. J.G. Dos Ramos, C.A. Silebi, *J. Coll. Interf. Sci.*, **135**, 165-177 (1990).

61. J. Venkatesan, J.G. Dos Ramos, C.A. Silebi, *ACS Preprints, PMSE,* **62**, 64-67 (1990)

62. J.G. Dos Ramos, C.A. Silebi, *ACS Preprints, PMSE,* **61**, 855-859 (1989)

63. G.J.M. Bruin, G. Stageman, A.C. van Asten, X. Xu, J.C. Kraak, H. Poppe, *J.Chromatogr.*, **559**, 163-181 (1991)

64. N.C. DeJaeger, J.L. Trappers, P. Lardon, *Part. Charact.*, **3**, 187 (1986)

65. H. Brenner, L.J. Gaydos, *J. Colloid Interface Sci.*,**58**, 312 (1977).

66. A.E. Hamielec, Chap. 6, in *Modern Methods of Particle Size Analysis*, H.G. Barth, ed., John Wiley & Sons, New York, 1984.

67. D.J. Nagy, C.A. Silebi, A.J. McHugh, in *Polymer Colloids II,* R.M. Fitch ed., Plenum Press, New York,1980.

68. C.A. Silebi, *FACSS Symp.* Abstr. 212, Philadelphia, PA. (1981).

69. M. Hess, R.F. Kratz, *J. Polym. Sci., A-2*, **4**, 731 (1966).

70. A. Revillon, J.F. Guilland, *J. Appl. Pol. Sci : Appl. Pol. Symp.* **45**, 125 (1990).

71. G. von Wald, M. Langhorst, *ACS Preprints, PMSE*, **62**, 77-80 (1990)

Received: December 28, 1993
Accepted: January 20, 1994

ORIGINAL PAPERS

JOURNAL OF LIQUID CHROMATOGRAPHY, 17(14&15), 3025-3041 (1994)

SEPARATION OF STYRENE-BUTYL METHACRYLATE COPOLYMERS BY HIGH PERFORMANCE LIQUID CHROMATOGRAPHY

KENJI OGINO, TOORU MARUO, AND HISAYA SATO
Department of Material Systems Engineering
Faculty of Technology
Tokyo University of Agriculture and Technology
Koganei, Tokyo 184, Japan

ABSTRACT

Styrene/*n*-butyl methacrylate (S/nBMA) and styrene/*t*-butyl methacrylate (S/tBMA) copolymers were separated by chemical composition using HPLC. In the case of normal phase HPLC using acrylamide gel or acrylonitrile gel as a stationary phase, S/nBMA and S/tBMA copolymers were separated by chemical composition. S/BMA copolymers were eluted from higher styrene content using dichloromethane/*n*-hexane as an eluent, while with the opposite elution order with tetrahydrofuran/iso-octane eluent. The difference of the elution order is explained by hydrogen bondings between the gel and the sample or eluent. In reversed phase HPLC using a styrene column and nonpolar eluent such as dichloromethane/acetonitrile, S/BMA copolymers were eluted from lower styrene content using any kind of eluent examined. On the other hand, an octadecyl methacrylate column provided no separation based on the composition. The separation using the styrene column was ascribed to the specific interaction of the phenyl groups in the sample and the gel. By the comparison of the content of good solvent in an eluent and clouds point of copolymers, it was confirmed that separation was done by adsorption mechanism for both of normal and reversed phase liquid chromatography.

INTRODUCTION

Copolymers usually have chemical composition distribution (CCD) and molecular weight distribution. It is important for the characterization of copolymers to acculately determine CCD, since polymer composition plays an important role in the physical and mechanical properties. Recently, HPLC has been applied to analyze the chemical composition distribution of copolymers[1-30]. It is found that polymers can be separated by the adsorption mechanism either with the combination of polar gel and nonpolar eluent (normal phase: NP) or of nonpolar gel and polar eluent (reverse phase: RP). Thus far, copolymers studied were mainly those consisting of monomers having different polarity, such as, styrene/methyl methacrylate[1-12] or acrylate[13-15], styrene/ethyl (meth)acrylate[16-20], or styrene/acrylonitrile copolymers[21-27].

We reported the separation of several copolymers depending on the chemical composition[4,8,29-31] and polybutadiene depending on the microstructure[32]. In this paper, we studied the separation of S/nBMA and S/tBMA copolymers, which consist of monomers having similar polarity, based on the chemical composition using normal and reversed phase HPLC. Specific interaction of the gel and the sample is discussed.

EXPERIMENT

Samples

Statistical copolymers of styrene-co-*n*-butylmethacrylate (S-nBMA) and of styrene-co-*t*-butylmethacrylate (S-tBMA) were prepared using benzoyl peroxide as an initiator in bulk. The conversion was regulated to be

less than 10% in order to obtain samples with a narrow chemical composition distribution. The composition was determined by ^{1}H-NMR measurement. Number and weight average molecular weights, M_n and M_w, respectively, were determined by GPC using a calibration curve for polystyrene. A survey of the samples used is given in TABLE 1 and TABLE 2.

HPLC Columns

Cross-linked acrylonitrile (AN) and octadecyl methacrylate (ODM) gels were prepared by a suspension copolymerization of the monomer and ethylene dimetharylate using 2,2'-azobis(2,4-dimethylvaleronitrile) as an initiator and poly(vinyl alcohol) as a suspensifier. Cross-linked styrene (St gel) was prepared by the smilar suspension copolymerization of styrene and

TABLE 1 Characteristic Data of S/nBMA Coplymers

sample	St unit mole%		Yield		
	in monomer	in polymer	(%)	Mn x 10^{-4}	Mw/Mn
A	84	78	3.7	9.8	1.8
B	70	64	3.8	10.0	1.9
C	55	52	4.5	16.0	2.1
D	29	32	5.3	19.3	1.5
E	14	21	7.4	23.6	1.4

TABLE 2 Characteristic Data of S/tBMA Coplymers

sample	St unit mole%		Yield		
	in monomer	in polymer	(%)	Mn x 10^{-4}	Mw/Mn
F	85	72	2.6	7.0	2.1
G	70	57	3.0	7.5	2.0
H	50	46	3.7	7.9	2.0
I	30	26	4.6	8.7	2.0
J	15	13	4.9	15.7	1.4

divinyl benzene. The resulting copolymers were successively washed with hot water, methanol, N,N-dimethylformamide (DMF), and chloroform. Cross-linked acrylamide gel (AA gel) was prepared by an inverse suspension copolymerization of acrylamide and bisacrylamide using 4,4'-azobis(4-cyanopentanoic acid) as a initiator and a mixture of DMF, water, and poly(ethylene glycol) as a diluent, and venton 27 and 34 (NL industries, inc.) as disperse reagents. The resulting copolymer was successively washed with hot water, acetone, DMF, and chloroform. The copolymer beads having diameter of 3-10μm were collected by decantation in acetone. Each gel was packed into a 4.6mm i.d. x 25cm stainless steel column by the slurry method. TABLE 3 shows the survey of HPLC columns.

TABLE 3 Characteristic Data of Packing Materials and Columns for HPLC

Gel	M/D[a)]	Divinyl monomer	Pressure (kg/cm^2)	Flow rate (ml/min.)	Ex.L[b)] ($x10^3$)	NTP[c)]
AA	50/50	BA	200	3.5	6000	2000
AN	67/33	EDMA	450	4.5	500	1800
St	64/36	DVB	300	6.4	500	2000
ODM	50/50	EDMA	90	2.0	500	4000

a):Volume ratio of monomer and divinyl monomer
b):Molecular weight at exclusion limit
c):Number of theoretical plates/25cm
AA, acrylamide; BA, N,N'-methylene-bis(acrylamide); AN, acrylonitrile
EDMA, ethylene dimethacrylate; DVB, divinylbenzene;
ODM, octadecyl methacrylate

HPLC Measurements

HPLC was carried out at room temperature (ca.25°C) using two Jasco 880-PU pumps, one for providing a poor solvent, and the other for a good solvent. The two solvents were mixed together after the pump and were delivered to the injector through a line filter. The flow rate was set at 0.5ml/min and the proportion of good solvent was linearly increased in 25min. A 10μl portion of a dichloromethane solution of the sample (10mg/ml) was injected through a Reodyne 7125 injector. The column

effluent was monitored with an ACS (United Kingdom) 750/14 evaporative mass detector.

RESULTS AND DISCUSSION

Separation by Normal Phase HPLC

It has been reported that styrene/methyl methacrylate copolymers can be separated according to the chemical composition by adsorption HPLC. By normal phase (NP) HPLC using a polar gel and a nonpolar eluent, the sample eluted in order of decreasing styrene content, while in the opposite elution order by reversed phase (RP) HPLC, regardless the type of eluent. It is interesting to know the elution behavior of the copolymers consisting of monomers with similar polarities.

A mixture of S-nBMA copolymers with different composition was separated by NP HPLC as shown in FIGURE 1. When a mixture of dichloromethane (DCM)/n-hexane or benzene/n-hexane was used as an eluent with AN or AA column, samples were eluted from higher styrene content. The AA column retarded the elution more than AN column, indicating that the former adsorbed the sample stronger than the latter. On the other hand, when tetrahydrofuran (THF)/iso-octane was used with AA column, samples were eluted from lower styrene content and with poor resolution. With THF/n-hexane or methyl acetate/iso-octane eluent, the same elution order was obtained as with THF/iso-octane eluent.

This is the first example that the elution order of a copolymer is dependent on the type of an eluent. The difference of elution order can be explained by the polarity difference among the sample and by the hydrogen

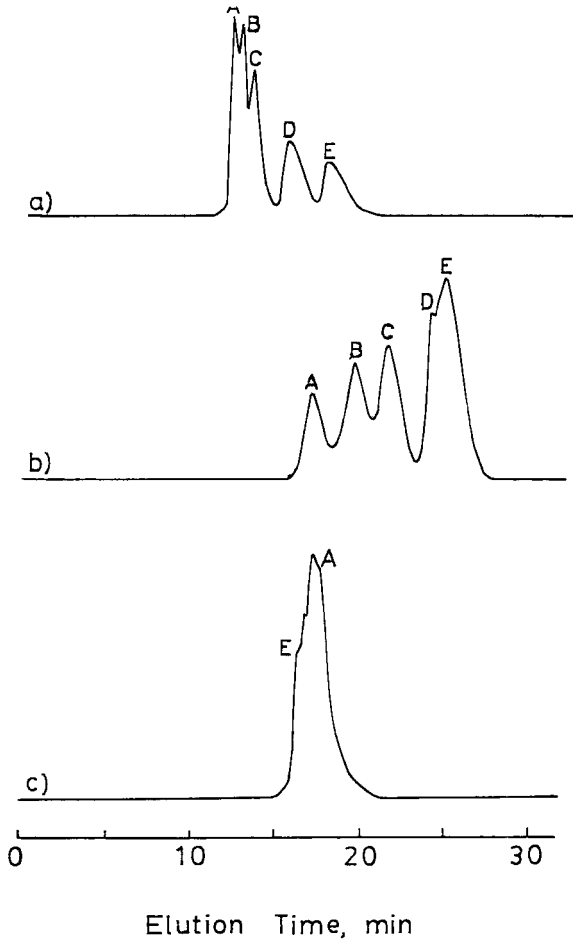

FIGURE 1. Separation of S/nBMA copolymers using (a) AN column and CH_2Cl_2/*n*-hexane eluent, (b) AA column and CH_2Cl_2/*n*-hexane eluent, (c) AA column and THF/iso-octane eluent. The content of CH_2Cl_2 or THF increased from 30 to 80 vol.% in 25 minutes.

bond between the gel and the sample or the eluent. By using DCM or benzene as a component of the eluent, the hydrogen bond was formed between the amide hydrogen in the gel and the carbonyl group in the sample. Since the polarities of both monomer units are similar, copolymer was separated based on the strength of hydrogen bonding with the gel; the sample having higher methacrylate unit eluted later. On the other hand, when oxygen containing solvent was used in the eluent, the hydrogen bond was formed between the gel and the eluent interrupting or reducing the hydrogen bond between the gel and the sample. Therefore, the sample is separated by the difference of the polarity of the sample or by the strength of the interaction between the sample and the eluent.

In FIGURE 2 the content of good solvent (DCM or THF) in the eluent at the peak maximum is plotted against the styrene content together with the cloud point. The content of good solvent is more than 20% higher than the cloud point. Therefore, it is concluded that the separation was governed by adsorption mechanism and not by phase separation one. It is also noteworthy that the cloud point curves have positive slopes for both solvent system indicating that the sample with lower styrene content is more soluble in both eluent. On the other hand, the elution curve for the eluent containing THF has a positive slope, while the slope of the curve for the DCM eluent was negative. Teramachi et al.[28] estimated that the resolution of copolymer would be improved when the slope of elution curve agree with that of cloud point. However, their estimation is not valid in our experiment. It can be concluded that the phase separation, or the solubility does not play signigicant role in the separation using adsorption mechanism.

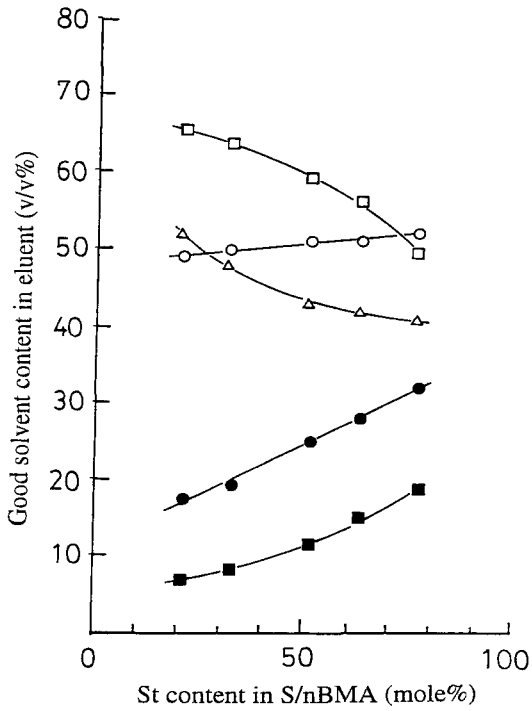

FIGURE 2. Good solvent content of the eluent at peak maximum (open symbols) and cloud point (filled symbol) for S/nBMA copolymers; (open) square: AA column with CH_2Cl_2/*n*-hexane eluent, triangle: AN column with CH_2Cl_2/*n*-hexane eluent, circle: AA column with THF/iso-octane eluent. (filled) square: CH_2Cl_2/*n*-hexane, and circle: THF/iso-octane.

FIGURE 3 shows the separation of S/tBMA copolymer using AA column. When DCM was used in an eluent, samples with higher styrene content eluted earlier, while opposite elution order was obtained by using THF in an eluent. This elution order is the same as that of S/nBMA.

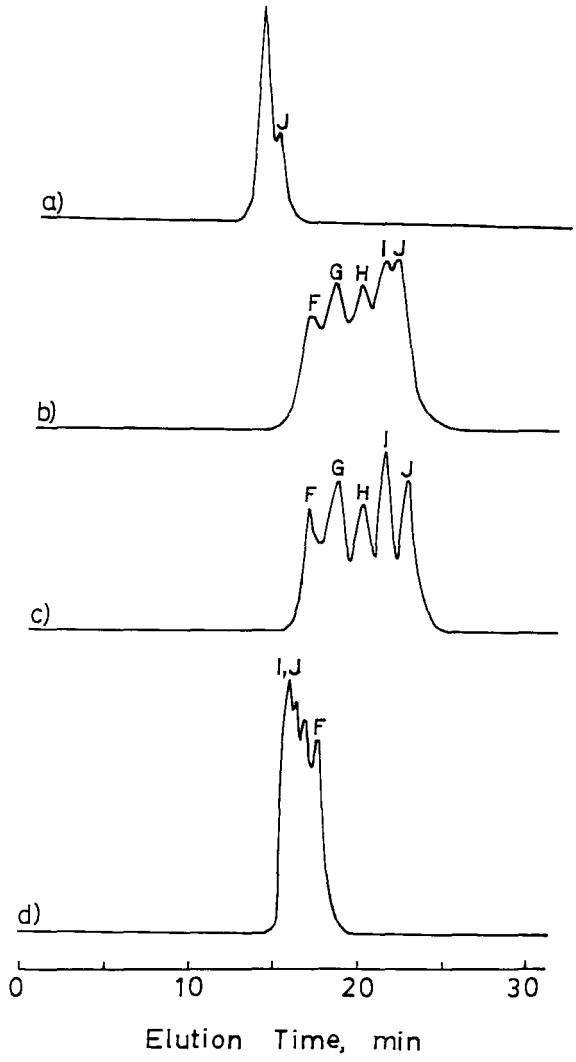

FIGURE 3. Separation of S/tBMA copolymers using (a) AN column and CH_2Cl_2/*n*-hexane eluent, (b) AA column and CH_2Cl_2/*n*-hexane eluent, (c) AA column and CH_2Cl_2/iso-octane eluent, (d) AA column and THF/iso-octane eluent.
The content of CH_2Cl_2 or THF increased from 30 to 80 vol.% in 25 minutes.

Furthermore, the elution volume of S/tBMA was almost the same as that of S/nBMA, if the sample had the same styrene content.

Separation by Reverse Phase HPLC

FIGUREs 4 and 5 show the elution patterns of a mixture of S/nBMA and S/tBMA copolymers, respectively, on the styrene (St) or octadecyl methacrylate (ODM) column using the eluent containing acetonitrile. These systems are reversed-phase (RP) HPLC, since a polar eluent was used with a nonpolar column. When St column was used, the copolymers eluted from the lower St content. This elution order was not changed by the type of good solvent such as THF or benzene. On the other hand, ODM column provided only one peak from a mixture containing 5 copolymers. The elution volumes of S/nBMA and S/tBMA copolymers were almost equal for both columns, when the styrene content was equal. It is noteworthy that the elution volume for ODM column was larger than that for St column, indicating that the sample was adsorbed on the ODM gel stronger than on the St gel.

Glöckner and Müller also found that retention of S/tBMA copolymer increased with styrene content, when THF/iso-octane was used with the phenyl silica column[28]. The elution behavior for the styrene column can be explained by the specific interaction between the phenyl groups of the gel and the copolymer. Thus, the sample was eluted in order of increasing styrene content. On the other hand, ODM column exhibited no specific interaction due to phenyl group providing only one overlapping peak, although it had a stronger hydrophobic interaction between the gel and the sample. Therefore, it can be concluded that the specific interaction such as

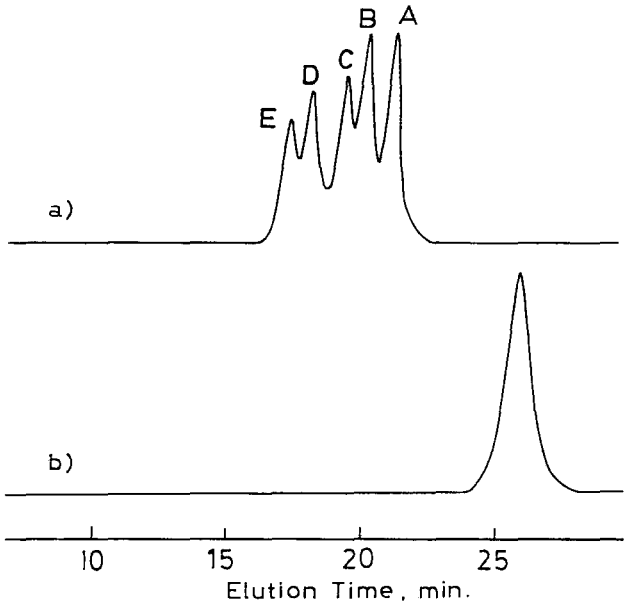

FIGURE 4. Separation of S/nBMA copolymers using (a)St column and (b)ODM column with CH_2Cl_2/CH_3CN (20/80-70/30) eluent.

the hydrogen bonding in NP HPLC or phenyl-phenyl interaction in RP HPLC is necessary to effectively separate the copolymer consisting of monomers with similar polarity.

The content of good solvent (DCM) in the eluent at the peak maximum is plotted against the styrene content together with the cloud point in FIGURE 6. The cloud point curve is lower than the good solvent content curve suggesting that the separation for the RP HPLC was also governed by the adsorption mechanism.

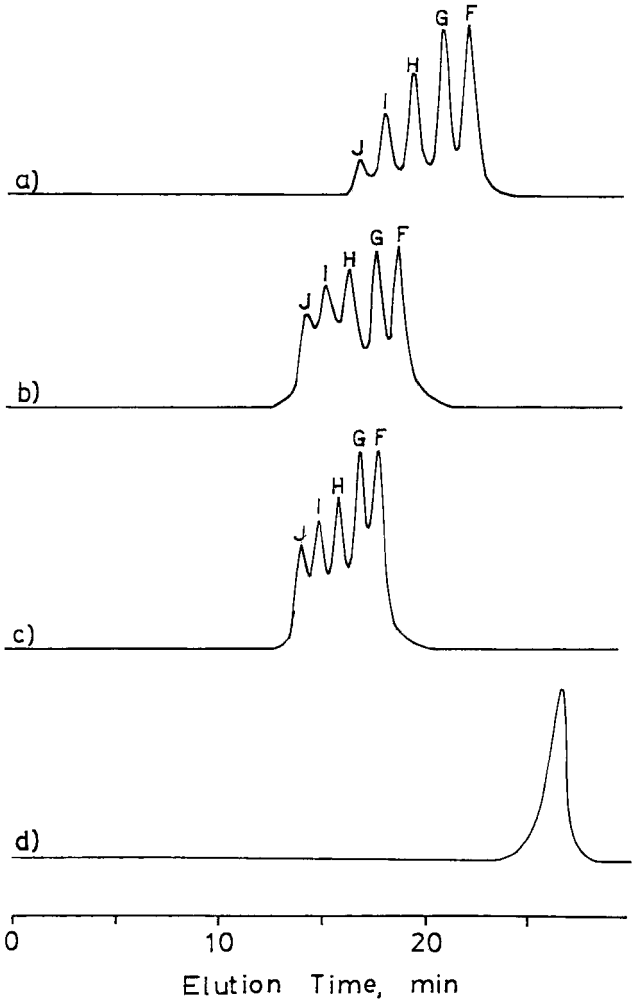

FIGURE 5. Separation of S/tBMA copolymers using St column and (a) CH_2Cl_2/CH_3CN, (b) THF/CH_3CN, and (c) benzene/CH_3CN eluent, and (d) ODM column and CH_2Cl_2/CH_3CN eluent. The content of CH_3CN decreased from 80 to 30 vol.% in 25 minutes.

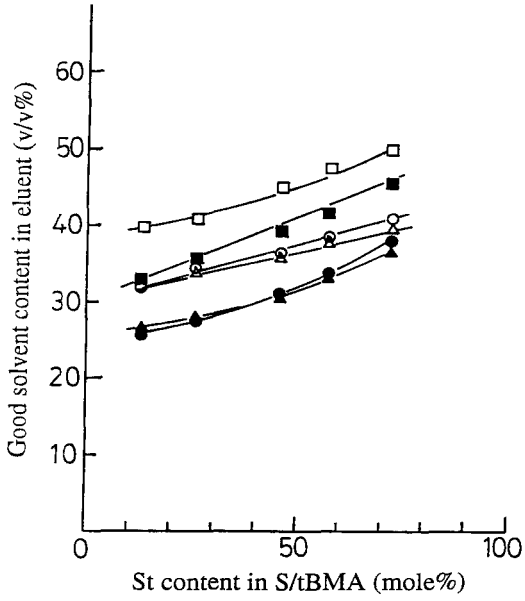

FIGURE 6. Good solvent content of the eluent at peak maximun (open symbols) and cloud point (filled symbols) for S/tBMA copolymers;St column with CH_2Cl_2/CH_3CN (square), THF/CH_3CN(circle) and benzene/CH_3CN(triangle).

The cloud point curve for St/BMA copolymers possessed a positive slope for NP and RP eluents. In the case of St/MMA copolymers, the slope for NP is negative and that for RP is positive when the cloud point is plotted against styrene content[31]. The solubility behavior of St/nBMA and St/tBMA copolymers indicates that the sample with a lower St content is soluble in a wider range of solvents. For example, a copolymer with 20% of St unit is soluble from 6/94 of DCM/n-hexane to 33/67 of DCM/acetonitrile and one with 80% of St unit from 18/82 of DCM/n-hexane to 46/54 of

DMC/acetonitrile. Since the solubility parameter (SP) values of n-hexane, DCM, and acetonitrile are 7.3, 9.6, and 11.8, respectively[33], the former copolymer is soluble in a soluvent with SP value between 7.4 and 11.8, and the latter between 7.7 and 10.8. The SP values of the center of the nonpolar and polar cloud points for the two copolymers are 9.30 and 9.25, which indicates that the St and BMA units has almost the same polarity.

REFERENCES

1) M. Danielewicz and M. Kubin, *J. Appl. Polym. Sci.*, **26**, 951 (1981).

2) G. Glöckner and J. H. M. van den Berg, *J. Chromatogr.*, **352**, 511(1986).

3) S. Mori, Y. Uno, and M. Suzuki, *Anal. Chem.*, **58**, 303 (1986).

4) H. Sato, H. Takeuchi, and Y. Tanaka, *Macromolecules*, **19**, 2613 (1986).

5) S. Mori and Y. Uno, *Anal. Chem.*, **59**, 90(1987).

6) S. Mori and Y. Uno, *J. Appl. Polym. Sci.*, **34**, 2689 (1987).

7) S. Mori, *J. Chromatogr.*, **411**, 355(1987).

8) H. Sato, K. Mitsutani, I. Shinizu, and Y. Tanaka, *J. Chromatogr.*, **447**, 387(1988).

9) S. Mori, *J. Appl. Polym. Sci.*, **38**, 95(1989).

10) S. Teramachi, A. Hasegawa, Y. Shigekuni, and S. Matunaga, *Polymer J.*, **21**, 803 (1989).

11) S. Mori, *J. Appl. Polym. Sci., Appl. Polym. Symp.*, **43**, 65 (1989).

12) S. Teramachi, A. Hasegawa, and K. Motoyama, *Polymer J.*, **22**, 489(1990).

13) S. Teramachi, A. Hasagawa, Y. Shima, M. Akatsuka, and M. Nakajima, *Macromolecules*, **12**, 992 (1979).

14) T. H. Mourey, *J. Chromatogr.*, **357**, 101(1986).

15) R. W. Sparidans, H. A. Claessens, G. H. J. van Doremaele, and A. M. van Herk, *J. Chromatogr.*, **508**, 319(1990).

16) S. Mori, and M. Mouri, *Anal. Chem.*, **61**, 2171(1989)

17) G. Glöckner, M. Stickler, and W. Wunderlich, *Fresenius. Z. Anal. Chem.*, **328**, 76 (1987).

18) G. Glöckner, M. Stickler, and W. Wunderlich, *Fresenius. Z. Anal. Chem.*, **330**, 46 (1988).

19) G. Glöckner, *J. Chromatogr.*, **403**, 280(1987).

20) G. Glöckner, H. Kroschwitz, and C. Meissner, *Acta. Polymerica.*, **33**, 614 (1982).

21) G. Glöckner, *Pure. Appl. Chem.*, **55**, 1553 (1983).

22) G. Glöckner, and J. H. M. van den Berg, *Chromatographia*, **19**, 55(1984).

23) G. Glöckner, J. H. M. van den Berg, N. L. Meijerink, T. G. Scholte, and R. Koningsveld, *Macromolecules*, **17**, 962(1984).

24) G. Glöckner, and R. Koningsveld, *Makromol. Chem. Raip Commun.*, **4**, 529 (1983).

25) G. Glöckner, and J. H. M. van den Berg, *J. Chromatogr.*, **384**, 135 (1987).

26) G. Glöckner, and J. H. M. van den Berg, *Chromatographia*, **24**, 233 (1987).

27) M. Danielewicz, M. Kubin, and S. Vozka, *J. Appl. Polym. Sci.*, **27**, 3629(1982).

28) G. Glöckner and A. H. E. Müller, *J. Appl. Polym. Sci.*, **38**, 1761 (1989).

29) H. Sato, H. Takeuchi, and Y. Tanaka, *Makromol. Chem. Rapid Commun.*, **5**, 719 (1984).

30) H. Sato, H. Takeuchi, and Y. Tanaka,
International Rubber Conf., Full Text, P. 596(Kyoto, 1985).

31) H. Sato, K. Ogino, S. Maruo, and M. Sasaki,
J. Polym. Sci., Polym. Phys. Ed., **29**, 1073(1991).

32) H. Sato, M. Sasaki, K. Ogino, *Polym. J.*, **23**, 23 (1991).

33) D. L. Saunders, *Chromatography*, 3rd Ed.,
p.96 (1975, Van Nostrand Reinhold, N. Y. Ed., E. Heftmann).

Received: November 5, 1993
Accepted: December 13, 1993

JOURNAL OF LIQUID CHROMATOGRAPHY, 17(14&15), 3043-3053 (1994)

COMPOSITIONAL SEPARATION OF POLY(VINYL ALCOHOL) USING A REVERSE PHASE PACKING IN HPLC

S. P. REID[1], E. MEEHAN[2], AND J. V. DAWKINS[1]
[1]*Loughborough University of Technology*
Loughborough
Leicestershire LE11 3TU, United Kingdom
[2]*Polymer Laboratories Ltd.*
Essex Road
Church Stretton
Shropshire SY6 6AX, United Kingdom

ABSTRACT

A reverse phase HPLC method has been developed for the separation of poly(vinyl alcohol) based on the chemical composition of the polymer. A fast gradient using water/THF results in elution based on both the degree of hydrolysis and the blockiness of the sample. The peak widths observed in this methodology are relatively broad indicating that partially hydrolysed poly(vinyl alcohol) exhibits a compositional distribution.

INTRODUCTION

Poly(vinyl alcohol) (PVOH) represents an important class of water soluble polymers used extensively in textile and paper treatments, adhesive technology and applications as emulsion stabilisers. PVOH is produced by the hydrolysis of poly(vinyl acetate) (PVAc) and the resultant polymers fall into two categories: fully hydrolysed (greater

than 98% hydrolysis) and partially hydrolysed (50-97% hydrolysis). Commercial PVOH grades are not homogeneous products and can be considered as a PVOH/PVAc copolymer system. A polymer sample consists of molecules exhibiting different degrees of hydrolysis, degrees of polymerisation and vinyl acetate sequence length distribution, dependant upon the method of hydrolysis. Alkaline hydrolysis results in relatively blocky copolymers whereas acid hydrolysis yields a more random distribution of vinyl acetate groups (1). Hence within a given sample a compositional distribution may well be superimposed upon a molecular weight distribution. For many applications of partially hydrolysed PVOH, particularly when used as an emulsifier, this compositional variation affects its properties and is therefore important in the characterisation of such copolymers.

Conventional methods of PVOH fractionation reported in the literature are based on precipitation or cloud point and are relatively time consuming methods relying on supportive analytical techniques (2). The application of adsorption chromatography to the characterisation of macromolecules has been of increasing interest over the last decade, mainly in the life science area but more recently in the field of synthetic polymer systems. HPLC separations of macromolecules generally utilise gradient elution although the actual separation mechanisms involved remain the subject of some debate (3,4). In the case of proteins it has been shown (5) that a strong interaction occurs with HPLC packings based on polystyrene/divinylbenzene (PS/DVB) and that the release of the protein occurs at a specific water/organic composition dependent on it's hydrophobicity. By a similar mechanism (6,7) PVOH polymers should be able to be separated as a function of hydrophobicity, that is degree of hydrolysis and/or vinyl acetate sequence length distribution (blockiness).

This paper describes the development of an HPLC method for the separation of PVOH polymers based on composition. Preliminary studies in this laboratory had indicated that under isocratic eluent

conditions (water /THF) some PVOH samples below a certain degree of hydrolysis did not elute from the column. Therefore the study described here concentrated on the development of a gradient elution separation in order to widen the applicability of the method. The use of THF as an organic modifier in gradient elution HPLC inhibits the use of conventional detectors (e.g. differential refractometer, UV absorbance) and the method described here employs an evaporative mass detector (8).

EXPERIMENTAL

HPLC measurements were carried out using a gradient system comprising two model 64 pumps controlled by a model 50 HPLC programmer, a dynamic mixing chamber (all Knauer, Germany), a model 7125 injection valve (Rheodyne, USA) and a model 950/14 evaporative mass detector (Applied Chromatography Systems, UK). The column used was a polymeric based reverse phase packing of polystyrene/divinylbenzene with a particle size of 8μm and pore size of 4000Å (PLRP-S 8μm 4000Å 50x4.6mm, Polymer Laboratories, UK). An eluent flow rate of 1.0ml/min was used for all experiments. All samples were analysed at room temperature using a linear gradient of 99%:1% (v/v) water:THF to 30%:70% (v/v) water:THF in 5 minutes. HPLC grade unstabilised THF (Fisons, UK) was used throughout. Model samples of PVOH polymers were derived from a single source of PVAc by alcoholysis in a methanol/methyl acetate medium (Harlow Chemical Company, UK). The degree of hydrolysis for each sample was determined by a titration method (9). Solutions for HPLC analysis were prepared by stirring an accurately weighed sample of the polymer in water and heating to 90°C to give a final concentration of 0.2% (w/v) and 50μl was injected. The mass detector was operated at an evaporation temperature of 90°C using compressed air as nebuliser gas at a flow rate of 16l/min. The signal from the detector was collected and analysed using a PL Caliber Workstation (Polymer Laboratories Ltd, UK).

RESULTS AND DISCUSSION

Typical HPLC chromatograms obtained for alkaline hydrolysed samples of different degrees of hydrolysis are shown in figure 1. The fully hydrolysed polymer always exhibited a relatively sharp, early eluting peak indicating limited interaction with the packing material. For the partially hydrolysed polymers broader and later eluting peaks were observed indicating stronger interaction for these samples.

The PVOH samples studied were prepared by alcoholysis of PVAc in the presence of methanol/methyl acetate. The resultant polymers had similar molecular weight distributions since they were all produced by the hydrolysis of one base PVAc polymer. The samples studied had different degrees of hydrolysis within the range 72.2%-100% as determined by the titration method. However it has been shown (10) that PVOH obtained by alcoholysis in the presence of methyl acetate exhibits relatively wide distribution of degree of hydrolysis. This may explain the broad peaks observed for partially hydrolysed polymers whereas in the case of the fully hydrolysed sample, where no such compositional variation exists, the peak width was much narrower.

To investigate this peak broadening effect further, 50/50 v/v blends of alkaline hydrolysed sample solutions were prepared. The chromatogram for the blend was compared with those of the constituent samples. For two samples of similar degree of hydrolysis, 72.2% and 77.7% (figure 2), the individual chromatograms revealed incomplete resolution of the two peaks. The chromatogram obtained after blending exhibited a single, broadened peak such that it enveloped the two constituent peaks. These observations would indicate that a relatively small increase in the distribution of degree of hydrolysis results in peak broadening and that the peak position, that is the maximum response, represents the average degree of hydrolysis for a given sample.

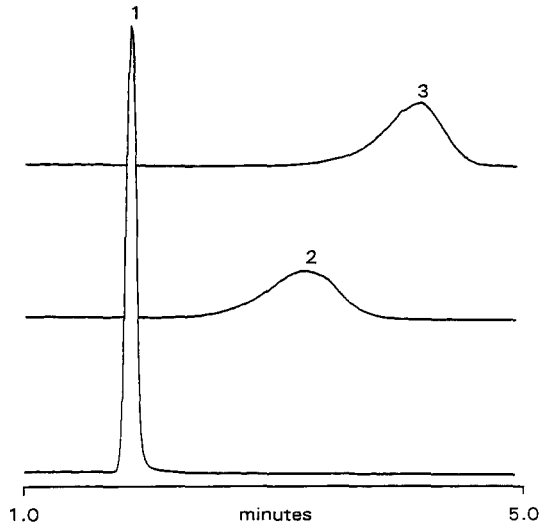

FIGURE 1 HPLC chromatograms of alkaline hydrolysed PVOH samples with different degrees of hydrolysis: 1 = 100.0%, 2 = 87.3%, 3 = 73.7%.

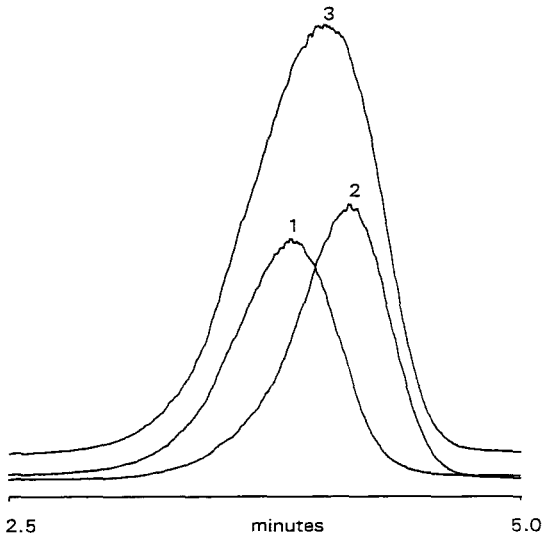

FIGURE 2 HPLC chromatograms of alkaline hydrolysed PVOH samples: 1 = 77.7% hydrolysed, 2 = 72.2% hydrolysed, 3 = 50/50 (v/v) blend of (1) and (2).

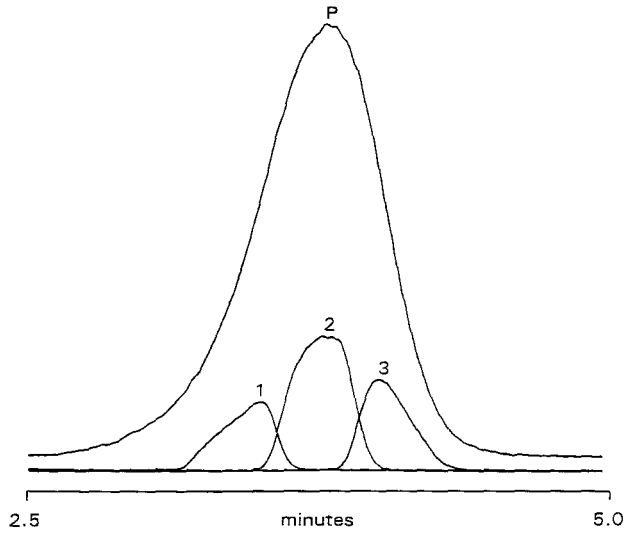

FIGURE 3 Chromatograms of alkaline hydrolysed PVOH and fractions collected from HPLC: P = whole polymer 79.6% hydrolysed, 1, 2 and 3 are fractions.

Confirmation of this theory was achieved by fractionation of alkaline hydrolysed PVOH samples as they eluted from the HPLC column. Based on previously observed elution times, three fractions were collected across the original whole sample peak after removal of the mass detector from the system. Figure 3 shows that the three fractions display individual peaks which all elute within the peak envelope of the original polymer which in this case was 79.6% hydrolysed. These results would suggest that the peak elution time is dependent on the degree of hydrolysis and that this sample, which was typical of all partially hydrolysed samples studied, exhibits a distribution of degree of hydrolysis consistent with alcoholysis in the presence of methyl acetate.

The distribution of acetate groups in partially hydrolysed PVOH obtained by acid alcoholysis is more random than that of PVOH

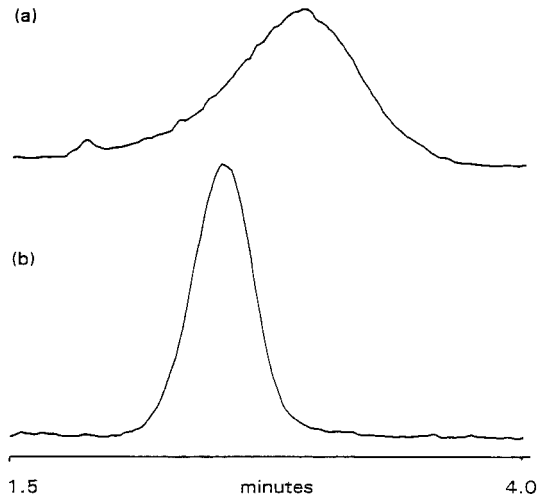

FIGURE 4 Comparison of HPLC chromatograms of PVOH 89.5% hydrolysed: (a) alkaline hydrolysis, (b) acid hydrolysis.

obtained by alkaline alcoholysis. A comparison of two polymers produced by alkaline and acid hydrolysis having the same nominal degree of hydrolysis (89.5%) is illustrated in figure 4. The acid hydrolysed sample displays a narrower peak than the alkaline hydrolysed sample. This could be due to the fact that the acid hydrolysis produces a narrower degree of hydrolysis distribution although there is no literature evidence to support this. The difference in peak width could be associated with the sequence length distribution in the alkaline hydrolysed sample being greater than that in the acid hydrolysed sample.

The basis of sample retention was explored by studying partially hydrolysed polymers covering a wide range of degree of hydrolysis, including both alkaline and acid hydrolysed PVOH. Typical chromatograms for acid hydrolysed samples, shown in figure 5, exhibited a similar trend to the alkaline hydrolysed samples shown in figure 1. At lower degrees of hydrolysis, the increasing acetate

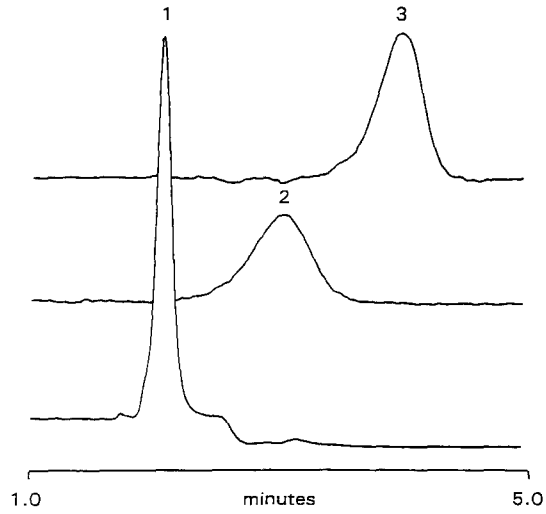

FIGURE 5 HPLC chromatograms of acid hydrolysed PVOH samples with different degrees of hydrolysis: 1 = 97.2, 2 = 84.6%, 3 = 72.2%.

content enhances the hydrophobicity of the polymer causing it to interact more strongly with the PS/DVB packing material at the start of the gradient (99% water/1% THF). Thus, a higher concentration of THF is required to release the sample from the column, resulting in increased elution time. It would appear that a specific water/THF composition is required to desorb polymers of a particular degree of hydrolysis. The elution characteristics observed suggest that the separation mechanism is by normal retention, i.e. adsorption, rather than precipitation/redissolution (3,4). A strong correlation was observed between elution time and degree of hydrolysis (figure 6) for both acid and alkaline hydrolysed samples. In general, the alkaline hydrolysed (blocky) polymers eluted later than the acid hydrolysed (random) polymers for the same degree of hydrolysis. A more blocky distribution of acetate groups, that is a longer sequence length, presents a more hydrophobic site for column attachment and requires

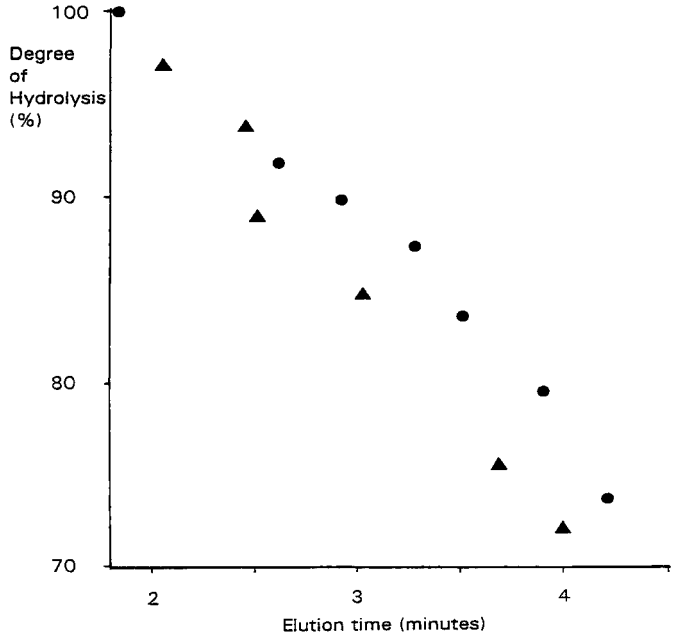

FIGURE 6 HPLC elution time as a function of degree of hydrolysis for both alkaline (●) and acid (▲) hydrolysed PVOH samples.

a correspondingly higher THF content to elute the sample. This difference is not observed at high degrees of hydrolysis, greater than 90%, where the sequence length in random and blocky samples is similar (9).

CONCLUSIONS

An HPLC method has been developed for the separation of PVOH polymers based on both degree of hydrolysis and the vinyl acetate sequence length distribution (blockiness). Gradient elution using water/THF results in the retention of solutes based on their

hydrophobicity. The retention mechanism is likely to be normal adsorption with polymers desorbing from the column at a specific water/THF composition. The peaks observed for partially hydrolysed PVOH samples are relatively broad indicating a distribution of composition. Fast gradients have been employed in this study but the application of slower gradients to yield more information regarding this compositional distribution merits further investigation.

ACKNOWLEDGEMENTS

The authors wish to express their thanks to European Vinyls Corporation (UK) Ltd, ICI Chemicals and Polymers Ltd and Harlow Chemical Company Ltd for their support in this work and to A.J. Handley, A. Nevin, S. Ormondroid, P.L. Shaw and F.P. Warner for helpful discussions.

REFERENCES

1. K. Noro, "Hydrolysis of polyvinyl acetate to polyvinyl alcohol", in Polyvinyl alcohol, C. A. Finch ed., John Wiley & Sons, London, 1973, pp. 91-120.

2. F. Lerner, M. Alon, J. Polym. Sci.:Part A:Polym. Chem.,25, 181-189 (1987).

3. M. A. Quarry, M. A. Stadalius, T. H. Mourey, L. R. Snyder, J. Chromatogr., 358, 1-16 (1986).

4. M. A. Quarry, M. A. Stadalius, T. H. Mourey, L. R. Snyder, J. Chromatogr., 358, 17-37 (1986).

5. L. L. Lloyd, F. P. Warner, J. Chromatogr., 512, 365-376 (1990).

6. T. van den Boomgaard, T. A. King, T. F. Tadros, H. Tang, B. Vincent, J. Colloid and Interfac. Sci., 66, 68-76 (1978).

7. M. C. Barker, M. J. Garvey, J. Colloid and Interfac. Sci., 74, 331-340 (1980).

8. T. H. Mourey, J. Chromatogr., 357, 101-106 (1986).

9. S. Ormondroid, personal communication

10. K. Noro, Brit. Polym. J., 2, 128 (1970)

Received: November 1, 1993
Accepted: December 17, 1993

JOURNAL OF LIQUID CHROMATOGRAPHY, 17(14&15), 3055-3068 (1994)

SEPARATION OF STYRENE-ACRYLONITRILE COPOLYMERS BY STEPWISE GRADIENT ELUTION – HIGH-PERFORMANCE PRECIPITATION LIQUID CHROMATOGRAPHY

SADAO MORI* AND HIROSHI TAZIRI
Department of Industrial Chemistry
Faculty of Engineering
Mie University
Tsu, Mie 514, Japan

ABSTRACT

With stepwise gradient elution of styrene-acrylonitrile copolymers from an ODS-silica column using chloroform - n-hexane mixtures as mobile phases, each copolymer was separated into six to eight peaks. The initial mobile phase was n-hexane and the content of chloroform in the mobile phase was increased 2% every five or ten minutes. Separated peaks were fractionated and the acrylonitrile (AN) content and molecular weight averages were measured. The copolymers were separated in order of increasing the AN content and molecular weight with a few exceptions. This explains that the fractions having lower molecular weight have lower AN content.

INTRODUCTION

Several attempts for the determination of chemical heterogeneity and chemical composition distribution for styrene-acrylonitrile copolymers P(S-AN) by high-performance liquid chromatography

(HPLC) have been reported. High-performance precipitation liquid chromatography (HPPLC), developed by Glőckner was applied to the separation of P(S-AN) according to composition (1,2). HPPLC uses a mixture of a good solvent and a non-solvent for the copolymer concerned as the mobile phase: tetrahydrofuran (THF) - n-hexane or THF - iso-octane in his work. The initial mobile phase consists of a non-solvent and the copolymer which is dissolved in a good solvent is injected into a column and is precipitated on top of the column. By applying a gradient elution as to increase the content of a good solvent in the mobile phase, the copolymer is redissolved and is eluted according to its solubility into the mobile phase.

The separation of P(S-AN) copolymers by HPPLC was found to be dependent on the combination of the stationary phase (RP-C18 or silica gel) and the mobile phase (a mixture of n-heptane and dichloromethane) (3). A system of silica gel with chemically bonded cyanoethyl groups / dichloroethane - heptane - acetonitrile has also been applied to the separation of P(S-AN) copolymers (4).

In our previous paper for the separation of P(S-AN) copolymers, the elution behaviour of P(S-AN) copolymers in HPPLC with mixtures of chloroform and n-hexane as mobile phases was evaluated (5). By applying isocratic elution with chloroform - n-hexane, next phenomena have been observed. The copolymers were eluted at retention volume corresponding to the interstitial volume (the volume of the mobile phase outside the gels in the column = the exclusion limit in size exclusion chromatography(SEC)) or retained in the column, depending on the compositions of the copolymers and of the mobile phases. The copolymers having much styrene could elute at the interstitial volume with the mobile phase of less chloroform. With increasing the content of n-hexane in the mobile phase, the copolymers were retained (precipitated) in the column. Besides the elution of the copolymers at the interstitial volume or precipitation of the copolymers in the column, the copolymers were eluted at the retention volume corresponding to the volume of the mobile phase in the column (the sum of the

interstitial volume and the pore volume of the packing materials in the column) with the mobile phase of the intermediate composition and this phenomenon was defined as the pre-precipitation state (a transition period).

In order to separate the copolymers according to composition, in other word, to observe different retention volumes among the copolymers having different composition, the linear gradient elution from 100% n-hexane to 100% chloroform has been performed and the elution was in order of increasing the acrylonitrile content in the copolymers. Although a linear relationship between retention volume and acrylonitrile content has been observed, the resolution between two copolymers was worse and the composition difference between the two copolymers should be more than 10% in the acrylonitrile content in order to get the complete resolution between two copolymers.

In the present report, stepwise gradient elution was performed for the purpose of increasing the resolution between two copolymers of which compositions were close each other. By this elution method, each copolymers could be separated into several peaks.

EXPERIMENTAL

HPPLC was performed with a high performance liquid chromatograph Model TRIROTAR-VI (Jasco Corp., Tokyo, Japan) equiped with an ultraviolet (UV) absorption detector Model UVIDEC-VI operated at 270 nm. The packing material was silica-ODS (Develosil, Nomura Chemical Co., Aichi, Japan) packed in a column of 250 mm x 4.6 mm I.D. The column was thermostated at 25 ^{o}C in a Model AO-30C column oven (Showa Denko Co., Tokyo, Japan).

Size exclusion chromatography (SEC) for the measurement of molecular weight averages of the fractions of P(S-AN) copolymers was performed with the same HPLC apparatus. A column for SEC was a Gelpak GL-W550 column (300 mm x 10.7 mm I.D.)(Hitachi Chemical

Co., Tokyo, Japan) packed with hydroxylated polymethacrylate gels. A UV detector was operated at 260 nm.

Samples used in this experiment were P(S-AN) copolymers prepared by suspension polymerization and supplied by Mitsubishi Monsant Co. (Yokkaichi, Japan). The acrylonitrile (AN) contents of these copolymers were measured by nitrogen analysis and were as follows: P(S-AN)-15, 14.8 wt%; P(S-AN)-20, 19.6 wt%; P(S-AN)-27, 26.2 wt%; and P(S-AN)-33, 32.3 wt%. These copolymers were dissolved in chloroform at a concentration of 0.1% for analytical separation and at a concentration of 0.5% for preparative separation. The injection volume for the sample solutions into the column was 0.1 mL.

The mobile phases for HPPLC were chloroform containing 1% ethanol as a stabilizer and n-hexan and their mixtures. Elution was performed by stepwise gradient. The initial mobile phase was n-hexane and ten or twelve minutes after the sample injection, the content of chloroform in the mobile phase was increased linearly in ten to seventeen minutes to specified concentration. Then the content of chloroform was increased 2% every five or ten minutes. The detailed programs are listed in Tables 1 (for analytical separation) and 2 (for preparative separation). The flow rate of the mobile phase was 0.5 mL/min.

The mobile phase for SEC was THF. Solvent in the fractions obtained by preparative separation was removed under reduced pressure and the residue was redissolved in THF.

RESULTS and DISCUSSION

In the previous report(5), adjacent peaks of the copolymers separated by linear gradient elution overlapped somewhat and in order to get complete resolution, the composition difference between the two copolymers should be more than 10 wt% in AN. A calibration curve of the peak retention volume vs. the composition of the copolymers can be constructed from Figure 6 in the previous

TABLE 1

Stepwise Gradient Program for Analytical Separation

Time, min	0	10*	20*	25	30	35	40	45	50	55
$CHCl_3$, %	0	0	20	22	24	26	28	30	32	34
Time, min	60	65	70	75	80	85	90	95	100	
$CHCl_3$, %	36	38	40	42	44	46	48	50	52	
Time, min	105	110	115	120	125	130	135	140		
$CHCl_3$, %	54	56	58	60	62	64	66	68		
Time, min	145	150	155*	175*						
$CHCl_3$, %	70	72	72	0						

* Linear gradient elution from 0% $CHCl_3$ to 20% $CHCl_3$ between 10 and 20 min and from 72% $CHCl_3$ to 0% $CHCl_3$ between 155 and 175 min.

report(5) and by using this calibration curve, the composition range of each copolymers can be calculated as follows: P(S-AN)-20, 16.5 - (34); P(S-AN)-27, 22.6 - (38)(AN wt%). The composition range calculated seems to be too broad and therefore, these peak widths must be affected not only by a composition distribution but also by a peak broadening effect during the elution in the column.

One of the possibilities to improve the peak resolution is to increase the programming time in the linear gradient elution. The difference in retention volume increased with increasing the programming time, but peak widths also increased and the improvement in the peak resolution was not much observed.

The second possibility to improve the peak resolution is to perform stepwise gradient elution. A stepwise gradient program operated in this work is listed in Table 1 for analytical separa-

TABLE 2

Stepwise Gradient Program for Preparative Separation

P(S-AN)-20 copolymer										
Time, min	0	12*	26*	36	46	56	66	76	86	96
$CHCl_3$, %	0	0	34	36	38	40	42	44	46	48
Time, min	106	116*	136*							
$CHCl_3$, %	50	50	0							
P(S-AN)-27 copolymer										
Time, min	0	12*	24*	34	44	54	64	74	84	94
$CHCl_3$, %	0	0	40	42	44	46	48	50	52	54
Time, min	104	114	124	134*	154*					
$CHCl_3$, %	56	58	60	60	0					
P(S-AN)-33 copolymer										
Time, min	0	12*	29*	39	49	59	69	79	89	99
$CHCl_3$, %	0	0	48	50	52	54	56	58	60	62
Time, min	109	119	129	139	149*	169*				
$CHCl_3$, %	64	66	68	70	70	0				

*Linear gradient elution between 12 and 26 min and between 116 and 136 min for P(S-AN)-20, between 12 and 24 min and between 134 and 154 min for P(S-AN)-27, and between 12 and 29 min and between 149 and 169 min for P(S-AN)-33.

tion and chromatograms obtained by the stepwise gradient elution are shown in Figures 1 and 2. Figure 1 is those for P(S-AN)-15 and P(S-AN)-20 and Figure 2 is those for P(S-AN)-27 and P(S-AN)-33. The programming time of stepwise gradient elution and the compositions of the mobile phase at the inlet of pump are also shown schematically. The compositions of the mobile phase listed in Table 1 and shown in Figures 1 and 2 are those at the system controller and the real compositions of the mobile phase in the column at the specified time are somewhat lower in the chloroform contents than those shown there. The monitoring at wavelength 260 nm caused the baseline drift and therefore, wavelength 270 nm was employed in this work.

P(S-AN)-20 copolymer was separated into 6 (+2) peaks and P(S-AN)-27 copolymer into 5 (+3) peaks by the stepwise gradient elution. Although some peaks of P(S-AN)-20 copolymer overlapped with those of P(S-AN)-15 copolymer, but all peaks of P(S-AN)-20 copolymer were not superimposed on those of P(S-AN)-27 copolymer. These results express that the range of composition for P(S-AN)-20 copolymer (and P(S-AN)-27 copolymer) is not wider than that calculated with a calibration curve mentioned above and peak broadening effect should be considered for the reason of broad peaks.

Stepwise gradient elution for analytical separation started at 20 min after the injection of the sample solution. This starting time affected retention volumes of separated peaks. In order to get good reproducibility for the elution positions of the resolved peaks, the starting composition of the mobile phase at a stepwise gradient elution should be lower in the chloroform content than the composition at which the copolymer started to elute.

Chloroform content in the mobile phase at which the copolymers started to elute from the column by linear gradient elution was different from that by stepwise gradient elution. P(S-AN)-15 copolymer started to elute at the composition of 75% chloroform in the mobile phase by linear gradient elution (5), while it started to elute at the composition of 34% chloroform in the mobile phase by stepwise gradient elution. Similarly, P(S-AN)-20

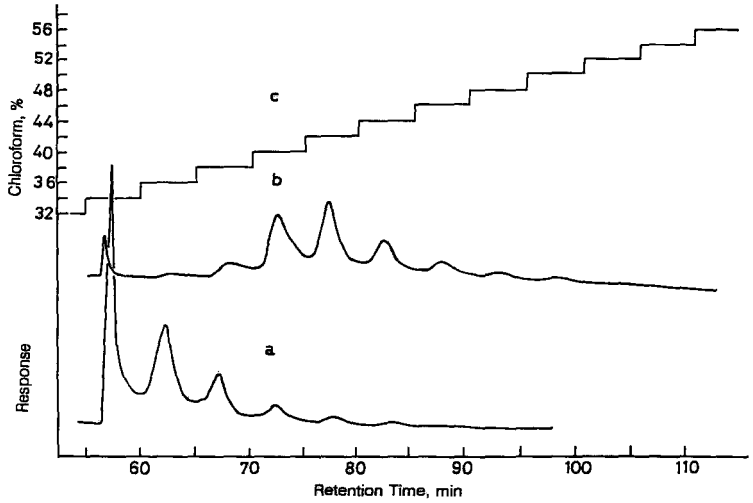

FIGURE 1. Chromatograms of P(S-AN) copolymers obtained by stepwise gradient elution (1). (a) P(S-AN)-15, (b) P(S-AN)-20, (c) composition profiles for the mobile phase; UV:270 nm, x0.16; sample concentration: 0.1%; injection volumne: 0.1 mL.

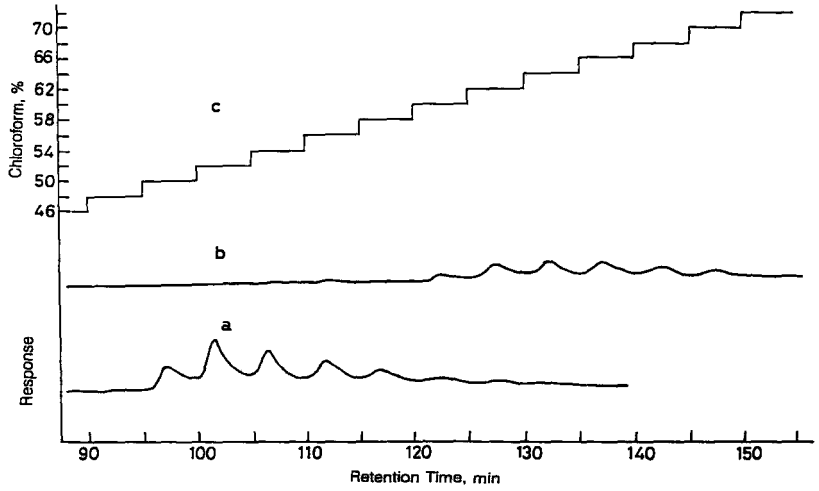

FIGURE 2. Chromatograms of P(S-AN) copolymers obtained by stepwise gradient elution (2). (a) P(S-AN)-27, (b) P(S-AN)-33, (c) composition profiles for the mobile phase; UV:270 nm, x0.16; sample concentration: 0.1%; injectiion volume: 0.1 mL.

copolymer started to elute at 82% chloroform in the mobile phase by linear gradient elution and 38% chloroform by stepwise gradient elution. Stepwise gradient elution required less good solvent than linear gradient elution. The composition in the mobile phase at which the copolymers started to elute by stepwise gradient elution (e.g., P(S-AN)-20, 38% chloroform, P(S-AN)-27, 50% chloroform) were nearly equal to those of mixtures of chloroform and n-hexane corresponded to cloud points (5) (e.g., P(S-AN)-20, 36% chloroform, P(S-AN)-27, 52.5% chloroform).

In order to measure the composition of each peak separated by the stepwise gradient elution, the peaks were fractionated by preparative separation. Gradient program for preparative separation is somewhat different from that for analytical separation and was indicated in Table 2. Chromatograms for P(S-AN)-20, P(S-AN)-27 and P(S-AN)-33 copolymers are shown in Figures 3, 4, and 5, respectively. Sample concentration was 0.5% and injection volume was 0.1 mL. No difference in peak retention volume was found in both sample concentrations, 0.1% and 0.5%. Chromatograms obtained with the 0.1% sample concentration are shown in Figures 3 and 4 for comparison purpose. Shaded parts in peaks indicate fractionated parts.

Four peaks of each samples were fractionated, the fractions were cast on a KBr disk, and then the infrared spectra of the fractions were measured by FTIR. A calibration curve was constructed by using the unfractionated P(S-AN) copolymers and the absorbance ratio of 2260 cm^{-1} and 1602 cm^{-1} was plotted against AN content. Composition of the fractions was determined by using this calibration curve. The results are shown in Table 3. From Table 3, it was found that P(S-AN)-33 copolymer was separated according to its composition and each peaks have about one percent difference in composition. Although fractions No. 1, 2, and 3 of P(S-AN)-20 copolymer were in order of increasing the AN content in the copolymer, fractions 3 and 4 were in reverse order. Fractions No. 1 and 2 of P(S-AN)-27 copolymer had the similar composition as well as those No. 3 and 4.

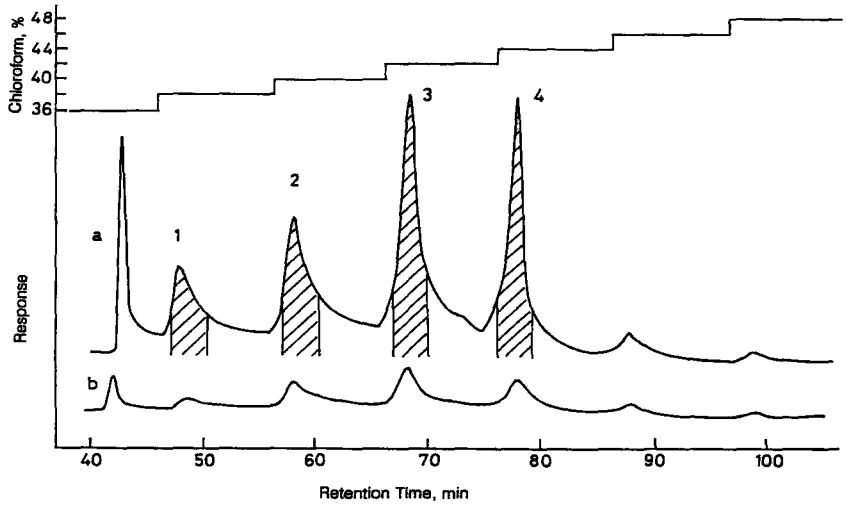

FIGURE 3. Chromatograms of P(S-AN)-20 copolymer obtained by stepwise gradient elution . Sample concentration: (a) 0.5%, (b) 0.1%; shaded parts in peaks indicate fractionation range and figures above the peaks represent the fraction numbers.

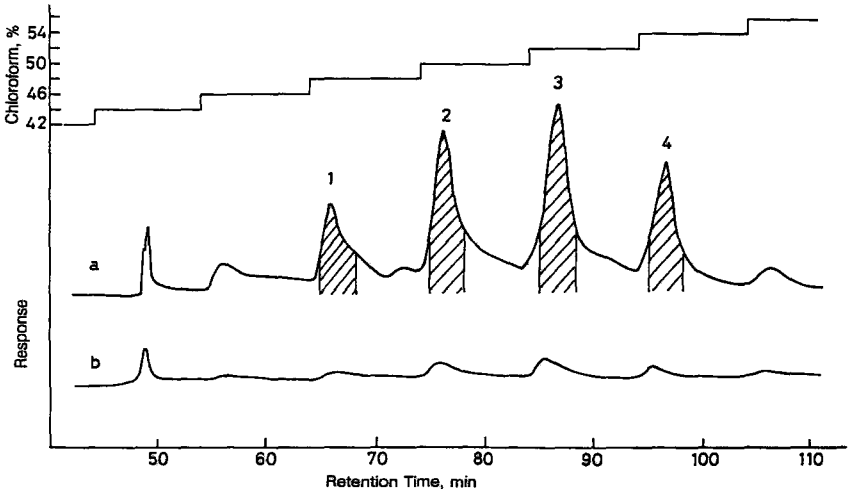

FIGURE 4. Chromatograms of P(S-AN)-27 copolymer obtained by stepwise gradient elution. Sample concentration: (a) 0.5%, (b) 0.1%; shaded parts and figures above the peaks were the same as in FIGURE 3.

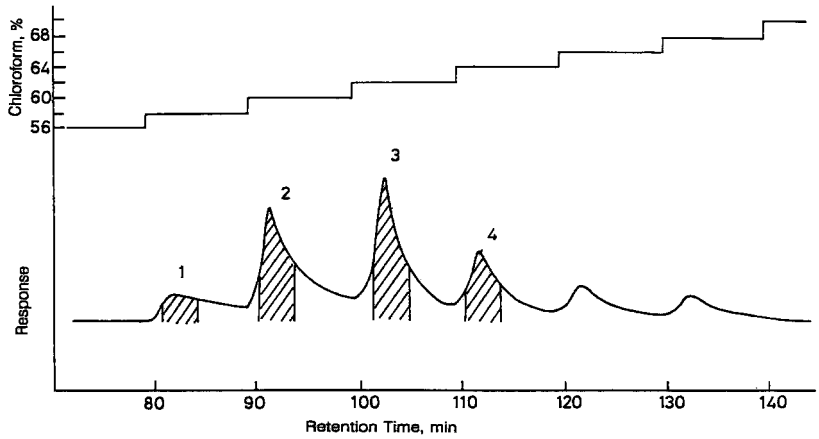

FIGURE 5. Chromatograms of P(S-AN)-33 copolymer obtained by stepwise gradient elution. Sample concentration: 0.5%; shaded parts and figures above the peaks were the same as in FIGURE 3.

TABLE 3

Composition of Fractions (AN, wt%)

Fraction number	P(S-AN)-20	P(S-AN)-27	P(S-AN)-33
1	18.0	25.4	30.5
2	19.2	25.8	31.8
3	21.8	27.3	32.8
4	20.5	27.3	34.0
Unfractionated	19.6	26.2	32.3

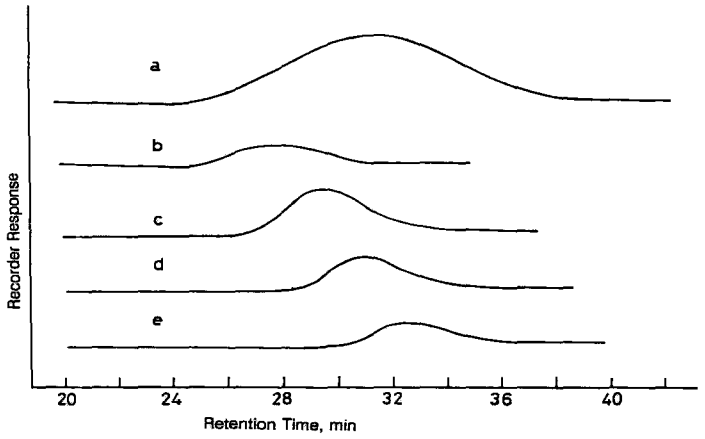

FIGURE 6. SEC chromatograms of P(S-AN)-20 copolymer and its fractions. (a):Unfractionated, (b): fraction number 4, (c):fraction number 3, (d):fraction number 2, (e):fraction number 1.

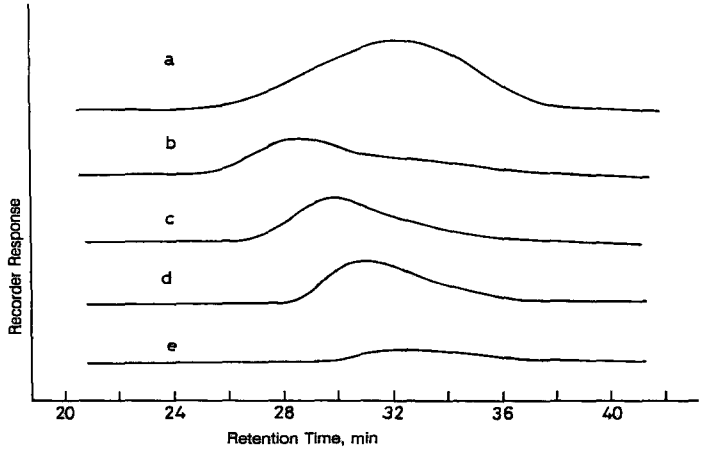

FIGURE 7. SEC chromatograms of P(S-AN)-27 copolymer and its fractions. a, b, c, d, and e are the same as in FIGURE 6.

TABLE 4

Molecular Weight Averages of Fractions as Polystyrene Equivalent

	Number average	Weight average
P(S-AN)-20	2.4×10^4	11.2×10^4
Fraction No. 1	2.8	4.7
Fraction No. 2	5.4	8.7
Fraction No. 3	11.7	15.5
Fraction No. 4	21.3	25.8
P(S-AN)-27	1.83	9.1
Fraction No. 1	2.6	5.2
Fraction No. 2	4.7	8.6
Fraction No. 3	6.6	12.9
Fraction No. 4	7.1	17.5

In order to consider this reverse order elution in composition, SEC of these fractions was performed and chromatograms are shown in Figures 6 and 7 and the molecular weight averages calculated are listed in Table 4 as polystyrene equivalent molecular weight. Elution of these fractions were in order of increasing molecular weight. It can be said that this elution method is affected by both the composition and the molecular weight of the copolymers. It is also possible to say roughly that the fractions having lower molecular weights have lower AN contents.

REFERENCES

1. G. Glöckner, Pure & Appl. Chem., 55: 1553-1562 (1983).

2. G. Glöckner, J. H. M. van den Berg, N. L. J. Meijerink, and T. G. Scholte, R. Koningsveld, Macromoleclules, 17: 962-967 (1984).

3. R. Schultz and H. Engelhardt, Chromatographia, 29: 325-332 (1990).

4. M. Danielewicz, M. Kubín, and S. Vozka, J. Appl. Polym. Sci., 27: 3629-3631 (1982).

5. S. Mori and M. Naito, J. Chromatogr., in press.

Received: October 16, 1993
Accepted: December 1, 1993

JOURNAL OF LIQUID CHROMATOGRAPHY, 17(14&15), 3069-3090 (1994)

DETERMINATION OF FUNCTIONALITY AND MOLAR MASS DISTRIBUTION OF ALIPHATIC POLYESTERS BY ORTHOGONAL LIQUID CHROMATOGRAPHY. I. OFF-LINE INVESTIGATION OF POLY(1,6-HEXANEDIOL ADIPATES)

R.-P. KRÜGER, H. MUCH, AND G. SCHULZ
Centre of Macromolecular Chemistry
Rudower Chaussee 5
D-12489 Berlin, Germany

ABSTRACT

During polycondensation of polyesters products are formed distributed in molar mass and functionality (end groups). Especially in polyurethane chemistry the knowledge of the distribution of terminal groups is necessary for correlating material properties containing different species in raw materials. The characterization of polyesters by "Liquid Adsorption Chromatography at Critical Conditions" (LACCC) is a new powerful tool for kinetics and modelling. Separation of polyesters according to their terminal groups independently of their molar mass is feasible at the critical conditions determined by the chromatographic system silica/acetone/hexane. Owing to side reactions, the number of combinations of COOH- and OH terminal groups identified was higher than expected. Cyclic species, hexanediol ether structures and alkyl-terminated homologues were identified. Model substances for all structures were synthesized. For orthogonal separation LACCC was combined off-line with SEC . With the help of preparative separation enough material was obtained to identify the species by spectroscopic methods (NMR, MALDI-TOF-MS) and to calibrate both the detector response and SEC. Finally, an algorithm is proposed for the characterization of end-group distributed reactive polymers by orthogonal liquid chromatographic methods.

INTRODUCTION

Polyesters from adipic acid and 1,6-hexanediol with an output of thousands of tons are manufactured for a wide field of applications. Polyester as intermediate product for polyurethanes are distributed in molar mass and are inhomogeneous with regard to end groups. The functionality type distribution (FTD) of these products is important for the properties of the final products, e.g. non-reactive cyclic species are responsible for the "fogging effect" in polyurethane systems. First ENTELIS et al. [1,2] investigated such reactive oligomers by means of liquid chromatography in mixed mobile phases near the "critical conditions of adsorption" of polymers and used this method for the determination of FTD. VAKTINA et al. [3] and TYUTYUNDZHAN et al. [4] separated aliphatic polyesters with OH- and alkyl-terminated groups by means of thin-layer chromatography (TLC) to characterize the thermal degradation. FILATOVA et al. [5] separated diethylene glycol adipic acid polyester with hexane/methyl ethyl ketone on silica gel by gradient elution and found an increasing OH-functionality with increasing elution force. FILATOVA et al. [6] were the first to determine "critical conditions of adsorption" in adipic acid polyesters using ethylene glycol, diethylene glycol, propylene glycol and dipropylene glycol with silica gel as stationary phase and mixed eluents of MEK / chloroform. Information about the existence of cyclic species and ether structures is given in the paper of WICK et al. [7], however, the quantitative separation and determination are not described. The state of the art of gradient HPLC is described by WICK and KRÜGER [8]. Size-exclusion chromatographic separations of aliphatic polyesters are reported in DMF [9], THF [10,11] and toluene [12] with standard polystyrene columns. Indications of the cyclic species are included in [10]. A comparison of SEC with gradient elution was done by GROS et al. [12] and KRÜGER [8].

The investigation of polymers by liquid chromatographic methods has shown that beside SIZE EXCLUSION CHROMATOGRAPHY (SEC) and interaction chromatography (LIQUID ADSORPTION CHROMATOGRAPHY, gradient HPLC), the Liquid Adsorption Chromatography of polymers at Critical Conditions (LACCC) is established and can contribute essentially to increasing the knowledge of the determination of the polymer structure [13]. The review on this liquid chromatographic mode [14] has shown that the critical conditions for the liquid adsorption chromatography of polymers are realized by using solvent mixtures as mobile phase. In SEC the chromatographic process of polymers in a good solvent is caused by a change in entropy, while the separation process of liquid adsorption

chromatography is based on the change in enthalpy in a thermodynamically poor solvent. At the critical point, the change in entropy will be compensated by the change in enthalpy. In that case, the basic unit of the polymer chain doesn't contribute to the separation process, the main chain has no chromatographic influence on retention. Under these conditions the retention is independent of the molar mass of the polymers investigated.

The chromatography at critical conditions of polymers can be used to determine the following distributions

- → functionality
- → chemical composition (blend)
- → block length distribution in copolymers
- → distributions according to structural and topological aspects (branching, cycles, tacticities)

The frequent attempts to determine the chemical composition and molar mass distribution of copolymers by orthogonal two-dimensional liquid chromatography (or so-called chromatographic cross fractionation) are incomplete, because the chromatographic mode beside the SEC does not separate independently of the molar mass. A purely orthogonal two-dimensional liquid chromatography is experimentally feasible by using liquid adsorption chromatography at critical conditions in the first dimension and SEC in the second one [15]. Subject of the present paper is the investigation of hexanediol adipate polyesters by two-dimensional liquid chromatography. The determination of functionality distribution by separation in LACCC is the aim in the first dimension. In the second dimension, the molar mass distribution of every functionally different fraction will be determined by SEC. All steps beginning with the determination of critical conditions up to the two-dimensional chromatography are presented. As a result, an algorithm for the systematic investigation by this technique will be proposed.

EXPERIMENTAL

Equipment

Investigations by gradient elution were performed with the modular equipment HP 1050 of Hewlett & Packard, consisting of a quaternary pump with membrane

solvent degasser, an auto sampler and a HP 1040 M series 2 diode array detector. 20 µl samples with a concentration of 5 mg / ml in acetonitrile were separated on a nucleosil column 250 x 4 mm ID with a 5 µm RP 18 phase of the AB type at 303 K. Data handling and computation was done by the HPLC 3D Chem Station with WIN-software.

The measurements for the determination of "critical conditions of adsorption of polymers" were performed on an equipment for isocratic separation mode, comprising a Jasco 880 PU pump, an auto sampler Marathon from Sparc (Netherlands) and an ERC 7511 differential refractometer detector. The chromatographic data were collected by a personal computer with a two-channel high special data acquisition with 24 bit resolution. The interactive processing of chromatographic data by the software NINA of Nuclear Interface (Germany). Stainless steel columns, of Tessek (Czechoslovakia), 250 x 4 mm ID with silica 7 µm with a mean pore diameter of 120 Å were used at 303 $\pm$ 1 K.

Preparative separation was carried out on an equipment of Shimadzu consisting of an LC 8 A pump, an SCL 8 A system controller, a 25 ml SIL 8 A autoinjector, a Waters R 401 differential refractometer detector, and an FCV 100 B fraction collector. A Latek Si 60 (20µm) column 500 x 40 mm ID was used with a flow rate of 30 ml min^{-1}. The Shimadzu C-R 4 AX Chromatospac integrator was applied for recording the chromatograms.

The SEC measurements were carried out at ambient temperature. The SEC system consisted of an HPLC pump (model 64 Knauer), a rheodyne injection valve with a 100 µl loop (Knauer), and a refraction index detector (Knauer). Two columns (300 x 8 mm ID), PL-gel, pore sizes of 50 Å and 100 Å, 5 µm particle diameter, separating in the molar mass range up to 10000 g mol^{-1} were used. Acetone was the mobile phase, with a flow rate of 1 ml min^{-1}. Data acquisition and calculation of calibration curves and molar mass distribution was done with the SEC software of Polymer Standard Mainz on an Atari computer.

MATERIALS AND SYNTHESIS

Chemicals and Solvents

The chemicals used in this study, were adipic acid (Merck, Darmstadt, Germany, for synthesis), caproic acid (Merck, for synthesis, distilled), 1,6-

hexanediol (Riedel-de Haën, Seelze, Germany, distilled under reduced pressure), thionyl chloride (Merck, destilled), 1-hexanol (Merck, distilled), 5-hexen-1-ol (Merck, distilled) and 4-toluenesulfonic acid (Merck, Germany). The solvents (methanol, toluene diethyl ether, and N,N-dimethylformamide obtained from Merck, pyridine obtained from Riedel-de Haën) were destilled freshly before application. Acetone, n-hexane and tetrahydrofuran (Baker, Deventer, Netherlands), HPLC grade reagents, were degassed by stitting under vacuum. The acid chlorides (adipic acid chloride, caproic acid chloride) were prepared by treatment of the corresponding carboxylic acid with thionyl chloride in the presence of nitrogen followed by distillation.

Sample Preparation

Definite model polyesters were prepared with favoured end groups to identify the HPLC peaks in the LACCC of industrially manufactured OH-terminated adipic acid / hexanediol polyesters.

For the modification of polyesters, polymer analogous reactions were performed. Polyesters with different end groups (favourably OH/OH, COOH/OH and COOH/COOH) were synthesized from adipic acid and 1,6-hexanediol by variation of stoichiometry in solution in the presence of 4-toluene-sulfonic acid and extra dry grade nitrogen. The water formed was permanently eliminated by toluene (towing agent) . The preparation was performed by precipitation in methanol or diethyl ether followed by sucking, washing and drying at reduced pressure. If adipic acid dichloride was applied, the reaction was carried out with hexanediol in the presence of pyridine by heating. Precipitation was performed in hydrochloric acid / ice water. The resulting product was sucked and washed, dissolved in toluene and precipitated in methanol followed by drying under vacuum. In all cases, white polyester powders were obtained .

The synthesized polyesters containing different end groups were converted once more to produce alkyl end groups. OH end groups were esterified with caproic acid chloride. By variation of stoichiometry (solvent pyridine) and heating polyesters were obtained containing end groups of different nature (Alk/COOH, Alk/OH, Alk/Alk). The purification was done as described above. An acid polyester containing one-sided hexenyl end groups was obtained from α,ω-COOH polyester

with 5-hexene-1-ol. Reaction was performed by heating in solution catalyzed by 4-toluenesulfonic acid. Potassium salts were synthesized yielding two excellent polyesters by accurate neutralisation of COOH-groups.

Moreover, oligomer diesters with special end groups were synthesized in order to facilitate the identification of polyester peaks owing to the excellent purity of those substances. These products were the first species of homologous series (six C-atoms in each component). All dihexyl adipates were obtained from adipic acid (or adipic acid dichloride) and excessive 1-hexanol in melt (or pyridine solution). The products were absorbed in diethyl ether and washed thoroughly with an aqueous solution of sodium carbonate. After the evaporation of ether, the substances were fractionated under reduced pressure. The reaction with 5-hexen-1-ol proceeded in the same manner. Analogously, all diesters obtained from 1,6-hexanediol and caproic acid chloride were prepared with a different excess of components (Alk/Alk-, Alk/OH-end groups). The diester with both alkyl and COOH end groups was obtained from adipic acid and 1-hexanol in melt.

In the literature [7] it is mentioned that etherdiol structures in polyesters have been detected too . Therefore, 1,6-hexanediol was treated with 4-toluenesulfonic acid in toluene under the same conditions as for the polyester preparation . The evaporated mixture was distributed between diethyl ether and water before the isolation of the product.

RESULTS AND DISCUSSION

For a complete description of the heterogeneity of polyesters the information of SEC and LACCC separation must be combined. Because the analysis of such a complex sample as a polyester containing small amounts of undesired structures (below three percent) is more difficult, the above-mentioned model polyesters were used for identification. For this purpose, the following experimental step must be solved.

Diagnosis of functionality distribution

Chemical heterogeneity can be recognize by comparing of chromatograms of samples with different end groups in SEC or in HPLC with gradient elution.

Therefore polyesters of adipic acid and 1,6-hexanediol with different structures were synthesized. The content of the expected terminal group combinations HO—OH, HO—COOH and HOOC—COOH depends on the molar ratio of dicarboxylic acid to diol in synthesis. The data of characterizing at the obtained model polyesters by classical mean values from chemical end-group analysis (OH- and COOH-value) and vapour pressure analysis are presented in Tab. 1. It reveals that no product has a mean functionality of whole numbers. In Tab. 2 the dates of other in this paper used AA-HD-polyesters are shown.

To indicate the influence of terminal groups on the elution behaviour of polyesters with preferred COOH end groups or OH end groups [Fig.1] they were separated with acetone as above for SEC defined conditions. The high-resolution separation system can distinguish between the low-molecular range of both the homologous series [Fig.1] and the raw materials. It must be checked if the reason for the differences in the elution volume is caused by adsorption or solvation. The calibration function should be controlled for the homogeneous series.

The gradient elution chromatogram [Fig.2] shows the separation of a sample PE2, preferred terminal OH-groups and a small carboxylic content. The shape of the eluted species clearly shows all homologues with two OH end groups, since the retention increases with molar mass. Between the main peaks there are some small peaks which are caused by other terminal groups. These species can't be separated at higher polycondensation degrees, because of the small difference of interaction. A quantitative determination of all existing homologous series by adding up the peaks in the adsorption or gradient mode of LC is not possible. Only in the LACCC separation mode all species with the same end groups will be eluated in one peak and can be determined quantitatively.

Selection of the phase system

Polyesters with typical terminal groups resulting from polycondensation and polyesters with other end groups caused by side reactions (cyclization, dehydration and thermal ester cracking) differ in a wide range of polarity. Silica gel and reversed phases were tested to separate HO—OH, HO—COOH and HOOC—COOH

TABLE 1: Selection of Synthesized Model Polyesters

Main structure of synthesized polyesters	Acid number (mgKOH/g)	Hydroxyl number (mgKOH/g)	Molar mass M_n (g mol^{-1})	Functionality
HOOC—PE—OH	9.2	7.0	6800	1.96
HO—PE—OH	1.2	86.2	1270	1.98
HOOC—PE—COOH	123.6	5.8	810	1.87
Alk—PE—Alk	0	0	2100	0
Alk—PE—OH	3.1	17.6	2520	0.93
Alk—PE—COOH	115.7	4.0	450	0.96
HOOC-PE-Alk(unsatur.)	19.6	0	2600	0.91
HO—O—OH	0	361	310	1.99

TABLE 2: Characterization of Polyester Samples

Polyester samples	Acid number (mgKOH/g)	Hydroxyl number (mgKOH/g)	Molar mass M_n (g mol^{-1})	Functionality
PE 1	0.16	110.3	930	1.83
PE 2	2.36	74.3	1300	1.78
PE 3	0.63	56.7	1650	1.69
PE 4	0.76	36.9	2400	1.61
PE 5	5.43	103.3	1020	1.98
PE 6	7.09	67.4	1400	1.86
PE 7	6.13	51.7	1810	1.86
PE 8	8.45	35.1	2220	1.73
PE 9	6.6	8.9	5940	1.64

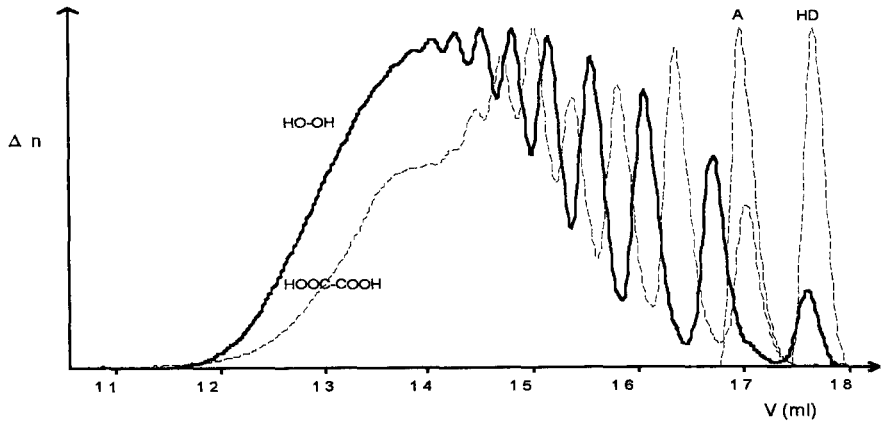

FIGURE 1: Separation of AA-HD polyester with preferred OH/OH- and COOH/COOH functionalities in SEC mode (see equipment)

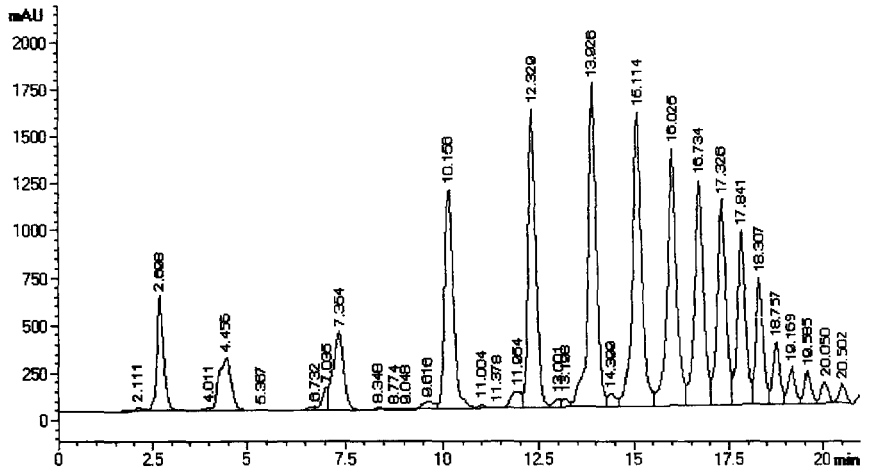

FIGURE 2: Gradient elution chromatogram of PE 2 with RP 18, 5μm column at 40°C, flow 1ml/min, solvent A: water, solvent B: ACN; gradient 65%B at the start, 1 min at 65%, in 15 min to 100%B, 5 min at 100%, detector wave length 210 nm

homologues. The reversed phase system was unsuitable because of unsufficient selectivity. The precipitation point was near the critical conditions, that means parts of polyester were precipitated on the column.

A mixture of acetone and hexane as mobile phase and silica gel as stationary phase was preferred because of the good solubility of polyesters, the possibility of evaporation after preparative separation, and low toxicity. The influence of small amounts of water (below 200ppm) could be neglected in the selectivity and retention of the peaks. At last, the mean pore diameter of the separation phase has to be optimized. Therefore were compared silica gels of different pore size of the same producer. It is necessary that all dissolved polymer molecules are able to contact the polar SiOH groups on the silica gel surface and that exclusion effects do not occur. The retention decreases with the mean pore size diameter of the phases. The phase ratio is proportional to the surface area. Nucleosil 50 Å, 100 Å, 300 Å and 500 Å were tested (Fig.3). Optimal resolution and peak shape were found with phase material of 100 Å mean pore diameter. For Nucleosil 50 Å not all pores of the phase were available for the polymer molecules, the transport of macromolecules was hindered. In that case the mean fraction was eluated as a broad peak. Retention and selectivity of Nucleosil 500 Å, however, exclude the separation of all species. For the measurements were used columns of Tessek, 120 Å, as written in "Equipment", with the same resolution. For the first orientation regarding the pore size selection of the stationary phase it is necessary that there are no exclusion peaks under conditions of SEC separation. Exactly the separation range must be checked by inversed liquid chromatography.

Determination of critical conditions of adsorption for AA-HD polyesters

For the determination of critical conditions it is necessary to separate samples with different molar masses. In that case the samples were in the molar mass range from 1000 to 6000 g mol^{-1} (see Tab.2) with preferably two OH groups in isocratic mode on the above-described chromatographic equipment. The mobile phase near the critical condition had to be premixed by weighing, the water content had to be controlled (<0.02%). The concentration of the samples in the mobile phase were about 1wt-%. It is favourable to begin the variation of the mobile phase with a thermodynamically good solvent in SEC mode thus avoiding precipitation or

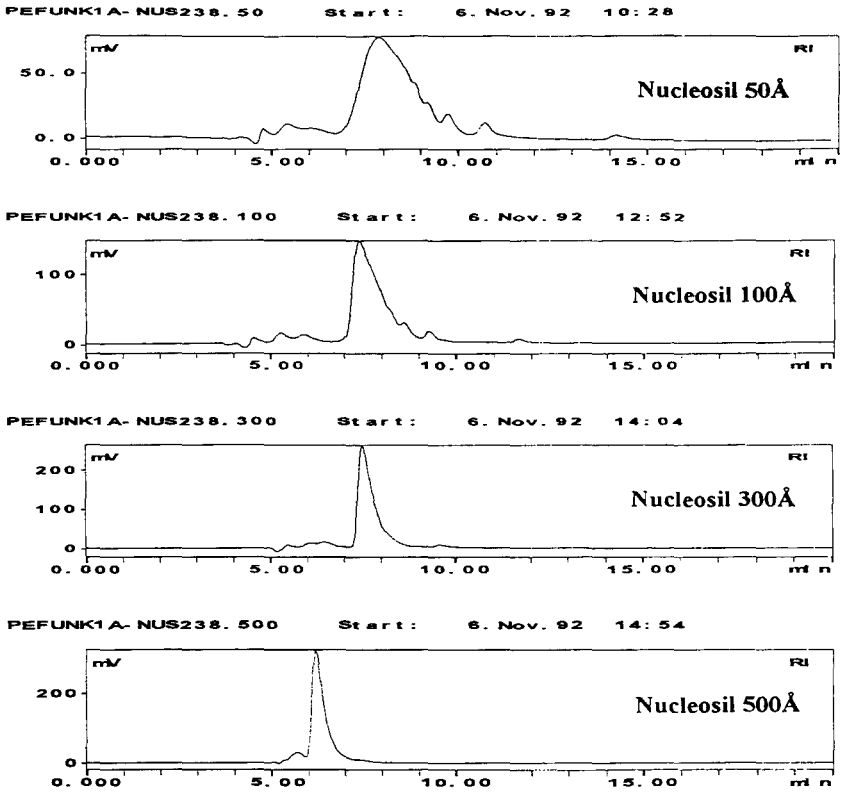

FIGURE 3: Separation of AA-HD polyester PE1 at critical conditions (49 Vol% hexane / 51 Vol% acetone) on Nucleosil 50 Å, 100 Å, 300 Å and 500 Å

irreversible adsorption on the stationary phase. In the size exclusion mode samples with higher molecular masses at lower elution volume were eluted in acetone (left series of peaks in Fig.4). By the addition of hexane, the difference in the elution volume of the used samples decreases. Near the critical conditions, at 47 vol-% hexane (Fig.4), the difference is very small. At critical conditions of adsorption, all standard samples elute at the same retention volume independent of their molar mass. The variation of the retention volume of the used standards should be smaller

than the measured standard deviation of the dead volume peak. In the right curve at 53 vol-% hexane the standards were eluted in adsorption mode (Fig. 4). The elution is reversed to the SEC mode. The peaks (Fig.5) are asymmetric near the critical point of eluent in the LAC mode and with higher molar masses they become very broad. The elution volume for a molar mass range can be tuned by the eluent mixture. The high-molecular part of the sample is adsorbed strongly, as for instance PE 9 in the right group of peaks in Fig. 5. For a complete elution in the adsorption mode the column must be washed by acetone between the separations.

Fig. 5 presents the dependence of elution volumes of polyesters with different molar masses (Tab. 2) on the composition of the mobile phase.

Identification of peaks at critical conditions of adsorption

Fig. 6 shows chromatograms of AA-HD polyesters with different molar masses of 930, 1300, 1650 and 2400 g mol^{-1}. The peaks representing different end-group combinations can be found in all four chromatograms independent of the molar mass. The relative amount of undesired structures in the products increases with higher molar masses.

The main peak 7 at 13 min. is caused by homologues with two OH-groups. The peak 10 eluated at 21 min. is related to 1,6-hexanediol as raw material. The rest of the peaks has to be identified by means of model polyesters. Polyesters with defined structures (see Tab.1) are separated at critical conditions for identification (Fig. 7) by retention data. The structures of the peaks 1 - 5 in the chromatogram (Fig.7) correspond with the models. After preparative separation, the NMR-spectra and MALDI-TOF-MS-spectra of the fractions agree with the proposed structures. Peak 8 and 9 could not be identified in such a way.

The possibility to synthesize ether structures from 1,6-hexanediol in acid medium under dehydration conditions was studied (substance with ether structures, Tab.1). In Fig. 8a the chromatogram of the polyester PE 3 is shown. The part which was saponified after preparative fractionation is marked. The separation of isolated diols after alkaline saponification and purification is shown in the chromatogram 8c. The retention of the dimer and trimer structures is identical with the synthesized

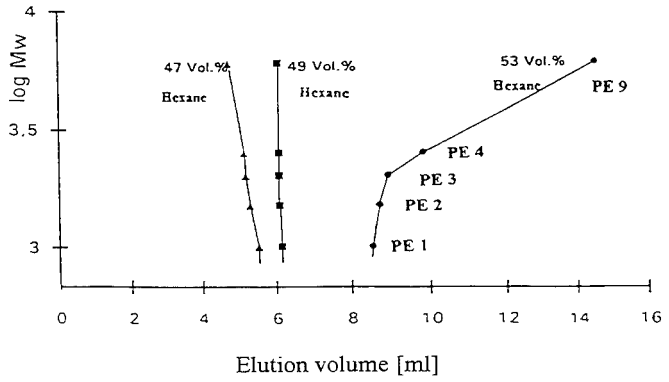

FIGURE 4: Dependence of the elution volume on molar mass (PE1,PE2,PE3,PE4,PE9) in eluents of 47% hexane / 53% acetone ▲, 49% hexane / 51% acetone ■ and 53% hexane / 47% acetone ●; silica gel column: Tessek 250x4 mm ID, 7µm, 120 Å

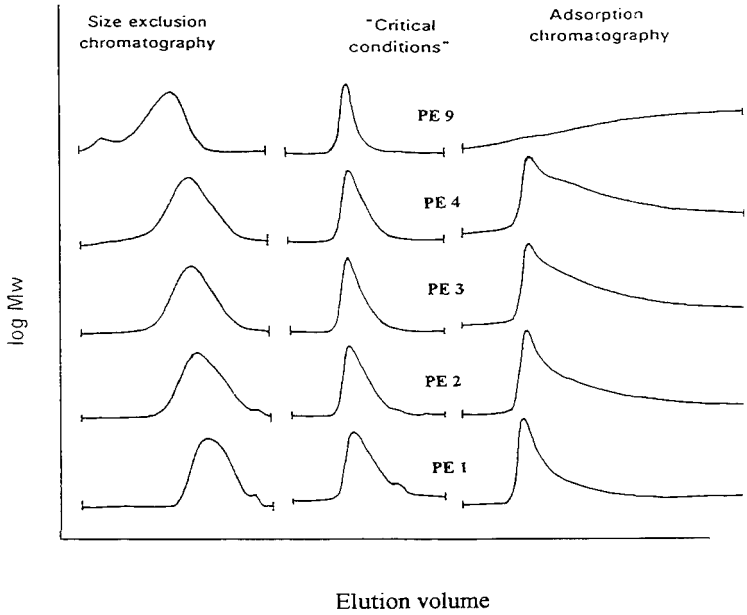

FIGURE 5: Peak shape of samples with different molar masses in dependence on the hexane / acetone ratio (left 47/53, middle 49/51, right 53/47)

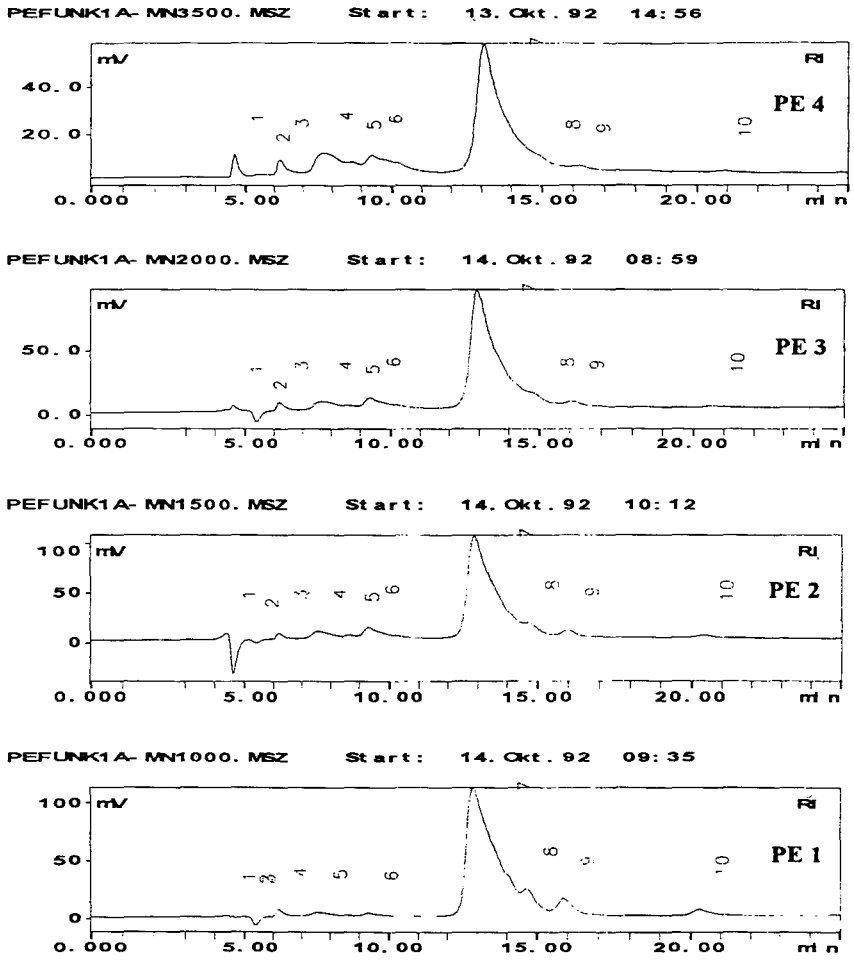

FIGURE 6: Chromatograms of AA-HD polyesters of different molar masses at critical conditions: 1: Alk-PE-Alk; 2: cycles; 3: Alk-PE-COOH; 4: Alk-PE-OH; 5: HOOC-PE-COOH, 6: HOOC-PE-OH, 7: HO-PE-OH; 8,9: HO-O-OH; 10: 1,6-hexanediol

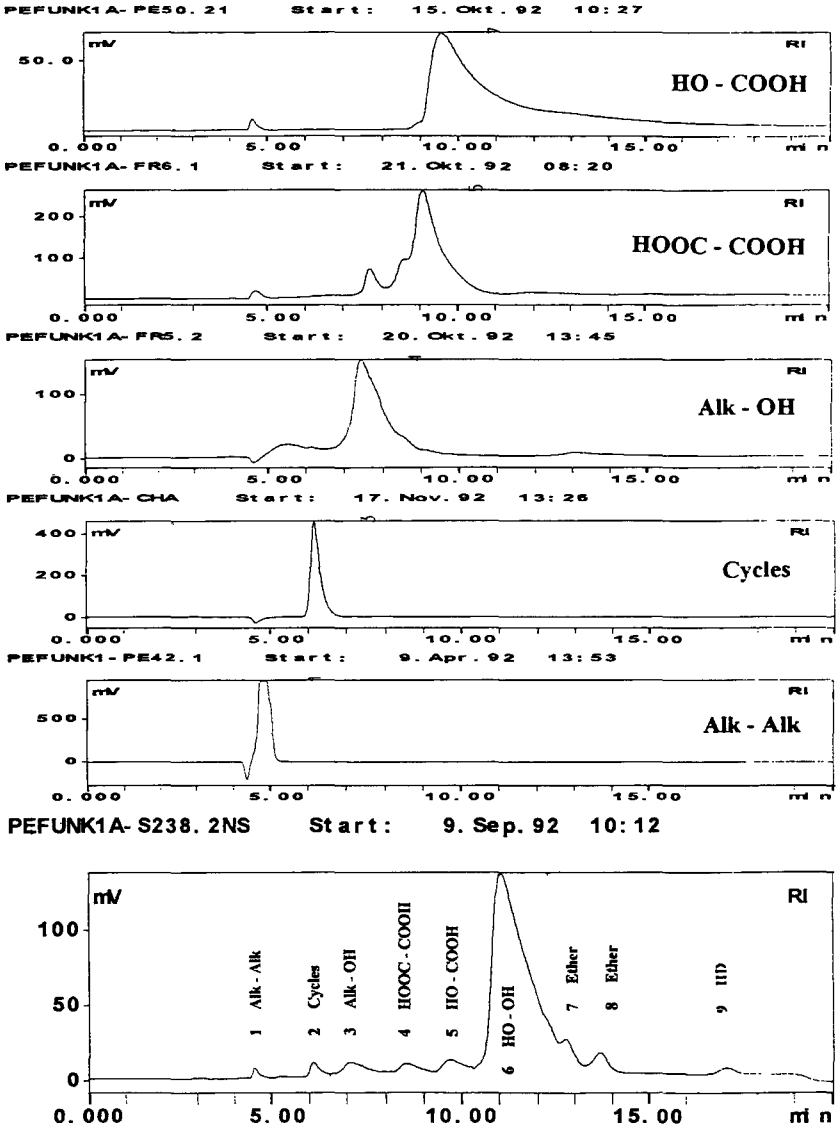

FIGURE 7: Chromatograms of AA-HD polyesters with defined structures of end groups

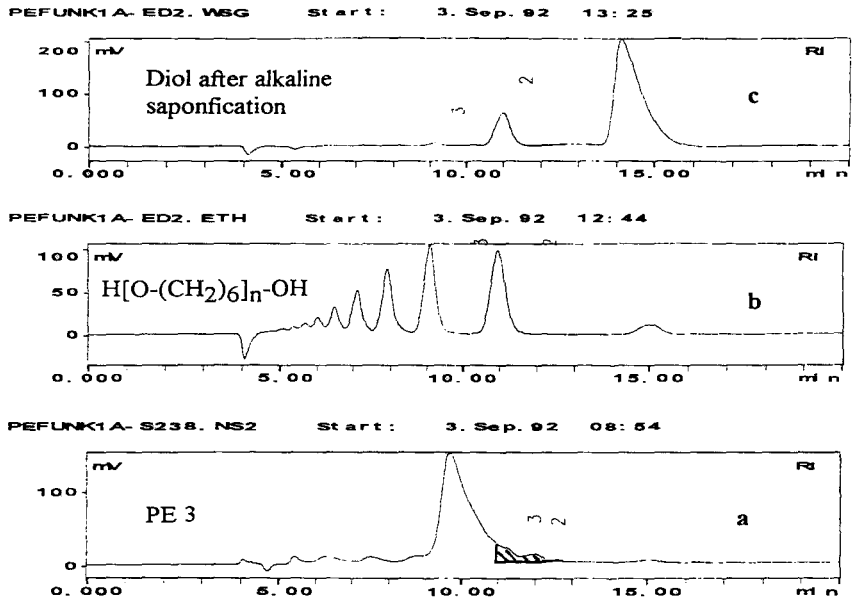

FIGURE 8: Chromatograms for the identification of ether structures in AA-HD polyester at critical conditions

oligomers of the chromatogram 8b. These ether structures are incorporated in all polyesters (Fig. 6). The content of these structures decreases in polyesters with higher molecular masses. It is well known that this ether structure is responsible for autoxidation processes.

Preparative fractionation

The preparative separation of manufactured products of AA-HD polyesters was performed on the equipment described above. About 5 g of sample were separated to isolate enough substance for the differentiation of alkyl / alkylene end groups by NMR. 10 ml of sample solution with about 800 mg of polyester were separated in one run. In the chromatogram (Fig. 9) typical overload effects by concentration or

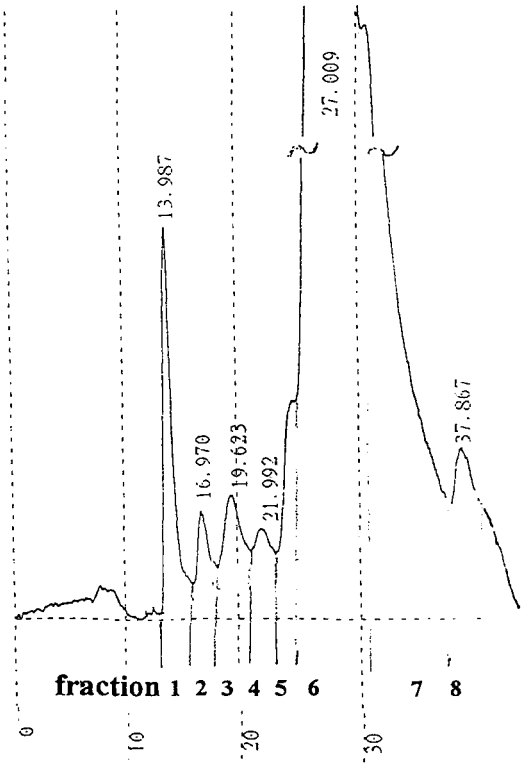

FIGURE 9: Preparative chromatogram with marked fractions

volume do not occur. The isolation of polymer fractions from the mobile phase was performed in a vacuum rotary evaporator. Degradation by saponification was not observed in the mobile phase used During a rechromatography of fractions the impurity peaks observed were ascribed to the mobile phase, they could not be observed using an evaporative light scattering detector (ELSD). After controlling by LACCC the fractions could be applied as calibration substances for the differential refractometer and ELSD. Finally, the fractions were measured by SEC to get the molar mass distribution in the second dimension of two-dimensional chromatography.

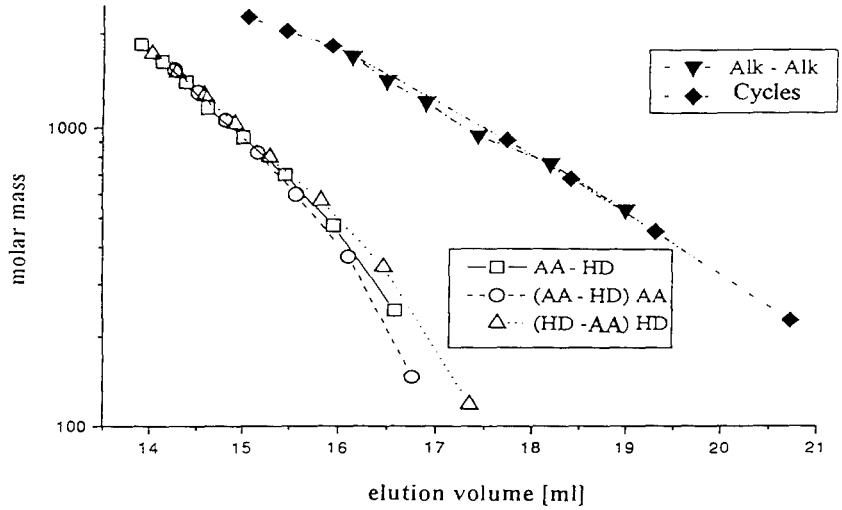

FIGURE 10: SEC calibration curves for AA-HD polyesters with different functionality

SEC

The resulting SEC calibration curves were obtained from the oligomer peaks of the homologous series of structurally different samples (Fig. 10). Therefore, the model substances described above and the synthesized first species of homologous series were used. In the case of cycles, substances were applied obtained from the former manufacturer of polyesters (Synthesewerk Schwarzheide).

Comparing the elution volumes of oligomer peaks of different end groups it could be observed that the calibration curves are different. The influence of the end group is remarkable in the first members of the homologous series. The elution volumes of polyesters with alkyl end groups and of cycles are significantly higher than of OH- or COOH- terminated polyesters. That means that in the case of comparable molar masses the hydrodynamic volumes are much smaller. The solvation of the end groups (OH or COOH) with molecules of the mobile phase could be the reason for that behaviour.

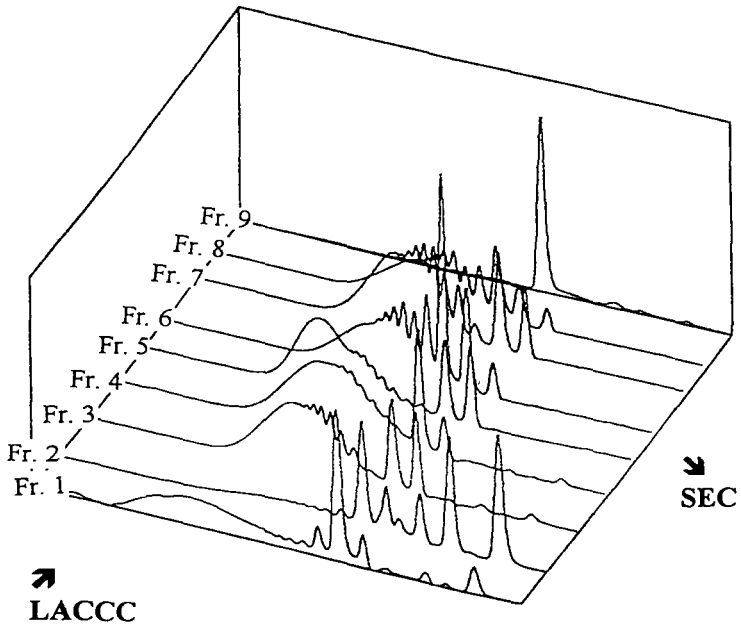

FIGURE 11: SEC chromatograms from LACCC preparative fractions of AA-HD polyester PE1

TABLE 3: Results of Off-Line Coupling LACCC / SEC (AA-HD Polyester PE1)

Structure	Fraction	M_n (SEC)	M_w (SEC)	Content from LACCC (%)
Alk—Alk	1	806	1740	0.2
Cycles	2	496	1165	0.5
Alk—OH	3	945	1190	1.1
HOOC—COOH	4	938	2071	1.2
HOOC—OH	5	1194	2863	1.3
HO—OH	6	986	1720	76.8
HO—O—OH	7	1400	2074	⎫ 16.3
HO—O—OH	8	760	1760	⎭
HD	9	112	118	2.6

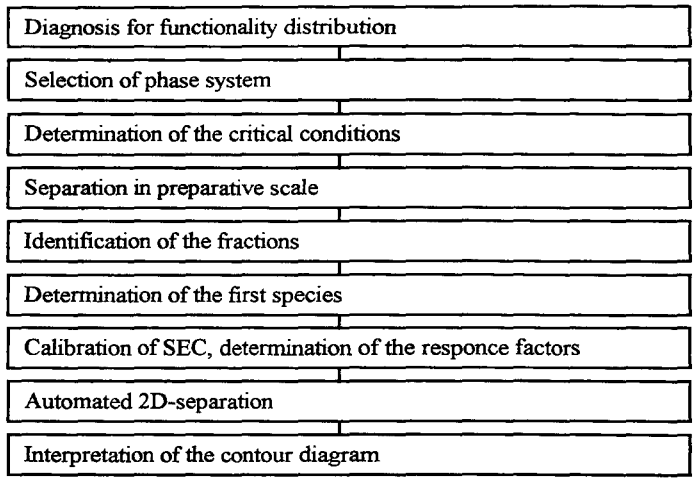

FIGURE 12: Algorithm of characterization molar mass distribution and chemical heterogeneity by two-dimensional liquid chromatography

In Fig. 11 the SEC curves of preparatively separated fractions are presented.

The molar masses, calculated from the corresponding calibration curves and the content of different species, measured in the LACCC mode by using the ELSD are presented in Tab. 3. The results differ strongly in M_n- and M_w-values of the species. Further investigations are necessary to cover and to interprete the data by kinetics and the technological process of polycondensation.

With the results of Tab. 3 a complete description of the polyester structure with regard to molar mass and functionality is given .

On the basis of the presented experiences it is possible to characterize other end-group distributed reactive polymers including macromers and telechelics. The following scheme for an algorithm is proposed (Fig. 12).

The last two operations in the algorithm will be discussed in part II, where the on-line coupling of the two chromatographic modes and their relations to synthesis will be presented.

ACKNOWLEDGMENT

Financial support from "Deutsche Forschungsgemeinschaft" is gratefully acknowledged.

REFERENCES

[1] S. G. Entelis, V. V. Evreinov, A. I. Kuzaev
Reactive Oligomers, Khimia, Moscow 1985

[2] S. G. Entelis, V. V. Evreinov, A. V. Gorshkov
Adv. Polym. Sci. 76, 129-175 (1986)

[3] I. A. Vaktina, A. G. Okunieva, R. Techritz, O. G. Tarakanov
Vysokomol. Soedin. A18, 471-474 (1976)

[4] I. P. Tjutjanshan, R. A. Schlachter, E. G. Ehrenburg, N. P. Anuchtina
Vysokomol. Soedin. A26, 104-107 (1975)

[5] N. N. Filatova, D. Ya. Rovina, V. V. Evreinov, S. G. Entelis
Vysokomol. Soedin. A20, 2367-2374 (1978)

[6] N. N. Filatova, A. V. Gorshkov, V. V. Evreinov, S. G. Entelis
Vysokomol. Soedin. A30, 953-957 (1988)

[7] G. Wick, H. Zeitler
Angew. Makromol. Chem. 112, 59-94 (1983)

[8] K. W. Krüger
GIT Fachz. Lab. 33, 1107-1110 (1989)

[9] G. Schulz
Plaste u. Kautschuk 23, 398-401 (1976)

[10] G. Müller-Hagen, P. Falke, H.-J. Oder, R. Tenner
III. Internat. PUR-Symp., SYS PUR-Reporter 19, 247-251 (1981)

[11] M. Szesztay, Zs. László-Hedvig, F. Tüdós
J. Appl. Polym. Sci., Appl. Polym. Symp. 48, 227-232 (1991)

[12] J. Gros, O. Fasko, D. Munteann, F. Pape
Plaste u. Kautschuk 30, 445-450 (1983)

[13] H. Pasch, H. Much, G. Schulz, A. V. Gorshkov
LC-GC Internat. 5, 38-43 (1992)

[14] H. Pasch, H. Much, G. Schulz
Trends in Polymer Sci. 1993, in press

[15] G. Schulz, H. Much, H. Krüger, C. Wehrstedt
J. Liqu. Chrom. 13, 1745-1763 (1990)

Received: November 3, 1993
Accepted: December 28, 1993

JOURNAL OF LIQUID CHROMATOGRAPHY, 17(14&15), 3091-3108 (1994)

CHROMATOGRAPHIC INVESTIGATIONS OF MACROMOLECULES IN THE CRITICAL RANGE OF LIQUID CHROMATOGRAPHY. VIII. ANALYSIS OF POLYETHYLENE OXIDES

H. PASCH AND I. ZAMMERT
Deutsches Kunststoff-Institut
Schloßgartenstraße 6
64289 Darmstadt, Germany

ABSTRACT

Alkyloxy and aryloxy terminated polyethylene oxides are analyzed with respect to their terminal groups by liquid chromatography at the critical point of adsorption. The molar mass distribution of the main functional fraction is determined by a modified size-exclusion chromatography technique using matrix assisted laser desorption/ionization mass spectrometry as an additional detector. The results are correlated with data obtained by supercritical fluid chromatography and mass spectrometry.

INTRODUCTION

Polyethylene oxides (PEO) are important intermediates in organic and polymer chemistry. In particular, alkyloxy and aryloxy terminated PEO's are in widespread use as surfactants. Depending on the molar mass and the chemical structure of the terminal groups the amphiphilic properties change, thus influencing the surface activity.

The chemical structure of alkyl/aryloxy PEO's is characterized by distributions in molar mass and functionality. Due to the different initiation, chain transfer and chain termination mechanisms and possible impurities in the reaction mixture, species having different terminal groups bound to the polyethylene oxide chain are formed. To elucidate the structure-property relationships of these products, it is important to know the chemical structure and the number of these terminal groups in addition to the molar mass distribution (MMD).

It has been shown previously, that the functionality type distribution (FTD) of PEO may be determined by liquid chromatography at the critical point of adsorption [1]. In brief, every chromatographic process is associated with the distribution of the solute between the mobile and the stationary phase. The distribution coefficient K_d relates to a change in free energy, ΔG, of the monomer unit when the solute molecule passes from the mobile into the stationary phase. ΔG depends on the energy of interaction of the monomer unit and the stationary-phase surface, and starting with a certain critical potential of interaction, ε_c, adsorption of the macromolecule takes place in the pore of the stationary phase. Therefore, if $\varepsilon>\varepsilon_c$, then the macromolecule is adsorbed and vice versa, such that $\varepsilon<\varepsilon_c$, then the macromolecule is unadsorbed and remains in the mobile phase. When $\varepsilon=\varepsilon_c$, the interaction energy is exactly compensated by the entropy losses. Corresponding to these three cases are the three modes of liquid chromatography of macromolecules: adsorption, exclusion, and critical. These modes relate to the different sequences in which macromolecules of various sizes elute. At the critical point, ΔG is zero, irrespective of the size of the macromolecule and all macromolecules elute within one retention time. The retention depends exclusively on the inhomogeneities of the polymer chain; that is, the nature and number of functional groups, grafts, blocks, or branches [2-4].

The determination of FTD and MMD of functional polyethers is possible by using two-dimensional chromatographic techniques, where liquid chromatography at the critical point of adsorption is carried out in the first dimension. After separating the reaction mixture with respect to functionality, the functionally homogeneous fractions may be subjected to SFC or SEC, delivering the MMD of each fraction [5,6].

In the present report a number of technical polyethylene oxides is investigated. The separation with respect to functionality is carried out using liquid chromatography at the critical point of adsorption, whereas MMD is determined by a modified SEC procedure and mass spectrometry.

MATERIALS AND METHODS

The polyethylene oxide samples were technical products of BASF, Ludwigshafen (Germany). The following average structures were given by the manufacturer:

Sample	Average Structure
C_{10}-PEO	$C_{10}H_{21}(OCH_2CH_2)_7OH$
C_{12}-PEO	$C_{12}H_{25}(OCH_2CH_2)_7OH$
C_{13}-PEO	$C_{13}H_{27}(OCH_2CH_2)_8OH$
C_{13},C_{15}-PEO	$C_{13}H_{27}$,$C_{15}H_{31}(OCH_2CH_2)_7OH$
Octylphenol-PEO	$C_8H_{17}C_6H_4(OCH_2CH_2)_6OH$
Nonylphenol-PEO	$C_9H_{19}C_6H_4(OCH_2CH_2)_{10}OH$

Liquid chromatography at the critical point of adsorption and modified SEC were carried out on a modular HPLC system, comprising a Waters model 510 pump, a Waters differential refractometer R401, a Knauer u.v./vis filter photometer, a Rheodyne six-port injection valve and a Waters column oven, keeping the temperature for all experiments at 25°C. The columns used were Macherey-Nagel Nucleosil RP-18 or RP-8, 125x4mm I.D. or 60x4mm I.D. Some preparative separations were carried out on a Nucleosil RP-18, 250x20mm I.D, column.
All solvents were Ferak HPLC grade.
The MALDI-MS investigations were conducted on a Kratos Kompact MALDI 3. The samples were dissolved in THF or the HPLC solvent and mixed with the matrix 2,5-dihydroxy benzoic acid. After drying the mixture of the sample and the matrix on the sample holder, the measurements were carried out using the following conditions: polarity-positive, flight path-reflection, mass-high (20kV acceleration voltage), 100 shots per sample.
The detailed description of the SFC experiments will be given in a forthcoming publication [10].

RESULTS AND DISCUSSION

In agreement with previous investigations, the separation of the functional PEO's according to functionality was carried out on a stationary phase RP-18 and

acetonitrile-water as the mobile phase [1]. However, using a column length of 250 mm or 125 mm, very strong retention of the functional PEO's was observed at the critical point of PEO due to the long hydrophobic chain end. To avoid irreversible adsorption on the stationary phase, a shorter column or a packing material of lower hydrophobicity was used.

The critical diagram M vs. retention time for a RP-18 column of 60 mm length is shown in Figure 1. At acetonitrile concentrations >47% by volume in the solvent mixture, the retention time decreases as the molar mass of the PEO calibration sample increases; per definition retention corresponds to a size-exclusion mode. The reverse behaviour is obtained at acetonitrile concentrations <45% by volume, where the retention time increases with increasing molar mass. At a solvent composition of acetonitrile-water 46:54% by volume, the retention time does not change with molar mass, and at this "critical point of adsorption" separation is accomplished exclusively with respect to functionality regardless of the molar mass.

The critical chromatograms of functional PEO's with different terminal groups at the critical point of adsorption of PEO are shown in Figure 2. As can be seen for the C_{10}- and C_{12}-PEO's, two distinctively different fractions are obtained, resulting in a very sharp peak at a retention time of about 35 s and a broad peak at higher retention times. For the Octylphenol-PEO RI and UV detection was used and the first peak appears only in the RI detector. By comparison with a standard sample the first peak was identified as polyethylene glycol, which is known to be formed as an unwanted by-product. In the case of the Octylphenol-PEO two additional peaks at retention times of 154 s and 303 s are detected, when UV detection at a wavelength of 280 nm is used. By comparison with the pure compound the peak at 154 s is found to be octylphenol. The second peak at 303 s is assumed to consist of Alkyphenol-PEO with a smaller alkyl substituent, which might have been formed due to impurities in the starting octylphenol.

The quantitative determination of the PEG fraction is carried out using a calibration curve amount PEG vs. refractive index response. The PEG content of the samples is in the magnitude of 1-3% by weight, which is typically for this type of commercial products, see Table 1.

In agreement with the expected behaviour for a reversed-phase column, the retention time of the samples increases with increasing hydrophobicity of the terminal group. Therefore, the elution order with respect to the terminal group is

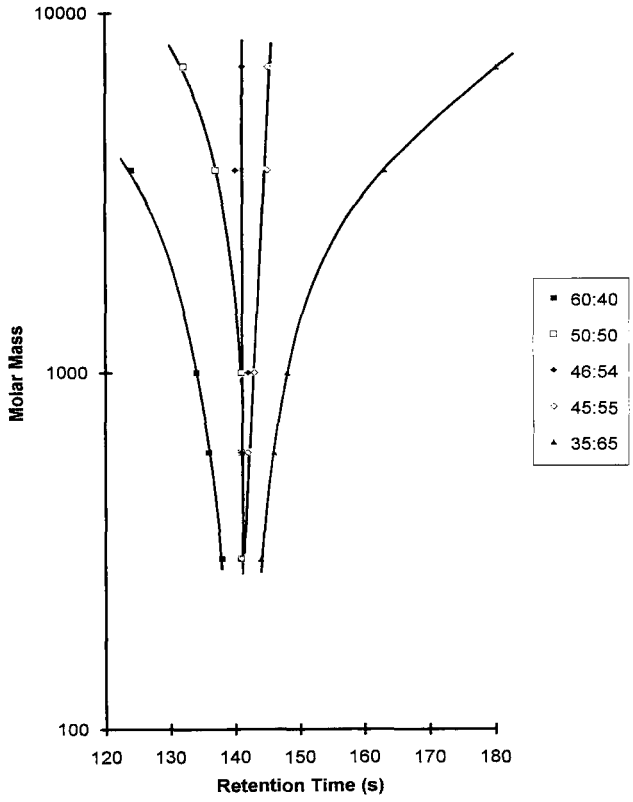

FIGURE 1 Critical diagram molar mass vs. retention time of polyethylene glycol, stationary phase: Nucleosil RP-18, 60x4mm I.D., solvent: acetonitrile-water

OH (PEG) << $C_{10}H_{21}$ < $C_{12}H_{25}$ < $C_{13}H_{27}$ < $C_{15}H_{31}$. The change of the retention times with changing the composition of the solvent mixture is given in Figure 3. The dramatic increase of the retention times near the critical point suggests, that PEO's with alkyloxy end groups greater than C_{13} may not be eluted from the column in reasonable times. In fact, it was found for C_{15}-terminated PEO and all following, that they do not elute from the column within 60 min.

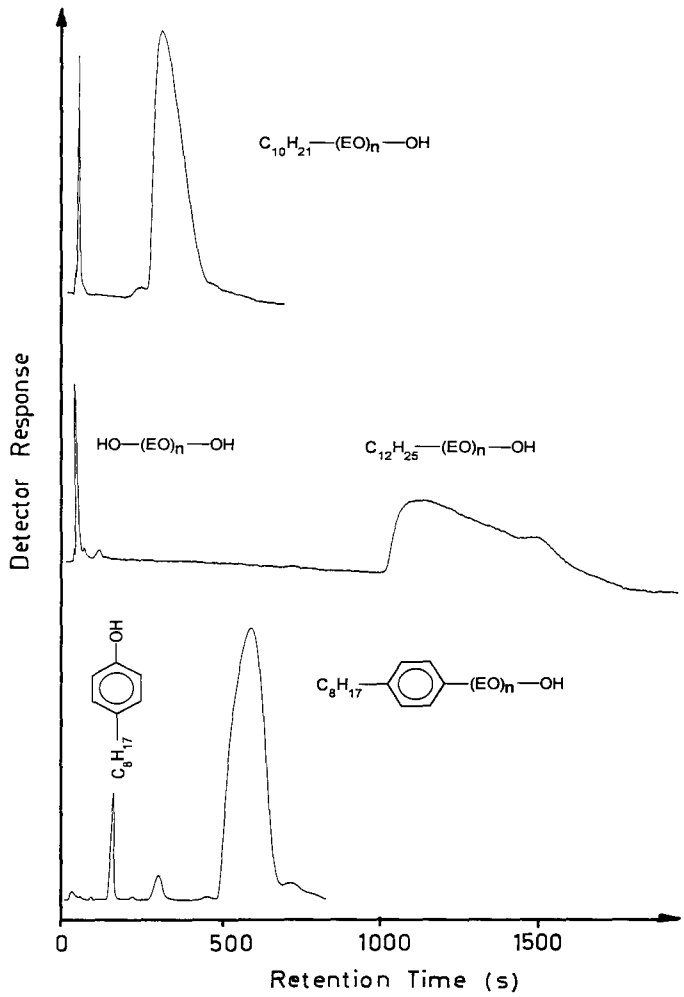

FIGURE 2 Chromatograms of functional PEO's at the critical point of adsorption of PEO, stationary phase: see Fig. 1, solvent: acetonitrile-water 46:54% by volume

TABLE 1

PEG Content of the Polyethylene Oxide Samples Determined by Liquid Chromatography at the Critical Point of Adsorption

Sample	PEG (% by weight)
C_{10}-PEO	3.27
C_{12}-PEO	2.50
C_{13}-PEO	2.32
C_{13},C_{15}-PEO	1.93
Octylphenol-PEO	1.32
Nonylphenol-PEO	1.58

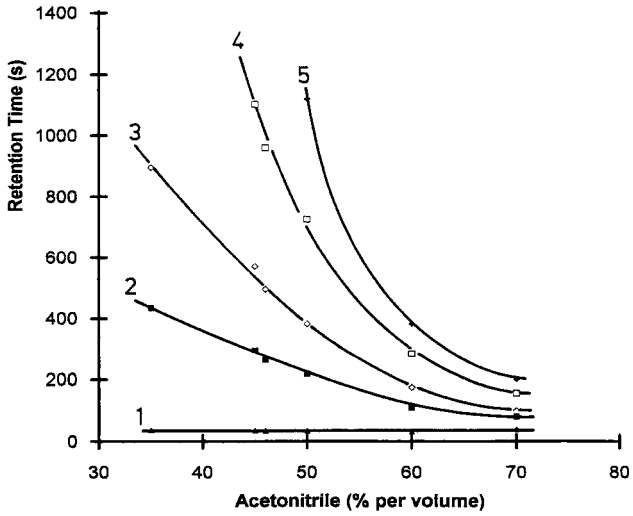

FIGURE 3 Diagram of retention time of the main functional fraction vs. composition of the solvent, stationary phase and solvent: see Fig. 1, samples: PEG (1), C_{10}-PEO (2), Octylphenol-PEO (3), C_{12}-PEO (4), C_{13}-PEO (5)

In order to decrease the hydrophobicity of the stationary phase and the retention times accordingly, a RP-8 instead of a RP-18 column is used. In this case C_{13}- and C_{15}-terminated PEO's elute from the column at the critical point of adsorption, see Figure 4. In addition to the previously detected peaks, for the aryloxy samples a third functionality fraction was eluted, which obviously corresponds to the α,ω-diaryloxy species. The concentration of this third functionality fraction, however, is very low and can be detected in the reaction mixture only with a 30 fold sensitivity of the UV detector.

As was mentioned before, on a RP-18 stationary phase the retention times of the functional PEO's increase dramatically by approaching the critical solvent composition. On the other hand, the differences in retention times at higher acetonitrile concentrations in the solvent suggest, that even in the size-exclusion region a separation into functionality fractions should be possible (see Figure 3). Assuming a mixed SEC-adsorption separation mechanism, at acetonitrile concentrations of 50-70% per volume at least the separation of the PEG fraction from the functional PEO is expected to occur. In order to increase resolution, a RP-18 column of 125 mm is used for this experiment.

The chromatograms of the samples at a solvent composition of acetonitrile-water 70:30% per volume are summarized in Figure 5. The inspection of the chromatograms reveals a separation into oligomer series for the C_{12}- and the C_{13},C_{15}-PEO's. Unexpectedly, for the C_{10}-, C_{13}- and aryloxy PEO's this type of separation is not obtained. However, regardless of the type of the functional group, in all cases a sufficient separation from the PEG and the diaryloxy fractions is obtained, thus allowing to determine all functionality fractions.

As can be seen from Figure 5, the proposed modified SEC separation technique is still very sensitive towards the chemical structure of the terminal groups. Even an increase of the substituent chain length by one methylene unit in the aryloxy PEO's (from octyl to nonyl) results in a significant increase in retention time. With a difference of two methylene units in the terminal group a complete separation of the functional fractions is obtained, see C_{13}- and C_{15}-fractions of C_{13},C_{15}-PEO in Figure 5.

From PEO chemistry it is known, that fatty alcohols of different structure are used as starting materials. They may not only differ in the length of the alkyl chain but also in the isomeric form (n-alcohol vs. iso-alcohol). From the technical point of view it is often more feasible to use mixtures of different isomers instead of pure

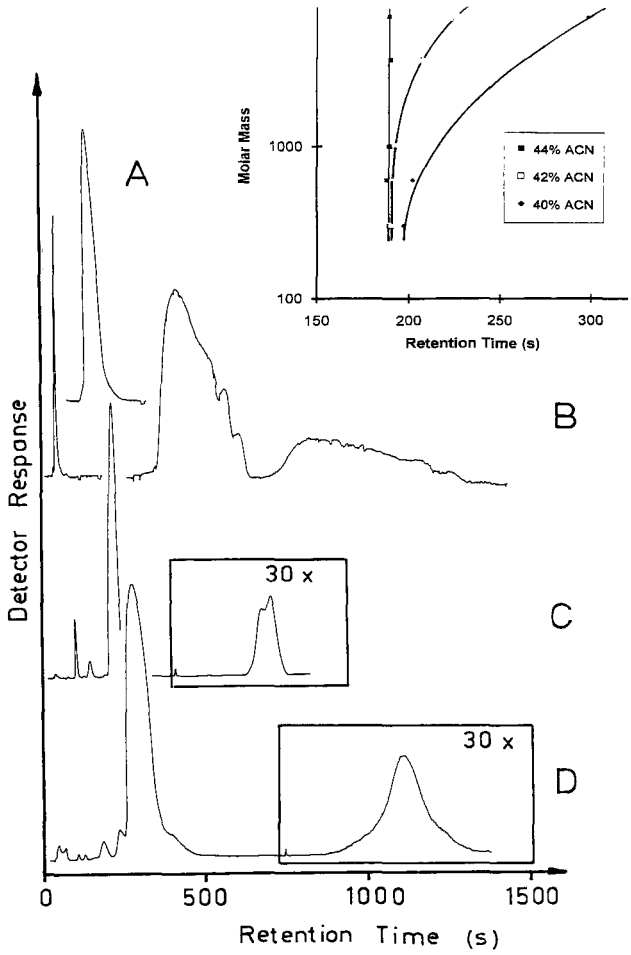

FIGURE 4 Critical diagram molar mass vs. retention time of polyethylene glycol (insert upper right corner) and chromatograms of functional PEO's at the critical point of adsorption of PEO, stationary phase: Nucleosil RP-8, 60x4mm I.D., solvent: acetonitrile-water 44:56% by volume, samples: C_{10}-PEO (A), C_{13},C_{15}-PEO (B), Octylphenol-PEO (C), Nonylphenol-PEO (D)

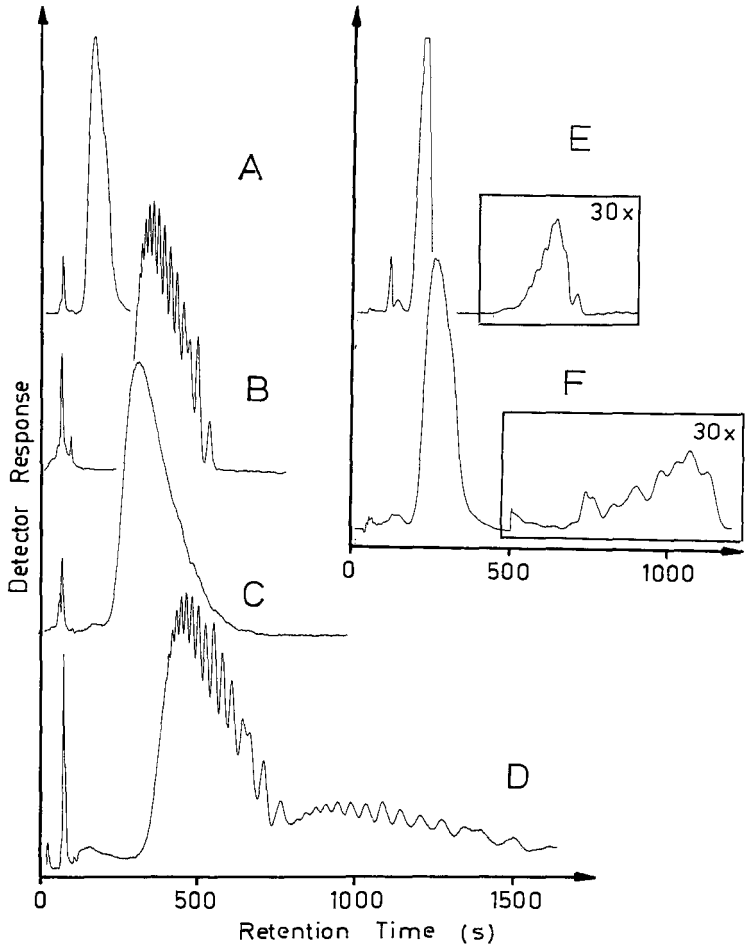

FIGURE 5 Chromatograms of the functional PEO's in a modified SEC mode, stationary phase: Nucleosil RP-18, 125x4mm I.D., solvent: acetonitrile-water 70:30% by volume, samples: C_{10}-PEO (A), C_{12}-PEO (B), C_{13}-PEO (C), C_{13},C_{15}-PEO (D), Octylphenol-PEO (E), Nonylphenol-PEO (F)

alcohols. The chromatographic behaviour of PEO's having isomeric structures as the terminal group is supposed to be different from that of uniform structures. Thus, an oligomer separation may be expected for uniform but not for isomeric terminal groups. With respect to retention, a higher retention time is expected for n-alkyl groups compared to branched iso-alkyl groups due to corresponding differences in hydrophobicity.

Considering these differences in retention behaviour with respect to the terminal group, the different chromatographic behaviour of the samples may be explained. For the C_{12}- and C_{13},C_{15}-PEO's, where oligomer separation takes place, a uniform n-alkyl terminal group may be assumed. The C_{10}- and C_{13}-PEO's are assumed to have iso-alkyl terminal groups. This explanation is in agreement with the lower retention time of the C_{13}-PEO compared to the C_{13}-fraction of the C_{13},C_{15}-PEO.

After separating the PEG fraction from the other functional species, and obtaining an oligomer separation for the main functional fraction, it should be possible to determine the molar mass distribution of the main functional fractions in the C_{12}- and C_{13},C_{15}-PEO's. Knowing the degree of polymerization or the molar mass at each oligomer peak in the chromatogram, a calibration curve log M vs. retention time may be obtained, thus allowing to calculate the M_n and M_w values. The molar mass at each oligomer peak may be determined by preparatively separating the samples into oligomer fractions and determining the molar masses of the individual fractions by an independent method. As this is rather time-consuming, a different approach was developed.

A new, most promising technique for the separation of large molecules according to their molar mass has been introduced recently. Matrix-assisted laser desorption/ionization mass spectrometry (MALDI-MS), developed by Karas and Hillenkamp in 1988 [7], has been successfully used to determine the mass of large biomolecules and synthetic polymers [8]. In principle, the sample to be investigated and a matrix solution are mixed in such a ration that matrix separation of the sample molecules is achieved. After drying, a laser pulse is directed onto the solid matrix to photo-excite the matrix material. This excitation causes the matrix to explode, resulting in the expulsion and soft ionization of the sample molecules without fragmentation. Once the analyte is ionized it is accelerated and analyzed in a time-of-flight (TOF) mass spectrometer. As a result, the analyte is separated according to molar mass of its components and in the case of heterogeneous

polymers a molar mass distribution may be obtained. In a recent paper it was shown by us that epoxy resins may be separated into their oligomers according to the degree of polymerization and the type of functional groups [9]. One major advantage of the method is, that minimum quantities of the magnitude of a few ng are sufficient for a proper analysis.

In order to assign the oligomer peaks in the chromatograms of C_{12}- and C_{13},C_{15}-PEO's, further chromatographic separations using the analytical RP-18 column are carried out and the oligomer fractions are collected, resulting in amounts of 5-20 ng substance per fraction in an acetonitrile-water solution. The solutions are directly mixed with the matrix solution and subjected to the MALDI-MS experiments. For C_{12}-PEO 14 fractions are collected, fraction 1 being the PEG and fractions 2-14 containing the C_{12}-terminated ethylene oxide oligomers.

The resulting spectra of some of the fractions are shown in Figure 6. The MALDI-MS spectrum of fraction 1 consists of peaks of major intensity, having a peak-to-peak mass increment of 44 Da, i.e. of one ethylene oxide unit. These peaks represent the $M+Na^+$ molecular ions of the PEG oligomers, whereas the peaks of minor intensity are due to the formation of $M+K^+$ molecular ions. The intensity of the peaks characterizes the relative abundance of the oligomers in the sample and from these the oligomer or molar mass distribution of the fraction may be calculated.

The MALDI-MS spectra of fractions 2-14 show one major peak each, representing the $M+Na^+$ molecular ion of the corresponding oligomer, and some minor peaks of neighbour oligomers due to incomplete separation. In all cases the main peak and its corresponding mass is used to assign a degree of oligomerization to the corresponding peak in the chromatogram. Similarly, the oligomer peaks in the C_{13},C_{15}-PEO sample are collected and subjected to MALDI-MS.

Once all peaks in the chromatograms are assigned to a degree of polymerization, the desired calibration curves log M vs. retention time may be obtained for the C_{12}-, C_{13}- and C_{15}-fractions, see Figure 7. using these calibration curves, the average molar masses and polydispersities are determined. They agree well with data obtained independently by SFC and MALDI-MS in a stand-alone mode, see Table 2. The detailed description of the SFC and MALDI-MS experiments will be dealt with in a separate publication [10].

As is shown in Figure 5, an oligomer separation is not obtained for the C_{10}- and C_{13}-PEO's as well as the aryloxy PEO's. Corresponding experiments using SFC

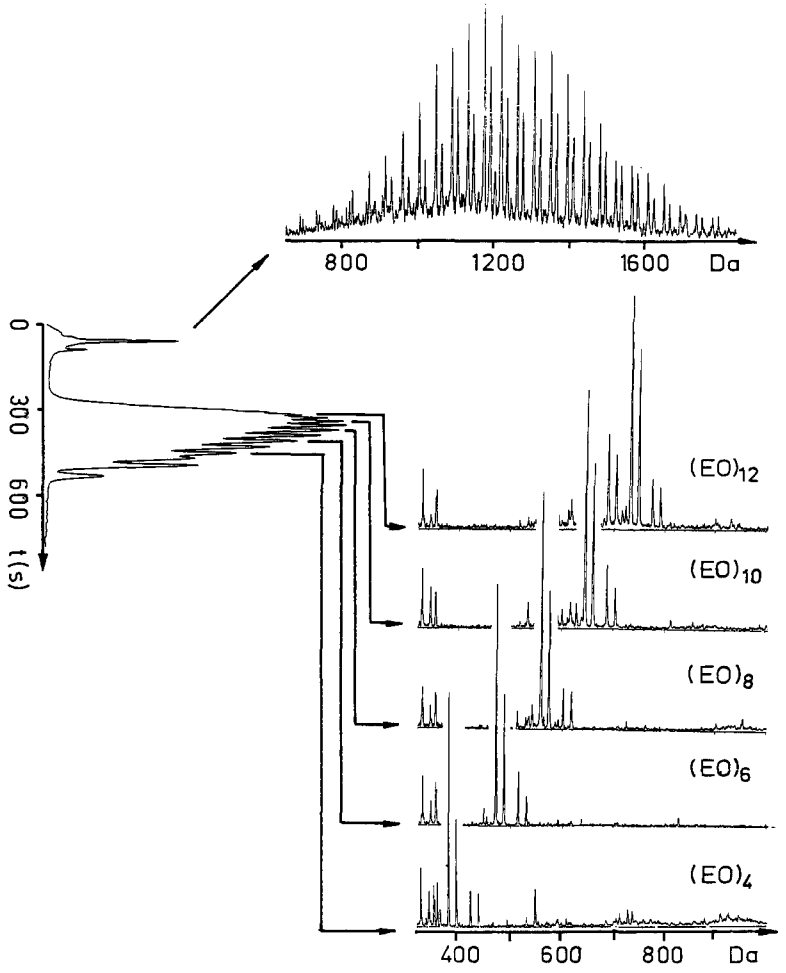

FIGURE 6 Identification of fractions of C_{12}-PEO by MALDI-MS, chromatogram taken from Fig. 5

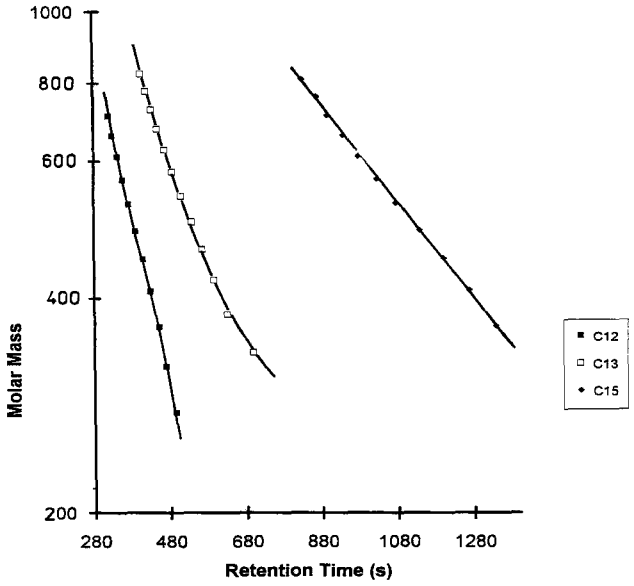

FIGURE 7 Calibration curves molar mass vs. retention time for the main functional fractions of C_{12}-PEO and C_{13},C_{15}-PEO, stationary phase and solvent: see Figure 5

reveal, that instead of one peak for each degree of polymerization, a number of overlapping peaks is obtained. This is a clear indication for the presence of isomeric structures, as was assumed from the HPLC behaviour. However, for the Octylphenol-PEO this behaviour is not obtained and, therefore, isomeric structures are not likely to be present in the sample.

As MALDI-MS separates exclusively with respect to mass per charge, isomerism does not interfer. Therfore, regardless of the isomeric endgroups the C_{10}-, C_{13}- and Nonylphenol-PEO's are separated with respect to their oligomer distribution and the molar mass can be calculated from the peak intensities, see Table 2.

The Octylphenol-PEO is investigated on a different column in order to obtain an oligomer separation. This is achieved on a preparative column Nucleosil RP-18, 250x20 mm I.D., using a solvent composition of acetonitrile-water 70:30 per

TABLE 2

Molar Masses and Polydispersities of the Polyethylene Oxides Determined by Modified SEC, MALDI-MS and SFC

Sample	SEC			MALDI-MS[1]			SFC[1]		
	M_n	M_w	U	M_n	M_w	U^2	M_n	M_w	U^2
C_{10}-PEO	----------			580	620	0.07	----------		
C_{12}-PEO	480	530	0.10	520	580	0.11	480	540	0.12
C_{13}-PEO	----------			690	740	0.07	----------		
C_{13},C_{15}-PEO									
C_{13}-fraction	550	610	0.11	580	620	0.07	540	590	0.09
C_{15}-fraction	480	520	0.08	570	620	0.09	----------		
Octylphenol-PEO									
	460	490	0.06	470	490	0.04	500	520	0.04
Nonylphenol-PEO									
	----------			630	660	0.05	----------		

[1] experimental details in [10]
[2] $U = M_w/M_n - 1$

volume, see Figure 8. Again, the different fractions are subjected to MALDI-MS and the molar mass is determined via a corresponding oligomer calibration curve. As can be seen, the first fraction, which elutes before the main functional fraction, consists of a number of oligomers. From the peak-to-peak mass increment of 44 Da it is clear, that these oligomers represent PEO's. However, the peak masses do not agree with the masses, obtained for Octylphenol-PEO oligomers. Instead, a mass of 131 Da is calculated for the endgroup. This mass agrees well with 133 Da calculated for a butylphenol endgroup and accordingly it is assumed, that the

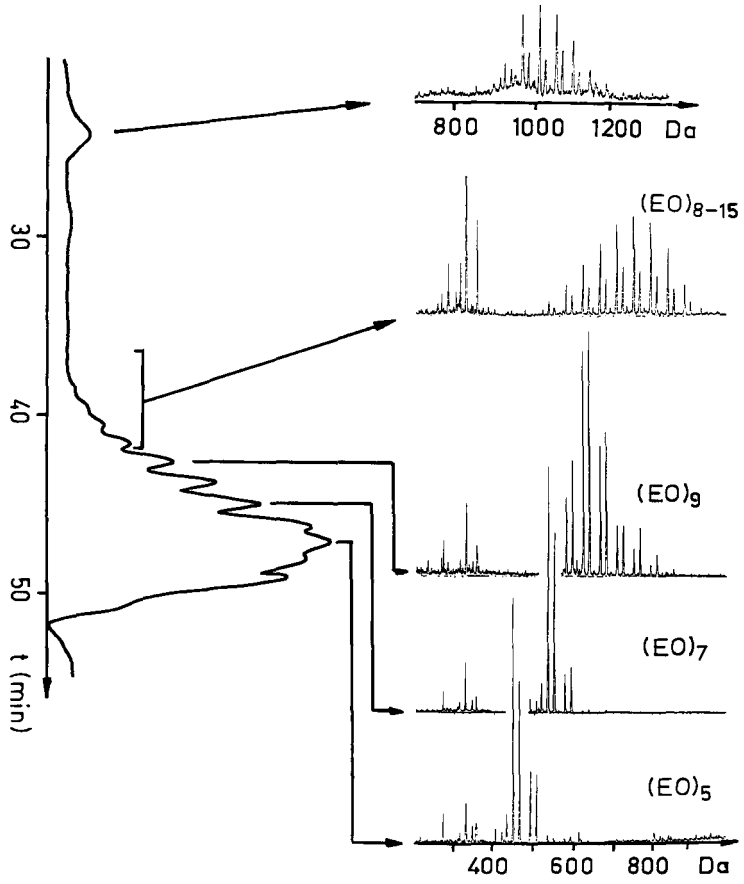

FIGURE 8 Chromatogram of Octylphenol-PEO and identification of fractions by MALDI-MS, stationary phase: Nucleosil RP-18, 250x20mm I.D., solvent: acetonitrile-water 70:30% by volume

starting octylphenol contained minor amounts of butylphenol. It is interesting, that the average molar mass of this fraction with M_n~1020 is distinctively higher than that of the main fraction.

Figure 5 shows, that in addition to the PEG and the main functional fraction, at higher retention times fractions are obtained, which may be visualized only using a very high UV detector sensitivity. These fractions, which are assumed to consist of α,ω-diaryloxy species, are separated as well. Unfortunately the amount of these fractions is too low for a proper characterization. Therefore, further efforts are necessary to accumulate enough material for analysis.

To summarize, liquid chromatography at the critical point of adsorption and modified SEC near the critical region have been shown to provide useful information on the functionality of alkyloxy and aryloxy polyethylene oxide. Using MALDI-MS as an additional detector, the molar mass distribution of the functional fractions may be determined. The average molar masses agree well with data, obtained independently by supercritical fluid chromatography and MALDI-MS alone.

Financial support from the Bundesminister für Wirtschaft through the Arbeitsgemeinschaft Industrieller Forschungsvereinigungen e.V. (AIF) is gratefully acknowledged (project No. 9287).

The authors are grateful to BASF, Ludwigshafen, for providing the polyethylene oxide samples.

REFERENCES

1. A.V. Gorshkov, H. Much, H. Becker, H. Pasch, V.V. Evreinov, S.G. Entelis, J. Chromatogr., 523: 91 (1990)

2. S.G. Entelis, V.V. Evreinov, A.V. Gorshkov, Adv. Polym. Sci., 76: 129 (1986)

3. B.G. Belenkii, E.S. Gankina, M.B. Tennikov, L.Z. Vilenchik, J. Chromatogr., 147: 99 (1978)

4. H. Pasch, H. Much, G. Schulz, A.V. Gorshkov, LC-GC International, 5: 38 (1992)

5. H. Pasch, H. Krüger, H. Much, U. Just, Polymer, 33: 3889 (1992)

6. H. Pasch, C. Brinkmann, H. Much, U. Just, J. Chromatogr., 623: 315 (1992)

7. M. Karas, F. Hillenkamp, Anal. Chem., 60: 2299 (1988)

8. R.C. Beavis, Rapid Commun. Mass Spectrom., 3: 233 (1989)

9. H. Pasch, R. Unvericht, Angew. Makromol. Chem., 212: 191 (1993)

10. H. Pasch, publication in preparation

Received: December 1, 1993
Accepted: December 27, 1993

JOURNAL OF LIQUID CHROMATOGRAPHY, 17(14&15), 3109-3132 (1994)

SEPARATION OF POLYETHYLENE GLYCOL OLIGOMERS ON NORMAL-PHASE AND REVERSED-PHASE MATERIALS BY GRADIENT HIGH PERFORMANCE LIQUID CHROMATOGRAPHY AND DETECTION BY EVAPORATIVE LIGHT SCATTERING. A COMPARATIVE STUDY

KLAUS RISSLER*, ULF FUCHSLUEGER, AND HANS JÖRG GRETHER

Polymers Division
CIBA-GEIGY Ltd.
K-401.2.08
CH-4002 Basel, Switzerland

Abstract

Separation of the polyethylene glycols PEG-200, PEG-300, PEG-600 and PEG-1000 by gradient high performance liquid chromatography is reported on a C_{18} as well as a Si 80 column in aqueous mixtures of acetonitrile, acetone and methanol as organic solvents. Detection was performed by means of evaporative light scattering. Further, the M_n and M_w values were determined by gel permeation chromatography and refractive index detection. Marked differences in the chromatographic behaviour occured between the two stationary phases with all three modifiers. Whereas PEG-200 and PEG-300 exhibited better peak resolution R_s on the C_{18} matrix, the inverse effect was observed with PEG-600 and PEG-1000, which reveal much better R_s on bare silica gel. Further, a dependence of the R_s of the PEG-600 and PEG-1000 samples (consisting of a substantially higher number of oligomers versus PEG-200 and PEG-300) from the organic modifier was seen, which increases in the range methanol < acetone < acetonitrile. A hypothetical view of the improved separation of

* Author for correspondence

PEG-600 and PEG-1000 oligomers is given on the basis of prevailing hydrophilic interactions between polar sites of polyethers and silanol groups of the stationary phase. Additionally a mechanistic hypothesis, which considers the superiority of acetonitrile and acetone versus methanol with respect to the R_s of oligomers is discussed by the assumption of different hydrogen bonding mediated solvent-stationary phase interactions implying a preponderance of adsorption (acetonitrile, acetone) versus partition chromatography (methanol).

Introduction

Polyethers of the polyethylene glycol (PEG) type as well as their derivatives (e.g. by substitution of one or both hydroxy groups by alkyl or aryl residues) have a broad application range in many different fields of chemistry. Among them important applications are the use as so-called non-ionic surfactants as well as emulsifiers for pharmaceuticals.

These facts suggest that elucidation of the molecular composition of polyethylene glycols will be of great scientific and industrial importance. For technical polymers knowledge of the homologous distribution is crucial because the products consist exclusively of oligomeric mixtures. This fact may essentially contribute to the physico-chemical properties of the products. Among chromatographic techniques used for characterisation, in general, gas chromatography (GC) is only applicable for separation of low molecular weight oligomers, whereas supercritical fluid chromatography (SFC) additionally includes measurement of medium sized samples. Although thin layer chromatography (TLC) has been frequently used for polyethylene glycol analysis and covers a wide molecular weight (M_r) range, peak resolution proves to be unsufficient in most cases. Gel permeation chromatography (GPC) covers the whole M_r range of polyethers because solute-matrix interactions can be neglected. Nevertheless satisfactory peak resolution is only achieved with low-molecular weight samples. Owing to the high number of mobile as well as stationary phases reversed-phase high performance liquid chromatography (RP-HPLC) is the preponderably used procedure for the separation of PEG oligomers. On the other hand chromatography has also been described on bare silica gel and so-called bonded phases, such as diol, aminopropyl and cyanopropyl matrices by use of non-aqueous ("normal-phase") solvents. Sufficient separation of the 3,5-dinitrobenzoyl derivatives of monoalkylated PEG oligomers on C_{18} and C_8 stationary phases (1) and of PEG dinitrobenzoyl derivatives on an ion-exchange matrix (2) was

reported. Isocratic elution of PEG mono- and dimethylethers as well as of the native samples on C_{18} materials has also been applied successfully (3,4). Similarly normal-phase partition chromatography of the native monoarylalkyl or monoalkyl substituted oligomers (5-7) on amino- and cyanopropyl bonded silica gel proved to be a reasonable alternative tool, whereas up to 40 oligomers were identified from ethoxylated octylphenol applying isocratic RP-HPLC on a C_1 matrix (8). Further, investigations of Alexander et al. (9) revealed that the R_s of PEG oligomers on C_{18} materials increased with decreasing carbon content, which may presumably be attributable to the influence of "polar sites" on the stationary phase surface. In a recent study we compared the chromatographic separation of different types of polyether with marked differences in polarity on different reversed-phase materials (10). In contrast to polybutylene glycol 1000 and polypropylene glycol 1200, which are well-resolved at least on C_{18} and C_8 stationary phases, unsufficient resolution was observed with PEG-1000. However, it should be remarked that in this case conditions of gradient HPLC had not been optimized for PEG 1000 due to the comparative purpose of the study requiring similar chromatographic conditions for all three types of polyether, which further markedly differ in polarity. For this reason we developed a more suitable chromatographic system for the separation of low-molecular weight PEG samples differing markedly in average molecular weight M_r. We applied gradient HPLC on both normal-phase and reversed-phase adsorbents by use of aqueous organic solvents prepared from different organic modifiers. Signal monitoring was performed by evaporative light scattering detection (ELSD). GPC coupled to refractive index detection (RI) was further carried out to evaluate the M_n, M_w and polydispersity index (M_w/M_n) values.

Materials

- Separation media:

For HPLC Spherisorb Si 80 bare silica (125 x 4.6 mm I.D., 5 μm particle size, 80 Å pore diameter) and Nucleosil $5C_{18}$ (125 x 4.6 mm I.D., 5 μm particle size, 100 Å pore diameter) were purchased from Metrohm-Bischoff (Wallisellen, Switzerland) and Macherey-Nagel (Oensingen, Switzerland), respectively. For GPC a series of four PLgel columns (each 300 x 7.5 mm I.D., 5 μm particle size) with pore diameters in

the range of 10^5 Å, 10^3 Å, 500 Å and 100 Å and a PLgel precolumn (50 x 7 mm I.D., 5 μm particle size, pore diameter 100 Å) for protection of the analytical columns were purchased from Polymer Labs. (Church Stretton, Shropshire, UK).

- Reagents and solvents:

Polyethylene glycol samples PEG-200[1)] PEG-300, PEG-600 and PEG-1000 ("pract." quality) were purchased from Fluka (Buchs, Switzerland). Narrow-range polystyrene molecular weight calibration standards for determination of M_n and M_w values were obtained from Polymer Labs. (Church Stretton, Shropshire, UK). Acetonitrile, methanol and acetone (all HPLC grade) were from Fluka. Water for the use in HPLC was purified with a Milli-Q reagent water system from Millipore-Waters (Milford, MA, USA). Tetrahydrofuran ("pro analysi") stabilised with 0.025 % of 2,6-di-tert. butyl phenol (Fluka) was used for GPC.

Methods

- Analytical equipment:

The HPLC apparatus consisted of a combined type SP 8100 system of HPLC pump and autosampler with a 10 μl sample loop, a PC 1000 data acquisition unit, all obtained from Spectra Physics (San Jose, CA, USA). For ELSD a type Sedex 45 apparatus from SEDERE (Vitry sur Seine, France) equipped with a 20 W iodine lamp was applied. For GPC a SP 8810 precision isocratic pump, a SP 8875 autosampler with a 100 μl sample loop, a SP 8430 refractive index detector, a SP 4270 integrator (all from Spectra Physics) and a column thermostat from Henggeler Analytic Instruments (Riehen, Switzerland) was used. A 2 micron filter (Rheodyne, Cotati, CA, USA) was inserted between pump and autosampler in order to avoid clogging of the columns by non-soluble solvent and sample impurities.

- Chromatographic separation:

Gradient system I (Table 1) was used for the separations on the C_{18} column, whereas gradient system II (Table 1) was applied for the Si 80 column. Separation

---

1) The numbers indicate the average molecular weight M_r as specified by the manufacturer.

Table 1: Gradient Systems I and II (Organic Solvents: Acetonitrile, Acetone, Methanol)

Gradient System	*Time (min.)*	*Organic Solvent (%)*	*Water (%)*
I	*0*	*0*	*100*
	40	*50*	*50*
	50	*50*	*50*
	51	*0*	*100*
	65	*0*	*100*
II	*0*	*10*	*90*
	40	*80*	*20*
	50	*80*	*20*
	51	*10*	*90*
	70	*10*	*90*

was performed at ambient temperature (ca. 22°C) at a flow-rate of 1.5 ml/min. PEG samples (2 %, w/v) were dissolved in methanol and 10 µl aliquots were injected. For detection by means of ELSD the nebulisation chamber was heated to 40°C and the nitrogen flow was adjusted to 4.5 l/min corresponding to an inlet pressure of 200 kPa. GPC was performed at a flow-rate of 1 ml/min and the column temperature was adjusted to 29°C. Aliquots of 100 µl of PEG samples (0.5 %, w/v) were injected and signals monitored at a range of 0.02 x 10^{-3} refractive index units full scale (RIUFS) measured against tetrahydrofuran in the reference cell.

- Calculation of M_n, M_w and M_w/M_n values:

This was performed on the basis of "low-molecular weight" calibration by use of 17 narrow range polystyrene calibration standards covering the M_r range from 104 D (styrene monomer) to 120'000 D (approx. n = 1150).

Results

We have investigated the separation of the low M_r polyethylene glycols PEG-200, PEG-300, PEG-600 and PEG-1000 on both bare silica gel (Si 80) and octadecylsilyl silica gel stationary phases (C_{18}) in aqueous organic solvents with acetonitrile, acetone and methanol as organic modifiers. All tested samples clearly reveal their oligomeric composition and marked differences in the chromatographic behaviour of the samples occurred on the two different stationary phases. The common feature on both sorbents is that the capacity factor values k' for the individual polyether samples show a marked dependence on the type of organic solvent and increase in the range methanol > acetonitrile > acetone. From the chromatographic patterns it is evident that the peak resolution R_s[2)] of PEG-200 and PEG-300 (Figs. 1-3a,b) on octadecylsilyl silica gel is better than that of PEG-600 and PEG-1000 (Figs. 1-3c,d). In contrast, on bare silica gel the R_s of PEG-600 and PEG-1000 oligomers increases substantially in comparison to the reversed-phase material (Figs. 4-6c,d), whereas the R_s of PEG-200 and PEG-300 decreases on this stationary phase (Figs. 4-6a,b). The R_s of PEG-600 and PEG-1000 on the Si 80 column reveals a dependence on the type of organic modifier and increases in the range methanol < acetone < acetonitrile. The protic solvent shows either decreased R_s values for PEG-600 and PEG-1000 or selectivity with respect to the separation of the whole series of tested low M_r PEGs. This means that a better distinction between the different types of polyether in mixtures is achieved with both aprotic modifiers as can be concluded from a superposition of the individual chromatographic patterns. Almost complete base-line separation of the whole quantity of PEG-1000 oligomers is achieved on a silica column with acetonitrile as organic modifier (Fig. 4d). It should be remarked that the R_s for the different oligomers of PEG-1000 on reversed-phases other than C_{18} decreases gradually in the range $C_8 > C_4 > C_{Phenyl} > C_1$ and the peak width of the poorly resolved peak, which covers the whole entity of oligomers becomes more and more diffuse (10). When compared with the elution using acetonitrile and acetone as modifier, differences in the chromatographic patterns of PEGs between bare silica and octadecylsilyl silica gel are less pronounced with

---

2) $R_s = (t_2-t_1)/w_2-w_1)$, where t_1 and t_2 are the retention times of two adjacent peaks and w_1 and w_2 their base-widths.

methanol (Figs. 3a-d, 6a-d). Within the group of investigated PEG oligomers the R_s decreases on both kinds of columns in the series PEG-200 ≅ PEG-300 > PEG-600 > PEG-1000 and the effect is stronger on the reversed-phase material. This general phenomenon can be satisfactorily explained by the higher relative mass difference of individual oligomers of PEG-200 and PEG-300 versus PEG-600 and PEG-1000. This means that in the case of both low M_r samples an increase of the number of repeating units n is associated with a more substantial relative increase of the sample surface and, as a consequence, by higher solute-matrix interactions. It should be remarked that the capacity factor of PEG-200 and PEG-300 is very low on bare silica gel and a decrease in the initial elution strength would surely effect a better resolution. However, the principal goal of this study was to improve separation of the two "high" M_r samples PEG-600 and PEG-1000.

The lack of a normally expected "Gaussian-like" distribution in particular of PEG-200 and partially of PEG-300 oligomers can presumably be ascribed to the high volatility of the low M_r members, which do not yield a response by ELSD. In these cases derivatisation with e.g. 3,5-dinitrobenzoyl chloride and UV detection would provide a more convenient means for signal monitoring. The first peak in PEG 200 seen in some chromatogrammes may be caused by the "residual" ELSD response of a low M_r homologue, which, due its high volatility will not reflect its true amount.

When compared with HPLC a marked lower separation efficiency of the four PEGs is observed by GPC. In our GPC system only PEG-200 and PEG-300 reveal at least partial peak resolution, whereas the PEG-600 and PEG-1000 samples elute as broad and unresolved peaks (results not shown). The values for the polydispersity index M_w/M_n are nearly identical for all four samples ranging from 1.05 to 1.095 (Table 2). Although the M_n and M_w values were determined with polystyrene calibration standards, which may not be an optimum means for an estimation of M_r on the basis of their hydrodynamic volumes, a relatively good agreement between the "true" M_r values of the PEG samples and those measured by GPC was obtained (Table 2).

Discussion

Based on our experience described recently (10), we applied gradient HPLC with a linear solvent strength (LSS) system and signal monitoring by ELSD, which has

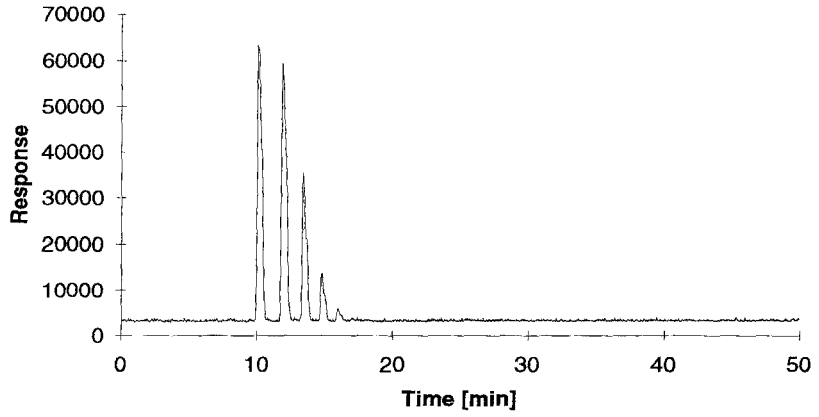

Figure 1a

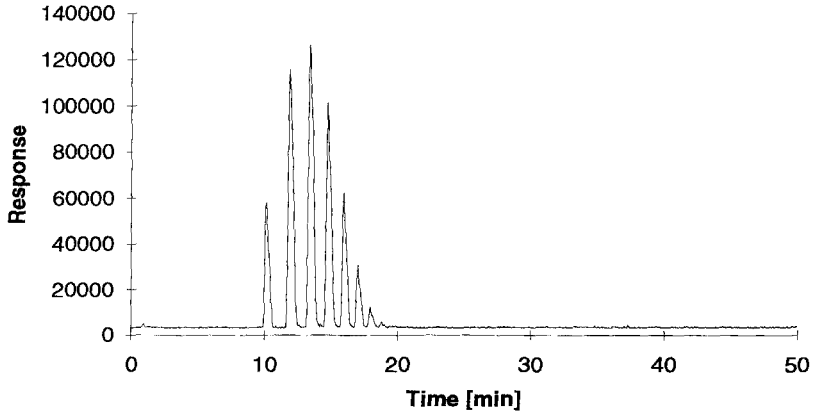

Figure 1b

Figures 1a-d: HPLC-chromatogrammes of a) PEG 200 b) PEG 300 c) PEG 600 d) PEG 1000 on a C_{18} column with acetonitrile as organic modifier

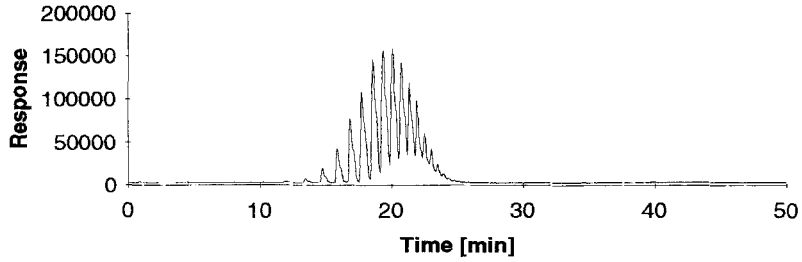

Figure 1c

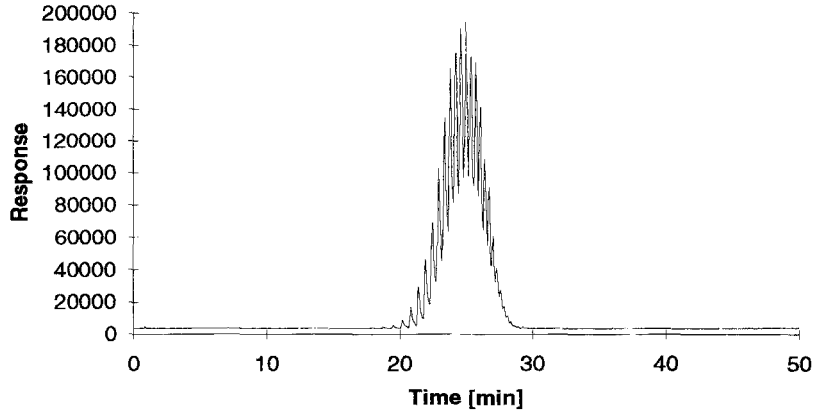

Figure 1d

been earlier reported for the measurement of signal responses of PEGs. This technique allows the additional use of acetone as organic solvent, which cannot be applied in UV detection due to its vast self-absorption. Further, detection by UV is inferior to ELSD in particular for gradient HPLC even at wavelengths < 200 nm owing to substantial baseline deterioration. Nevertheless several authors have described addition of trace amounts (5 ppm) of nitric acid (11) or sodium azide (12) to the aqueous phase to compensate for the baseline drift invoked by the gradual increase

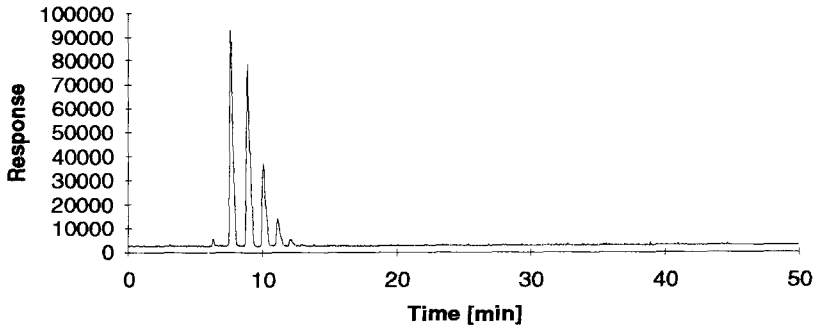

Figure 2a

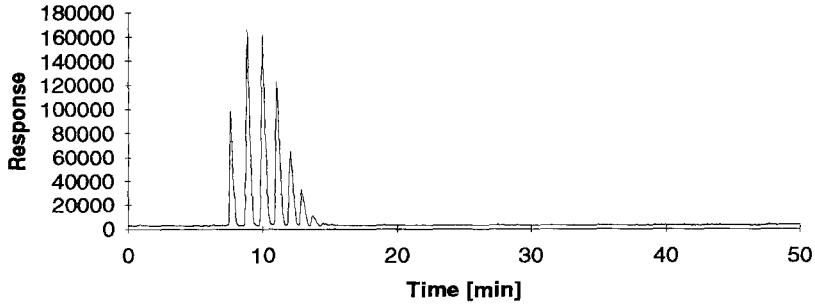

Figure 2b

Figures 2a-d: HPLC-chromatogrammes of a) PEG 200 b) PEG 300 c) PEG 600 d) PEG 1000 on a C_{18} column with acetone as organic modifier

of the concentration of organic modifier. On the other hand pre-chromatographic tagging of the α,ω- dihydroxy groups by a chromophoric agent (1,10,13) would make the polyethers amenable to the detection at the usual wavelength range. However, as shown recently (10), derivatisation of free hydroxy groups of polyethylene glycols with 3,5-dinitrobenzoyl chloride rather decreases the R_s of oligomers and thus contrasts with the results of Desbène et al. (1). Detection of PEG and its alkylated or arylated

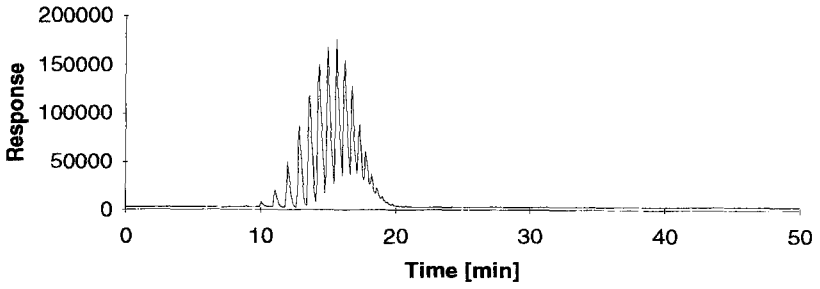

Figure 2c

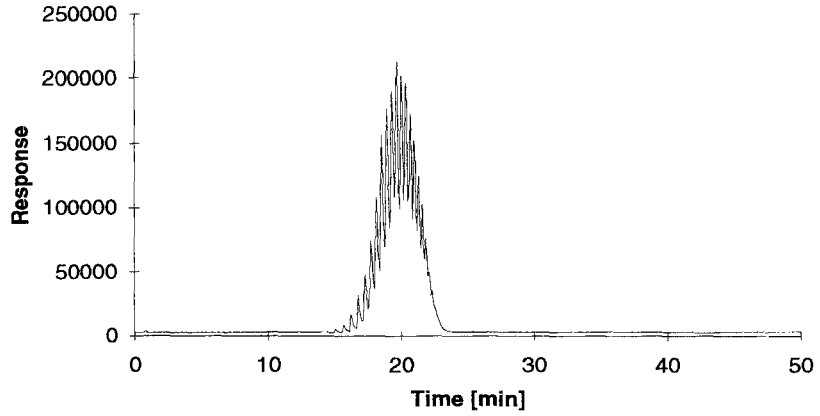

Figure 2d

derivatives by refractive index measurement is restricted to isocratic LC. Although isocratic reversed-phase HPLC yields excellent separation of low to medium M_r oligomers, the higher M_r sample constituents eluting at higher t_R values exhibit marked peak-tailing as seen from the investigations of Trathnigg et al. (3,4). Further, quantitative elution of PEG samples with M_r > 1000 will be difficultly to achieve in the isocratic mode. Thus the gradient technique promises to be the method of choice in particular for samples showing a broad M_r distribution of oligomers.

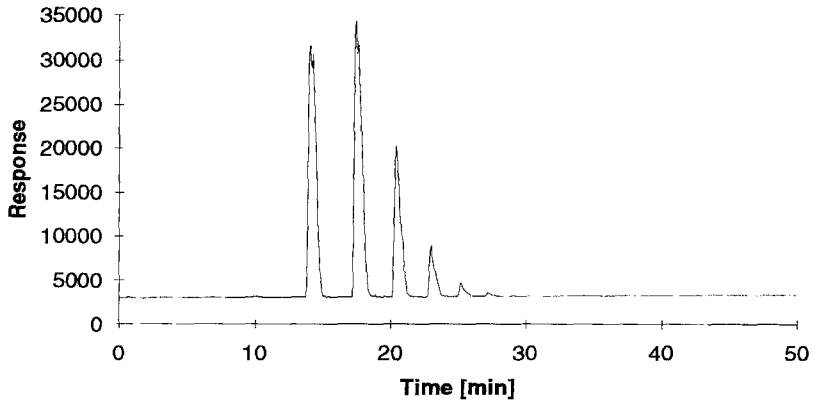

Figure 3a

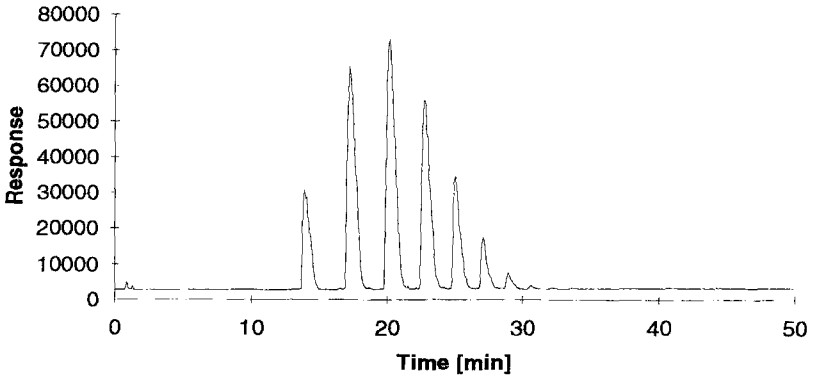

Figure 3b

Figures 3a-d: HPLC-chromatogrammes of a) PEG 200 b) PEG 300 c) PEG 600 d) PEG 1000 on a C_{18} column with methanol as organic modifier

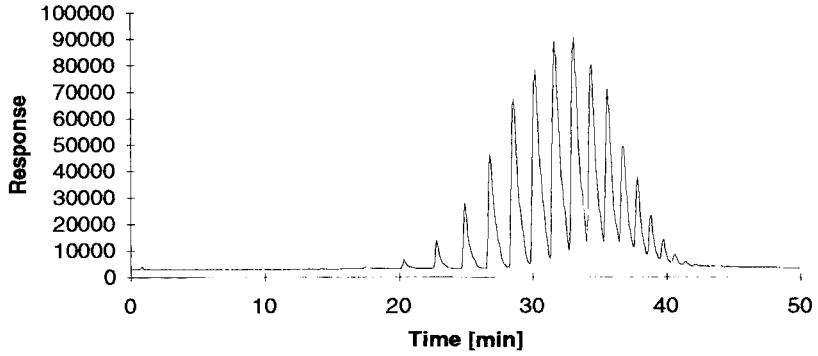

Figure 3c

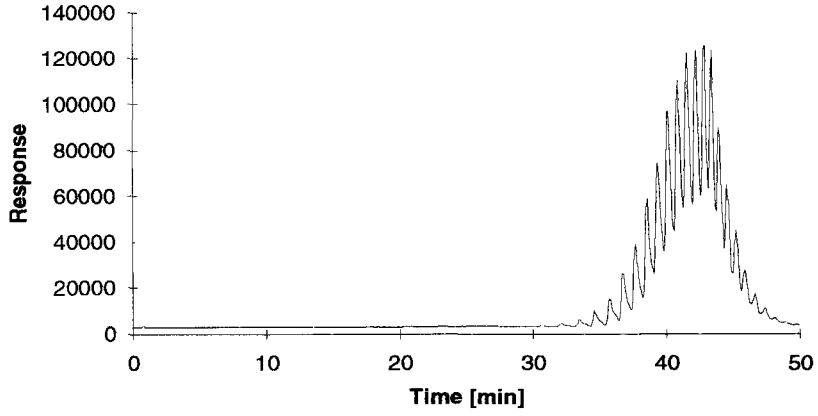

Figure 3d

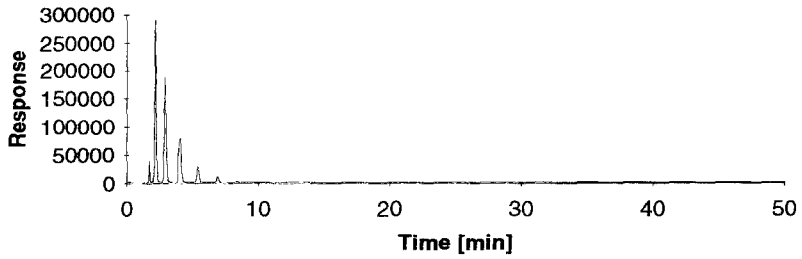

Figure 4a

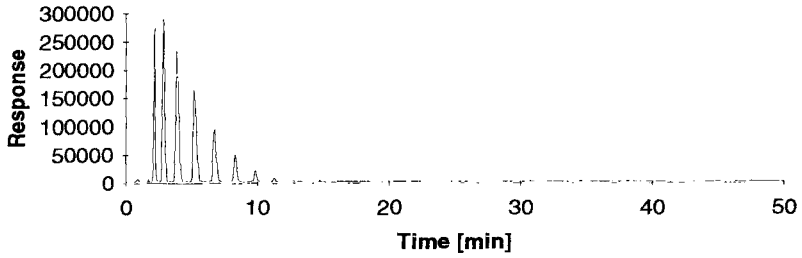

Figure 4b

Figures 4a-d: HPLC-chromatogrammes of a) PEG 200 b) PEG 300 c) PEG 600 d) PEG 1000 on a Si 80 column with acetonitrile as organic modifier

Our aim in searching for a new powerful technique of an efficient separation of low M_r polyethylene glycols has been stimulated by the investigations of Alexander et al. (9). The authors observed a dependence of the R_s of PEGs on the extent of silica gel matrix coverage by octadecylsilyl groups and found that the lower the "saturation" of silanol groups by alkyl residues the better the peak resolution. Indeed chromatography of PEG-1000 on C_{18} matrices, which have been used for a high number of injections revealed substantial improvement of oligomer separation with respect to a new one (results not shown). This may be attributable to a "column ageing-invoked" depletion of marked amounts of octadecylsilyl substituents from the

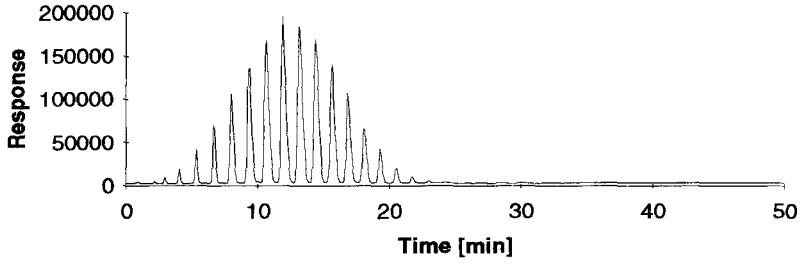

Figure 4c

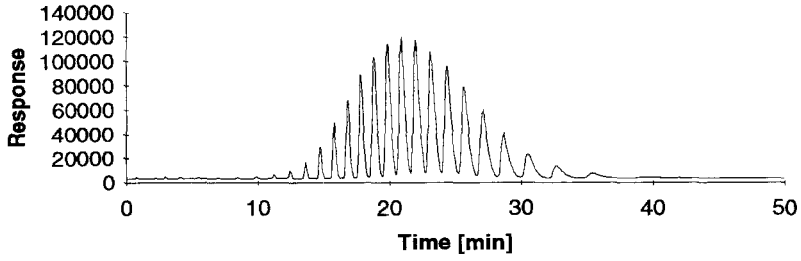

Figure 4d

silica backbone. Starting from this observation we assumed that a more extended or even complete "dissociation" of octadecylsilyl substituents from the RP matrix should further increase the R_s of PEG-1000 oligomers. However, aqueous organic solvents are rarely used for the separation on "normal-phase" materials, which may primarily be attributed to the relatively long equilibration times postulated after changes of the solvent composition, as is the case particularly in gradient chromatography. For this reason "normal-phase sorbent - reversed-phase solvent" chromatography is usually restricted to isocratic LC and the LSS gradient technique would normally be associated with poor chromatographic performance due to an expected slow adjustment of the sorption-desorption equilibrium during sample elution. On the other hand it is known that even small amounts of water in organic mobile phases are able to deactivate the stationary phase surface and thus increase the rate of adjustment of

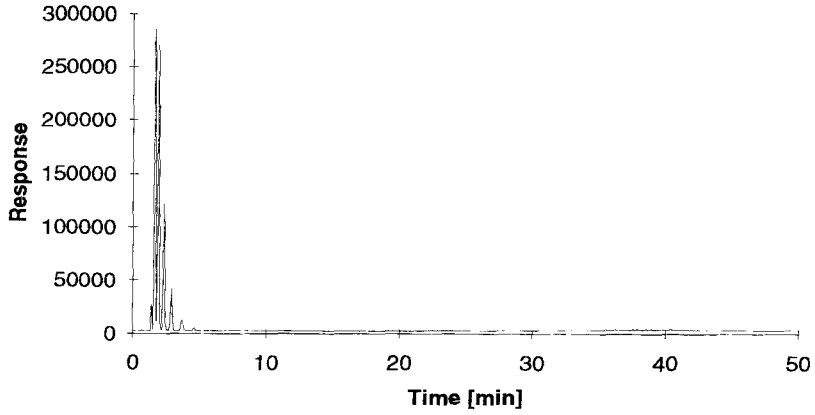

Figure 5a

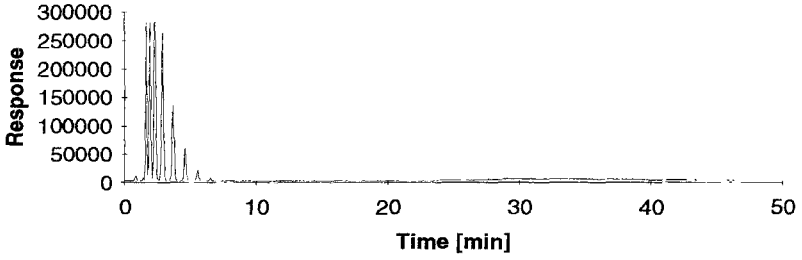

Figure 5b

Figures 5a-d: HPLC-chromatogrammes of a) PEG 200 b) PEG 300 c) PEG 600 d) PEG 1000 on a Si 80 column with acetone as organic modifier

the sorption-desorption equilibrium (14,15). Nevertheless extended reequilibration times should be expected, which would render the HPLC analysis unattractive within an adequate time range at least when LSS gradient HPLC is used. Surprisingly we did not encounter any of these problems and even reestablishment of initial gradient conditions within 1 min (e.g. from 90 % to 10 % of organic modifier) followed by reequilibration for 19 min proved to be sufficient and neither significant changes in t_R

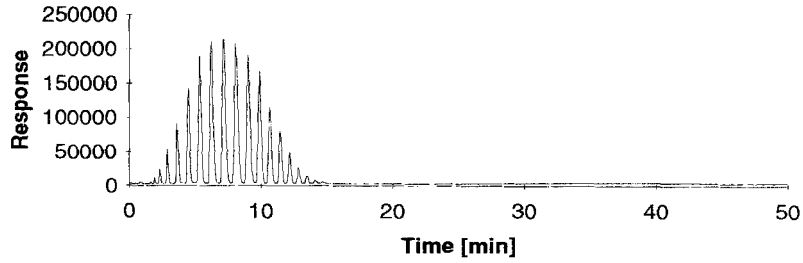

Figure 5c

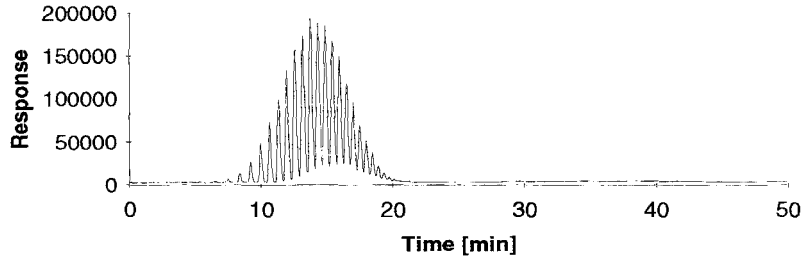

Figure 5d

values nor base-line deterioration and peak distortion were observed after a multitude of injections of the same sample. The successful use of bare silica gel in LSS gradient RP-HPLC may be astonishing at first sight. However, it must be taken into account that according to Horvath et al. (16,17) reversed-phase chromatography can also be achieved on "naked" silica by use of excessive water in the mobile phase due to its extensive silanol-coating effect. The marked increase in band broadening of PEG-1000 oligomers at higher t_R values in particular by use of methanol and acetonitrile may thus be in accordance with their hypothesis of a typical reversed-phase behaviour of "naked" silica at higher concentrations of water. It may be explained by the continuous replacement of water by organic solvent during gradient elution, which in turn, may lead to a decrease in silanol-coating efficiency. Thus the "normal" chromatographic behaviour of acetone (i.e. negligible band broadening of

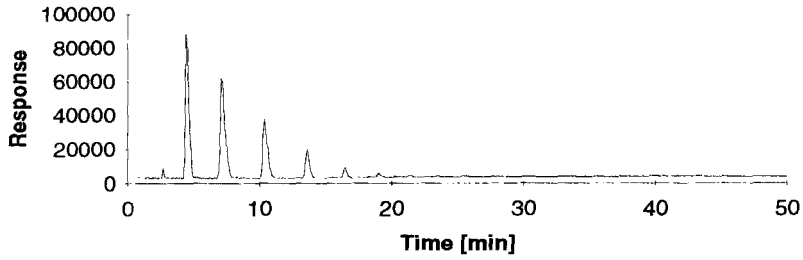

Figure 6a

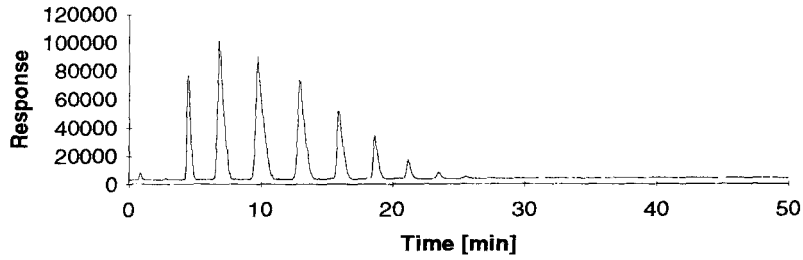

Figure 6b

Figures 6a-d: HPLC-chromatogrammes of a) PEG 200 b) PEG 300 c) PEG 600 d) PEG 1000 on a Si 80 column with methanol as organic modifier

later eluting homologues) may be attributed to elution of the whole amount of oligomers at a water content already being sufficient to mask the silanol groups. It is worthy to note that isocratic separation of basic drugs was also performed on bare silica gel with "reversed-phase" eluents. In these cases solute-matrix interactions were suppressed by addition of ammonia to the mobile phase and the excellent separation characteristics observed were ascribed to a combination of adsorption and ion-exchange.

Whereas separation improvement of PEG-200 and PEG-300 on a Si 80 column should approximate to the similar pattern obtained with the C_{18} matrix by use of a more shallow gradient starting with e.g. 0 % of organic modifier, substantial

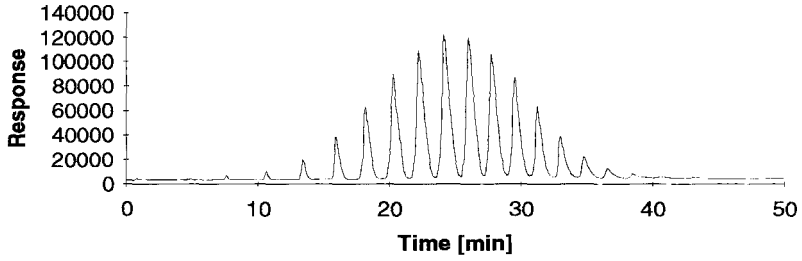

Figure 6c

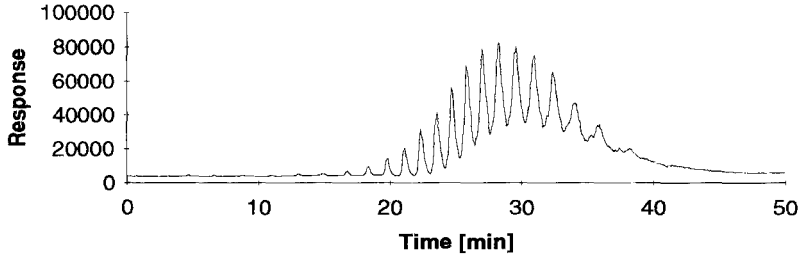

Figure 6d

refinement of peak resolution of PEG-600 and particularly of PEG-1000 on a C_{18} column, as compared with bare silica, could be achieved with difficulty. Therefore we have concentrated on a possible hypothesis of the excellent separation of PEG-600 and PEG-1000 oligomers on silica gel adsorbents with acetonitrile and acetone as the organic modifier. The observations of Alexander et al. (9) imply that the separation characteristics are essentially governed by the polar superficial layer of free matrix silanols rather than by interactions with ether-like oxygens of the polysiloxane backbone, which in turn, may be responsible for distinct "modulating" effects during the separation process. This view is further corroborated by the observation that a better accessibility of solute molecules to polysiloxane oxygens as it should be the case with the "short-chain" substituted silica gels, such as C_8, C_4, C_{Phenyl} and C_1 matrices did not result in improvement of the R_s of PEG-1000 oligomers (10).

Table 2: M_n , M_w and Polydispersity Index (M_w/M_n) Values of Polyethylene Glycol Samples

	PEG 200	*PEG 300*	*PEG 600*	*PEG 1000*
M_n	*244*	*326*	*673*	*1205*
M_w	*265*	*357*	*724*	*1265*
M_w/M_n	*1.086*	*1.095*	*1.075*	*1.050*

Further, the R_S seems to be preponderably influenced by interactions between the polyether backbone of the PEGs and the hydrophilic stationary phase and only to a small extent by those between the silica matrix and the hydroxy endgroups of the solute. This is supported by an almost identical chromatographic pattern after conversion of the PEGs to their diacetates (results not shown).

The marked delay of oligomer elution with methanol as organic modifier versus acetone and acetonitrile may be attributed to a partial sorbent-invoked demixing of methanol from the aqueous organic phase. Effects like these, presumably due to strong adsorption of the more polar component of binary mixtures of pure organic solvents to the hydrophilic silica gel matrix are well-known in liquid solid chromatography (LSC) and are often responsible for vast discrepancies from the theoretically calculated t_R values (18). Thus in order to explain the increased retention with methanol both a delay in gradient onset and/or a more shallow gradient profile of organic solvent concentration at the start of sample elution (18) should be considered. On the one hand "selective retention" of methanol on the polar sorbent would be facilitated by very tight hydrogen bonding to either silanol groups or ether-like oxygens of the polysiloxane backbone. On the other hand "extraction" of water should be favoured due to its excess at the gradient starting conditions as well as by the assumption of a better compatibility in polarity towards the stationary phase compared with methanol. However, the marked hydrophobic properties of the siloxane backbone (19,20) should also be taken into consideration, which in turn, imply a preferable interaction with the organic solvent component. Substantially lower

k'- values of PEG 1000 are observed with ethanol and isopropanol as organic modifiers, although it might be expected that their lower polarities with respect to methanol would yield an increase in retention at least on bare silica (results not shown). This observation would thus be in accordance with a preferable "extraction" of methanol and may be ascribed to a lower actual concentration in the mobile phase as calculated from the gradient profile at the start of chromatographic separation. Acetonitrile as well as acetone are also able to undergo hydrogen bonding at least with silanol groups, which implies a "fine-tuning" effect of both modifiers on separation characteristics.

In order to attempt an explanation of the marked separation improvement on bare silica gel with the aprotic modifiers acetonitrile and acetone compared with methanol we have developed a possible mechanistic hypothesis, which will be discussed briefly. As already mentioned above the polar solvents are able to mask residual silanol groups in reversed-phase materials and according to Horvàth et al. (16,17) this effect is stronger with methanol than with acetonitrile. Whereas methanol is a proton acceptor, i.e. in terms of Pearson's classification (21,22) a hard base, acetonitrile and acetone are weak dipolar bases. Methanol exhibits hydrogen bonding by interactions of either its free pair of electrons on the oxygen with silanol protons or by the inverse interaction between its hydroxy proton with free pairs of electrons on the ether-like siloxane oxygens. These synergistic effects may lead to a strong attachment of methanol molecules to the silica gel surface. Thus possible "localisation" of methanol on the silica surface will favour partition of the solute between this dense surface layer and the neighbouring solute transporting aqueous methanolic layer in a corresponding way as stated for normal bonded phase liquid chromatography (NBP-LC) on aminopropyl silica gel (23). Owing to their lack of exchangeable ("acidic") protons, which will cause a less marked coverage of surface silanols, acetonitrile as well as acetone are only able to undergo hydrogen bonding with silanol groups and adsorption chromatography may prevail in this case. A simplified presentation of the hypothetic solvent-stationary phase hydrogen bonding sites is given in Figure 7.

It should be stated that effects quite different from the afore-mentioned may also be of importance. This would include a differential "solvation" of polyether samples in the mobile phase by hydrogen bonding between the hydroxy protons of methanol and

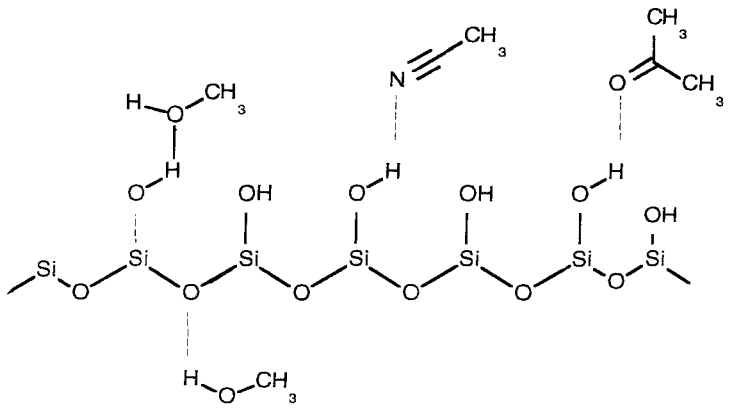

Figure 7: *Simplified model of possible interactions between organic solvent, silanol groups and polysiloxane oxygens at the surface of bare silica gel stationary phases*

ether oxygens of the solute, which is not achievable with the aprotic solvents and thus additionally may "superimpose" solute-matrix interactions. Further, a continuous transition from a "reversed-phase-like" behaviour to "normal-phase" (adsorption) chromatography owing to the gradual replacement of water by organic solvent during gradient elution may also be operating. Nevertheless at the moment the hypothesis discussed above may represent a reasonable preliminary attempt to explain the separation improvement of PEG 600 and PEG-1000 with the change from a reversed-phase to a normal-phase matrix.

Conclusions

To our knowledge, gradient HPLC of polyethylene glycol samples with aqueous organic solvents typically used in classical RP-HPLC on bare silica gel has not previously been reported. The feasibility of the method with respect to its analytical power has been demonstrated and thus offers an attractive alternative way to the generally used reversed-phase materials. From the investigations it is evident that the

higher the number of oligomers within a PEG sample the better the peak resolution compared with reversed-phase matrices. The main advantage of the silica stationary phase over its octadecylsilyl derivative consists of its higher selectivity with respect to an assigment of the resulting chromatographic patterns to individual PEG samples, which will be of great technical importance due to "recognition" of the type of PEG within mixtures. In contrast to the findings with bare silica the more pronounced overlap of peaks from different samples by use of reversed-phase separation media would make a selective attribution more difficult. Improvement of chromatographic performance on bare silica may presumably be attributed to specific interactions between polar sites on the polyethers and the vast amount of silanol groups on the stationary phase surface. Owing to the high water content at the start of gradient elution a "reversed-phase like behaviour" of the silica gel can additionally be postulated, which is also in agreement with the marked hydrophobic properties of the polysiloxane backbone, whereas, at higher concentrations of organic solvent adsorption may prevail. Taken together the improved separation characteristics of polyethylene glycols on "naked" silica opens up an efficient tool for characterising the oligomeric distribution of polar polyethers.

References

1) *P. L. Desbène, B. Desmazières, J. J. Basselier, A. Desbène-Monvernay, J. Chromatogr., 461: 305- 313 (1989)*
2) *T. Okada, J. Chromatogr., 609: 213-218 (1992)*
3) *B. Trathnigg, D. Thamer, X. Yan, S. Kinugasa, J. Liq. Chromatogr., 16: 2453-2467 (1993)*
4) *B. Trathnigg, D. Thamer, X. Yan, S. Kinugasa, J. Liq. Chromatogr., 16: 2439-2452 (1993)*
5) *F. P. B. van der Maeden, M. E. F. Biemond, P. C. G. M. Janssen, J. Chromatogr., 149: 539-552 (1978)*
6) *A. M. Rothmann, J. Chromatogr., 253: 283-288 (1982)*
7) *F. Bogatski, H. Lippmann, Acta Polymerica, 34: 219- 223 (1983)*
8) *Z. Wang, M. Fingas, J. Chromatogr., 673: 145-156 (1993)*
9) *J. N. Alexander, M. E. McNally, L. B. Rogers, J. Chromatogr., 318: 289-298 (1985)*
10) *K. Rissler, H.-P. Künzi, H.-J. Grether, J. Chromatogr., 635: 89- 101 (1993)*
11) *S. van der Val, L. R. Snyder, J. Chromatogr., 255: 463-474 (1983)*
12) *G. Barka, P. Hoffmann, J. Chromatogr., 389: 273-278 (1987)*
13) *A. Nozawa, T. Ohnuma, J. Chromatogr., 187: 261-263 (1980)*

14) T. Okhuma, S. Hara, J. Chromatogr., 400: 47-63 (1987)
15) J. J. Kirkland, C. H. Dilks Jr., J. J. De Stephano, J. Chromatogr., 635: 19-30 (1993)
16) A. Nahum, Cs. Horvàth, J. Chromatogr., 203: 53-63 (1981)
17) K. E. Bij, Cs. Horvàth, W. R. Melander, A. Nahum, J. Chromatogr., 203: 65-84 (1981)
18) M. A. Quarry, R. L. Grob, L. R. Snyder, J. Chromatogr., 285: 19-51 (1984)
19) R. K. Iler, The Chemistry of Silica, John Wiley & Sons, Inc., New York, 1978
20) K. Unger, Porous Silica, Elsevier Publishers, Amsterdam, 1979
21) M. T. W. Hearn, B. Grego, J. Chromatogr., 218: 497- 507 (1981)
22) R. G. Pearson, J. Songstad, J. Amer. Chem Soc., 89: 1827-1836 (1967)
23) C. W. Hsu, W. T. Cooper, J. Chromatogr., 603: 63- 71 (1992)

Received: October 18, 1993
Accepted: December 1, 1993

JOURNAL OF LIQUID CHROMATOGRAPHY, 17(14&15), 3133-3143 (1994)

CRITICAL RETENTION BEHAVIOR OF HOMOPOLYMERS

PAUL J. C. H. COOLS[1], ALEX M. VAN HERK[1], ANTON L. GERMAN[1]*, AND WIM STAAL[2]

[1]Laboratory of Polymer Chemistry
Eindhoven University of Technology
P.O. Box 513, 5600 MB Eindhoven
The Netherlands

[2]Millipore, Waters Chromatography Division
P.O. Box 166, 4870 AD Etten-Leur
The Netherlands

ABSTRACT

The isocratic retention behaviour of a homopolymer at a specific temperature and varying solvent compositions can be divided into three modes: exclusion mode, transition mode (critical conditions) and adsorption mode. Under critical conditions (a specific non-solvent/solvent composition at a specific temperature) the retention of a homopolymer is independent of the molar mass. The critical conditions depend upon the temperature, the type of polymer and the type of non-solvent/solvent mixture. A difference in the critical conditions between polystyrene standards and polybutadiene standards was found. No significant influence of different types of column packing on the critical solvent composition was noticed. The exact mechanism of the retention of a polymer under critical condition is not clear yet.

In order to determine the critical conditions, a new method has been developed. The method can be easily performed on existing equipment. The method contains a different setup of the data acquired by isocratic HPLC than methods described in literature. Therefore, less experiments need to be performed to determine the critical conditions compared to the current method. The newly developed method is more efficient than the methods described in the literature.

*Author to whom correspondence should be sent.

INTRODUCTION

The interest in the separation of polymers by liquid chromatography has grown during the last decade. New high performance liquid chromatography (HPLC) methods have been developed to characterize polymers.

In order to obtain the chemical composition of a polymer the HPLC method gradient polymer elution chromatography (GPEC®) can be used. Methods resembling GPEC® have been described in literature as high performance precipitation liquid chromatography HPPLC [1] or liquid adsorption chromatography [2]. The separation of polymers by GPEC® is based on the differences in solubility of polymers. The molar mass distribution (MMD) of a polymer can be determined by the isocratic HPLC method size exclusion chromatography (SEC).

The isocratic retention behaviour of a homopolymer can be divided into three different modes: an exclusion mode, a transition mode and an adsorption mode. The isocratic retention behaviour of a homopolymer depends on the solvent conditions at a specific temperature. By changing the non-solvent/solvent composition at a constant temperature the three retention modes can be observed.

In the exclusion mode a strong solvent is used. Therefore no interaction between the column packing and the polymer occurs. The polymer molecules move through the column and are excluded from the pores of the column packing. As can be seen in figure 1(A), the retention increases with decreasing molar mass of the polymer molecules.

By increasing the volume percentage of non-solvent (vol% NS) at a specific temperature the solvent strength decreases. The retention mode changes from exclusion mode to the adsorption mode. At high %NS the

GPEC® is a registered trademark of Millipore, Waters Chromatography Division

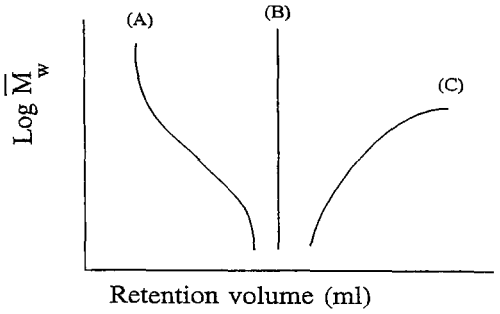

FIGURE 1

Plot of log $\overline{M}_w$ Versus Retention Volume (ml) at Different Vol% NS; (A) %NS < CSC, (B) %NS is CSC and (C) %NS > CSC.

solvent strength is so low that interaction between the column packing and the polymer molecules occurs. As a result the sequence of retention in adsorption mode is proportional to the increase of the molar mass of the polymer molecules (see figure 1(C).

In between the two modes a transition mode exists. If the polymers differ in molar mass but not in chemical structure a non-solvent/solvent composition is reached at which the polymer molecules elute simultaneously. The combination of the non-solvent/solvent composition and the particular temperature is called the critical conditions [3] and the composition is referred to as the critical solvent composition (CSC).

The CSC depends upon the temperature, the non-solvent/solvent mixture and the type of polymer. At the CSC, the separation is independent of the molar mass of the polymer molecules (see figure 1(B)).

Gorshkov *et al.* [3-7] have studied the critical retention behaviour and the influence of the temperature on the critical conditions of a solvent/column system. The same authors have also described the three isocratic retention modes in thermodynamic terms.

The isocratic HPLC method performed at the critical conditions is called critical polymer chromatography (CPC). Polymers which only differ in functionality or end-groups can be separated by CPC [3-7]. Additionally, polymers which differ in topology (*e.g.* grafted, linear) can be separated under critical conditions [8,9].

A method to determine the critical solvent conditions at a specific temperature is described by Gorshkov *et al.* [3-7]. Many experiments are necessary to obtain the critical conditions of a specific system (column, solvents, polymer). The retention volume of polymer standards at different non-solvent/solvent compositions at a constant temperature are obtained. The molar mass of each polymer standard is plotted versus the retention volume of the polymer standards at a certain non-solvent composition. The curves of the molar mass of the polymer versus the retention volume at different non-solvent/solvent compositions can be plotted in one figure (see figure 1). Under critical conditions the retention volume is independent of the molar mass. Therefore, the slope of the critical curve becomes infinite.

In order to determine the critical conditions using the method according to Gorshkov *et al.* [3-7], many experiments are needed and therefore the method is time consuming. In order to reduce the time and number of experiments a new simple method of determining the critical conditions will be introduced.

EXPERIMENTAL

Materials

Equipment : the equipment consisted of a Waters 600E gradient controller and pump, a Waters U6K variable loop injector and a column oven.

Two detectors were used: the Waters 484 variable wavelength ultra violet absorbance (UV) detector (254 nm) and the ACS 750/14 mass detector. The mass detector is an evaporative light-scattering detector [10] and was used to detect polybutadiene (polybutadiene has no significant UV absorbance). The eluent flow was established at 0.5 ml/min.

Columns : the used columns were Deltapak C18 100 Å (pore size= 100 Å, d_p= 5 μm, 3.9x150 mm, Waters Part No. 11795), Deltapak C18 300 Å (pore size= 300 Å, d_p= 5 μm, 3.9x150 mm, Waters Part No. 11793), Novapak C18 (pore size= 60 Å, d_p= 4 μm, 3.9x300 mm, Waters Part No. 11695), μStyragel HT (pore size= linear, d_p= 10 μm, 7.8x300 mm, Waters Part No. 3554). The column temperature was (in all experiments) 30°C.

Solvents : the used solvents were tetrahydrofurane (THF) Westburg HPLC grade (not stabilized) and water of the Milli-Q water system of Millipore. During the experiments Helium was sparging the solvents.

Polymer samples : the polymers used in the experiments were polystyrene standards of TSK ($\overline{M}_w$: 500, 3000, 5600 and 9100 g/mol). The polybutadiene standards are from Polymer Labs ($\overline{M}_w$: 900, 3000, 8000 and 9300 g/mol). It is important that the standards used for each experiment have the same functionalities, because under critical conditions the adsorption of the functional group effects the retention. In order to guarantee the same end-group of each standard type the standards used for one experiment had to be of the same company. The concentration of the polymer solutions in THF was 0.1% (g/l). The injected volume of the sample was 25 μl.

Methods

The retention volumes of the different polymer standards were obtained isocratically at different volume %NS, starting with 100% solvent at constant

temperature. By increasing the non-solvent composition the retention volume increases. The retention volume of each polymer standard can be plotted versus the non-solvent composition.

The curves (k' versus non-solvent composition) of all polymer standards can be plotted in one figure (see figure 2). This figure is called the CSC plot. The intersection point relates to the non-solvent composition at which the polymer standards with the same chemical structure but with different molar mass elute simultaneously. The critical conditions or the critical solvent composition (CSC) can be defined by this particular non-solvent composition and the specific temperature.

RESULTS AND DISCUSSION

Method to determine the critical conditions

Few experiments are necessary to determine the critical conditions in contrast to the method of Gorshkov *et al.* [3-7]. The retention volumes of the polymer standards of the same chemical type but with different molar mass are obtained at different non-solvent/solvent compositions at a specific temperature. In the figures 2 and 3 the retention volume (V_R) is replaced by a coefficient k' which is defined as $(V_R-V_0)/V_0$. V_0 is the zero retention volume of the system.

The accuracy of the determination is about ± 1%NS. The exact critical solvent composition is defined more accurately than within 1%. Especially near the critical solvent composition, small variations in the %NS have great influence on the retention behaviour. Since the solvent composition can not be established more accurately than 1%, the exact critical solvent composition can be obtained by fine tuning of the temperature.

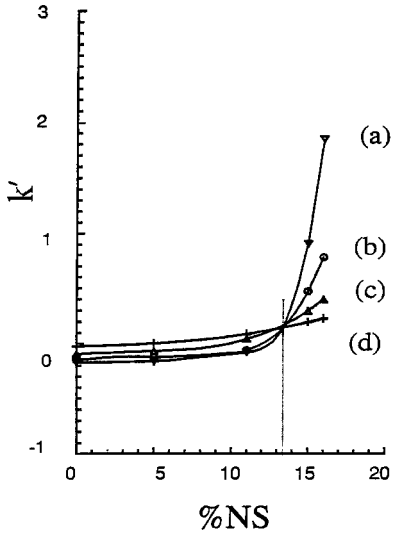

FIGURE 2

CSC Curve of Polystyrene in the Solvent System Water/THF on a Novapak C18 Column at 30°C and a Flow Rate of 0.5 ml/min; Detection: UV 254 nm; Polystyrene Standards: (a) $\overline{M}_w$=9100, (b) $\overline{M}_w$=5570, (c) $\overline{M}_w$=2980 and (d) $\overline{M}_w$=500 g/mol.

In order to compare the method described in literature and the introduced method, the acquired data (figure 2) are presented in figure 4 according to the technique developed by Gorshkov *et al.* [3-7]. The curves show the relation between the molar mass and the retention volume at certain %NS. As can be seen in figure 4 the critical solvent composition cannot be determined. No curve is obtained with infinite slope. More specific experiments have to be performed when using the method of Gorshkov *et al.* [3-7].

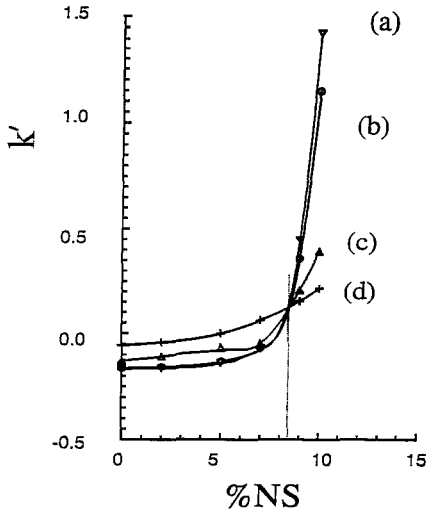

FIGURE 3

CSC Curve of Polybutadiene in the Solvent System Water/THF on a Novapak C18 Column at 30°C and a Flow Rate of 0.5 ml/min; Detection: Mass Detector; Polybutadiene Standards: (a) $\overline{M}_w$=9300, (b) $\overline{M}_w$=8000, (c) $\overline{M}_w$=3000 and (d) $\overline{M}_w$=900 g/mol.

Polystyrene

The CSC plot of the polystyrene standards is shown in figure 2. The used column is the Novapak C18 (4.0x300 mm). The increase of the flow in the range form 0.5 - 1.0 ml/min had no influence on the critical solvent composition. The critical solvent compositions determined for water/THF systems using different types of column packing were determined (see Table 1). With respect to the pore size distribution and the type column packing similar critical solvent compositions were obtained.

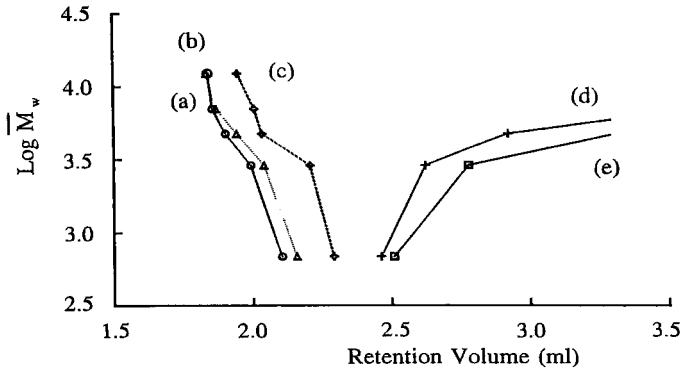

FIGURE 4

Log $\overline{M}_w$ Versus the Retention Volume of Polystyrene Standards at Different Vol% NS ; (a) %NS=0, (b) %NS=5, (c) %NS=11, (d) %NS=15 and (e) %NS=16; Solvent System Water/THF at 35°C on a Novapak C18 Column; Detection: UV 254 nm; Polystyrene Standards: $\overline{M}_w$=9100, $\overline{M}_w$=5570, $\overline{M}_w$=2980 and $\overline{M}_w$=500 g/mol.

TABLE 1

Critical Solvent Composition (CSC) of Polystyrene Standards in the Solvent Mixture Water/THF at 30°C and Different Types of Columns.

Column	CSC (%water)
Novapak C18	13
μStyragel HT	11
Deltapak C18 (100Å)	11
Deltapak C18 (300Å)	12

Polybutadiene

In order to determine the influence of the chemical composition of the polymer on the critical solvent composition, polybutadiene was studied. The critical solvent composition in the system water/THF, Novapak C18 of polybutadiene (see figure 3) was determined. The CSC of polybutadiene appeared to be different from the CSC of polystyrene in the system water/THF, Novapak C18. The CSC of polybutadiene is 8% water and the CSC of polystyrene is 13% water.

CONCLUSIONS

The new method is accurate in determining the critical conditions at a certain temperature. By presenting the results as in the figures 2 and 3 the transition from exclusion mode to adsorption mode can easily be noticed. The newly introduced method is more efficient as compared with the existing method.

The critical solvent composition depends on the following parameters: the temperature, the type of polymer, and the solvent/non-solvent mixture. The exact contribution of each parameter in respect to the mechanism of critical polymer chromatography is still unclear. Especially the role of the temperature is not completely understood. Moreover, the theory of adsorption of polymer molecules does not satisfactorily describe the critical retention behaviour.

Additionally no significant differences in the critical solvent composition occur when different types of column packing are used. This implies that the adsorption of a polymer molecule is more dependent on the polymer type than on the type of column packing.

In conclusion, in order to understand the mechanism, the contributions of the column, temperature and eluent mixture should be studied.

REFERENCES

1. G. Glöckner, Gradient HPLC of Copolymers and Chromatographic Cross Fractionation, Springer-Verlag, Berlin, 1991.

2. S. Mori, Anal. Sci., 4, 365-369 (1988).

3. S.G. Entelis, V.V. Evreinov, A.V. Gorshkov, Adv. Polym., 76, 129-175 (1985).

4. A.V. Gorshkov, T.N. Prudskova, V.V. Gur'yanova, V.V. Evreinov, Polym. Bulletin, 15, 465-468 (1986).

5. A.V. Gorshkov, V.V. Evreinov, B. Lausecker, H. Pasch, H. Becker, G. Wagner, Acta Polymerica, 37, 740-741 (1986).

6. A.V. Gorshkov, S.S. Verenich, V.V. Evreinov, S.G. Entelis, Chromatographia, 26, 338-342 (1988).

7. A.V. Gorshkov, H. Much, H. Becker, H. Pasch, V.V. Evreinov, S.G. Entelis, J. Chromatography, 523, 91-102 (1990).

8. G. Schultz, H Much, H. Krüger, C. Wehrstedt, J. Liq. Chromatography, 13(9), 1745-1763 (1990).

9. H. Krüger, H. Much, G. Schultz, C. Wehrstedt, Makromol. Chem., 191, 907-920 (1990).

10. Th. Mourey, L.E. Oppenheimer, Anal. Chem., 56, 2427-2434 (1984).

Received: November 5, 1993
Accepted: December 1, 1993

JOURNAL OF LIQUID CHROMATOGRAPHY, 17(14&15), 3145-3177 (1994)

THEORY OF HOMOPOLYMER RETENTION IN THE WEAK ADSORPTION LIMIT

RICHARD E. BOEHM AND DANIEL E. MARTIRE
Department of Chemistry
Georgetown University
Washington, D.C. 20057-2222

ABSTRACT

The theory of homopolymer fractionation in mixed mobile phase solvent, high performance liquid chromatography (HPLC) developed previously by Boehm, Martire, Armstrong and Bui [12-14] for strongly adsorbed homopolymers is modified for the case where weak polymer adsorption and/or sorption prevails in the stationary phase. A weakly adsorbed homopolymer of degree of polymerization, M, is assumed to consist of a single adsorbed contiguous train of M^{γ} segments where $0 < \gamma < 1$ ($\gamma = 1$ corresponds to strong adsorption) and a tail of $M - M^{\gamma}$ segments which protrudes into the mobile phase. The analysis predicts that the homopolymer capacity factor, k', depends upon the mobile phase composition, ϕ, of the better polymer solvent in the vicinity of the critical composition, $\phi_c \equiv \phi_c(M)$, which renders $k' = 1$ for an M-unit homopolymer, according to

$$\ell n\ k' = S(\phi_c(M) - \phi)$$

where the slope, $S = -\partial \ell nk'/\partial\phi_c \sim M^{\gamma}$. Experimental measurements of S for different chromatographic systems are discussed within the framework of the theory.

I. INTRODUCTION

Considerable interest exists in the analysis and separation of synthetic macromolecules by high performance liquid chromatography (HPLC). For

instance, Armstrong and Bui [1-4] and Snyder and coworkers [5-11] have demonstrated that molecular weight separation of synthetic homopolymers such as polystyrene can be achieved by reversed-phase gradient elution HPLC using a mixed solvent mobile phase such as $MeCl_2$/MeOH or THF/H_2O. In contrast to size exclusion chromatography (SEC), a single reversed phase column can be utilized to separate homopolymers over essentially the entire molecular weight spectrum (oligomer-high polymer) by gradient elution HPLC.

A statistical thermodynamic theory of homopolymer fractionation and its application to gradient elution HPLC has been developed by Boehm, Martire, Armstrong and Bui (hereafter BMAB) to describe the retention behavior of an isolated flexible chainlike homopolymer molecule distributed between a binary mixed mobile phase and an idealized stationary phase of sorbed solvent(s) forming a monolayer on a chemically homogeneous planar surface [12-14]. The BMAB theory assumes that a retained polymer molecule is strongly sorbed in that the number of surface-polymer segment contacts is directly proportional to the degree of polymerization, M. The present investigation seeks to ascertain the modifications required of the original BMAB theory when the retained polymer molecule is weakly sorbed having only a fraction of its M segments in contact with the stationary phase surface monolayer.

Of general interest is the predicted dependence of $\ell nk'$ on mobile phase composition, ϕ, where k' is the solute capacity factor and ϕ is the volume fraction of the better polymer solvent. Of even greater significance are the predicted dependences on M of the critical mobile phase composition, ϕ_c, at which $k'=1$ ($\ell nk'=0$) and the local slope, $S = -\partial \ell nk'/\partial \phi_c$, of the $\ell nk' - \phi$ isotherm at $\phi = \phi_c$. The ϕ_c-M and S-M dependences are important components in the BMAB description of homopolymer retention and fractionation and they are experimentally accessible from isocratic $\ell nk'$-ϕ measurements performed on several different molecular weight homopolymers

on the same HPLC column [15,16,17]. Less reliable estimates of ϕ_c and S and their variation with M can also be obtained from gradient elution measurements [16,18,19].

Isocratic measurements of $\ell nk'$ - ϕ isotherms have been performed for several polystyrene standards of different molecular weights with narrow distributions by several different groups. For example, Lochmüller and McGranaghan [15] have employed both THF/H_2O and $MeCl_2$/ACN mobile phases with a C-8 300 Å mean pore diameter chemically bonded phase; Alihedai et. al. [16] have utilized $MeCl_2$/MeOH mobile phases with both 100 Å and 300 Å mean pore diameter C-18 chemically bonded phases and Northrup et. al. [17] have used both THF/ACN and $MeCl_2$/MeOH mixed mobile phases and a C-4 bimodal pore diameter reversed phase column consisting of a 48%-52% blend of 80 Å and 500 Å silica [20]. Generally a monotonic increase of ϕ_c and S with M is observed although variations in the ϕ_c - M and especially the S-M dependences have been determined from isocratic measurements performed on these different chromatographic systems. Experimentally one finds that $S \sim M^{\gamma}$ (or $\ell nS \sim \gamma \ell nM$) where the positive exponent, γ, typically ranges between $0.35 < \gamma < 1$ (see Table 1 which summarizes the experimental data).

The BMAB theory predicts that $\gamma \Rightarrow 1$ as $M \Rightarrow \infty$ if strong polymer sorption prevails on an idealized planar stationary phase surface with a sorbed solvent monolayer compositionally enriched in the better polymer solvent. Experimentally determined values of $\gamma < 1$ suggest that for those chromatographically relevant values of k' where $0 < k' \leq 1$ weak adsorption of the polymeric solute with considerable penetration into the mobile phase may be more realistic physically.

In Sec. II we present a brief summary of the original BMAB theory. In Sec. III a statistical thermodynamic treatment is given for the adsorption behavior of an ideal isolated polymer chain which interacts with a chemically

homogeneous adsorption surface with a segment-surface contact free energy, ϵ. The analysis reveals that there is a transition region between the strong adsorption ($\epsilon < 0$) and desorption ($\epsilon > 0$) limits where the average number of polymer segment-surface contacts is proportional to $M^{1/2}$ (rather than M for strong adsorption). The range of ϵ values over which the transition from strong adsorption to desorption occurs is found to decrease as $M^{-1/2}$.

In Sec. III we also discuss the Monte-Carlo calculations performed by Lal and Stepto [21,22] on the configurational behavior of adsorbed freely rotating polymer lattice chains where excluded volume interactions are included. The average configurational behavior is described in terms of the fraction of segments adsorbed, thickness of the adsorbed layer and the average lengths of train, loop and tail sequences of segments. Under conditions where weak (strong) adsorption prevails it is found that the average number of segment-surface contacts goes as $M^{.58}$ ($M^{1.1}$) for $30 \leq M < 100$. Also for weak adsorption the adsorbed layer was determined to be dominated by the lengths of the tail segments.

In Sec. IV we utilize the results and insights obtained in Sec. III to develop a modified BMAB theory of homopolymer retention which applies under conditions where weak polymer sorption is anticipated. It is assumed that the average configurational behavior of a weakly sorbed chain can be described by a single adsorbed train sequence of M^{γ} segments where $0 < \gamma < 1$ and a single tail of $M\text{-}M^{\gamma}$ segments which extends into the mobile phase. The subsequent analysis predicts that $S \sim M^{\gamma}$ for large M and that the predicted dependence of ϕ_c on M is somewhat sensitive to the assumed behavior of the adsorbed train of M^{γ} segments. However, the basic physical description of the homopolymer retention process and mechanism in the modified BMAB approach remains similar to the original treatment.

Finally in Sec. V we compare and discuss the predictions of the modified BMAB analysis and the experimental results and suggest possible extensions.

II - SUMMARY OF THE BMAB THEORY OF HOMOPOLYMER RETENTION IN THE STRONG SORPTION LIMIT

The BMAB theory applies statistical thermodynamics to predict the equilibrium distribution of an isolated flexible chainlike homopolymer molecule between a binary solvent mobile phase and an idealized planar stationary phase surface with sorbed solvent(s). The relative phase preference of the polymer molecule depends on M, ϕ, all possible types of nearest neighbor interactions such as solvent molecule-polymer segment, solvent molecule-solvent molecule, polymer segment-polymer segment, solvent molecule and/or polymer segment-stationary phase surface site, and also the configurational entropy of the flexible polymer molecule in each chromatographic phase. The flexible polymer coil plus the entrained solvent molecules are assumed to behave as a swollen spherical (thin cylindrical) gel in a favorable mobile (stationary) phase environment. Also it is assumed that strong polymer molecule sorption prevails upon retention in the stationary phase with M polymer segment-surface contacts.

In its simplest form, the BMAB theory predicts

$$\ell n\ k' = S(\phi_c - \phi) \equiv |A_1|M(\phi_c - \phi)$$

or

$$k' = \exp[S(\phi_c - \phi)] = \exp[|A_1|M(\phi_c - \phi)] \qquad \text{(II-1)}$$

where $S \equiv -\partial \ell n\ k'/\partial\phi_c = |A_1|M$ and A_1 asymptotically approaches a constant value independent of M for large M which is typically negative for chromatographically reasonable selections of the mixed solvents. When sorption of the better polymer solvent onto the stationary phase dominates, the following predictions for ϕ_c and A_1 result:

$$\phi_c \equiv \phi_c(M) = \phi_c^{\infty} - |a|M^{-1/2} + bM^{-4/5} + c_1M^{-1} + c_2M^{-1}\,\ell nM \qquad \text{(II-2)}$$

and

$$A_1 = X_{12} + X_{13} - X_{23} + dM^{-4/5} + eM^{-1} \qquad \text{(II-3)}$$

Here, ϕ_c^∞ ($0 \leq \phi_c^\infty \leq 1$) is the asymptotic limiting value of the critical composition as $M \rightarrow \infty$ and $X_{ij} \equiv \beta c_m(w_{ij} - (w_{ii} + w_{jj})/2)$, (i,j = 1-3) represents the reduced interchange energy (in units of $(\beta c_m)^{-1} \equiv kT/c_m$ where c_m is the mobile phase coordination number) required to form an i-j nearest neighbor pair with energy w_{ij} from i-i and j-j nearest neighbor pairs with energy w_{ii} and w_{jj}. The indices 1 and 2 respectively denote the better and poorer mobile phase solvents and 3 corresponds to a monomeric segment of the homopolymeric solute. The quantities a, b, c_1, c_2, d and e introduced in eqs. (II-2) and (II-3) are independent of M and depend on the interchange energies and weakly upon the mobile phase composition.

Eq. (II-1) indicates that for large M polymers, $k' \equiv \exp[|A_1|M(\phi_c - \phi)]$ undergoes an abrupt transition from a very large to a very low value within a very narrow mobile phase composition range centered at ϕ_c. Thus a very small change in the mobile phase composition from $\phi_c(1 - \Delta)$ to $\phi_c(1 + \Delta)$ where Δ is a small positive infinitesimal ($\lim \Delta \rightarrow 0$ as $M \rightarrow \infty$) generates an increasingly abrupt change from very large to very low solute retention as M increases. Eq.(II-2) predicts that ϕ_c becomes a monotonically increasing function of M for large M which asymptotically tends to ϕ_c^∞ as $M \rightarrow \infty$.

The BMAB analysis indicates that fractionation of homopolymers with respect to M is possible over a wide spectrum of M values (oligomer-high polymer) on a single column provided certain conditions are satisfied: (1) The polymer molecules are flexible; (2) A combination of a good (1) and a poor (2) solvent for the polymer is employed for the mobile phase such that $X_{12} + X_{13} - X_{23} < 0$; (3) The better solvent is preferentially sorbed onto the stationary phase. Fractionation of the higher M homopolymers usually requires gradient elution which commences at an initial mobile phase composition that is less than the critical composition of the lowest molecular weight homopolymer in the sample and the mobile phase composition is then temporally enriched with the better solvent to a value which exceeds the critical composition of the highest M homopolymer present. For very high

values of M, ϕ_c increases only slightly with M making fractionation more difficult.

In a linear gradient, the temporal variation of the mobile phase composition is

$$\phi(t) = \phi(0) + Bt \quad t \geq 0 \tag{II-4}$$

where $\phi(t)$ ($\phi(0)$) is the mobile phase composition at the column entrance at time t (time t = 0) and B is the rate of increase of the volume fraction of the favorable solvent. The solute retention time, t_R, in linear gradient elution and if Eq. (II-1) applies for k' is

$$t_R = t_0 + (|A_1|MB)^{-1} \ln[1 + |A_1|MBt_0\exp[|A_1|M(\phi_c - \phi(0))]] \tag{II-5}$$

where t_0 represents the column dead time. When

$$|A_1|MBt_0\exp[|A_1|M(\phi_c - \phi(0)] >> 1,$$

eq. (II-5) simplifies to

$$t_R \approx t_0 + (\phi_c - \phi(0))/B + (SB)^{-1} \ln(SBt_0) \tag{II-6}$$

where $S \equiv |A_1|M$. This result can be utilized to determine ϕ_c and S by gradient elution measurements provided the linear approximation to $\ln$ k' given by eq.(II-1) is valid over the entire mobile phase composition range where chromatographically significant values of k' are encountered ($10 \geq$ k' ≥ 0.1) [14]. A linear relationship between $\ln$k' and ϕ over the relevant composition is likely to become more accurate as M increases.

The BMAB theory predicts in general that

$$\ln k' = |A_1|M(\phi_c - \phi) + \sum_{j=2}^{\infty} A_j M(\phi_c - \phi)^j \tag{II-7}$$

where the A_j $j \geq 2$ are monotonically decreasing functions of M which vanish as $M \to \infty$. Non-linear corrections to $\ell nk'$ appearing in the sum $\sum_{j=2}^{\infty} A_j M(\phi_s - \phi)^j$ contribute whenever the difference $|\phi - \phi_c|$ becomes appreciable and M is sufficiently small so that k' is chromatographically measurable over a considerable composition range.

III. STATISTICAL THERMODYNAMIC BEHAVIOR OF A CHAINLIKE POLYMER MOLECULE NEAR A PLANAR ADSORPTION SURFACE

Here we consider the statistical thermodynamic behavior of a completely flexible chainlike homopolymer molecule near a chemically homogeneous planar adsorption surface. The polymer chain consists of M freely rotating links each of length b confined to the halfspace $z > 0$ by an impenetrable adsorption surface with which the polymer can interact on a per segment basis. Both the diffusion equation - Green's function approach [23,24] and the Monte Carlo calculations performed by Lal and Stepto [21] for determining the equilibrium configurational behavior of an adsorbed polymer chain will be discussed.

The equilibrium configurations of a flexible homopolymer chain without intrachain interactions can be simulated from the trajectories assumed by a particle undergoing an unrestricted three dimensional random walk [23,24]. This means that the probability density (i.e. Green's function) $G(\underline{r}, 0; M)$ that one end of a chain of M segments is located in a small volume element centered about $\underline{r}$ given that the other end is located at the origin can be obtained by solving a diffusion equation in a local one-particle potential $\beta\phi(r)$ (in units of $\beta^{-1} = kT$)

$$\frac{\partial G(\underline{r}, 0; M)}{\partial M} = \left(\frac{b^2}{6}\right) \nabla_r^2 G(\underline{r}, 0; M) - \beta\phi(\underline{r})\, G(r, 0; M) \qquad \text{(III-1)}$$

subject to the initial condition $G(\underline{r}, 0; M=0) = \delta^3(r) \equiv \delta(x)\delta(y)\delta(z)$. When $\phi(r) = 0$,

$$G(r,0;M) = (3/2\pi Mb^2)^{3/2}\exp[-3r^2/2Mb^2] \qquad \text{(III-2)}$$

which is the familiar Gaussian solution of Eq.(III-1), and it represents the probability density that an ideal chain has an end-to-end separation, r, when it assumes an equilibrium distribution of configurations. The mean square end-to-end separation is $\langle r^2\rangle = \int_0^\infty 4\pi r^4 G(r,0;M)dr = Mb^2$ and $\langle r^2\rangle^{1/2} = M^{1/2}b$ where b is the length of a (statistical) segment.

When a chainlike polymer molecule interacts with a surface, the number of accessible configurations is reduced relative to a completely isolated coil. If the interaction between a polymer segment and the surface is a contact potential

$$\beta\phi(r) = \beta\epsilon' b\delta(z) \qquad \text{(III-3)}$$

where ϵ' has the units of energy and the delta function, $\delta(z)$, has units of reciprocal length, then the probability density for a polymer chain which interacts with the surface is obtained by solving the differential equation

$$\frac{\partial G(\underline{r},0;M)}{\partial M} = \left\{\left(\frac{b^2}{6}\right)\left[\frac{\partial^2}{\partial x^2} + \frac{\partial^2}{\partial y^2} + \frac{\partial^2}{\partial z^2}\right] - \beta\epsilon' b\delta(z)\right\} G(\underline{r},0;M) \qquad \text{(III-4)}$$

where for an impenetrable surface $z \geq 0$. It is possible and convenient to remove the constraint that $z > 0$ by including polymer configurations which penetrate through the surface and then removing them by the device of introducing a 'sink' term to the diffusion equation. This loss term has the form $-(\ln \upsilon)b\delta(z)\, G(\underline{r},0;M)$ where υ represents the ratio of the number of ways a given segment of the polymer chain can be generated from a random-walk trajectory starting at the surface to a point above the surface ($z > 0$) (and hence generate an allowed configuration) to the total number of ways the segment could be generated in the absence of the surface. For a completely

flexible one-dimensional polymer chain $\upsilon = ½$ [25,26] which means that whenever a chain segment makes contact with the surface the next segment must be diverted away from the surface. For a three dimensional polymer chain whose configurations are simulated by a particle taking a random walk on a cubic lattice, $\upsilon = 5/6$ for a chain which can fold back on itself and $\upsilon = 4/5$ when only one segment is allowed per lattice site.

The modified diffusion equation which incorporates the 'sink' term is congruent to eq. (III-4) when ϵ' is replaced by

$$\epsilon = \epsilon' - kT\ell n\upsilon \qquad 0<\upsilon\leq 1 \tag{III-5}$$

and with the restriction $z > 0$ removed. The solution of eq.(III-4) with the modification (III-5) subject to the initial condition $G(\underline{r},0;\ M=0) = \delta^3(r)$ gives the probability density $G(\underline{r},0;\ M)$ that an isolated polymer chain of M links without intrachain segment-segment interactions (i.e. excluded volume interactions) has its terminal segment between $\underline{r}$ and $\underline{r} + d\underline{r}$ given that its initial segment is at the origin in contact with the surface.

The behavior of $G(\underline{r},0;\ M)$ depends on ϵ. When $\epsilon < 0$ adsorption of the chain occurs since contact with the surface is energetically favored and overcomes the loss of configurational entropy. If $\epsilon = 0$, that is, $\epsilon' = kT\ell n\upsilon$, the polymer chain behaves as if the surface were absent, and when $\epsilon > 0$, the polymer molecule is essentially desorbed from the surface except for the initial segment which becomes irrelevant for long chains. Once $G(\underline{r},0;M)$ is obtained the canonical partition function, $Q \equiv Q(M, \beta)$, is determined from

$$Q = \int_{z>0} d^3r G(\underline{r}, 0; M) \tag{III-6}$$

and from Q, the statistical thermodynamic properties of the ideal polymer chain-surface system can be extracted.

The solution of eq.(III-4) with eq. (III-5) is facilitated by taking the Laplace transform of eq. (III-4) with respect to M and then the Fourier transform with respect to the x and y coordinates which are parallel to the plane of the adsorption surface. These transformations convert eq. (III-4) to

$$\left(\frac{b^2}{6}\right)\frac{d^2\bar{G}^*}{dz^2} - \left(\lambda + \left(\frac{b^2}{6}\right)(k_x^2 + k_y^2) + \beta\epsilon b\delta(z)\right)\bar{G}^* = -\delta(z) \tag{III-7}$$

where

$$\bar{G}^* \equiv \bar{G}^*(k_x, k_y, z; \lambda) = \int_{-\infty}^{\infty} dx \int_{-\infty}^{\infty} dy \exp[i(k_x x + k_y y)] G^*(x, y, z; \lambda) \tag{III-8}$$

and

$$G^* \equiv G^*(x, y, z; \lambda) = \int_0^{\infty} dM e^{-\lambda M} G(x, 0; M) \tag{III-9}$$

Eq. (III-7) has the general solution

$$\bar{G}^* = A \exp[-\kappa z]\theta(z) + \beta \exp[\kappa z]\theta(-z) \tag{III-10}$$

where $\kappa \equiv \kappa(\lambda, k_x, k_y) = (6b^{-2}(\lambda + (b^2/6)(k_x^2 + k_y^2)))^{1/2}$ has the units of inverse length, A and B are constants, and $\theta(z) = 1$ for $z > 0$ and $\theta(z) = 0$ for $z < 0$ is the Heaviside unit step function. The constants are determined by requiring that $\bar{G}^*$ be continuous at $z = 0$ and that

$$\left(\frac{b^2}{6}\right)\left[\frac{d\bar{G}^*}{dz}\Big|_{z=0^+} - \frac{d\bar{G}^*}{dz}\Big|_{z=0^-}\right] - \beta\epsilon b\bar{G}^*(z=0) + 1 = 0$$

which is obtained by integrating (III-7) across the singularity at z=0. These conditions are satisfied if $A=B=(\kappa b^2/3 + \beta\epsilon b)^{-1}$
and $\overline{G}^*=(\kappa b^2/3 + \beta\epsilon b)^{-1}\{\exp[-\kappa z]\theta(z) + \exp[\kappa z]\theta(-z)\}$.
Performing the inverse Laplace transformation on $\overline{G}^*$ gives

$$\overline{G}=\overline{G}(k_x, k_y, z; M) =$$
$$\exp[-Mb^2(k_x^2+k_y^2)/6]\{(\frac{3}{(2\pi Mb^2)})^{1/2}\exp[-3z^2/2Mb^2]$$

$$-\frac{3\beta\epsilon}{2b}\exp[(\frac{3\beta\epsilon}{b})(z+M\beta\epsilon b/2)]\,erfc((\frac{3}{2Mb^2})^{1/2}(z+Mb\beta\epsilon))]$$

(III-11)

$$where\ erfc(u) = 2\pi^{-1/2}\int_u^\infty e^{-\mu^2}d\mu$$

is the complementary error function.
Taking the inverse Fourier transformation gives

$$G(x, 0; M) = (2\pi)^{-2}\int_{-\infty}^{\infty}dk_x\int_{-\infty}^{\infty}dk_y\exp[-i(k_x x+k_y y)]\,G(k_x, k_y, z; M)$$

$$= (\frac{3}{2\pi Mb^2})^{3/2}\exp[-3(x^2+y^2+z^2)/2Mb^2]$$

$$x\{1-\beta\epsilon(\frac{3\pi M}{2})^{1/2}\exp[(\frac{3\beta\epsilon}{b})(z+\frac{M\beta\epsilon b}{2}) + \frac{3z^2}{2Mb^2}]$$
$$x\ erfc((\frac{3}{2Mb^2})^{1/2}(z+Mb\beta\epsilon))\}$$

(III-12)

When $\epsilon\equiv\epsilon'-kT\ell n\upsilon=0$, eq. (III-12) reduces to eq. (III-2) which is the Gaussian distribution for an unperturbed three dimensional polymer coil. When $\beta\epsilon << 0$ which corresponds to strong polymer adsorption the last term

on the RHS of eq. (III-12) dominates and as erfc(u) ~ 2 for u→-∞, eq. (III-12) reduces to

$$G(\underline{r},0;M) = \left(\frac{3}{2\pi Mb^2}\right)\frac{3\beta|\epsilon|}{b}\exp\left[\frac{3M(\beta\epsilon)^2}{2}\right]\exp\left[\frac{-3\beta|\epsilon|z}{b}\right] \times \exp\left[-3(x^2+y^2)/2Mb^2\right] \tag{III-13}$$

The average thickness of the strongly adsorbed polymer molecule normal to the surface is

$$d = \langle z\rangle = \int d^3r\theta(z)\; zG(\underline{r},0;M) / \int d^3r\theta(z)\,G(\underline{r},0;M) = b/3\beta|\epsilon| \tag{III-14}$$

The average thickness of the polymer layer varies inversely with $\beta|\epsilon|$ and the polymer assumes configurations in the strong adsorption mode which are closely associated with the surface and the polymer assumes a geometry which resembles a thin cylindrical disc or pancake.

When $\beta\epsilon >> 0$ the asymptotic expansion

$$erfc(u) = \pi^{-1/2}u^{-1}e^{-u^2}$$

for large positive u applies and

$$G(\underline{r},0;M) \rightarrow \left(\frac{3}{2\pi Mb^2}\right)^2\pi^{1/2}z\exp\left[-3(x^2+y^2+z^2)/2Mb^2\right]\theta(z) \tag{III-15}$$

The average value $\langle z\rangle = (M/6)^{1/2}b$ is independent of ϵ and the polymer molecule assumes dimensions characteristic of a coil removed from the surface.

The configurational partition function for the adsorbed polymer molecule is obtained from eq. (III-6) with G(r,0;M) given by eq. (III-13) and

$$Q = Q(M, \beta) = (1/2) \exp[3M\beta^2\epsilon^2/2]\, erfc((\frac{3M}{2})^{1/2}\beta\epsilon) \qquad \text{(III-16)}$$

The partition function assumes the following limiting forms

$\beta\epsilon << 0$	$Q \sim \exp[3M\beta^2\epsilon^2/2]$	(III-17a)
$\beta\epsilon >> 0$	$Q \sim 1/(6\pi M)^{1/2}\beta\epsilon$	(III-17b)
$0 \leq (3M/2)^{1/2}\beta\lvert\epsilon\rvert < 1$	$Q \simeq 1/2[1-(6M/\pi)^{1/2}\beta\epsilon]$	(III-17c)

The average energy of adsorption in units of kT is calculated from $\beta<E> = -\partial \ell nQ/\partial \ell n\beta$ and has the following limiting forms

$\beta\epsilon << 0$	$\beta<E> \simeq -3M(\beta\epsilon)^2$	(III-18a)
$\beta\epsilon >> 0$	$\beta<E> \simeq 1$	(III-18b)
$0 \leq (3M/2)^{1/2}\beta\lvert\epsilon\rvert < 1$	$\beta<E> \simeq (6M/\pi)^{1/2}\beta\epsilon$	(III-18c)

Clearly in the strong adsorption limit where $-\infty < \beta\epsilon << -(2/3M)^{1/2}$, $\beta<E>$ is proportional to the number of chain segments or degree of polymerization, M which indicates that the average number of contacts with the surface, $\overline{C} \equiv \beta<E>/\beta\epsilon$, is also proportional to M. Thus in the limit of strong adsorption, the polymer molecule assumes trainlike configurations which extend over the entire length of the chain and are in contact with the surface.

For $0 \leq \beta\lvert\epsilon\rvert < (2/3M)^{1/2}$ a transition from strong adsorption to desorption occurs and, in this region of weak adsorption which narrows as $M^{-1/2}$, $\overline{C} \propto M^{1/2}$. Also, the probability distribution given by eq. (III-12) reduces to a Gaussian distribution for sufficiently large values of z ($z \geq (2M/3)^{1/2}b$). These results suggest that a weakly adsorbed polymer chain assumes configurations which consist of an adsorbed train of $\sim M^{1/2}$ segments and one or two terminal tails which involve $M\text{-}M^{1/2}$ segments which are desorbed from the surface. Finally when $\beta\epsilon >> 0$, $\beta<E> \simeq 1$ becomes independent of M which indicates that only the initial segment is attached to the surface and hence desorption of the remainder of the polymer chain has occurred.

The above results essentially have been obtained by many investigators employing both discrete and continuum (diffusion) models for determining the

configurational behavior [27, 28, 29]. This model of an adsorbed polymer chain, however, fails to include excluded volume interactions between chain segments.

Lal and Stepto [21] have performed Monte Carlo calculations of the configurational behavior of an adsorbed polymer chain which include excluded volume interactions. They analyzed freely rotating lattice chains consisting of 30, 50, 75 and 100 bonds adsorbing from athermal solutions onto an impenetrable planar adsorption surface for different adsorption energies which are defined as the energy changes, $\Delta\epsilon_s$, for breaking a segment-solvent interaction to form a segment-surface bond. Strong and weak adsorption were respectively simulated by the selections $\beta\Delta\epsilon_s$=-0.9 and $\beta\Delta\epsilon_s$=-0.5. When the chains are strongly adsorbed they are found to possess extended configurations dominated by trains and loops and short tails. For weak adsorption, however, the chain configurations develop longer tails and the thickness of the adsorbed homopolymer layer is dominated by the lengths of the tails. Indeed, proportionality was obtained between tail length and chain length for the chains investigated (M=30, 50, 75, 100) in the weak adsorption case with about one third of the segments in each tail at all chain lengths.

The average number of contacts, $\overline{C}$, obtained by Lal and Stepto as a function of M (the number of bonds) in their Monte-Carlo calculations satisfy the following relationships obtained by linear regression over the range $30 \leq M \leq 100$ (See TABLE I of ref. 21)

$$\beta\Delta\epsilon_s=-0.9; \quad \overline{C}=.38\ M^{1.08};\ \text{c.c}=.999 \qquad \text{(III-19a)}$$

$$\beta\Delta\epsilon_s=-0.5; \quad \overline{C}=.99M^{0.582};\ \text{c.c.}=.997 \qquad \text{(III-19b)}$$

where c.c. $\equiv$ correlation coefficient. These results determined from the Monte-Carlo calculations in the strong and weak adsorption limits reinforce and agree rather well with the predictions of the ideal chain-surface analysis based on the diffusion equation.

IV. MODIFICATION OF THE BMAB THEORY FOR THE CASE OF WEAK POLYMER SOLUTE ADSORPTION IN THE STATIONARY PHASE

Here we apply the insights and results discussed in III to modify the original BMAB theory (see sec. II) when weak polymer adsorption or sorption characterizes its retention in the stationary phase. In general, the configurations of an adsorbed polymer chain can be described in terms of (1) trains which are contiguous sequences of segments in contact with the surface; (2) loops which are successive segments which protrude into the solution or solvent phase and connect adjacent trains, and (3) tails which represent terminal sequences of segments that extend away from the surface into the solvent phase [21,22]. When strong adsorption prevails the chain configurations are dominated by long train sequences connected by loops and short or nonexistent tails with the average number of segment-surface contacts proportional to M. For weak adsorption the chain configurations develop longer tails which determine the thickness of the adsorbed layer and a concomitant decrease in the number and length of the train-loop sequences with an average number of segment-surface contacts proportional to M^{γ} where $0<\gamma<1$.

In the subsequent proposed modification of the original BMAB theory to weak polymer sorption, we assume an average configurational behavior which is characterized by a single adsorbed train of M^{γ} segments and a single tail of $M-M^{\gamma}$ segments which extends into the mobile phase environment beyond the surface-sorbed solvent monolayer. Thus when a polymer molecule exits from the stationary to the mobile phase (or vice versa) a concomitant displacement of M^{γ} monomeric solvent molecules from the mobile to the stationary phase is assumed to occur. Other configurations for the weakly adsorbed homopolymer are viable possibilities such as one which consists of an adsorbed train of M^{γ} segments and two tails comprised of a total of $M-M^{\gamma}$ segments which can be apportioned between the tails in $(M-M^{\gamma}+1)/2$ (((M-

$M^{\gamma})/2)+1)$ distinguishable ways if $M-M^{\gamma}$ is an odd (even) integer. It turns out, however that if each configuration composed of one train and one or two tails is equally probable, then it suffices for the subsequent analysis to consider the single train-single tail adsorbed configuration since all other configurations of this class will generate the same result. Those configurations for which the M^{γ} ($M-M^{\gamma}$) segments in contact (not in contact) with the surface appear in multiple train-loop sequences and thus shorter tails are expected to be energetically and entropically less favorable for real polymer chains with definite bond angles and steric hindrances and are not considered in the present investigation.

In ref. [14] (see eq. (22)) the following expression was derived for the capacity factor ($k_3 \Rightarrow k'$) of a chainlike homopolymer solute (component 3) of M monomeric units distributed between a mobile phase (m) consisting of a binary solvent mixture of components 1 and 2 and a stationary phase (s) consisting of a planar chemically homogeneous support surface with a monolayer of sorbed solvents 1 and 2.

$$k_3 \Rightarrow k' = \Phi \frac{c_s(c_s-1)^{M-2}}{c_m(c_m-1)^{M-2}} \left(\frac{N_s P_s}{N_m P_m}\right) \frac{(1-M/N_s)^{M-N_s}}{(1-M/N_m)^{M-N_m}}$$

$$\exp\left((1/2 - g_s)\frac{M^2}{N_s} - (1/2 - g_m)\frac{M^2}{N_m}\right)\left(\sum_{i=1}^{2} f_i\right)^M \qquad \text{(IV-1)}$$

where

$$f_i = x_{is}\exp\left[\beta\Delta e(i,3;s) + \left((1-x_{is})(c_s/c_m) - (1-x_{im})\right)(X_{i3}^m + X_{12}^m - X_{j3}^m)\right] \qquad \text{(IV-2)}$$

($i=1,2$ $j\neq i$). Eq. (IV-1) was derived in the strong adsorption (or sorption) limit where all M units of the homopolymer reside in the surface monolayer when retained in the stationary phase and M (monomeric) solvent molecules

are exchanged between chromatographic phases whenever a polymeric solute makes a concomitant transition. In eqs. (IV-1) and/or (IV-2), Φ represents the phase ratio; c_a ($a \equiv m,s$) represents the coordination number in phase a; N_a ($a \equiv m,s$) denotes the volume (or area) occupied by the polymer molecule and entrained solvent molecules in chromatographic phase a; $P_a \equiv P_a(N_a)$ represents the probability that a polymeric solute molecule and entrained solvent molecules occupies a volume (or area) given by N_a; $\beta\Delta e(i,3;s) \equiv \beta(e_{is}-e_{3s}+w_{i3}-w_{ii})$ $i=1,2$ represents the free energy change associated with removing a polymer segment from the stationary phase surface to the mobile phase with the corresponding exchange of a type i ($i=1,2$) solvent molecule; the e_{is} $i=1,2$ and e_{3s} respectively represent the interaction free energy of a type i solvent molecule and a polymer segment with the surface while w_{ii} and w_{i3} $i=1,2$ respectively denote nearest neighbor solvent i-solvent i and solvent i-polymer segment interaction energies; $X_{ij}^m \equiv \beta c_m(w_{ij} - (w_{ii} + w_{jj})/2)$ $(i,j=1\text{-}3)$ represents the reduced interchange energy required to form an i-j nearest neighbor pair from an i-i and a j-j nearest neighbor pair; the x_{ia} $i=1,2$ $a=m,s$ represent the volume fractions of solvent component i in phase a; and finally

$$g_a = \tfrac{1}{2} - \sum_{i=1}^{2} x_{ia}X_{i3}^a + x_{1a}x_{2a}X_{12}^a \quad (x_{ia}+x_{2a}=1) \quad a=m,s.$$

We seek to modify eq. (IV-1) for k′ to make it applicable when weak homopolymer adsorption (and/or sorption) characterizes the retention behavior in the stationary phase. The weakly adsorbed chain is assumed to consist of a single train of M^γ segments (actually the nearest integer to M^γ) where $0<\gamma<1$ and then a tail of $M\text{-}M^\gamma$ segments which is desorbed from the surface monolayer and penetrates into the mobile phase. In the present treatment the configurational behavior of the train and tail portions are taken to be independent. Also polymer desorption from the stationary phase is accompanied by the sorption of M^γ solvent molecules.

The proposed generalization of eq. IV-1 in the weak adsorption case is

$$k' = \Phi \frac{c_s (c_s-1)^{M^\gamma-1} (c_m-1)^{M-M^\gamma-1} N_s^* P_s(N_s^*) N_m^* P_m(N_m^*) (1-M^\gamma/N_s^*)^{M^\gamma-N_s^*}}{c_m (c_m-1)^{M-2} N_m P_m (1-M/N_m)^{M-N_m}}$$

$$X(1-(M-M^\gamma)/N_m^*)^{M-M^\gamma-N_m^*} \exp[-(1/2-g_m) M^2/N_m]$$

$$x \exp[(1/2-g_m)(M-M^\gamma)^2/N_m^* + (1/2-g_s)(M^\gamma)^2/N_s^*] (\sum_{i=1}^{2} f_i)^{M^\gamma}$$

(IV-3)

where N_s^* and N_m^* respectively represent the area and volume occupied by the train and tail portions of the weakly sorbed polymer molecule and entrained solvent molecules and N_m is the volume of the solvent swollen polymer coil in the mobile phase. N_s^*, N_m^* and N_m are determined by free energy minimization of the respective polymer train, tail or coil entrained solvent system. The minimization conditions are

$$\frac{\partial \ln P_s(N_s^*)}{\partial N_s^*} + (N_s^*)^{-1} - \ln[1-\frac{M^\gamma}{N_s^*}] - \frac{M^\gamma}{N_s^*} - (\frac{M^\gamma}{N_s^*})^2 [1/2-g_s] = 0$$

(IV-4a)

$$\frac{\partial \ln P_m(N_m^*)}{\partial N_m^*} + (N_m^*)^{-1} - \ln[1-\frac{(M-M^\gamma)}{N_m^*}] - \frac{(M-M^\gamma)}{N_m^*} - (\frac{M-M^\gamma}{N_m^*})^2 [1/2-g_m] = 0$$

(IV-4b)

and

$$\frac{\partial \ln P_m(N_m)}{\partial N_m} + N_m^{-1} - \ln[1-M/N_m] - \frac{M}{N_m} - (\frac{M}{N_m})^2 [1/2-g_m] = 0$$

(IV-4c)

Employing the approximations $P_s(N_s^*) \approx M^{-\gamma}\exp[-N_s^*/M^\gamma]$, $P_m(N_m^*) \approx (M-M^\gamma)^{-3/2}$ $\exp[-3N_m^{*2/3}/2(M-M^\gamma)]$ and $P_m(N_m) \approx M^{-3/2}\exp[-3N_m^{2/3}/2M]$ in eqs. (IV-4a)- (IV-

4c), respectively, give $N_s^* = g_s^{1/2} M^{3\gamma/2}$, $N_m^* = g_m^{3/5}(M-M^\gamma)^{9/5}$ and $N_m = g_m^{3/5} M^{9/5}$ and whenever $M^\gamma/N_s^* << 1$, $(M-M^\gamma)/N_m^* << 1$ and $M/N_m << 1$, which corresponds to polymer swelling in good solvent environments. These results for N_s^*, N_m^* and N_m are the standard Flory predictions [29, 30, 31] for the dimensions of a solvent swollen cylindrical disc or spherical coil.

Substitution of the above results for $P_s(N_s^*)$, $P_m(N_m^*)$, $P_m(N_m)$, N_s^*, N_m^* and N_m into eq. (IV-1) gives after some simplification [e.g. replacing

$$\frac{c_s(c_s-1)^{M^\gamma-1}}{c_m(c_m-1)^{M^\gamma-1}} \quad by \quad \left(\frac{c_s-1}{c_m-1}\right)^{M^\gamma}$$

for large M^γ]

$$M^{-\gamma}\ell nk' =$$

$$\ell n\left(\sum_{i=1}^{2} x_{is}\exp\left(\beta\Delta E(i) + \left(\frac{C_s}{C_m}(1-x_{is}) - (1-x_{im})\right)(X_{i3}^m + X_{12}^m + X_{j3}^m)\right)\right)$$

$$-M^{-\gamma/2}(2g_s^{1/2}) + \tfrac{1}{2}M^{-4/5}g_m^{2/5} + M^{-\gamma}\ell n[\Phi(1-M^{\gamma-1})^{3/10}M^{\gamma/2}g_s^{1/2}] \qquad \text{(IV-5)}$$

where $\beta\Delta E(i) = \beta(\epsilon_{is} - e_{3s} + w_{i3} - w_{ii}) + \ell n[(c_s-1)/(c_m-1)]$ $i = 1,2$. The solvent compositions x_{im} and x_{is} are related by the equilibrium adsorption isotherm of the solvents distributed between the binary solvent mobile phase and the adsorbed surface monolayer, which is [14]

$$x_{1s}(1-x_{1s})^{-1}\exp\left[X_{12}^m\frac{C_s}{C_m}(1-2x_{1s}) + \beta(e_{1s}-e_{2s})\right] =$$

$$x_{1m}(1-x_{1m})^{-1}\exp\left[X_{12}^m(1-2x_{1m}) + \beta(w_{11}-w_{22})/2\right] \qquad \text{(IV-6)}$$

In many applications of interest $\beta(e_{1s}-e_{2s}) << 0$, $\exp[-\beta(e_{1s}-e_{2s})] >> 1$ and $x_{2s} << x_{1s} \simeq 1$ and to an excellent approximation $x_{1s} \simeq u/(1+u)$ and $x_{2s} \simeq (1+u)^{-1}$ where with $x_{1m} \equiv \phi$ and $X_{12} \equiv X_{12}^m$

$u \equiv u(\phi) = \phi(1-\phi)^{-1}\exp[X_{12}(1-2\phi+c_s/c_m)-\beta(e_{1s}-e_{2s})+\beta(w_{11}-w_{22})/2]$ (IV-7)

In this approximation eq. (IV-5) can be expressed directly as a function of the mobile phase composition of the better solvent, ϕ,

$$M^{-\gamma}\ell nk' = \ell n\left[u(1+u)^{-1}\exp\{\beta\Delta E(1) + \left[\frac{C_s}{C_m}(1+u)^{-1}-1+\phi\right]\left[X_{12}+X_{13}-X_{23}\right]\}\right.$$

$$\left. + (1+u)^{-1}\exp\{\beta\Delta E(2) + \left[\frac{C_s}{C_m}u(1+u)^{-1}-\phi\right]\left[X_{12}+X_{23}-X_{13}\right]\}\right]$$

$$-M^{-\gamma/2}2g_s^{1/2}+1/2M^{-4/5}g_m^{2/5}+M^{-\gamma}\ell n\left[\Phi(1-M^{\gamma-1})^{3/10}M^{\gamma/2}g_s^{1/2}\right] \quad \text{(IV-8)}$$

where $g_s = 1/2 - (c_s/c_m)[u(1+u)^{-1}X_{13}+(1+u)^{-1}X_{23}-u(1+u)^{-2}X_{12}]$ and we have deleted the 'm' superscript from the $[X_{ij}]$ (i,j,= 1-3).

The last three terms on the RHS of both eq. (IV-5) and (IV-8) depend on M and they vanish as $M\to\infty$. The retention behavior for sufficiently large M solutes depends on whether $M^{\gamma}\ell nk'$ is positive (high retention) or negative (low retention). A transition from high to low retention is anticipated to occur abruptly for sufficiently large M solutes as ϕ is systematically increased. If, for example, when $\phi=\phi_c<1$, $\ell nk' = 0$, a transition from high to low retention occurs whenever the mobile phase composition changes from $\phi_c(1-\Delta)$ to $\phi_c(1+\Delta)$ where $\Delta \equiv \Delta(M)$ is a small positive number which becomes smaller as M increases. Also, ϕ_c depends on M since $M^{\gamma}\ell nk'$ depends on M and this suggests that fractionation of homopolymers by molecular weight should be viable by gradient elution HPLC [1] and in some systems even isocratic elution [15-17].

In the immediate vicinity of ϕ_c, where $F(\phi_c) \equiv M^{\gamma}\ell nk'(\phi_c)=0$, the capacity factor can be expressed as

$$k' = \exp\left[M^{\gamma}\sum_{j=1}^{\infty} D_j(\phi-\phi_c)^j\right] \quad \text{(IV-9)}$$

where $D_j \equiv (j!)^{-1}\partial^j F(\phi_c)/\partial\phi_c^j$. If $|D_j(\phi-\phi_c)^j| << |D_1(\phi-\phi_c)|$ for all $j \geq 2$, then a linear approximation $M^{-\gamma}\ell nk' = D_1(\phi-\phi_c)$ is sufficiently accurate. In general, determining $F(\phi_c)=0$ requires numerical methods as does the evaluation of D_1 and if necessary the remaining coefficients D_j for $j \geq 2$. When the stationary phase exhibits a decided preference for the better solvent than $x_{1s} \simeq 1$ which corresponds to $u >> 1$ (strictly $u \to \infty$ as $x_{1s} \to 1$) and (IV-8) reduces to:

$$\overline{F} \equiv M^{-\gamma}\ell nk' = \beta\Delta E(1) - (1-\phi)[X_{12}+X_{13}-X_{23}] - M^{-\gamma/2}\, 2\overline{g}_s^{\,1/2} + \tfrac{1}{2}M^{-4/5}g_m^{\,2/5} + M^{-\gamma}\ell n[\Phi(1-M^{\gamma-1})^{3/10}M^{\gamma/2}\overline{g}_s^{\,1/2}] \qquad \text{(IV-10)}$$

where $\overline{F}, \ell n\overline{k}'$ and $\overline{g}_s$ indicates that the $x_{1s} \to 1$ or $u \to \infty$ limit has been taken. The mobile phase composition, ϕ_c, which renders $F(\phi_c)=0$ satisfies

$$\phi_c = \phi_c^{\infty} + (X_{23}-X_{12}-X_{13})^{-1}[-2\overline{g}_s^{\,1/2}M^{-\gamma/2} + \tfrac{1}{2}g_m^{\,2/5}M^{-4/5} + M^{-\gamma}\ell n[\Phi(1-M^{\gamma-1})^{3/10}M^{\gamma/2}\overline{g}_s^{\,1/2}]] \qquad \text{(IV-11)}$$

where

$$\phi_c^{\infty} = 1 + (X_{23}-X_{12}-X_{13})^{-1}\beta\Delta E(1) \qquad \text{(IV-12)}$$

A physically meaningful result requires that $-1 \leq (X_{23}-X_{12}-X_{13})^{-1}\beta\Delta E(1) \leq 0$ for $0 \leq \phi_c^{\infty} \leq 1$. Also

$$\overline{D}_1 \equiv \frac{\partial \overline{F}}{\partial \phi_c} = X_{12} + X_{13} - X_{23} + \frac{1}{5} g_m^{-3/5} M^{-4/5} \frac{\partial g_m}{\partial \phi_c} \qquad \text{(IV-13)}$$

$$\overline{D}_j = \frac{1}{j!}\frac{\partial^j \overline{F}}{\partial \phi_c^j} = (j!)^{-1}\left[\frac{1}{2}M^{-4/5}\right]\frac{\partial^j g_m^{2/5}}{\partial \phi_c^j} \qquad j \geq 2 \qquad \text{(IV-14)}$$

As $M \to \infty$ $\overline{D}_1 \to X_{12} + X_{13} - X_{23}$ and $\overline{D}_j \to 0$ for all $j \geq 2$. Furthermore, as $M \to \infty$ eq. (IV-10) can be expressed as

$$\overline{F} = M^{-\gamma}\ell n\, \overline{k}' = (X_{23}-X_{12}-X_{13})(\phi_c^{\infty}-\phi) \qquad \text{(IV-15)}$$

When M is large but finite it still remains an excellent approximation to use

$$\overline{F} = M^{-\gamma}\ell n\, \overline{k}' \simeq |\overline{D}_1|(\phi_c-\phi) \qquad \text{(IV-16)}$$

where $\phi_c \equiv \phi_c(M)$ and $\overline{D}_1$ are given by eqs. (IV-11) and (IV-13), respectively. If $X_{23}-X_{13}-X_{12} > 0$, ϕ_c is a monotonically increasing function of M which

asymptotically approaches ϕ_c^∞ as $M\to\infty$. Provided $0 < \phi_c \leq \phi_c^\infty \leq 1$ a transition from high to low solute retention is predicted to occur over a mobile phase composition interval centered about ϕ_c which becomes narrower as M increases.

Inspection of eq. (IV-11) reveals that the dependence of ϕ_c on M enamates from contributions of the form $-|\overline{a}|M^{-\gamma/2}+\overline{b}M^{-4/5}+\overline{c}M^{-\gamma}\ell nM$ which depend sensitively upon the value of the exponent γ $(0<\gamma<1)$. Comparison can be made with eq. (II-2) for the strong adsorption case. Also from the linear approximation for $\ell n\ \overline{k}'$ given by eq. (IV-16) we obtain

$$S = -\partial n\ \overline{k}'/\partial\phi_c = |\overline{D}_1|M^\gamma$$

$$\text{or} \qquad \ell nS=\gamma\ell nM+\ell n|D_1| \qquad \text{(IV-17)}$$

This result predicts that measurements of S as a function of M plotted as ℓn S vs. ℓn M should be linear with slope given by the exponent γ $(0<\gamma<1)$. Thus the predicted slope of a ℓn S-ℓn M plot becomes smaller when weak adsorption prevails since for strong adsorption $\partial\ell nS/\partial\ell nM\to1$ when M is large. If $\gamma=½$, which corresponds to an 'ideal' adsorbed chain $\partial\ell nS/\partial\ell nM=½$ for sufficiently large M and $\phi_c=\phi_c^\infty$ + $(X_{23}-X_{13}-X_{12})^{-1}$ $[-2\overline{g}_s^{½}M^{-1/4}+½g_m^{2/5}M^{-4/5}+M^{-½}\ell n[\Phi M^{1/4}\overline{g}_s^{½}(1-M^{-½})^{3/10}]]$.

An explicit expression for the retention time, t_R, as a function of M for linear gradient elution where $\phi\equiv\phi(t)$ is temporally increased in linear fashion, $\phi(t) = \phi(0)+Bt$, can be obtained readily when $k'=|D_1|M^\gamma(\phi_c-\phi)$ and is

$$t_R = t_o+(|D_1|M^\gamma B)^{-1}\ell n[1+|D_1|M^\gamma Bt_o\exp[|D_1|M^\gamma(\phi_c-\phi(0))]] \qquad \text{(IV-18)}$$

Here t_o is the time required for unretained solute to pass through the column, $\phi(0)$ is the mobile phase composition at the start of the gradient and B is the time rate of change of the composition gradient. Whenever $|D_1|M^\gamma Bt_o\exp[|D_1|M^\gamma(\phi_c-\phi(0))]>>1$ eq. (IV-18) reduces to

$$t_R = t_o+B^{-1}(\phi_c-\phi(0))+(|D_1|M^\gamma B)^{-1}\ell n(|D_1|M^\gamma Bt_o) \qquad \text{(IV-18*)}$$

Clearly for large M and $\phi(0)<\phi_c$, $t_R\simeq t_o+B^{-1}(\phi_c-\phi(0))=t_o+t_c$ where t_c is the time required for the mobile phase composition at the inlet to develop to ϕ_c when a linear gradient is sustained. Also, utilization of eq. (IV-18*) allows

one to express asymptotically for large M that $\ln t_R \simeq \ell n\, t_R^{\infty}$-const.$M^{-\gamma/2}$ where $t_R^{\infty} \equiv t_o + B^{-1}(\phi_c - \phi(0))$.

Equations (IV-18) or (IV-18*) provide a relationship between t_R and M and predict that a very dilute homopolymer mixture can be separated into molecular weight fractions by linear gradient elution HPLC when $\phi(0)$ is less than the critical composition of the lowest M homopolymer present. The order of elution then proceeds successively from the lowest to the highest molecular weight constituent since $\phi_c(M)-\phi(0)$ monotonically increases with M.

If the adsorbed train of M^{γ} contiguous segments behaves as a 'rigid' moiety whose dimensions are unaltered by solvent uptake, then eq. (IV-3) for k' is modified by replacing the factor(s)

$$N_s^* P(N_s^*)\,(1-M^{\gamma}/N_s^*)^{(M^{\gamma}-N_s^*)} \exp\left((1/2-g_s)M^2/N_s^*\right)$$

by unity and k_R' becomes

$$k_R' = \Phi \left(\frac{C_s - 1}{C_m - 1}\right)^{M_\gamma} \frac{N_m^* P_m(N_m^*)}{N_m P_m(N_m)} \quad \frac{(1-(M-M^{\gamma})/N_m^*)^{(M-M^{\gamma}-N_m^*)}}{(1-M/N_m)^{(M-N_m)}}$$

$$\times \exp\left[-(1/2-g_m)\left[\frac{M^2}{N_m} - \frac{(M-M^{\gamma})^2}{N_m^*}\right]\right] \left(\sum_{i=1}^{2} f_i\right)^{M^{\gamma}} \qquad \text{(IV-19)}$$

where f_i is again given by eq. (IV-2) and the 'R' subscript on k' indicates the rigidity of the adsorbed train. Employing the same approximations for N_m, N_m^*, $P_m(N_m)$ and $P_m(N_m^*)$ as in eq. (IV-5) for eq. (IV-19) gives after some manipulations which assume $M^{\gamma-1} << 1$:

$$M^{-\gamma}\ell n k_R' = \ell n\left(\sum_{i=1}^{2} x_{is} \exp\left[\beta \Delta E(i) - 1 + \left(\frac{C_s}{C_m} x_{js} - x_{jm}\right)(X_{i3} + X_{12} - X_{j3})\right]\right)$$

$$+ 1/2 g_m^{2/5} M^{-4/5} + M^{-\gamma} \ell n\left[\Phi (1-M^{\gamma-1})^{3/10}\right] \qquad \text{(IV-20)}$$

where again $\beta\Delta E(i)=\beta(\epsilon_{is}-e_{3s}+w_{i3}-w_{ii})+\ell n[(c_s-1)/(c_m-1)]$ $i=1,2$ and eq. (IV-6) must be utilized to obtain the x_{1s}-x_{1m} adsorption isotherm.

If $x_{1s}\simeq 1$, $x_{2s}\simeq 0$ and $x_{1m}\rightarrow\phi$, eq. (IV-20) simplifies to

$$\overline{F_R} = M^{-\gamma}\ell n\overline{k_R'}=\ell n\left[\exp\left[\beta\Delta E(1)-1-(1-\phi)\left(X_{13}+X_{12}-X_{23}\right)\right]\right]+\tfrac{1}{2}g_m^{2/5}M^{-4/5} + M^{-\gamma}\ell n\left[\Phi\left(1-M^{\gamma-1}\right)^{3/10}\right] \tag{IV-21}$$

where the 'bar' above the k_R' again indicates the limit $x_{1s}=1$ has been taken. Also $\overline{k}_R'$ may be expressed as

$$\overline{k_R'} = \exp\left[M^{\gamma}\sum_{j=1}^{\infty}\overline{D}_j(\phi-\phi_c)^j\right] \tag{IV-22}$$

where $\overline{D}_j\equiv (1/j)(\partial^j\overline{F}_R/\partial\phi_c^j)$ if $\ell n\overline{k}_R'=0$ when $0\leq\phi=\phi_c\leq 1$. The critical composition is given by the solution of

$$\phi_c=\phi_c^{\infty}+(X_{23}-X_{13}-X_{12})^{-1}\left[\tfrac{1}{2}M^{-4/5}g_m^{2/5}(\phi_c)+M^{-\gamma}\ell n[\Phi(1-M^{\gamma-1})^{3/10}]\right] \tag{IV-23}$$

where

$$\phi_c^{\infty} = 1+(X_{23}-X_{13}-X_{12})^{-1}[\beta\Delta E(1)-1] \tag{IV-24}$$

which differs slightly from eqs. (IV-11) and (IV-12). In linear approximation with respect to ϕ_c-ϕ, eq. (IV-21) (or IV-22) reduces to

$$M^{-\gamma}\ell n\overline{k_R'}= (\phi_c-\phi)\left[X_{23}-X_{13}-X_{12}-(1/5)\ g_m^{-3/5}(\phi_c)\frac{\partial g_m}{\partial\phi_c}M^{-4/5}\right]+O(\phi_c-\phi)^2 \tag{IV-25}$$

and

$$S_R=-\frac{\partial\ell n\overline{k_R'}}{\partial\phi_c}=M^{\gamma}\left[X_{23}-X_{13}-X_{12}-(1/5)\ M^{-4/5}g_m^{-3/5}(\phi_c)\frac{dg_m}{d\phi_c}\right] \tag{IV-26}$$

which establishes that $S_R\propto M^{\gamma}$ for sufficiently large M.

V. DISCUSSION AND COMPARISON OF THEORY AND EXPERIMENTAL RESULTS

Several sets of experimental measurements which can give the dependence of the slope $S = -\partial \ell nk'/\partial \phi_c$ on M have been performed on polystyrene standards using both isocratic and gradient elution HPLC using a variety of mixed solvent combinations and chemically bonded stationary phases of different pore sizes and hydrocarbon chain lengths.

A summary of the experimentally determined S-M results are recorded in Table I along with the mixed mobile phase solvents and the stationary phases employed. Linear regression was utilized to obtain the best empirical fit of the form $\ell nS = \ell n\alpha + \gamma \ell nM$ or $S = \alpha M^{\gamma}$ to the experimental S-M data, where α and γ are optimally selected empirical parameters. Inspection of Table I reveals considerable variation in the experimental S-M results which depend upon the mobile phase mixtures, stationary phases, molecular weight range and number of homopolymer solutes utilized and the method(s) used to obtain the S-M data-isocratic or linear gradient elution or some combination thereof.

Whenever possible or feasible, measurements of $S \equiv -\partial \ell nk'/\partial \phi_c$ derived from isocratic measurements of $\ell nk'$-ϕ isotherms for a given homopolymeric solute are more reliable than the corresponding linear gradient elution measurements. If the $\ell nk'$-ϕ dependence were strictly linear over the relevant mobile phase composition range centered about ϕ_c, then the isocratic and gradient elution measurements of S and ϕ_c should agree. In general such agreement does not occur although it improves as M increases since the transition from high to low retention occurs over a decreasing mobile phase composition range. Specifically for $\phi \sim \phi_c$ linear $\ell nk'$-ϕ behavior is observed irrespective of the value of M. However, as $|\phi - \phi_c|$ increases, departures from linearity develop especially for the lower M solutes. These non-linear contributions to $\ell nk'$ for $\phi < \phi_c$ can generate a compositionally averaged gradient determined slope, S_G, which overestimates $S = -\partial \ell nk'/\partial \phi_c$ [16].

TABLE I

Reference	$S = \alpha M^{\gamma}$ γ	α	Solute Molecular Weight Range (kD)	Mobile Phase Solvents	Bonded Stationary Phase (Pore Size Å)
11, 18[a]	0.50	2.25	2-233	THF/H_2O	C-18 (150 Å)
15[b]	0.654	0.472	4-300	$MeCl_2/ACN$	C-8 (300 Å)
15[b]	0.669	1.03	17.5-35	THF/H_2O	C-8 (300 Å)
16[a]	0.472	3.41	2-390	$MeCl_2/MeOH$	C-18 (100 Å)
16[a]	0.517	2.03	2-390	$MeCl_2/MeOH$	C-18 (300 Å)
16[b]	0.730	0.452	2-100	$MeCl_2/MeOH$	C-18 (100 Å)
16[b]	0.586	0.668	2-100	$MeCl_2/MeOH$	C-18 (300 Å)
16[c]	0.732	0.446	2-390	$MeCl_2/MeOH$	C-18 (100 Å)
16[c]	0.735	0.334	2-390	$MeCl_2/MeOH$	C-18 (300 Å)
16[c]	0.770	0.343	17.5-390	$MeCl_2/MeOH$	C-18 (100 Å)
16[c]	0.877	0.124	17.5-390	$MeCl_2/MeOH$	C-18 (300 Å)
16[c]	0.768	0.345	50-390	$MeCl_2/MeOH$	C-18 (100 Å)
16[c]	0.994	0.0515	50-390	$MeCl_2/MeOH$	C-18 (300 Å)
17[b]	0.55	0.0054	4-390	THF/ACN	C-4[d]
17[b]	0.35	0.201	30.7-390	$MeCl_2/MeOH$	C-4[d]

[a]Gradient elution measurements
[b]Isocratic measurements
[c]Isocratic measurements for 2-100 kD polystyrene samples. Gradient elution measurements for polystyrene samples greater than 100 kD.
[d]Bimodal pore diameter column composed of a 48% 80 Å and 52% 500 Å mixed silica support surface.

The first S-M measurements on a series of polystyrene homopolymers were performed by Snyder and coworkers using THF/H_2O mixed mobile phases and a 150 Å mean pore diameter C-18 chemically bonded phase and linear gradient elution HPLC [11, 18]. They obtained the empirical fit $S_G = 2.25\ M^{.50}$ where the subscript 'G' denotes gradient elution. The best linear regression fits to the S_G-M measurements obtained by Alihedai et. al. on polystyrene solutes ranging from 2-390 kD using gradient elution HPLC with $MeCl_2/MeOH$ mixed mobile phases and either a 100 Å or 300 Å mean pore size diameter C-18 stationary are $S_G = 3.41\ M^{.472}$ (c.c. = 0.982) and $S_G = 2.03\ M^{.517}$ (c.c. = 0.977), respectively. These results compare favorably with

those of Snyder et. al. although different chromatographic phases were utilized.

Measurement of S for any M taken from isocratic $\ell nk'$-ϕ measurements in the vicinity of and including $\phi_c(M)$ are more reliable and Alihedai et. al. [16] obtained the following best linear regression fits for solutes between 2 - 100 kD; $S = 0.452\ M^{.730}$ (c.c. = 0.993) and $S = 0.668\ M^{.586}$ (c.c. = 0.995) for the 100 Å and 300 Å C-18 columns respectively using $MeCl_2$/MeOH mobile phases. For comparison the isocratic measurements of the slopes of $\ell nk'$-ϕ isotherms reported by Lochmüller and McGranaghan [15] for five polystyrene solute samples with molecular weights between 4 kD and 300 kD eluted with $MeCl_2$/ACN mobile phases and a C-8 bonded phase of 300 Å mean pore diameter can be fit by linear regression to $S = 0.472\ M^{.654}$ (c.c = 0.994). Also their isocratic measurements of the slopes for three polystyrene solute samples of 4, 17.5 and 35 kD using THF/H_2O mobile phases and a 300 Å C-8 bonded phase can be represented by $S = 1.03\ M^{.669}$ (c.c. = 0.993).

When the isocratic measurements performed by Alidhedai e. al. in $MeCl_2$/MeOH mobile phases for 2-100 kD polystyrene standards are supplemented by gradient elution determined S_G for 233 kD and 390 kD polystyrene solute standards, then $S = .446\ M^{.732}$ (c.c. = 0.994) for the 100 Å C-18 column and $S = .334\ M^{.735}$ (c.c. = 0.980) for the 300 Å C-18 column. Also recorded in Table I are the linear best fits of the isocratic S-M data reported in [16] for smaller sets of solute standards which include the highest molecular weights studied. The exponent γ in the best fit of the form $S = \alpha M^{\gamma}$ tends to increase towards unity for the 300 Å C-18 column when the set of polystyrene standards is limited to molecular weights between 50 kD and 390 kD. This perhaps suggests that strong adsorption may be the dominant mode of retention for these higher M solutes.

Utilization of $MeCl_2$/MeOH mobile phases with a C-18 column tends to generate $\ell nk'$-ϕ isotherms which change rather abruptly from high to low retention over a narrow composition range about $\phi_c(M)$ even for the lower M

polystyrenes. As a result, isocratic measurements of the $\ell nk'$-ϕ isotherms in the vicinity of $\phi_c(M)$ become extremely difficult and uncertain for $M > 10^3$ (i.e., mol. wt. > 100 kD) polystyrenes. Northrup et. al. [17] observed, however, that by selecting THF/ACN mobile phases and a bimodal pore size C-4 stationary phase [20], isocratic measurements of $\ell nk'$-ϕ isotherms for five polystyrene standards with 4 kD $\leq$ mol. wt. $\leq$ 390 kD were possible. These isocratic measurements lead to the linear regression best fit $S = .0054\ M^{.55}$ (c.c. = .997). Northrup et. al. [17] also utilized $MeCl_2$/MeOH mobile phases along with the same C-4 bimodal stationary phase to obtain $\ell nk'$-ϕ isotherms isocratically for the same five polystyrene standards. Their corresponding best linear regression fit is $S = .201\ M^{.35}$ (c.c. = .973) for the four highest molecular weights (30, 50, 100 and 390 kD). These results are obtained from lower capacity columns and none of the isocratic $\ell nk'$-ϕ measurements involved the region where $\ell nk' \geq 0$ and thus did not include compositions where $\phi \leq \phi_c(M)$. Hence the relevant ϕ range for determination of $S \equiv -\partial \ell nk'/\partial \phi_c$ was not probed directly by the measurements and only values of S extrapolated to the relevant composition, $\phi_c(M)$, from higher compositions $\phi > \phi_c(M)$ for each solute were obtained.

The experimentally determined S-M behaviors exhibit considerable variation and clearly depend on the chromatographic conditions and the range of M values probed. The values of the exponent γ in the relationship $S \sim M^{\gamma}$ were obtained from linear regression fits to the various experimental measurements and have been found to range between $0.35 \leq \gamma < 1$ with most of the results confined to the range $0.5 < \gamma < 0.75$. These results suggest that the polymeric solutes are generally weakly adsorbed and/or sorbed in the stationary phase with a considerable portion of the solute penetrating into the mobile phase environment over the composition range of chromatographic significance where $0 < k' \leq 10$. The experimental results for γ agree reasonably well with the theoretical estimates $\gamma = \frac{1}{2}$ for an ideal adsorbed chain and $\gamma = 0.582$ [21] for the Monte-Carlo generated adsorbed

chains with excluded volume interactions included. The modified BMAB theory introduced in the previous section predicts that $S \sim M^{\gamma}$ where M^{γ} corresponds to the number (to the nearest integer) of polymer segments sorbed contiguously as a single train sequence onto the idealized stationary phase monolayer. The case $\gamma = 1$ corresponds to the strong adsorption limit treated in the original BMAB analysis.

A more realistic model of the adsorption surface which explicitly incorporates the pore structure and the bonded alkyl chains would clearly be a desirable improvement of the BMAB theory. It is anticipated that configurations where trains of adsorbed segments reside in neighboring pores connected by a loop or bridge sequence of segments protruding into the mobile phase might contribute significantly to the retention in real systems, especially for large M solutes and small diameter pores. Despite its shortcomings, however, the present model does suggest that consideration of weak adsorbed and/or sorbed states can rationalize the numerous experimental observations from many chromatographic systems that $S \sim M^{\gamma}$ where $\gamma < 1$ rather than the strong adsorption prediction that $S \sim M$ for sufficiently large M.

Since the ϕ_c - M dependence is predicted to depend on the exponent γ, this dependence also correlates with the extent of sorption of the polymeric solute in the stationary phase especially for the lower M solutes. The ϕ_c - M dependence on γ is sensitive to whether the adsorbed train sequence is solvent swollen or is better characterized as a rigid chain skeleton which is more likely for smaller M.

For chromatographic conditions where $k' >> 1$ homopolymer retention is anticipated to be determined by strong adsorption. However, under chromatographic conditions where $0 < k' < 1$ weaker adsorption modes are more likely to dominate. The transition from strong to weak adsorption behavior for large M homopolymers may be abrupt or rather gradual functions of ϕ depending upon the chromatographic system involved. An abrupt transition for a fixed M solute is more likely to occur if the mobile

phase consists of a mixture of a good and relatively poor solvent for the polymeric solute, and there exists a strong preference for sorption of the better solvent and a preference for the solute in the stationary phase. Mixed mobile phases of $MeCl_2$/MeOH and THF/H_2O and well end-capped C-18 chemically bonded stationary phases tend to exhibit increasingly abrupt transitions from high to low retention as M increases which suggests strong polymer adsorption for $\phi < \phi_c(M)$ and weaker adsorption for $\phi > \phi_c(M)$. If, however, the mobile phase solvents have similar affinities for the polymeric solute and the stationary phase exhibits only slight preference for the better solvent and has lower capacity for the solute, then low retention $0 < k' < 1$ may prevail over a considerable range of ϕ and weak adsorption of the polymeric solute is anticipated. The THF/ACN mixed mobile phase and C-4 stationary phase utilized by Northrup et. al. [17] represents a chromatographic system where weak polymer sorption behavior is likely to dominate. Indeed isocratic $\ell nk'$-ϕ measurements have been performed directly for polystyrene standards up to 390 kD with this system.

Finally it should be mentioned that explicit *a priori* determination of the actual mobile and stationary phase conditions which lead to weak homopolymer adsorption is beyond the scope of the present investigation.

ACKNOWLEDGMENT

This material is based upon work supported by the National Science Foundation under Grant CHE-8902735.

REFERENCES

1. D. W. Armstrong, K. H. Bui, Anal. Chem., 54: 706 (1982).

2. D. W. Armstrong, K. H. Bui, R. E. Boehm, J. Liq. Chromatogr., 6: 1 (1983).

3. K. H. Bui, D. W. Armstrong, J. Liq. Chromatogr., 7: 29 (1984).

4. K. H. Bui, D. W. Armstrong, J. Liq. Chromatogr., 7: 45, (1984).

5. J. P. Larmann, J. J. DeStefano, A. P. Goldberg, R. W. Stout, L. R. Snyder, M. A. Stadalius, J. Chromatogr., 255: 163 (1983).

6. L. R. Synder, M. A. Stadalius, M. A. Quarry, Anal. Chem., 55: 1412A (1983).

7. M. A. Stadalius, H. S. Gold, L. R. Snyder, J. Chromatogr., 296: 31 (1984).

8. M. A. Stadalius, H. S. Gold, L. R. Snyder, J. Chromatogr., 327: 27 (1985).

9. M. A. Stadalius, M. A. Quarry, L. R. Snyder, J. Chromatogr., 327: 93 (1985).

10. R. W. Stout, S. I. Sirakoff, R. D. Ricker, L. R. Snyder, J. Chromatogr., 353: 439 (1986).

11. M. A. Quarry, R. L. Grob, L. R. Snyder, Anal. Chem., 58: 907 (1986).

12. R. E. Boehm, D. E. Martire, D. W. Armstrong, K. H. Bui, Macromolecules, 16: 466 (1983).

13. R. E. Boehm, D. E. Martire, D. W. Armstrong, K. H. Bui, Macromolecules, 17: 400 (1984).

14. R. E. Boehm, D. E. Martire, Anal. Chem., 61: 471 (1989).

15. C. H. Lochmüller, M. B. McGranaghan, Anal. Chem., 61: 2449 (1989).

16. A. Alhedai, R. E. Boehm, D.E. Martire, Chromatographia, 29: 313 (1990).

17. D. M. Northrop, D. E. Martire, R. P. W. Scott, Anal. Chem., 63: 1350 (1991).

18. M. A. Stadalius, M. A. Quarry, T. H. Mourey, L. R. Snyder, J. Chromatogr., 358: 1 (1986).

19. M. A. Stadalius, M. A. Quarry, T. H. Mourey, L. R. Snyder, J. Chromatogr., 358: 17 (1986).

20. D. M. Northrop, R. P. W. Scott,, D. E. Martire, Anal. Chem., 63: 1350 (1991).

21. M. Lal, R. F. T. Stepto, J. Polym. Sci., 61: 401 (1977).

22. Yu. S. Lipatov, Russ. Chem. Revs., 50: 196 (1981).

23. M. Doi, S. F. Edwards, The Theory of Polymer Dynamics, Clarendon Press: Oxford, 1986, Chap. 2.

24. K. F. Freed, Adv. Chem. Phys., 22: 1 (1972).

25. E. A. DiMarzio, J. Chem. Phys., 42: 2101 (1965).

26. E. A. DiMarzio, F. L. McCrackin, J. Chem. Phys., 43: 539 (1965).

27. R. J. Rubin, J. Chem. Phys., 43: 2392 (1965).

28. D. Chan, D. J. Mitchell, B. W. Ninham, L. R. White, J. Chem. Soc., Faraday Trans. 2, 71: 235 (1975).

29. P. G. deGennes, Scaling Concepts in Polymer Physics, Cornell University Press: Ithaca, NY, 1979.

30. P. J. Flory, Principles of Polymer Chemistry, Cornell University Press: Ithaca, NY 1971.

31. T. L. Hill, An Introduction to Statistical Thermodynamics, Dover: New York, 1986, Chap. 21.

Received: November 12, 1993
Accepted: December 7, 1993

JOURNAL OF LIQUID CHROMATOGRAPHY, 17(14&15), 3179-3189 (1994)

RETENTION BEHAVIOR OF POLY(L-TRYPTOPHAN)S AND POLY(D,L-TRYPTOPHAN)S IN REVERSED-PHASE LIQUID CHROMATOGRAPHY

C. H. LOCHMÜLLER[1]*, CHUN JIANG[1], AND MATTI ELOMAA[2]

[1]P. M. Gross Chemical Laboratory
Department of Chemistry
Duke University
Durham, North Carolina 27708
[2]University of Helsinki
Department of Polymer Chemistry
Meritullinktu 1 A
SF-00170 Helsinki, Finland

ABSTRACT

The reversed-phase liquid chromatographic retention behavior of poly(l-tryptophan)s and poly(d,l-tryptophan)s) whose molecular weight ranged from 5.4 kD to 37.25 kD is examined using a C-8 chemically bonded stationary phase and binary mobile phases of tetrahydrofuran (THF)-water and ternary mobile phases of THF-water-methanol. The retention of poly(l-tryptophan)s is compared with that of poly(d,l-tryptophan)s. Linear-Solvent-Strength (LSS) model is examined in describing the retention behavior. The effect of adding a third solvent to the binary mobile phase is also discussed.

INTRODUCTION

The use of reversed-phase liquid chromatography (RPLC) in polymer separation and characterization has drawn considerably large interest since 1980s [1-14]. The reversed-phase chromatographic method, which involves no size-exclusion, complements the widely used size-exclusion chromatographic method in which polymers are separated according to their sizes. It has been shown that using RPLC it is possible to separate a variety of polymers, especially copolymers [15] which has been a difficult task with size-exclusion chromatography. However, the retention mechanism of polymers in RPLC remains unclear and several models have been suggested [3,6,7,8,9,10,11,12,13]. A true and clear retention mechanism is needed in order to fully exploit the power of RPLC, such as optimizing separation and predicting retention. Central to the debate on polymer retention mechanism is that whether or not isocratic retention can be obtained. Lochmüller and McGranaghan [14] found that retention behavior of poly(styrene) that is similar to that found in small molecules could be obtained only when the sample was adequately mixed with the mobile phase using a low dispersion, crocheted mixer before the solute-column contact occurred. They reported that isocratic retention of polystyrenes of molecular weight ranged from 2000 Daltons to 2,800,000 Daltons could be obtained with binary mobile phases of tetrahydrofuran/H_2O and dichloromethane/ acetonitrile. Finite, non-zero k' values and linear relationships in the plots of log k' versus the volume percentage of tetrahydrofuran and dichloromethane were observed [14].

Characterization of rigid polymers with size-exclusion chromatography is difficult because the calibration curve that is derived from flexible polymers is no longer applicable [16,17,18,19]. If a polymeric sample contains both rigid and

flexible polymers, it is even more difficult to assign the peaks in the size-exclusion chromatogram. RPLC can be a good method for characterizing rigid polymers because of its partition/adsorption retention mechanism and its independence of calibration. It is also highly desirable to be able to control the retention with current available separation optimization knowledge developed from small molecules, such as the "third solvent" strategy [20]. In this report, Poly(l-tryptophan)s and poly(d,l-tryptophan)s are chosen as model polymers because (1). the former is a rigid and helical polymer which is rod-like, and the later a flexible and globular one; (2). a very small amount (less than 0.5 nanogram) of poly(tryptophan)s can be detected with fluorescence detection and this insures that solution of poly(tryptophan) is close to infinitely dilute; (3). poly(tryptophan)s are actually synthetic peptides and this study may shed some light on the future study of separation of synthetic peptides and proteins. It is found that poly(l-tryptophan)s show longer retention times than poly(d,l-tryptophan) of the same molecular weight. For all poly(tryptophan)s samples, linear plots of the logarithm of the capacity factor (k') versus volume fraction (ϕ) of the strong solvent are obtained. The LSS model is examined via inter-relating isocratic and gradient elution. With the volume fraction of THF kept constant, the effect of adding a small amount of methanol in THF-water mobile phase on the retention time is discussed.

EXPERIMENTAL SECTION

HPLC. A Perkin-Elmer Series 4 liquid chromatograph and 420B autosampler (Perkin-Elmer, Norwalk, CT) was used. Detector used was a Perkin-Elmer 850-

10LC Fluorescence Spectrometer with excitation wavelength at 280 nm and emission wavelength at 350 nm. Flow rate was 1 mL/min. A sample loop of 5 μL was used. Retention data were collected using a Nelson Analytical Chromatography package (Nelson Analytical, Inc., Cupertino, CA). Samples were dissolved in the mobile phase collected right before injection. The concentrations of all samples were 50 μg/mL. Before each injection the samples were vigorously agitated by a shaker for 10-20 minutes. Capacity factor k' was calculated by the equation of $k'=(t_r-t_o)/t_o$, where t_r is the retention time of polymer peak maximum and t_o is the void time. The standard deviation of k' calculated from three measurements was within 2% error.

Materials. Columns used were 25cmX4.6mm ones with Partisil 10 C8 bonded phase (Whatman, Clifton, NJ). HPLC grade methanol, tetrahydrofuran (THF) and water were used as received. Poly(tryptophan) standards were purchased from Sigma (St. Louis, MO, USA). Their molecular weights are: poly(l-tryptophan) 5,400 Daltons (Mw/Mn=1.45), 115,000 Daltons (Mw/Mn=1.24), 37,250 Daltons (Mw/Mn=1.11) and poly(d,l-tryptophan) 5,700 Daltons (Mw/Mn=1.47) and 14,500 Daltons (Mw/Mn=1.42).

RESULTS AND DISCUSSION

In reversed-phase chromatography of polymers, a pair of good and poor solvents are often used [1-15]. In this study, THF and H_2O were used. THF is the "good" solvent and H_2O is the "poor" or hostile one. The sample chromatograms from isocratic elution are shown in Figure 1. It is interesting to observe that at the same mobile phase composition, poly(l-tryptophan) 11.5 kD has longer retention

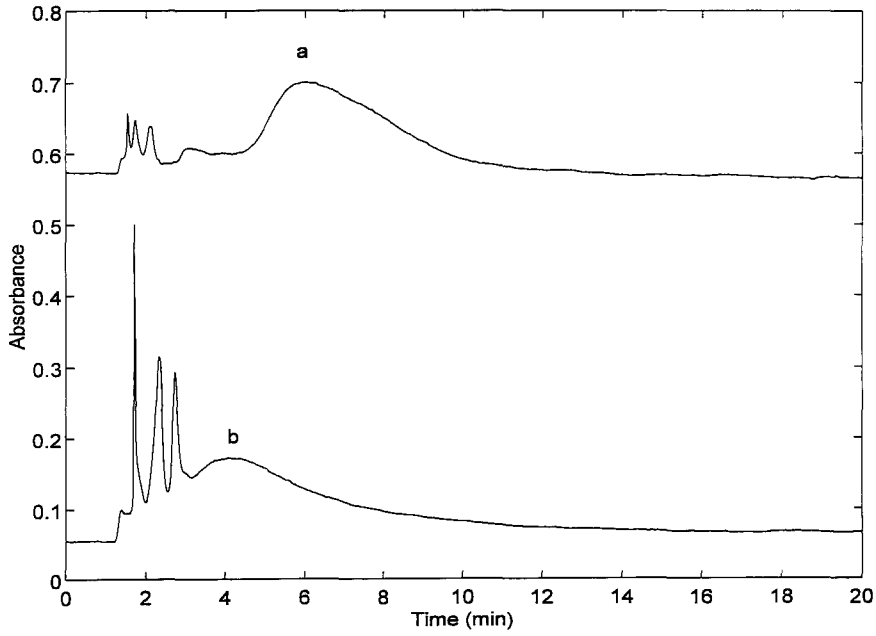

FIGURE 1. Chromatograms of poly(tryptophan)s Mobile phase THF:water 77:23, (a). 11.5 kD poly(l-tryptopahn), (b). 14.5 kD poly(d,l-tryptophan). The sharp peaks are from oligomers.

time than its counterpart 14.5 kD poly(d,l-tryptophan)s within the range of mobile phase compositions used in the experiments. The difference in retention time between 5.4 kD poly(l-tryptophan) and 5.7 kD poly(d,l-tryptophan)s is small. It has been reported that the predicted order of solute retention is: rigid-rod solutes>plate solutes>flexible chain solutes [21]. There have been many reports and debates on whether the retention mechanism for small molecules is an adsorption process ("Solvophobic" model), or a partition process, or both [22]. For the high molecular weight polymer case, if retention only involves adsorption mechanism

in which solute-stationary phase interaction only takes place at the surface of the stationary phase, the retention of poly(l-tryptophan)s should be shorter than that of poly(d,l-tryptophan)s because the average surface area of the polymer solute in contact with the stationary phase of poly(l-tryptophan) is smaller than that of poly(d,l-tryptophan). The bulky globular poly(d,l-tryptophan)s may not be able to enter the bonded phase of alkyl chains, whereas a part of the rod-like poly(l-tryptophan)s may get intercalated in the bonded alkyl chains. If the molecular weight is low, there may not be dramatic difference in retention time as we observed in 5.4 kD and 5.7 kD poly(tryptophan)s. Therefore, the rationale can be suggested as that high molecular weight poly(d,l-tryptophan)s may experience a mechanism of adsorption, on the other hand, poly(l-tryptophan)s and low molecular weight poly(d,l-tryptophan)s may have a combined partition and adsorption mechanism. The results here support that for RPLC of polymers the stationary phase plays a very important role. More mechanistic study can be done by varying the alkyl chain length of stationary phase and studying the retention of polymers of different size and/or shapes.

In Figure 2 are shown the plots of log k' versus the volume fraction of THF (ϕ) in binary THF-water mobile phase. These plots fit linear relationships (log k'= A-Sϕ) where A is the intercept and S is the slope.

Linear-Solvent-Strength has been applied to optimization of separation and prediction of retention [23,24,25]. From the LSS theory, gradient retention time t_g is given by:

$$t_g = t_o \log[2.3k_o/k'] + t_o + t_D \qquad 1$$

where t_D is the dwell time of the gradient system (the time between the beginning of the gradient at the pump and its reaching the inlet of the column), k'

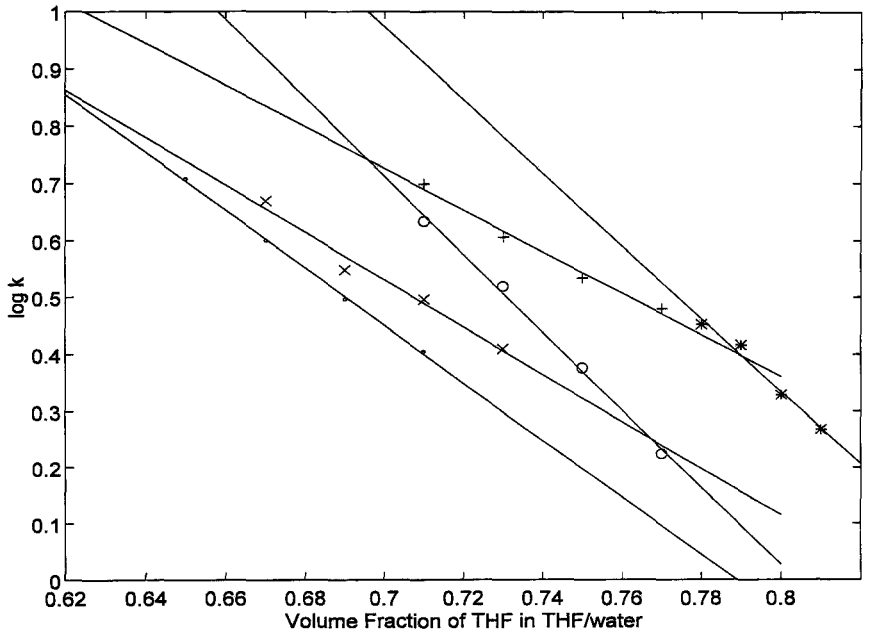

FIGURE 2. Plots of log k' versus volume fraction of THF Poly(l-tryptophan)s: (*) 37.25 kD; (+) 11.5 kD; (x) 5.4 kD; Poly(d,l-tryptopahn)s: (o) 14.5 kD; (·) 5.7 kD.

is the average capacity factor of gradient elution and k_o is the capacity factor from pure weak solvent. Since

$$k'_1 = t_G/(\Delta\phi S t_o) \quad (2)$$

where t_G is the gradient time and $\Delta\phi$ is the change of mobile phase composition. With two gradient runs, k'_1 can be calculated as:

$$k'_1 = [t_{g1}-(t_{g2}/\beta)-(t_o+t_D)(\beta-1)/\beta]/(t_o \log\beta) \quad (3)$$

$$\beta = t_{G2}/t_{G1} \quad (4)$$

Given a known k'_1, S can be calculated as:

$$S = t_{G1}/(\Delta\phi k'_1 t_o) \quad (5)$$

TABLE 1: Predicted S Values from LSS Model and Actual S Values *

	37.25 kD (l)	11.5 kD (l)	5.4 kD (l)	14.5 kD (d,l)	5.7 kD (d,l)
predicted S	6.68	4.2	4.5	7.5	5.5
actual S	6.42	3.6	5.1	6.94	5.1

* In the table, (l) stands for poly(l-tryptophan)s, (d,l) for poly(d,l tryptophans).

If the gradient retention time from two runs is known, S can be calculated by equation 5. The predicted and actual S and t_r values are listed in Table 1. The prediction is moderately accurate, considering the fact that the plot of log k' versus ϕ is not perfectly linear over a large range of mobile phase composition and LSS model is a empirical model.

Mobile phase plays an important role in RPLC [20,22]. Many optimization techniques center around using combinations of different mobile phase. Using ternary solvent mixture as mobile phase to precisely control the elution strength and polarity of mobile phase has been studied for a long time [20]. However, to our best knowledge there is no report on studying the effect of ternary mobile phase on the polymer retention. In this work, methanol is added into THF-water mobile phase as the third solvent. Methanol is a poor solvent for poly(tryptophan)s, but it is a better solvent than water. This is verified by mixing the same amount of poly(l-tryptophan) 11.5 kD with the same volume of methanol, and water and taking fluorescence intensity measurements of the supernatant. The normalized fluorescent intensities at 350 nm indicate that methanol and acetonitrile are better solvents than water, e.g., the intensity at 350nm for methanol solution is 7 times larger than that for water. While the volume fraction of THF is kept constant, the fraction of water is decreased with the increase of the fraction of methanol. Since methanol is a better solvent than

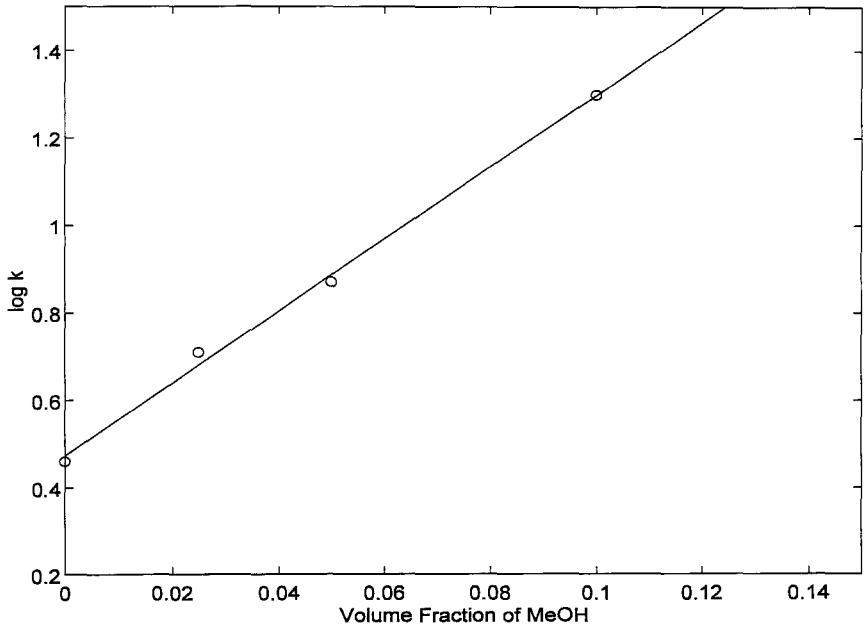

FIGURE 3. Plot of log k' versus volume fraction of methanol in THF-water-methanol tenery mobile phase.

water, one would expect that replacing water with methanol should decrease retention of poly(l-tryptophan) 11.5 kD. However, we observed the opposite. The plot of log k' versus the volume fraction of methanol shows a linear relationship (Figure 3). This unusual retention behavior was observed in small molecules by Lochmüller and co-workers[26]. They found that water actually was freed from the methanol-water associates when a small amount of acetonitrile or THF was added into the methanol-water mobile phase and the increased content of "free" water led to the increase of the retention time within a certain range. The small addition of methanol into THF-water mixture also frees water from the

associated THF-water complex and caused the increase in retention time. More study will be directed to understand the selectivity and optimization of separation of polymers with different mobile phases.

CONCLUSION

The retention behavior of poly(l-tryptophan)s and poly(d,l-tryptophan)s were examined. It is found that their retention behavior can be explained in terms of LSS model. It is observed that retention time for high molecular weight poly(l-tryptophan)s is longer than that of poly(d,l-tryptophan)s under the same mobile phase composition. When methanol is added into THF-water mobile phase, the retention time becomes larger. The mechanism and explanation are suggested for such retention behavior.

REFERENCES

1. Barth, H. G.; Mays, J. W. eds Modern Methods of Polymer Characterization, Wiley, New York, 1991.
2. Glöckner, G. Polymer Characterization by Liquid Chromatography; Elsevier, 1987.
3. Armstrong, D.W.; Bohem, R.E. J. Chromatogr. Sci., 22: 378 (1984).
4. Jandera, P.; Rozkosna, J. J. chromatogr. 362: 325 (1986).
5. Kirkland, J. J. J. Chromatogr., 125: 231 (1976).
6. Stadalius, M. A.; Quarry, M.A.; Mourey, T. H.; Snyder, L. R. J. Chromatogr., 358: 1 (1986).
7. Stadalius, M. A.; Quarry, M.A.; Mourey, T. H.; Snyder, L. R. J. Chromatogr., 358: 17 (1986).

8. Snyder, L.R.; Stadalius, M.A.; Quarry, M.A. Anal. Chem., 55: 1412 A (1983).

9. Glöckner, G.; VanDen Berg, J. H. M. Chromatographia, 19: 55 (1984).

10. Glöckner, G.; Van Den Berg, J. H. M. J. Chromatogr., 317: 615 (1984).

11. Armstrong, D.W.; Bui, K. H. Anal. Chem., 54: 706 (1982).

12. Glöckner, G.; Van Den Berg, J. H. J. Chromatogr., 352: 511 (1986).

13. Bohem, R. E.; Matire, D. E.; Armstrong, D. W.; Bui,K.H. Macromolecules, 17: No. 3, 400 (1984).

14. Lochmüller, C. H.; McGranaghan, M. B. *Anal. Chem.*, 61: 2449 (1989).

15. Barth, H. G., Janca, J., Polymer Analysis and Characterization, Wiley, New York, 1992.

16. Yau, W.W.; Kirkland, J. J.; and Bly, D.D., Modern Size Exclusion Chromatography, Wiley, New York, 1979.

17. Hager, D., J. Chromatogr., 187: 285 (1980).

18. Grubistic, Z.; Rempp, P., and Benoit, H., Polymer Lett., 5: 753 (1967).

19. Giddings, J. C.; Kucera, E.; Russell, C. P.; and Myers, M.N., J. Phy. Chem., 72: 4397 (1968).

20. Snyder, L.R.; Kirkland, J. J., Introduction to Modern Liquid Chromatography, Wiley, New York, 1979.

21. Matire, D. E. and Bohem, R. E., J. Phys. Chem., 87, 1045 (1983).

22. Lochmüller, C. H., and Wenzel, T. J., in Physical Methods of Chemistry, 2nd ed., Vol. X., eds. Rossiter, B. W. and Baetzold, R.C., pp 85-161, Wiley, New Nork, 1993.

23. Snyder, L.R.; Stadalius, M. A.; Quarry, M. A. Anal. Chem., 55, 1413A (1983).

24. Snyder, L. R.; Dolan, J. W. DrylabG Users Manual; LC Resources; California, 1986.

25. Quarry, M. A.; Grob, R. L.; Snyder, L. R. Anal. Chem., 58: 907 (1986).

26. Lochmüller, C. H.; Hamzavi-Abedi, M.A.; and Ou, Chu-Xiang, J. Chromatogr., 387: 105 (1987).

Received: January 19, 1994
Accepted: February 1, 1994

JOURNAL OF LIQUID CHROMATOGRAPHY, 17(14&15), 3191-3199 (1994)

MONITORING OF ORIGINATED POLYMER IN PURE MONOMER WITH GRADIENT POLYMER ELUTION CHROMATOGRAPHY (GPEC)®*

W. J. STAAL[1], P. COOLS[2], A. M. VAN HERK[2], AND A. L. GERMAN[2]
[1]Waters Chromatography Group
Penningweg 33
P.O. Box 166
4870 AD Etten-Leur, The Netherlands
[2]Eindhoven University of Technology
Laboratory of Polymer Chemistry and Technology
P.O. Box 513
5600 MB Eindhoven, The Netherlands

ABSTRACT

The analysis of the amount of polymer in pure monomer with cloudpoint measurements gives, only a qualitative answer. Now by use of a liquid chromatograph and gradient elution the amount of polymer can be measured fully automated. Also an impression of the molar mass can be achieved.

INTRODUCTION

One of the important parameters in polymerization is the purity of the monomers.The factors that have a negative influence on the polymerization process are, contaminants and polymer formed during storage. One of the most

* GPEC is a registered trademark of the Waters chromatography group

common tests to check the precense of polymer in the monomer is the cloudpoint test. This test is described in the ASTM method 2010, polymer content of styrene monomer [1].

By adding a nonsolvent to the monomer the polymer will precipitate. This can be visually observed as a cloudpoint. This test gives a qualitative answer. In this case polystyrene and its monomer are taken as example. As a nonsolvent, methanol is used the most for this application.The problem with methanol is that the oligomers of polystyrene are soluble up to n = 5. Therefore these oligomers are not detectable with the methanol cloudpoint test. Another reason that this test is just a qualitative one is because of the amount of methanol, required for the precipitation, is dependent of the molecular mass of polystyrene [2].

Chromatography can also be applied for this application. With Gel Permeation Chromatography (GPC) a separation can be achieved on molecular mass. The problem with this technique is the limited separation. For separating traces of polymer from the monomer, the monomer must be injected without dilution. This leads to an overload of the column and as result a bad separation.With Gradient Polymer Elution Chromatography (GPEC) traces of polymer and oligomers [3] can be separated from the pure monomer.

The styrene monomer is injected pure in a stream of a nonsolvent (water). In this nonsolvent, monomer, oligomers and polymer are retained on the top of the column or a guard column [4] as suspension.

By adding a solvent (THF) to the nonsolvent (water) in a gradient the monomer, oligomers and polymer will redissolve and elute from the column [5]. The separation is so good that even oligomers are also separated from the monomer. Very small amounts of polymer can be detected with this method. Also the molecular mass can be calculated referring to well defined polymer standards [4], [6].

EXPERIMENTAL

HPLC Equipment

Gradient elution was performed with a 4 solvent gradient pump (Waters Model 600E). A Waters intelligent sample processor (WISP, Model 712B) was used to inject 5μl pure styrene. A Waters photodiode array detector (Model 996) was used to monitor the formed polystyrene scanning from 200 to 345 nm. The chromatogram was reproduced by the Waters Millennium 2010 photodiode array software and recorded by a NEC Powermate 486/33i computer. The Waters group is located in the U.S.A.

The water was purified with a Milli-Q system from the Millipore Corporation. Tetrahydrofuran (THF) without stabilizer was obtained from Rathburn U.K.

HPLC Conditions

The injection volume of the monomer samples was 5 μl without dilution. A linear gradient was used starting with 100% water (as nonsolvent) to 100% THF (as good solvent) in 30 min. The eluent flow was 1 ml/min. The temperature was 30°C.

The column was a Waters Nova-Pak CN, 3.6 x 150 mm, column packed with spherical 4μ, 60Å particles. The polystyrene sample was the DOW 1683 broad standard (U.S.A.). The polystyrene narrow standards were obtained from Polymer Laboratories (U.K.). The styrene monomer (polymer free) was obtained from Nevcin Polymer, the Netherlands. With this monomer all dilutions were made. The stored styrene (containing polymer) was obtained from the University of Technology, Eindhoven, the Netherlands.

Cloudpoint Observations

The micro cloudpoint titrations were performed in a 4 ml Waters WISP vial, sealed with a self sealing septum. The temperature was at roomtemperature (24°C.). The

nonsolvent, methanol was added with a 100 µl syringe, Hamilton (U.S.A.) The cloud-cloudpoints were observed visually, using a black background. The mixing was performed by intensive shaking during titration. The methanol was obtained from Rathburn (U.K.).

RESULTS AND DISCUSSION

It is demonstrated in Table 1 that the cloudpoint is strongly dependent of the molecular mass and a little dependent of the amount of polymer. With spectro-photometers the intensity of the cloudiness can be measured as indication of the amount of polymer except for the oligomers [1]. The problem is that this suspensions are not stable. In some cases it takes 5-15 min. before the suspension is formed. With polymers at the level of molecular mass a million and more immediately flocculation takes place. This makes a quantitative spectrofotometric method complicated.

With the gradient method the concentration (peak hight or peak area of oligomers and polymer) can be calculated. Also an indication of the molecular mass can be achieved. In Figure 1 the contour plot of a test mixture of styrene and polystyrene standards is shown. This is a good demonstration of the separation power of a water/THF gradient between monomer, oligomers and polymer.

Figure 2 is a contour plot of one month stored destillated styrene at -4°C. Oligomer formation (A) and polymer formation (B) has already taken place. The level is about 1500 ppm (calculated from Figure 1).

In Figure 3 polystyrene (Dow 1683 Mw = 250,000) has been spiked to the styrene sample from Figure 2. The benefit of using a photodiode array detector is to monitor differences in the UV spectrum. Normally the UV spectrum from a molecular mass 1000 up to 20 million g/mol polystyrene is uniform. When the UV spectrum is different, other response factors have to be applied with GPEC. Two different response factors have to be applied. One for dissolved polystyrene and one for a turbid suspension of polystyrene in a nonsolvent water-THF

TABLE 1

Cloudpoints of polystyrene in styrene*

Sample	Conc. Mg/ml (PPM)	Sample volume µl styrene (Containing polymer)	Added NS µl methanol at cloudpoint*	Nonsolvent % methanol
Polystyrene Dow 1683 (Mw 250,000)	12,000	400	130	24,5
	1,200	400	150	27,3
	120	400	200	33,3
	12	400	Not visually detectable	-
Polystyrene (Mw 11,600)	10,000	400	265	39,8
	1,000	400	370	48,1
	100	400	520	56,5
	10	400	Not visually detectable	-
Styrene TUE	unknown	400	150	27,3

** Visual observation of the cloudpoint at a temperature at 24,0°C.*

combination. This colloidal suspension formation from molar mass 50,000 g/mol and larger was described by Engelhart and others [7].

In figure 3 the appearance of this colloidal suspension is clearly demonstrated by the spiked Dow 1683. This peak gives a response, far in the visual wavelength area. Comparing with dissolved polystyrene, the normal UV absorption spectrum of polystyrene is from the maximum at 261 nm to 300 nm.

CONCLUSIONS

Gradient Polymer Elution Chromatography is an easy technique to monitor the amount of polymer in pure monomer. Also an indication of the molar mass of the polymer can be achieved. No sample preparation is needed, pure monomer can be

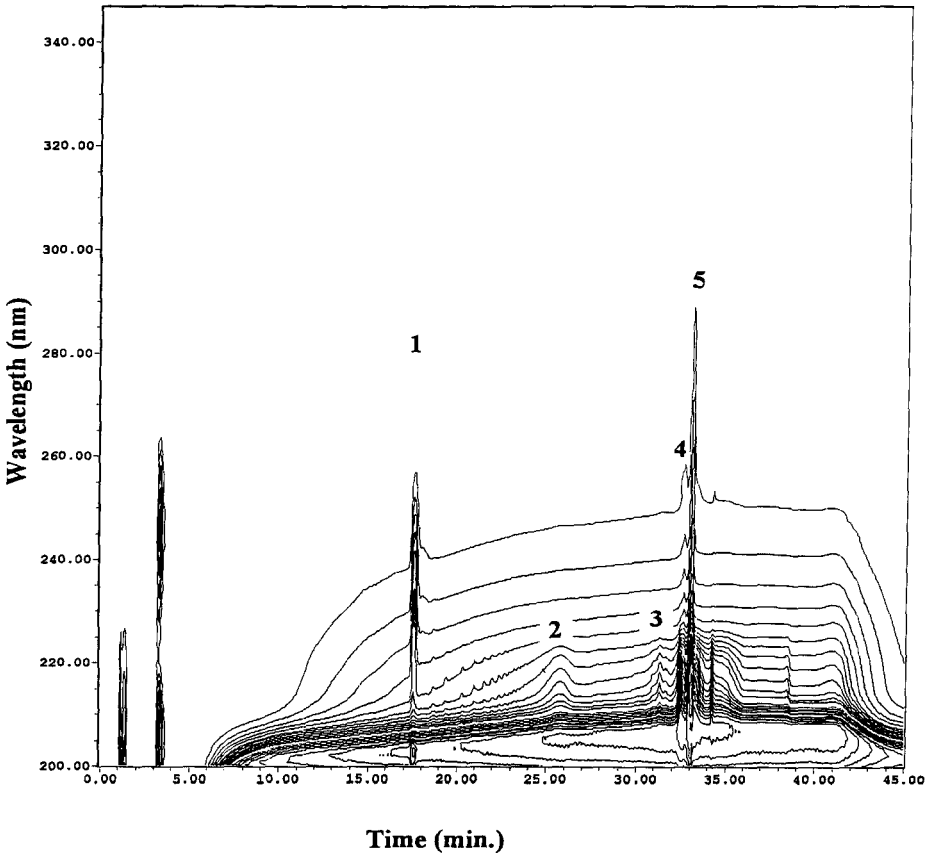

FIGURE 1. Retention time behaviour of styrene monomer and narrow polystyrene standards. Styrene monomer (1), oligomer Mw 2,020 (2), polymer Mw 50,000 (3), Mw 340,000 (4) and the summation of Mw 3,000,000 and Mw 8,000,000 (5). Concentration 2.7 mg/ml THF.

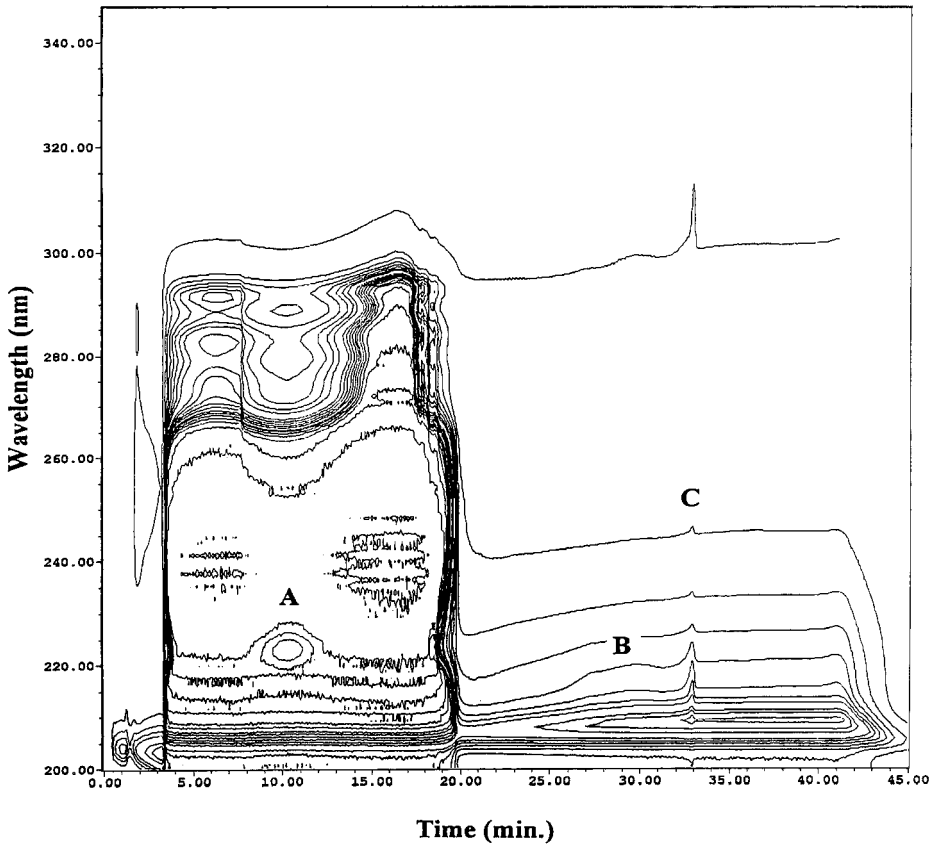

FIGURE 2. Stored styrene monomer and formed oligomer and polymer. Styrene monomer (A), oligomer content (B) and polymer content (C).

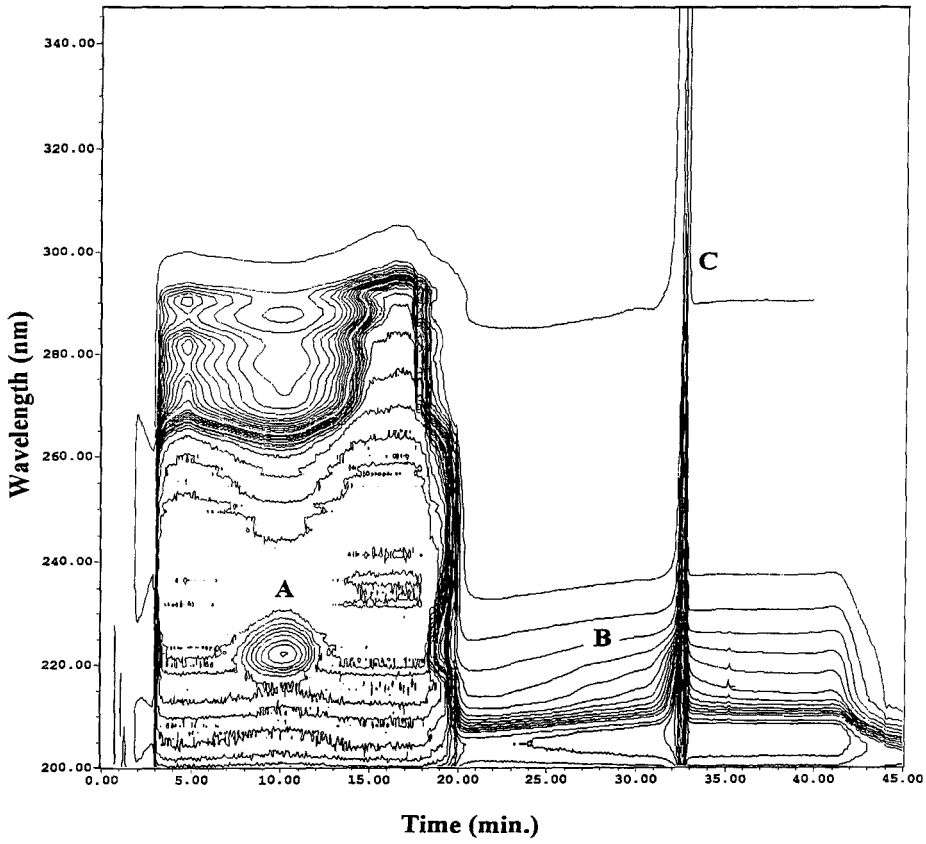

FIGURE 3. A mixture of stored styrene monomer and polystyrene (Dow 1683 Mw 250,000, 12,000 ppm). Styrene monomer (A), oligomer (B) and polymer (C / Dow 1683)

injected. With the use of an autosampler large numbers of samples can be handled. With the use of a photodiode array detector differences in response factors can be monitored. In the case of non absorbing polymers a mass detector can be used. This method can be very useful to monitor the start of a polymerization process, if no initial inhibition takes place.

FUTURE OUTLOOK

For detection at a level of 10 PPM and lower, more UV transparant solvents like dichloromethane and cyclohexane are advisable. In the case of non-UV absorbing polymers an Evaporative Light Scattering Detector (ELSD) can be applied.

ACKNOWLEDGMENT

Special aknowledgements are given to mr. J. Brassers and mr. C.Evers, arranging the equipment, and miss G. King of General Electric-ABS, from the plant in Amsterdam, for doing the HPLC analysis work.

REFERENCES

1. ASTM method D2121-68.
2. A.R. Mathieson, J. Colloid Sc. 15, 387-401 (1960).
3. J.J. Lewis, L.B. Rogers, R.E. Pauls, J. Chromatogr., 264, 339-356 (1983).
4. G. Glöckner, Chromatographia, 25, 854-860 (1988)
5. W.J. Staal, proceedings of the international technical symposium on the GPC and HPLC analysis of polymers and additives, Oct. 1989, Newton, Mass, U.S.A., p.518.
6. R.A. Shalliker, P.E. Kavanagh, I.M. Russel, J. Chromatogr., 558, 440-445 (1991)
7. R. Schultz, H. Engelhart, Chromatographia, 29, 205-213 (1990).

Received: October 29, 1993
Accepted: December 17, 1993

JOURNAL OF LIQUID CHROMATOGRAPHY, 17(14&15), 3201-3219 (1994)

TEMPERATURE RISING ELUTION FRACTIONATION (TREF) CHARACTERIZATION OF POLYPROPYLENE COPOLYMERS

FRANCIS M. MIRABELLA, JR.
Quantum Chemical, Corp.
Process Research Center
8935 North Tabler Road
Morris, Illinois 60450

ABSTRACT

The fractionation by temperature rising elution fractionation (TREF) of poly(propylene–ethylene) copolymers containing a minor fraction of ethylene was described. A method was developed to determine the ethylene concentration distribution in these copolymers. A poly(propylene–ethylene) copolymer containing 29% wt. ethylene was fractionated by preparative TREF. The fractions were analyzed by analytical TREF, and by ^{13}C NMR spectroscopy to determine the average ethylene concentration in each fraction. A calibration curve relating analytical TREF elution temperature and ethylene concentration was established. It was shown that the weight–average TREF elution temperature was the appropriate average elution temperature to correlate with the weight percent ethylene determined by ^{13}C NMR spectroscopy. This calibration curve was used to obtain the ethylene concentration distribution for a series of poly(propylene–ethylene) copolymers from their analytical TREF elution temperature chromatograms. The average ethylene concentration was calculated from these ethylene concentration distributions and found to be in good agreement with the ethylene concentration determined by ^{13}C NMR. Extrapolation of the calibration curve to 0% ethylene yielded a predicted analytical TREF elution temperature of 108.7°C, which was in excellent agreement with the experimental elution temperature for isotactic polypropylene of 108.7°C.

INTRODUCTION

The development of polymeric materials has increasingly been in the direction of more complex mixtures of polymers. This has emphasized the need for methods to separate the components of such mixtures, and to fractionate component polymers in order to reveal their structural distribution by subsequent analysis and characterization. For example, a formulation of A, B, C, etc. polymers can be separated into each polymer type in order to gain an understanding of the basic composition of the formulation. Each polymer type can be further fractionated into a sufficient number of narrow fractions based on chemical composition in order to gain an understanding of the copolymer composition distribution, stereochemical distribution, monomer sequence distribution, etc. Separations and fractionations of these types have been accomplished by a variety of techniques. However, the technique which has emerged as that of choice is temperature rising elution fractionation (TREF). This technique has been highly developed for both analytical and preparative fractionations over the last 40 years with the major developments occurring during the last 15 years.[1]

The TREF technique is based on the crystallizability of the polymer for the purpose of achieving a compositional separation of molecular species. It is composed of two basic steps. In the first step a very slow crystallization is done to predispose the molecular species to sequential elution from low to high crystallizability. In the second step the crystallized sample is loaded onto a steel column through which a good solvent is passed, as the temperature is uniformly increased. When each molecular species is subjected to its melting temperature in the presence of the solvent, it melts and rapidly dissolves, and elutes from the column to be detected by a concentration detector. The separation is based on composition, as the major determining parameter of crystalizability, and is little influenced by molecular weight for high polymers. A recent review considers details of the technique.[1]

The TREF technique has been frequently applied to the fractionation of poly(ethylene–α–olefin) copolymers, which are rich in ethylene, in order to

determine the short–chain branching distribution (SCBD).[1] The TREF technique was used to elucidate the structure of such ethylene copolymers.[2–4] Other applications have been to the determination of the composition distribution of low density polyethylene, ethylene–vinyl acetate copolymers and polypropylene, as discussed in the review by Wild.[1] The structure of a high impact strength ethylene/propylene copolymer was comprehensively determined with the use of preparative and analytical TREF, as the central techniques for separating and characterizing the components of this complex mixture of copolymers.[5] In that work the components of the impact poly(ethylene–propylene) were separated by preparative TREF and identified as isotactic polypropylene, essentially amorphous ethylene/propylene rubber (EPR), polyethylene with a small fraction of propylene comonomer and a distribution of poly(ethylene–propylene) copolymers with partial crystallinity. Further, analytical and preparative TREF were used to fractionate and subsequently characterize the stereoregularity distribution of the polypropylene homopolymer and the chemical structure distribution of the EPR and semicrystalline poly(ethylene–propylene) copolymers.

The purpose of this work was to develop additional applications of the TREF technique. Specifically, the characterization of ethylene/propylene copolymers was extended to the fractionation of statistical copolymers of ethylene and propylene in order to determine the distribution of ethylene over all copolymer chains.

EXPERIMENTAL

Materials

A series of commercial poly(propylene–ethylene) copolymers with a small fraction of ethylene comonomer and a commercial isotactic polypropylene homopolymer were used in this study. Relevant data are given in Table 1 for these polymers.

Preparative TREF

Large fractions of the resin sample E/P–A were obtained by preparative TREF. The apparatus and procedure have been described elsewhere.[5] Specifics of

TABLE 1

Properties of Random Polypropylene Copolymers and Polypropylene Homopolymer.

	Ethylene* % wt	$\bar{M}_n$ x 10^{-4}	$\bar{M}_w$ x 10^{-4}	Calculated** Ethylene %
E/P–A	2.9	5.6	40.0	2.8
E/P–B	2.3	4.9	40.9	1.9
E/P–C	3.0	3.0	20.5	3.1
E/P–D	3.2	4.7	27.9	2.9
PP	0	–	–	–

*^{13}C NMR, precision is ± 0.2% wt.
** From equation 6, using Te (w)

the procedure used in this work were as follows. The resin was dissolved at a concentration of 4.0 g in 600 ml p–xylene and solution achieved at 130°C with gentle stirring. The solution was cooled in a programmable oil bath at –5°C/hr from 120°C to room temperature. This precipitate suspended in the p–xylene was poured into 100 ml of cold acetone to complete the precipitation of all polymers. The precipitate was slurried with about 35 g of diatomaceous earth, filtered and dried to recover a free flowing solid. This was introduced into the preparative TREF unit as shown schematically in Figure 1. P–xylene solvent was introduced, also. Fractions were taken by incrementally raising the temperature of the p–xylene while gently stirring the solvent in order to dissolve all polymers which melt and dissolve at the specified fraction temperature. A period of 1.5 hours was employed for complete dissolution. Temperature was very carefully controlled to ± 0.5°C of the specified temperature. The fractions were then removed at the specified temperature through a valve at the bottom of the apparatus. The polymer fractions dissolved in xylene were then poured into 1500 ml of cold acetone, the precipitate was filtered and dried to constant weight. The fractionation temperatures and fraction weights of the E/P–A resin are given in Table 2. The recovery was 93% by weight.

Analytical TREF

Polymer samples were dissolved at a concentration of 2 to 5 mg in 10 ml of p–xylene and solution achieved at 130°C with gentle stirring. The solutions were

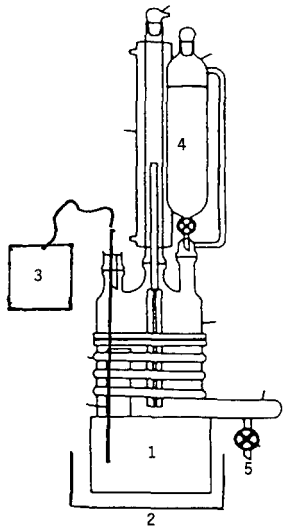

Figure 1 – Preparative temperature rising elution fractionation apparatus: 1. sample chamber, 2. heating mantle, 3. temperature sensor, 4. solvent reservoir, and 5. take–off valve.

TABLE 2

Characterization Data on the Preparative TREF Fractions of the Random Polypropylene Resin E/P–A

Fraction Number	Maximum Preparative TREF Temperature	Fraction Weight Percent	Weight Percent Ethylene ^{13}C NMR E	Molecular Weight x 10^{-4} Mn	Mw	Weight Average Analytical Elution Temperature Te(w)°C	Calculated Weight Percent Ethylene From Equation 6
1	86	35.7	4.9	2.8	17.4	83.6	5.2
2	90	9.4	4.6	2.2	4.8	90.0	3.8
3	94	8.5	3.0	3.2	9.6	92.8	3.3
4	98	15.5	2.0	6.7	22.1	97.7	2.3
5	104	24.0	1.7	10.8	46.2	101.0	1.6
Whole Polymer	–	–	2.9	5.6	40.0	95.3	2.8

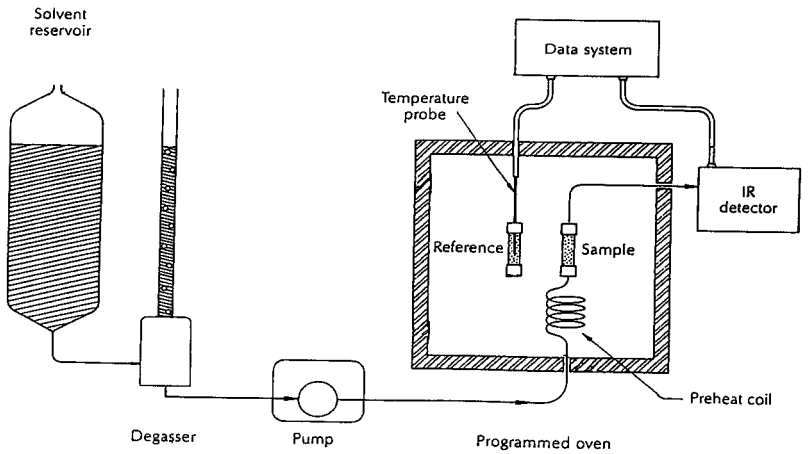

Figure 2 – Analytical temperature rising elution fractionation apparatus.

cooled in a programmable oil bath at –5°C/hr from 120°C to room temperature. Then 10 ml of cold acetone was added to the precipitated polymer in p–xylene and shaken gently. About 1 g of diatomaceous earth was added to the slurry and the entire contents were quantitatively loaded onto a steel column (250 mm x 10 mm i.d.). The column was connected into a system as shown schematically in Figure 2. Orthodichlorobenzene was pumped through the column at a rate of 3.0 ml/min while the temperature was increased at 4°C/min. The species eluting from the column were detected with an infrared detector set at a detection wavelength of 3.41μm (C–H stretch). The temperature inside a reference column with no sample but packed identically to the sample column was monitored with a temperature probe. This temperature was taken as that in the sample column. This procedure was expected to account for any temperature lag between the oven temperature and that inside the sample column and to give an accurate indication of the temperature inside the sample column. The detector response and elution temperature were digitized and stored in a computer. Subsequent computations were performed on digitized data.

^{13}C Nuclear Magnetic Resonance

^{13}C nuclear magnetic resonance was done on a Varian Gemini 200 super–conducting NMR system. Typical conditions were: 300 scans, 90° pulse angle, 10 sec. pulse delay (ca. 1 h scan accumulation); 10 mm tubes were used for relatively small sample mass (ca. 400 mg). Samples were swelled with a minimum volume (ca. 2 ml) of TCB. Data were handled according to standard techniques.[6]

Gel Permeation Chromatography

Molecular weight distributions were determined on a Waters 150C GPC at 140°C in trichlorobenzene.

RESULTS AND DISCUSSION

Modern polymer formulations routinely produced by the plastics industry have tended to become more complex in the number of chemically different polymer components and the structural distributions of each of the polymer components. The TREF technique is ideally suited to the compositional separation of the components and to fractionate the individual components to reveal their structural distribution. The TREF technique is effectively insensitive to molecular weight variations for polymer species with $>10^4$ molecular weight.[1]

Polypropylene and its copolymers represent such a complex array of formulations. In previous work it was shown that polypropylene homopolymer and copolymers were readily separable by TREF.[5] The analytical TREF technique was used to separate the components and to tentatively identify each component by developing a list of elution temperature ranges for a set of known polymer types. Preparative TREF was then used to obtain large fractions of polymer from a series of elution temperature ranges. The fractions were then characterized to confirm the identity of the components and the structural distributions within each component, as previously indicated by the analytical TREF.

Currently, the only calibration of analytical TREF is for the determination of the comonomer distribution [i.e. the short–chain branching distribution (SCBD)] in

poly(ethylene–α–olefin) copolymers which are rich in ethylene.[1] Other common copolymers related to these are so–called random polypropylenes, as they are known in the industry, which contain a minor amount (ca. 1–5% weight) of ethylene comonomer and are known to be statistical copolymers. These random polypropylenes are used in a variety of applications, including film, sheet, bottles, etc. The distribution of ethylene over all copolymer chains is an important variable in the determination of the polymers performance in such properties, such as stiffness, impact, hardness, hot–tack, etc. The TREF technique may be used to determine the ethylene distribution over all copolymer chains, if a calibration of ethylene concentration as a function of TREF elution temperature were available.

The analytical TREF elution temperature chromatogram for random polypropylene resin E/P–A is shown in Figure 3. The elution temperature range is from approximately 75°C to 105°C. This broad range of elution temperature implies a rather broad distribution of ethylene concentration over all copolymer chains. The E/P–A resin was fractionated in the preparative TREF into five fractions with the upper fractionation temperature for each fraction as given in Table 2. The fractions were analyzed by ^{13}C NMR and GPC to determine the average weight percent of ethylene and molecular weight for each fraction, and these data are given in Table 2, also.

Each fraction was run in the analytical TREF and the elution temperature chromatograms are presented in Figures 4 and 5. The analytical TREF chromatograms reveal that the preparative TREF fractions tend to be broad and in some cases multimodal. It would be desirable to obtain very narrow fractions, however, a relatively large amount of material (ca. 200–400 mg) is needed for the ^{13}C NMR analysis of each fraction and this would require significantly more preparative fractionation work to be done.

The average weight percent of ethylene in each preparative TREF fraction is known (Table 2). In order to calibrate the analytical TREF it is necessary to

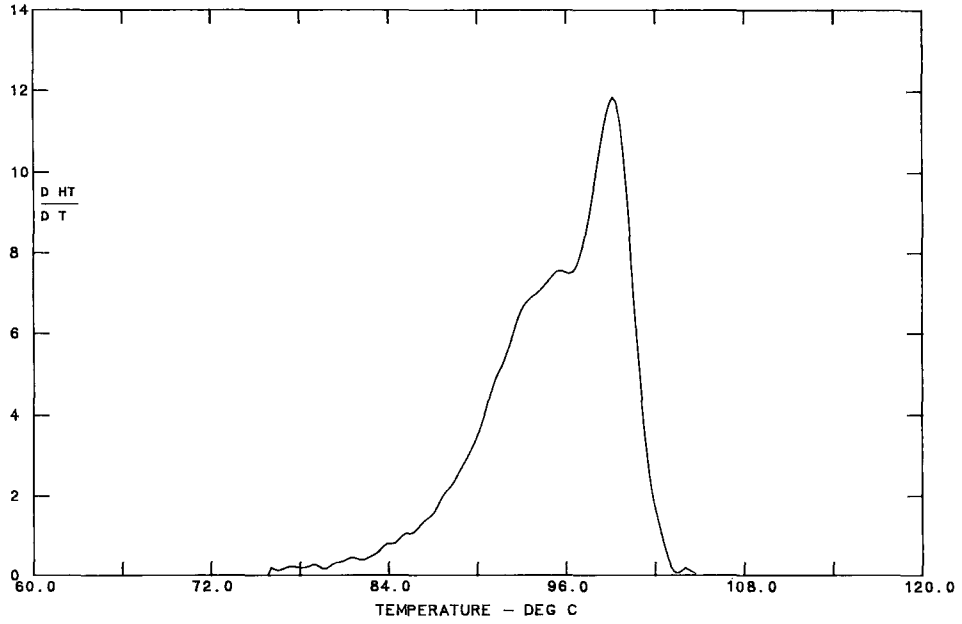

Figure 3 – Analytical TREF temperature chromatogram of random poly(propylene–ethylene) copolymer E/P–A.

determine the correct "average" elution temperature from the analytical TREF curves (Figures 4 and 5). This may be accomplished by making the following two critical assumptions. First, it is assumed that the average weight percent ethylene in the fractions determined by NMR spectroscopy (E) is the summation of the ethylene concentration (E_i) in all concentration "slices" of the distribution (C_i):

$$E = \sum_i C_i E_i \qquad (1)$$

Second, it is assumed that the correlation of analytical TREF elution temperature (T_e) with average weight percent ethylene for the fractions is represented by a straight line equation:

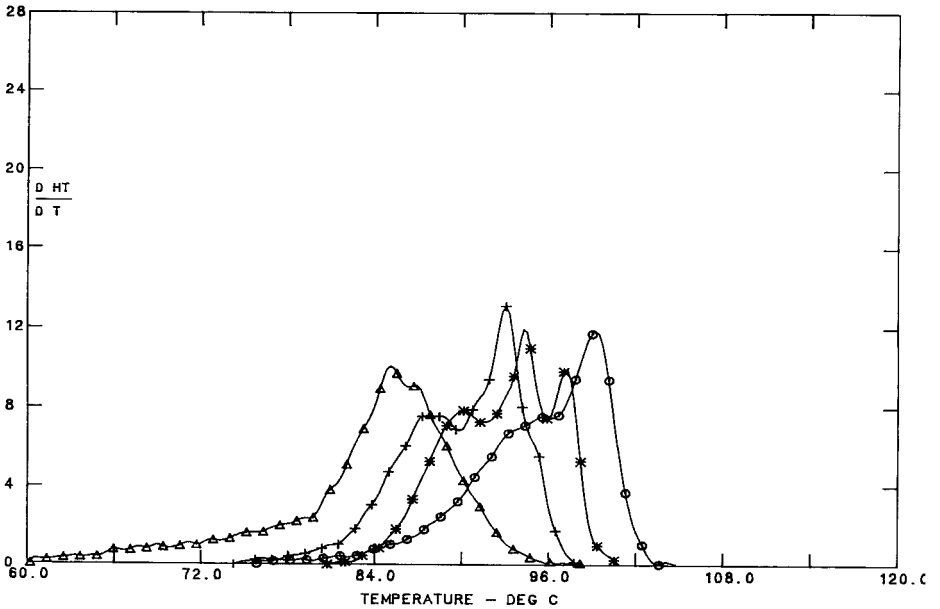

Figure 4 – Analytical TREF temperature chromatograms of preparative TREF fraction 1 Δ, fraction 2 +, fraction 3 ✱, and whole polymer E/P–A O.

$$E = a\,Te + b \qquad (2)$$

where a is the slope and b is the intercept of the straight line. This second assumption limits the calibration curve to a specified range of E values, and it also ignores band–broadening effects in the analytical TREF. If equation 2 is substituted for E_i in equation 1 we obtain:

$$E = \sum_i C_i\,(aTe_i + b) \qquad (3)$$

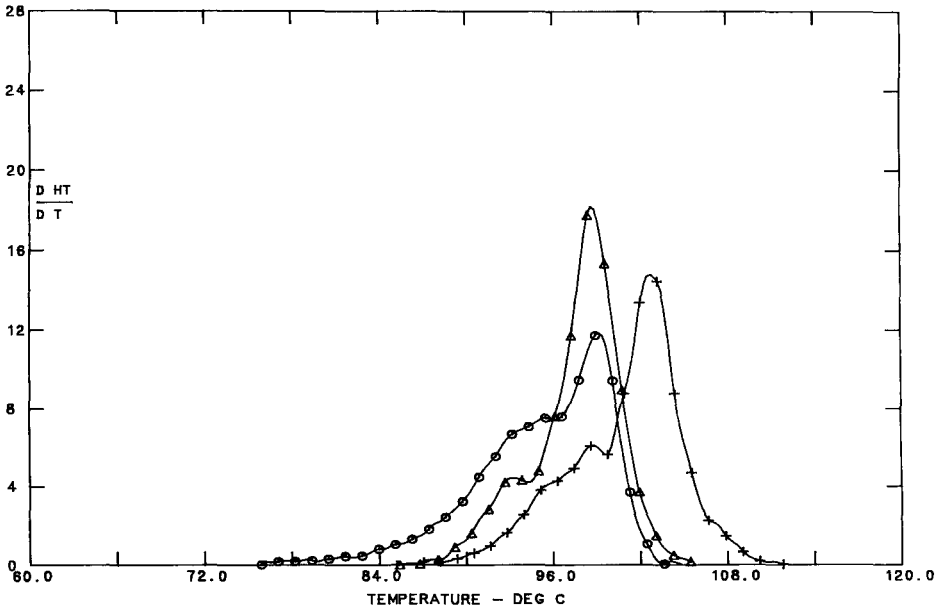

Figure 5 – Analytical TREF temperature chromatograms of preparative TREF fraction 4 Δ, fraction 5 +, and whole polymer E/P–A O.

Expanding equation 3 and dividing by $\sum_i C_i$, which is normalized to unity, yields:

$$E = a \sum_i C_i \, Te_i / \sum_i C_i + b \qquad (4)$$

Equation 4 shows that the average weight percent of ethylene determined by NMR spectroscopy (E) is correlated with the weight–average TREF elution temperature ($T_e(w)$) where $T_e(w) = \sum_i C_i Te_i / \sum_i C_i$. The data obtained from the analytical TREF is in terms of concentration "slices" from the infrared detector (i.e.

heights, H_i, where H_i = absorbance at each point on the elution curve) and an elution temperature (Te_i). Therefore, the weight–average elution temperature is:

$$Te(w) = \sum_i H_i \, Te_i / \sum_i H_i \qquad (5)$$

The weight–average elution temperature was calculated for each fraction and these are presented in Table 2. The values of average ethylene concentration (E) and weight–average analytical TREF elution temperature ($T_e(w)$) from Table 2 were fitted to a straight line by linear regression in order determine the constants in equation 2 and this resulted in the calibration curve:

$$E = -0.206Te + 22.39 \qquad (6)$$

The correlation coefficient for the linear regression was r = 0.95. The calibration curve is plotted in Figure 6. Equation 6 is the calibration curve for deconvoluting analytical TREF elution temperature chromatograms into ethylene concentration distribution curves. The range of validity of equation 6 is up to about 10% wt. of ethylene. The analytical TREF elution temperature chromatogram of E/P–A in Figure 3 was deconvoluted into the ethylene concentration distribution curve in Figure 7 by the use of equation 6. The weight–average elution temperature (Te (w)) for resin E/P–A was 95.3°C, as given in Table 1. From equation 6 this gives an ethylene weight percent of 2.8% wt. which is in good agreement with that determined by ^{13}C NMR of 2.9% wt. It should be noted that equation 6 implies that at zero weight percent ethylene (polypropylene homopolymer) the elution temperature is Te = 108.7°C. The analytical TREF elution temperature chromatogram for a polypropylene homopolymer (PP) is shown in Figure 8. The peak elution temperature of this narrow peak is 108.7°C in excellent agreement with that calculated from equation 6.

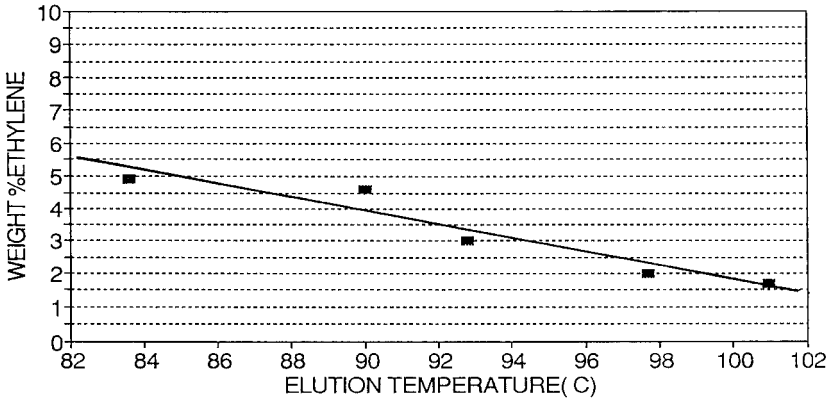

Figure 6 – Calibration curve for analytical TREF relating percent ethylene and TREF weight–average elution temperature.

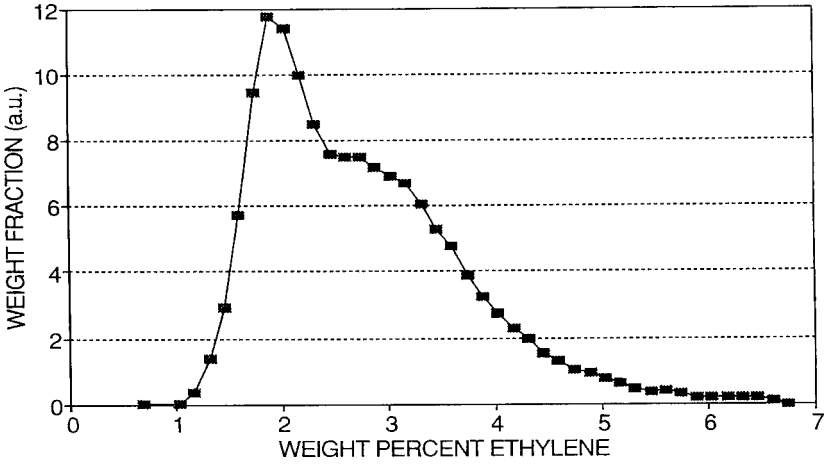

Figure 7 – Ethylene concentration distribution of random copolymer E/P–A.

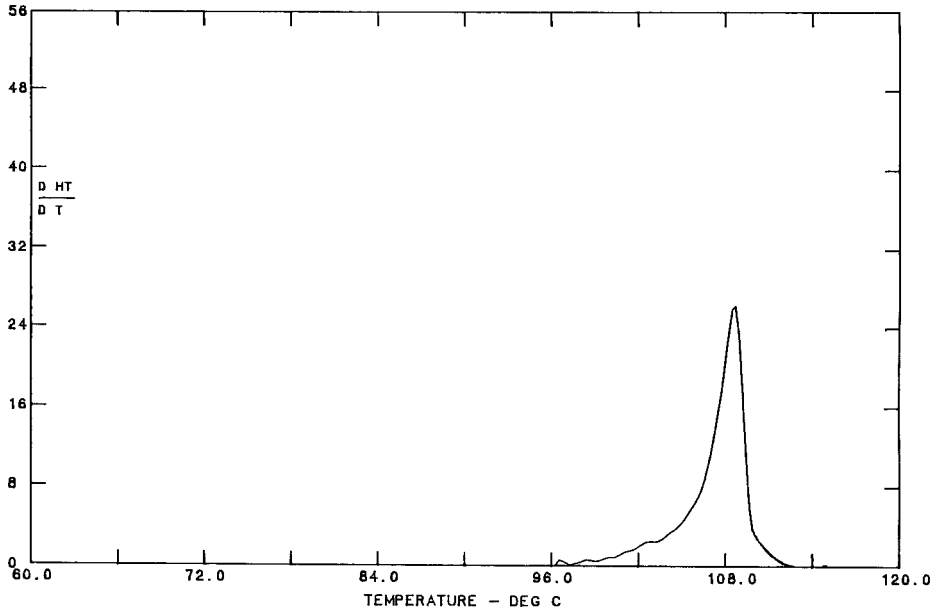

Figure 8 – Analytical TREF temperature chromatogram of isotactic polypropylene.

The analytical TREF elution temperature chromatograms and the ethylene concentration distribution curves, obtained by deconvolution of the chromatograms with equation 6, are shown in Figures 9–11 for random polypropylene resins E/P–B, E/P–C and E/P–D, respectively. It may be observed in Figures 7 and 9–11 that the ethylene concentration distributions of the four random polypropylene resins differ considerably. The weight percent ethylene for random polypropylenes E/P–B, E/P–C and E/P–D were calculated from equation 6 using the weight–average elution temperature, Te(w), obtained from the TREF elution temperature chromatograms, shown in Figures 9–11. These data are presented in Table 1. The agreement between the calculated and experimentally determined NMR values of weight percent ethylene in Table 1 may be seen to be quite good within the precision of the NMR

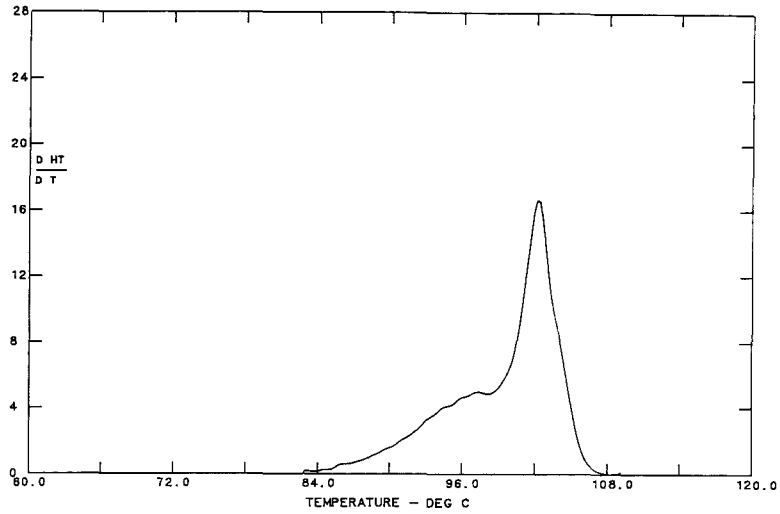

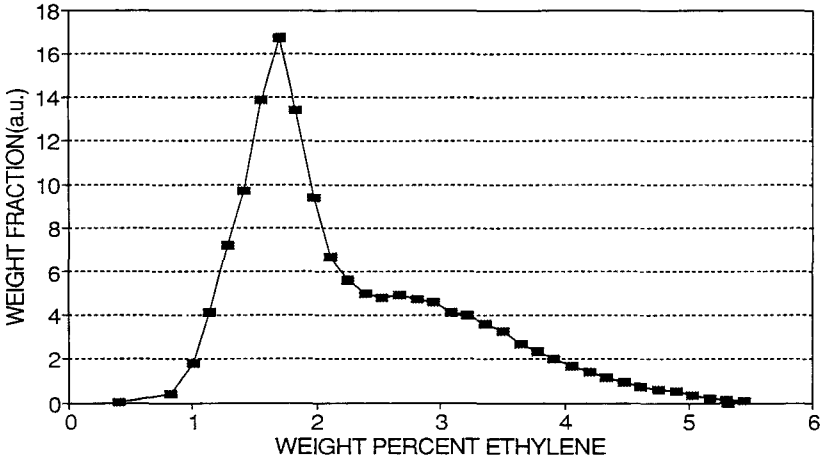

Figure 9 – Analytical TREF temperature chromatogram and ethylene concentration distribution of random copolymer E/P–B.

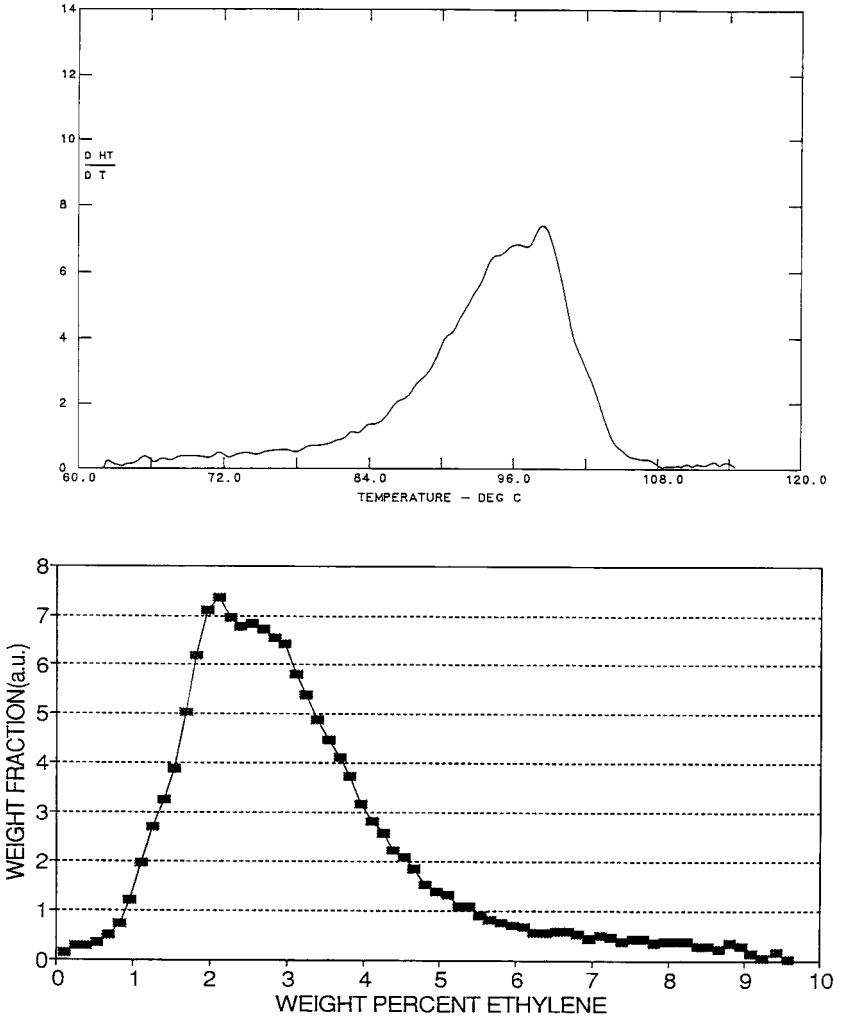

Figure 10 – Analytical TREF temperature chromatogram and ethylene concentration distribution of random copolymer E/P–C.

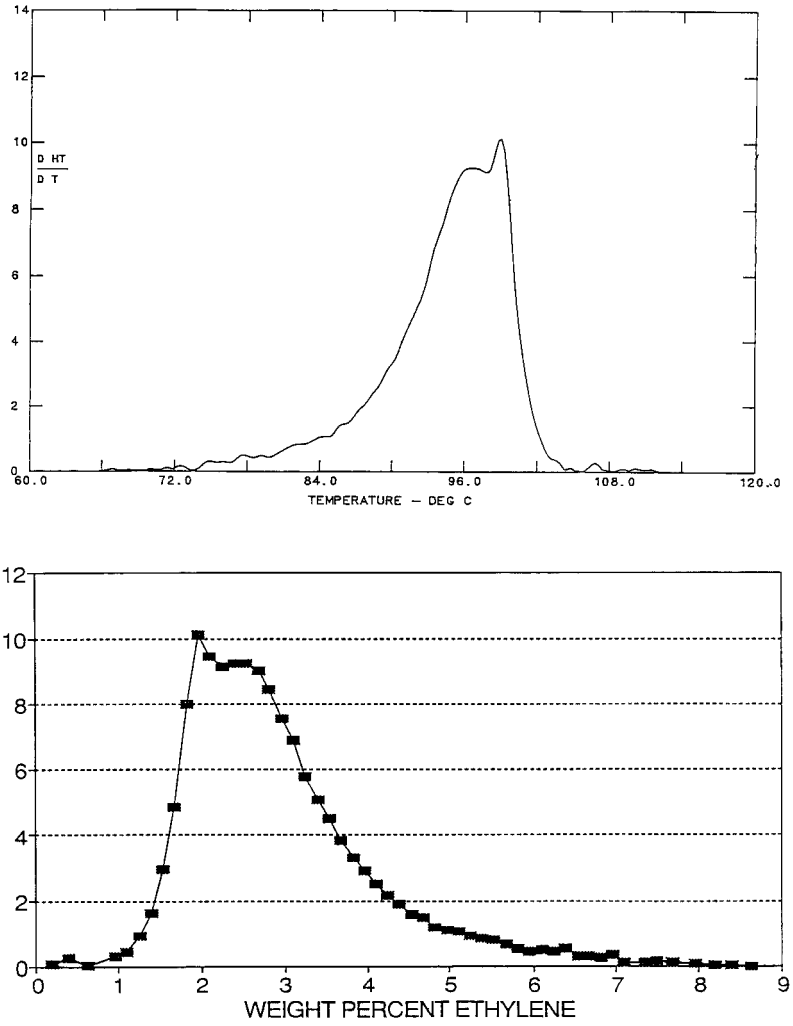

Figure 11 – Analytical TREF temperature chromatogram and ethylene concentration distribution of random copolymer E/P–D.

measurements of ± 0.2% wt. ethylene. The fact that the ethylene content of the random polypropylenes may be recovered from TREF elution temperature chromatograms with the use of equation 6 provides further evidence of the validity of the TREF calibration described herein.

CONCLUSIONS

Application of analytical temperature rising elution fractionation to the composition distribution of polypropylene copolymers was described. In the present work a method was developed to determine the ethylene concentration distribution in poly(propylene–ethylene) copolymers (called random polypropylenes) with a minor fraction of ethylene (ca. 1 to 5 weight percent). A calibration of the analytical TREF was developed correlating elution temperature and ethylene concentration. It was shown that it was the weight–average elution temperature from the analytical TREF chromatogram that correlated with the weight percent ethylene determined by ^{13}C NMR spectroscopy. It should be noted that this also applies to the short–chain branching distribution in poly(ethylene–α–olefin) copolymers; i.e. it is the weight–average TREF elution temperature that correlates with the average short–chain branching in these copolymers. It was also shown that the ethylene concentration distributions of a series of commercial random polypropylene resins were broad and differed in their characteristic shapes. The weight percent ethylene estimated from these distributions was shown to agree with that determined by ^{13}C NMR spectroscopy. The calibration curve was used to predict the TREF elution temperature of polypropylene homopolymer, which agreed well with the experimental value. This indicated that the calibration curve was valid to low levels of ethylene concentration and extrapolation may be used up to about 10% weight of ethylene.

The ethylene concentration distributions of polypropylene containing a minor fraction of ethylene should prove useful in studies of the crystallization behavior of these copolymers in analogy to the use of short–chain branching distributions in crystallization studies of poly(ethylene–α–olefin) copolymers, such

as linear low density polyethylene (LLDPE). Such studies of the crystalline morphology of random polypropylene should prove useful for the correlation of the solid–state structure with mechanical properties, such as stiffness, impact, hardness, hot tack, etc.

ACKNOWLEDGEMENTS

The author would like to acknowledge the expert assistance of Susan Barnett for the preparation of the TREF fractions and the analytical TREF measurements. The author is also grateful for helpful discussions with Dr. H. Mavridis.

REFERENCES

1. L. Wild, Adv. Polym. Sci., 98, 1 (1990).
2. L. Wild, D. Ryle, D. Knobeloch and I. Peat, J. Polym. Sci., Polym. Phys. Ed., 20, 441 (1982).
3. T. Usami, Y. Gotoh and S. Takayama, Macromol., 19, 2722 (1986).
4. F. M. Mirabella, Jr. and E. A. Ford, J. Polym. Sci., Polym. Phys. Ed., 25, 777 (1987).
5. F. M. Mirabella, Jr., Polymer, 34, 1729 (1993).
6. J. C. Randall, Polymer Sequence Determination: Carbon–13 NMR Method, Academic Press, New York, 1977.

Received: November 24, 1993
Accepted: January 20, 1994

JOURNAL OF LIQUID CHROMATOGRAPHY, 17(14&15), 3221-3238 (1994)

SEPARATION OF CHARGED LATEX PARTICLES BY ELECTRICAL FIELD-FLOW FRACTIONATION

MARTIN E. SCHIMPF*, DALE D. RUSSELL, AND J. KATHLEEN LEWIS
Department of Chemistry
Boise State University
Boise, Idaho 83725

ABSTRACT

The retention of both underivatized and carboxylated polystyrene latex beads by electrical field-flow fractionation (ElFFF) was investigated using a 2 mM aqueous solution of quinone-hydroquinone as the carrier liquid. The quninone-hydroquinone redox couple passes current with less polarization of the electrodes than carrier liquids previously employed. Underivatized beads, ranging in diameter from 0.15 to 0.74 μm eluted in the normal mode, while carboxylated beads larger than 1 μm eluted in the steric mode. Normal mode retention increases with flow rate, probably due to shearing of the polarization layer, which increases the working field. At a constant field and flow rate, normal-mode retention is inversely related to the product of a particle's size and electrophoretic mobility, in accordance with retention theory. Thus, ElFFF can be used to obtain both the size and electrophoretic mobility of particle suspensions.

INTRODUCTION AND BACKGROUND

Electrical field-flow fractionation (ElFFF) was introduced in 1972 as a promising method for the separation of proteins (1). However, retention and resolution fell short of theoretical predictions. One problem was polarization of the electrodes by buffers used to dissolve the proteins and carry current across the channel. Polarization caused the channel to behave like a capacitor, with most of the potential drop occurring within a short distance from the channel walls, leaving a very weak field in the bulk of the channel. Polarization was overcome by increasing the field, but the electrodes had to be separated from the channel proper by a porous surface, which allowed current to flow while minimizing the effect of electrolysis products. Unfortunately, the porous surface reduced uniformity in the channel walls and resolution remained poor (2). Later channels were designed with more rigid surfaces (3) to improve channel uniformity, but performance remained significantly below expectations, and the method remained unproductive for over a decade.

In 1990, renewed interest in ElFFF was stimulated by the work of Gau and Caldwell, who developed a new channel design and the methodology for separating charged particles (4). In their design, current-conducting walls serve as electrodes for generating the electrical potential across the channel. Polarization is reduced by adding the redox couple quinone-hydroquinone to the aqueous carrier liquid.

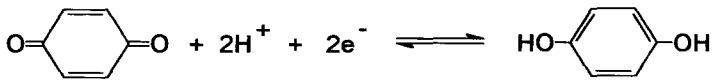

Since no new products are generated in electrode reactions with this redox couple, concentration gradients are not established and polarization of the electrodes is reduced. Using a simple 1.5 volt battery as a power supply, the new system was used to separate underivatized polystyrene particles.

Motivated by their success, Caldwell and Gau built their next-generation channel of resin-impregnated graphite (5), which has the advantage of being both rugged and inexpensive while offering low resistance to current flow. Although the graphite channel failed to yield consistent retention with the quinone-

hydroquinone carrier liquid, other electrolyte solutions were shown to produce efficient separations as long as the ionic strength was kept low. Using the graphite channel, Caldwell and Gau separated a wide range of particles sizes, and demonstrated the expected linear dependence of retention time on field strength.

In the work reported here, we further characterize the retention behavior of underivatized polystyrene latex beads, as well as carboxylated polystyrene, using the quinone-hydroquinone carrier liquid. Our experimental configuration is based on the original design of Gau and Caldwell (4), using gold-coated glass plates as the channel walls. We characterize the dependence of retention on field strength, flow rate, and the size and electrophoretic mobility of the particles.

THEORY

Retention in ElFFF, like other FFF techniques, is based on the application of a force field perpendicular to the separation axis of a thin channel. The field, which is applied across the thin dimension of the channel, interacts with analyte, forcing it to one of the walls (referred to as the accumulation wall). Due to viscous drag, the velocity is reduced toward the walls, and therefore the volume V_r of carrier liquid required to flush the analyte through the channel is related to analyte interactions with the field. Several comprehensive summaries of FFF retention theory can be found in the literature (see for example references 5,6), including those specific to ElFFF (7). Below is a condensed summary of the relevant concepts and equations applicable to ElFFF.

There are two forms of particle retention in FFF; they are referred to as the "normal" and "steric" modes. In both forms, a zone of injected particles is forced to the accumulation wall through interactions with the field. In the normal mode, Brownian motion of the particles cause them to back-diffuse from the accumulation wall toward the center of the channel. A balance is struck whereby the field-induced motion and back-diffusion are balanced, and the zone relaxes into a dynamic but steady-state distribution of particles in which the concentration is highest at the accumulation wall and decreases exponentially toward the center of the channel. The thickness l of the compressed zone is related to the magnitude of the voltage drop ΔV applied across the channel and to the diameter d and electrophoretic mobility μ of the particles

$$\lambda = \frac{\ell}{w} = \frac{kT}{3\pi\eta} \cdot \frac{1}{\mu d} \cdot \frac{1}{\Delta V} \quad (1)$$

Here kT is the thermal energy, w is the channel thickness (typically 0.1-0.2 mm), and η is the viscosity of the carrier liquid. The ratio ℓ/w is termed the retention parameter λ, and is fundamental to all FFF techniques.

Because flow of the carrier liquid is laminar, λ can be related precisely to the volume V_r of carrier liquid required to flush the zone through the channel

$$R = V^o/V_r = 6\lambda[\coth(1/2\lambda) - 2\lambda] \quad (2)$$

Here V^o is the geometric volume of the channel and R is termed the retention ratio. When retention is sufficiently strong ($R < 0.2$), equation 1 simplifies to

$$R = 6\lambda \quad (3)$$

Equations 1 and 3 can be combined to yield

$$V_r = \frac{\pi\eta V^o}{2kT} \cdot d\,\mu\,\Delta V \quad (4)$$

As indicated by equation 4, smaller particles generally elute ahead of larger ones in the normal mode (i.e. they have a smaller retention volume). This is because their Brownian motion carries them further from the accumulation wall, where the carrier liquid is moving at a higher velocity through the channel. Larger particles, on the other hand, move more slowly through the channel because they are compressed more tightly against the accumulation wall, where the velocity of the carrier liquid is reduced.

Previous studies indicate that much of the applied voltage ΔV is lost by polarization of the electrode walls, so that the working field responsible for particle retention is significantly reduced. For example, when the carrier liquid is a 49 μM aqueous solution of NaCl (conductivity 5 μS/cm), more than 99% of the applied potential is dropped across the polarization layers (5). As the ionic strength of the carrier liquid is increased, polarization becomes more severe, and retention

decreases accordingly. A potential method for combating the buildup is to increase the flow rate of carrier liquid in order to perturb the polarization layers via shearing action of the carrier flow.

When the particle size and/or voltage drop is sufficiently large, the particles are forced to the wall so strongly that the magnitude of l approaches the size of the particles. When this occurs, Brownian motion is negligible and the physical size of the particles governs how far they protrudes into the faster flow lines. In this steric mode of retention, the elution order reverses, with larger particles eluting ahead of smaller ones. The relationship between steric-mode retention and particle size is given by the following approximate expression (8)

$$V_r = \frac{wV^o}{3} \cdot \frac{1}{d} \tag{5}$$

In order to quantify the ability of FFF to separate particles according to their size, we define the size-based selectivity s_d as follows

$$s_d = \left| \frac{d \ln V_r}{d \ln d} \right| \tag{6}$$

In both the normal and steric mode, V_r is related linearly to particle diameter, so that s_d is expected to have a value of unity. The transition between the normal and steric modes is fairly abrupt. In the transition region, selectivity is diminished. At the inversion diameter (9), which is the particle size where the elution order reverses, s_d falls to zero. Particle size distributions that span the inversion diameter are difficult to characterize because two different particle sizes coelute. Fortunately, the inversion diameter can be shifted somewhat by adjusting experimental conditions (10), such as flow rate and field strength. However, for separating samples having extremely broad size distributions, it may not be possible to shift the inversion diameter outside of the distribution, and a pre-fractionation must be performed in order to obtain two or more fractions that can be subsequently separated individually.

MATERIALS AND METHODS

The ElFFF channel is illustrated in Figure 1. A 76 μm-thick mylar spacer is sandwiched between two glass plates that have been coated with gold by vacuum deposition. The glass plates are clamped between two sheets of Plexiglass using several bolts to provide a leak-proof seal. Holes in the plates provide an inlet and outlet to the channel, which is 37 cm long, 2 cm wide and 76 μm thick; the resulting void volume V^o is 0.65 mL. Sample and carrier liquid enter and exit the channel through pieces of Teflon tubing that are friction fit to the holes. An injection valve with a 3 μL loop for sample loading is connected to a four-way manual switching valve and mounted near the channel inlet. The switching valve allows the flow of carrier liquid to be routed around the channel during a stop-flow procedure, in which flow in the channel is halted after sample injection to allow the particles to reach their equilibrium distribution at the accumulation wall in the absence of downstream flow. The stop-flow procedure eliminates band broadening associated with sample relaxation (11), resulting in more efficient separations. By comparing retention times and peak areas using different stop-flow times, we found that 6 minutes of stop-flow time was sufficient for all experiments.

The gold faces of the channel are charged with a 20-volt adjustable power supply whose output is attenuated 20:1 by a voltage divider built in-house. The voltage supply is wired to five contact points along the length of each glass plate to provide a uniform field. The channel is placed in a vertical position so that gravitational forces do not affect retention. The carrier liquid is delivered with a single-piston HPLC pump, and the channel effluent is monitored with a variable wavelength UV detector set at 270 nm. The detector signal is sent to a chart recorder for visual display of the fractogram.

The carrier liquid was a solution of 2 mM quinone in deionized water, adjusted to pH 4.7 with HCl; the resulting solution has a conductivity of 18 mS/cm. The polystyrene latex standards were obtained from Polysciences, Inc. (Warrington, PA). Electrophoretic mobilities were determined on several of the standards (Table 1) using an electrokinetic sonic analyzer (Maytec Instruments, Hopkington, MA), which relies on the generation of a pressure wave by the sample in response to an oscillating electric field.

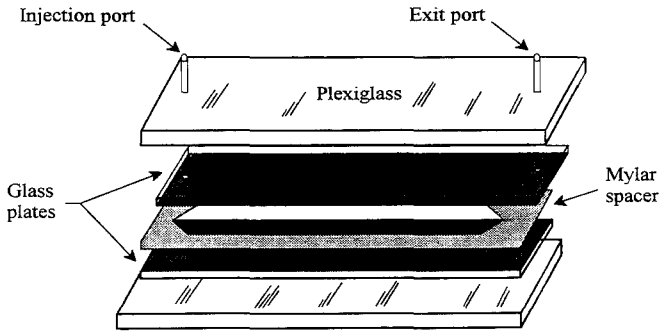

FIGURE 1. Schematic of the ElFFF channel.

TABLE 1.

Electrophoretic Mobility μ of Underivitized and Carboxylated Polystyrene Latex Standards.

	Diameter (μm)	Mobility (10^4 $cm^2s^{-1}V^{-1}$)
Underivitized Polystyrene	0.15	1.77
	0.22	2.26
	0.37	2.35
	0.48	1.83
	0.74	1.40
Carboxylated Polystyrene	0.10	2.05
	0.21	2.53
	0.55	2.29
	0.79	2.12
	1.07	1.32

RESULTS AND DISCUSSION

According to equation 4, retention parameter λ should vary inversely with the magnitude of the working field when the normal mode of retention is at work. Consequently, as the field is increased, λ should decrease toward a limiting value equal to the radius of the particle. Figure 2 plots a series of λ-values, measured at various field strengths, on an underivatized polystyrene (UPS) standard having a diameter of 0.37 μm. Fields above 1 V lead to irregular peaks and an irregular baseline, presumably due to gas bubbles formed by the electrolytic decomposition of water. Between 0.3 V and 1.0 V, the expected linear increase in λ with 1/V is observed. However, the slope is much larger than predicted by equation 1 because the working field is much less than the applied field. Thus, the abscissa in Figure 2, which reflects the applied field, is greatly compressed compared to the range of working 1/V-values. Based on the particle's electrophoretic mobility, equation 1 predicts a slope of 5.6×10^{-4} V for normal-mode retention of the 0.37 μm-diameter standard. The slope in figure 2 is 5.0×10^{-3} V, or 9 times the predicted value, which indicates a working field that is only 11% of the applied field. This compares favorably with the use of NaCl solutions as the carrier liquid, where the working field is only 0.2% of the applied field (5). The precipitous drop in retention (increase in λ) below 0.3 V (3.33 V^{-1} in Figure 2) presumably signifies the charging potential of the two electrode surfaces.

As we discussed above, an increase in flow rate should raise the working field by shearing the polarization layers. We tested this hypothesis on the 0.37 μm UPS standard using a field of 0.3 V. As illustrated in Figure 3, V_r continues to increase with flow rate up to a flow rate of 2.0 mL/min. Further flow increases were not possible due to leakage of the channel. The increase in retention with flow rate is a new factor to ElFFF separations that is not present in other FFF techniques, or in chromatography-like techniques in general. The major outcome of the flow rate dependence of retention is the need to use consistent flow rates in applying calibration curves to the analysis of unknown samples. However, this is a minor inconvenience--consistent flow rates are commonly used anyway. The flow rate dependence must also be considered in methods development. For example, in characterizing an unknown sample by FFF, a preliminary fractogram is often obtained at a high flow rate to determine the proper field strength. The higher flow rate minimizes development time. (One of the advantages of FFF is that the

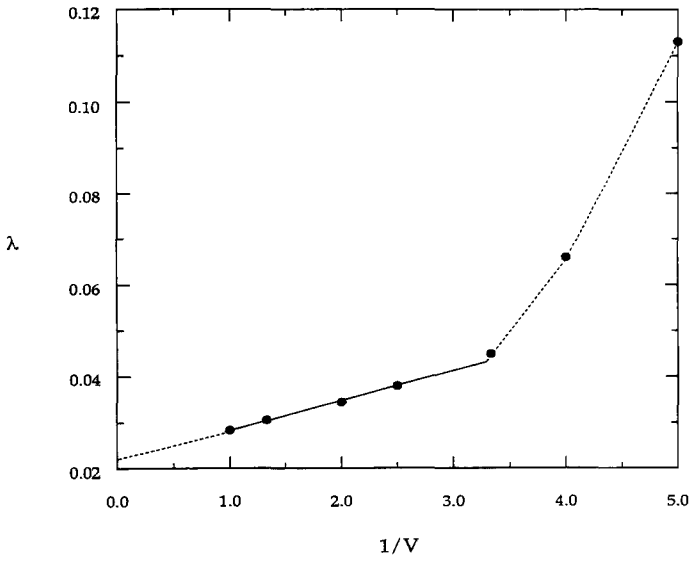

FIGURE 2. Dependence of retention parameter λ on the inverse of the applied voltage V. The sample is a 0.37 μm UPS standard; the flow rate is 1.82 mL/min.

field can be readily controlled and optimized for a given separation.) Once the preliminary run is completed, the required field is easily determined, and the flow is reduced for sample analysis. With ElFFF, either the flow rate used in the preliminary run will need to match that of the analytical run, or the retention dependence will have to be accounted for in determining the proper field strength.

In characterizing sub-micron particles by FFF, a low flow rate is typically used (< 1.0 mL/min) in order to minimize band broadening and thereby maximize resolution. However, the recent trend has been to utilize faster flow rates and/or lower fields in order to decrease run time at the expense of resolving power. Figure 4 illustrates the separation of two polystyrene standards in about 3 minutes using a ΔV of 0.3 V and a flow rate of 1.50 mL/min. Here, the run time was made as short as possible without losing the indication of a bimodal distribution.

According to equation 4, normal mode retention is governed by both size and electrophoretic mobility. For colloidal particles, the electrophoretic mobility in a

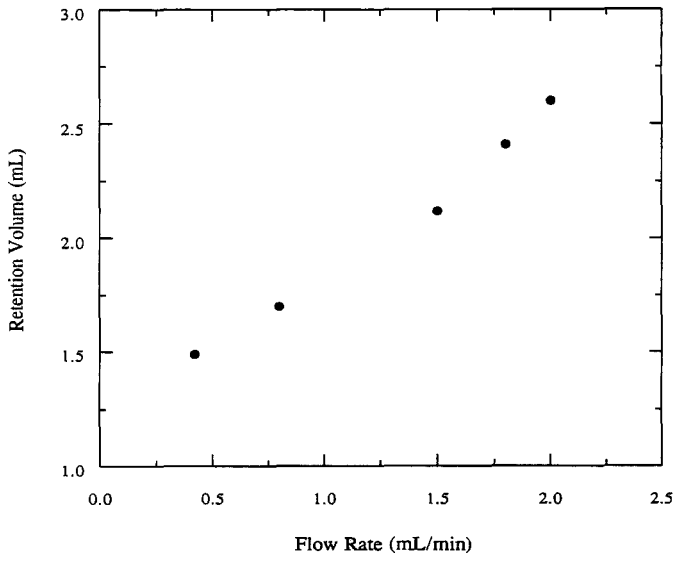

FIGURE 3. Dependence of retention volume on flow rate. The sample is a 0.37 μm UPS standard; the applied potential is 0.30 V.

given medium is fairly insensitive to particle size, provided the surface composition is relatively invariant (12). However, in the submicron size range, a small but measurable size effect on mobility is predicted. Fortunately, the size effect is consistent for a given type of particle, and therefore ElFFF retention can be calibrated to particle size without knowing the electrophoretic mobilities. This is illustrated in Figure 5, where retention volume is plotted against UPS particle size at both low and high flow rates. The curvature in these plots is due to the effect of size on electrophoretic mobility, particularly for the smallest particle (d = 0.15 μm), which has a significantly reduced μ-value. The two plots diverge initially, then parallel one another. The divergence is expected because the magnitude of the working field increases with flow rate and equation 4 predicts an increase in V_r/d with increasing field strength. It is unclear why the plots do not continue to diverge beyond particle diameters of 0.4 μm.

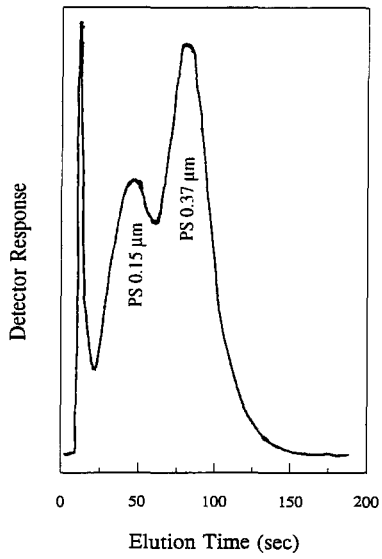

FIGURE 4. EIFFF fractogram illustrating the separation of two UPS standards. The applied potential is 0.30 V; the flow rate is 1.50 mL/min.

Next, we evaluate the retention behavior of several carboxylated polystyrene (CPS) standards ranging in diameter from 0.15 to 4.55 μm. Figure 6 illustrates the dependence of retention on particle size at a flow rate of 1.82 mL/min and a ΔV of 0.3 V. The steric transition occurs at an inversion diameter of 1.0 μm. As discussed in the Theory section, when particles are compressed into layer thicknesses approaching the size of the particle, their retention is determined by physical exclusion from the wall. When this happens, the elution order is reversed, and larger particles elute ahead of smaller ones. Based on the value of λ (0.03) where inversion occurs, the most highly retained particles are still 2 μm from the channel wall, a distance which is significantly greater than their radius of 0.5 μm. The additional exclusion distance is due to two factors -- a large double layer on the particles, as a result of the low ionic strength of the carrier liquid, and lift forces at the accumulation wall. Although lift forces are not well understood, they are known to elevate the particle from the wall, resulting in decreased retention.

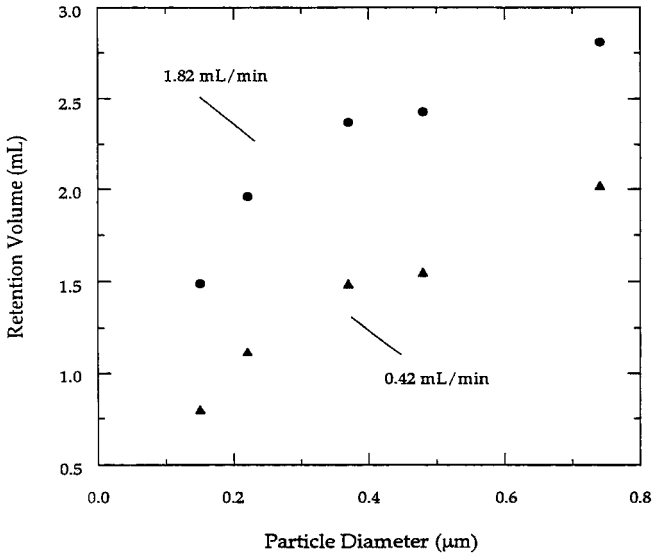

FIGURE 5. Dependence of retention volume on particle size of UPS standards at low and high flow rates. The applied potential is 0.30 V; the flow rate is 1.82 mL/min.

In the normal mode, lift forces are not a factor; in the steric mode, the lift force is a function of many factors, including the particle size and flow rate of the carrier liquid. The increase in lift force with particle size is responsible for the non-linear dependence of retention on particle diameter in the steric mode, as illustrated in Figure 6.

As we mentioned in the Theory section, we expect a size-based selectivity of 1 in both the normal and steric modes, based on the definition given in equation 6. (In the steric mode, lift forces cause the selectivity to drop from a maximum of 1 with increased particle size.) Experimentally, we obtain selectivities that are only about 0.6 in the normal mode for both UPS and CPS. In the steric mode, the data is limited, but the selectivity is approximately 0.6 near the inversion diameter. While the size-based selectivity is affected by a slight dependence of electrophoretic mobility on size, this does not account for the discrepency. The

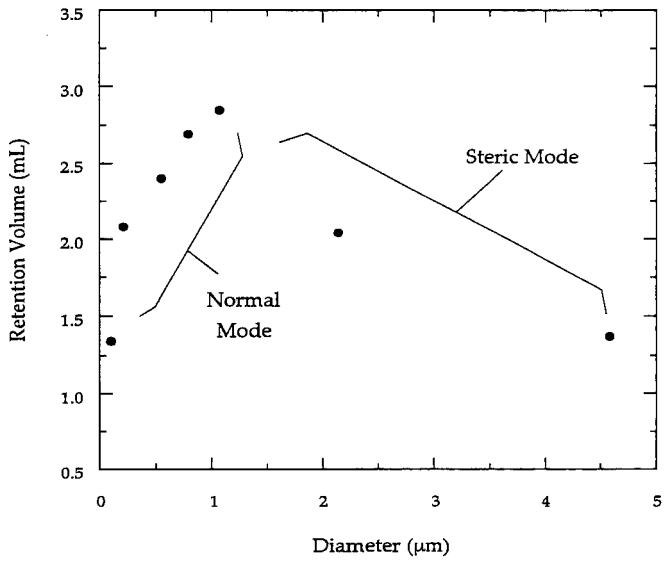

FIGURE 6. Dependence of retention volume on particle size of CPS standards. Both normal- and steric-mode retention are illustrated. The applied field is 0.30 V; the flow rate is 1.82 mL/min.

reason for the reduced selectivity remains unclear. However, one contributing factor is the presence of double layers surrounding the particles, which should add significantly to their effective size in the low ionic strength mediums used in this work. The double layer thickness should be fairly uniform over the size range examined, so the apparent selectivity, which is calculated using core diameters, will be artificially low.

A mixture of particles having a size range that spans the inversion diameter can lead to erroneous information on particle size. As an example, the fractogram illustrated in Figure 7 was obtained on three CPS standards; the particle sizes are 0.10 μm, 0.55 μm, and 2.1 μm. The center peak contains the larger standard, which elutes in the steric mode with a retention volume that is intermediate between the other two standards. Suppose the particle sizes were unknown and this fractogram was used to establish the size distribution based on the calibration

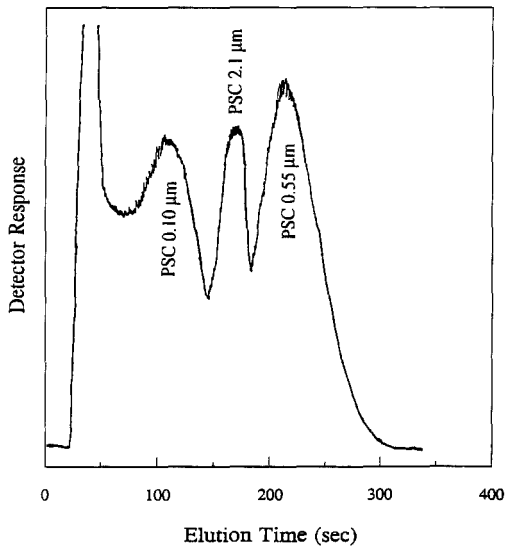

FIGURE 7. ElFFF fractogram illustrating the separation of three CPS standards. The center peak contains a standard that has eluted in the steric mode. The applied field is 0.30 V; the flow rate is 1.02 mL/min.

curve in Figure 6. One might assign the center peak a diameter of 0.2 µm, which coelutes in the normal mode with 2 µm particles eluting in the steric mode. An experienced FFF practitioner might suspect the center peak because it is particularly narrow compared to the other two. Often, however, polydisperse samples elute as a single broad peak, which may or may not contain particles coeluting in both modes of retention. Fortunately, an experienced FFF user can also identify coelution in broad distributions by a steep edge on the high-V_r side of the elution profile. For a detailed discussion on the coelution of particles in the normal and steric modes, the reader is referred to reference 10.

If we compare the normal-mode retention of CPS to that of UPS, we find that CPS retention is slightly greater than that of similarly sized beads of UPS, at the same flow rate and field strength. For example, the retention volume of 0.21 µm CPS particles is 2.08 mL, while that of 0.22 µm UPS particles is only 1.96 mL.

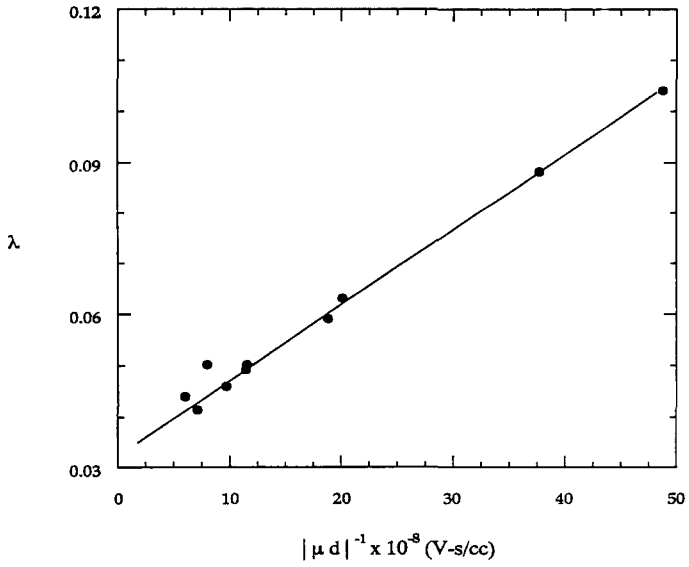

FIGURE 8. Dependence of retention parameter λ on the inverse product of the electrophoretic mobility μ and particle diameter d. The applied potential is 0.3 V; the flow rate is 1.82 mL/min.

The difference lies in their electrophoretic mobilities, which are slightly higher in CPS. The larger electrophoretic mobilities translate into a stronger force driving the CPS particles to the accumulation wall, hence greater retention in the normal mode. If the electrophoretic mobilities are known, retention of different particle types can be represented by a single calibration plot of retention parameter λ versus the reciprocal product of particle diameter and electrophoretic mobility. Such a plot is illustrated in Figure 8. Here, the retention data on CPS is combined with the UPS data taken at the same flow rate of 1.82 mL/min. Since the field strength, flow rate, and carrier-liquid composition were held constant for all the data, a linear relationship is obtained, in accordance with equation 1. The slope of the plot in Figure 8 is 1.4×10^{-11} cc/V-sec; equation 1 predicts a slope of 1.6×10^{-12} cc/V-sec. As was the case in Figure 2, the discrepancy lies in the magnitude of the working field, which is greatly reduced from the applied potential

by polarization of the electrodes. Comparing the slope in Figure 8 with that expected from theory indicates a working field that is 11% of the applied field, consistent with previous indications.

Caldwell and Gau demonstrated that polarization differs with the nature and conductivity of the carrier liquid. As we have shown, the flow rate is also important, and certainly we can expect the nature of the electrode surface to be a factor. However, by careful control of the field strength, as well as the nature and flow rate of the carrier liquid, Figure 8 illustrates the potential of ElFFF for characterizing charged particles. If the particle size is known, ElFFF can be used to obtain electrophoretic mobilities, and even distributions in μ. By measuring retention under several different sets of experimental conditions, both size and electrophoretic mobilities could be obtained by ElFFF. Finally, if ElFFF is used in combination with a light scattering detector, both the size and electrophoretic mobility could be obtained from a single fractogram.

CONCLUSIONS

The newly designed ElFFF channel shows potential as an alternative method for analyzing charged particles. The channel is inexpensive and easy to assemble. The major difficulty with the technique lies in the dependence of retention on parameters that influence polarization of the electrodes. As a result, several parameters associated with the carrier liquid must be carefully controlled in addition to the field strength. With the 2 mM quinone-hydroquinone carrier used in this work, critical parameters include the flow rate, pH, and conductivity. Although 89% of the field is lost at the electrode surface due to polarization of the electrodes, applied potentials of less than one volt still result in efficient separations of both micron and sub-micron sized particles whose electrophoretic mobilities are in the range of 10^{-4} $cm^2/V\text{-}s$.

In the work reported here, we obtained a size-based selectivity of ~0.6, which is significantly lower than the expected value of unity predicted by retention theory. Caldwell and Gau reported a selectivity of ~0.7 using a solution of NaCl as the carrier liquid. However, the apparent discrepancy between theory and experiment probably arises from the double layer on the particle, which is not accounted for in empirical determinations of selectivity. If instead of using core

diameters to calculate selectivity, the thickness of the double layers were known and accounted for, the apparent selectivity would increase. Nevertheless, for measuring core diameters, the selectivity is lower than other FFF techniques, including flow FFF and sedimentation FFF. Yet, flow and sedimentation instruments are significantly more expensive than ElFFF equipment, so the reduced selectivity may well be worth the cost savings for many applications.

The unique feature of ElFFF is its ability to separate particles based on their charge, or electrophoretic mobility. While the resolution of the technique is comparable to that of capillary zone electrophoresis (CZE) (5, 13), the speed of CZE is significantly greater. However, ElFFF can deal with much higher sample loadings than CZE, which is conducive to sample collection and subsequent analysis by secondary methods, such as photon correlation spectroscopy. The two-dimensional capability that becomes available when fractions can be collected may be critical for analyzing unknown samples of a complex or polydisperse nature.

ACKNOWLEDGMENTS

We thank Dr. Karin Caldwell and Dr. Yu-Shu Gau for their valuable counsel. We thank Hewlett-Packard Corp. for supporting the initial work, and for their assistance in determining particle mobilities. This work was supported by the NSF-Idaho EPScOR program and by National Science Foundation grant number OSR-9350539.

REFERENCES

1. K. D. Caldwell, L. F. Kesner, M. N. Myers, J. C. Giddings, Science 176: 296 (1972).

2. L. F. Kesner, K. D. Caldwell, M. N. Myers, J. C. Giddings, Anal. Chem., 48: 1834 (1976).

3. J. C. Giddings, J. C. Lin, M. N. Myers, Sep. Sci., 11: 553 (1976).

4. Y.-S. Gau, K. D. Caldwell, The Second International Symposium on Field-Flow Fractionation, Salt Lake City, Utah, 1991.

5. J. C. Giddings, J. Chem. Phys., 49: 81 (1968).

6. M. N. Myers, J. C. Giddings, Anal. Chem., 54: 2284 (1982).

7. K. D. Caldwell, Y.-S. Gao, Anal. Chem., 65: 1764 (1993).

8. J. C. Giddings, M. N. Myers, Sep. Sci., 13: 637 (1978).

9. J. C. Giddings, M. H. Moon, Anal. Chem., 64: 3029 (1992).

10. S. K. Ratanathanawongs, J. C. Giddings, in Chromatography of Polymers: Characterization by SEC and FFF, T. Provder, Ed., ACS Symp. Series No. 521, American Chemical Society, Washington, DC, 1993, pp. 47-62.

11. M. E. Schimpf, M. N. Myers, J. C. Giddings, J. Appl. Polym. Sci., 31: 117 (1987).

12. D. C. Henry, Proc. R. Soc. Lodon, Ser. A, 133: 106 (1931).

13. S. L. Petersen, N. E. Ballou, Anal. Chem., 64: 1676 (1992).

Received: November 8, 1993
Accepted: January 7, 1994

JOURNAL OF LIQUID CHROMATOGRAPHY, 17(14&15), 3239-3260 (1994)

SEPARATION OF POLYSACCHARIDES BY THERMAL FIELD-FLOW FRACTIONATION

JIANZHONG LOU, MARCUS N. MYERS, AND J. CALVIN GIDDINGS
Field-Flow Fractionation Research Center
Department of Chemistry
University of Utah
Salt Lake City, Utah 84112

ABSTRACT

Polysaccharides are complex polymers of great biological and industrial importance. The fractionation and determination of molecular weight distributions of these substances are required for many applications. Thermal field-flow fractionation (thermal FFF) is shown to be applicable to the separation and characterization of a variety of polysaccharides in dimethyl sulfoxide (DMSO). Samples of pullulans, dextrans, and Ficolls are readily fractionated according to differences in molecular weight. Calibration plots have been developed to obtain molecular weight distributions. More complex polysaccharides, such as starch and cellulose, have also been investigated. This study is complicated by the poor solubility of these materials. Nonetheless, starch can be successfully separated into amylose and amylopectin fractions, the latter consisting of an ultrahigh molecular weight polymer with a highly branched structure. A cationic corn starch has also been resolved into its components. These examples suggest that thermal FFF is widely applicable to polysaccharides.

INTRODUCTION

Polysaccharides are biopolymers of both biological and industrial importance. The occurrence and applications of polysaccharides are ubiquitous [1-4]. These polymers usually exhibit a wide molecular weight distribution (MWD). Many applications require the isolation, fractionation, and molecular weight determination

of these substances. For this reason, we have investigated the applicability of field-flow fractionation (FFF) to the separation of a variety of polysaccharides. Specifically, pullulans, dextrans, Ficolls, and starch polymers dissolved in dimethyl sulfoxide (DMSO) are fractionated by thermal FFF.

Pullulan, dextran, and Ficoll span a broad range of polysaccharide branching structures, and have been the subject of some extensive studies [5-7]. Pullulan is a linear polymer of glucose, produced by enzymes secreted by *Aureobasidium* bacteria. The chain is linked by one α-D-(1-6)-glycosidic bond and two α-D-(1-4)-glycosidic bonds alternating regularly. Pullulan is manufactured commercially by enzymatic fermentation processes. In medicine, pullulan solutions can be used to extend plasma supply and pullulan gel can be used to purify enzymes. In addition, pullulan can be used in diet foods as a starch substitute because pullulan cannot be degraded by *in vivo* digestive enzymes. In industry, pullulan films are used as packaging materials for drugs and coatings for electrodes [5]. Pullulan can be used as a gelling agent in food [8] and a protective coating on stainless steel during annealing [9].

Dextran is a partially branched, high molecular weight polymer of glucose, synthesized by the enzyme on the cell surface of *Leuconostoc* or *Streptococcus* bacteria. The backbone of dextran is linked through α-D-(1-6)-glycosidic bonds and the branches are linked by α-D-(1-3)-glycosidic bonds. Dextran also has many uses [6]. Dextran fractions of relatively low molecular weights (~40,000) are used in blood substitutes. Dextran crosslinked with epichlorohydrin, called Sephadex, has been widely used for the fractionation of proteins, nucleic acids, and polysaccharides. The "salting-out" effect of dextran on proteins makes dextran very useful for tests of antigen-antibody reactions. Dextran is also used to stabilize isolation media for subcellular species. It is reported that dextran can be used in veterinary work [10] and in human immunization [11].

Ficoll is a densely branched copolymer of sucrose and epichlorohydrin (1-chloro-2,3-epoxypropane). Ficoll is widely used as a material to form density gradient in various centrifugations of biological species such as blood granulocytes [7, 12, 13] and as a polysaccharide antigen for clinical tests [14]. Ficoll is also used as model for inert spheres in aqueous SEC calibrations [15].

The physical, biological, and clinical properties of these polysaccharides vary with MWD. For example, native dextrans are too high in molecular weight (up to 10^8) to be used in blood substitutes [6].

Apart from our interest in the foregoing polysaccharides, we have also investigated some more complex industrial polysaccharides such as starch, cellulose, and their derivatives. Starch contains amylose and amylopectin in different proportions depending on the plant source. About 97% of all the industrial starch is obtained from corn [16]. Cellulose occurs in cotton, wood, and other plant cell walls [17]. Amylose is a linear polymer of glucose linked by α-D-(1-4)-glycosidic bonds [16]. Amylopectin is linked by both α-D-(1-4)-glycosidic and α-D-(1-6)-glycosidic bonds, probably with random-branching structure [18]. Some researchers believe starch is a giant macromolecule, and that the appearance of amylose and amylopectin is the result of polymer degradation occurring during sample processing [16]. Cellulose is also a linear polymer of glucose but differs from amylose in that it is linked by β-D-(1-4)-glycosidic bonds [17]. Derivatives of starch and cellulose generally have backbone configurations resembling those of their parent polymers [16, 17]. Because the processing rheology and the quality of end products are correlated with MWD, techniques for determining MWDs for these polysaccharides are needed by industry for both processing equipment design and quality control.

MWD can be crudely estimated by some non-fractionation methods such as dynamic light scattering (DLS) [19], which generally requires some assumption about the distribution function, thus often eliminating the possibilities of detecting multimodal distributions or the existence of tails in MWD. In many engineering applications, the presence of a small fraction of ultrahigh molecular weight polymer can strongly influence key material properties, such as normal stresses [20], drag reduction [21], and fracture strength [22].

For the past three decades, size exclusion chromatography (SEC) has been the standard method for polymer separation and MWD determination. However, SEC is not ideally suited for separating ultrahigh molecular weight polymers, due in part to the difficulties in preparing robust packings with sufficiently large pores to allow the permeation of large macromolecules [23-24]. The possibility of the shear degradation of large, fragile macromolecules in porous media [24-27] is another shortcoming of SEC. Cationic polymers may experience sample adsorption on the packing of SEC [27-30]. SEC columns are vulnerable to clogging. Filtration is generally required prior to SEC, which can leave out tails in MWD. Other limitations of SEC for ultrahigh molecular weight applications have been described [31].

Several attempts have been made to use SEC to separate starch polymers [32-36], but the results are still being debated. In order to overcome the drawbacks of SEC, other alternatives have been considered for application to starch polymers, such as flow separation [37], thin-layer chromatography (TLC) [38], radial migration [39], multicell membrane dialysis [40], capillary hydrodynamic chromatography (CHDC) [41, 42], and continuous sedimentation-velocity separation [43].

Field-flow fractionation (FFF) is a relatively new family of elution methods that offer a promising solution to some of the problems of ultrahigh molecular weight polysaccharide separation. In FFF, separation is achieved in a ribbon-like thin channel with no packing inside. A parallel-plate Poiseuille flow is established in the channel. An external field is applied across the channel thickness to drive molecules to different velocity streams and cause separation [44-52]. First proposed in 1966 [44], FFF has now evolved to many techniques, including thermal FFF, sedimentation FFF, flow FFF, and electric FFF [51].

Of all the FFF techniques, thermal FFF has been most widely applied to polymer separations [45-48, 50, 51]. Thermal FFF offers some unique advantages for the study of polymers. Because thermal FFF utilizes an open channel, it has a minimal surface area exposed to polymer molecules. The choice of surface material (or coating) is quite freely made and therefore the problem of sample adsorption can be controlled. Polymer recovery is high. There is no need for sample filtration. Shear degradation is also minimized. Most important of all, thermal FFF can be extended into the ultrahigh molecular weight range.

Despite its broad potential for polymer analysis, much of the research on thermal FFF to date has been devoted to the separation of well-understood synthetic linear polymers. These polymers permit the use of conventional solvents and detection systems [45, 47, 50]. The existence of narrow molecular weight standards has allowed the development of calibration procedures for many of these polymers [50]. A great deal of work has been done on polystyrene standards, some with molecular weights up to 20 million daltons, by thermal FFF [47]. Very little FFF work has been performed on polysaccharides. Myers et al. first subjected a water-soluble blue dextran to thermal FFF, but observed no retention in water because the thermal diffusion effect in water was too weak. They found that the thermal diffusion of blue dextran was enhanced in a mixed solvent of water and DMSO [45]. The lack of retention in water was confirmed by Kirkland and Yau for

polysaccharides [48]. More recently, Wahlund and Litzen used flow FFF to fractionate an aqueous solution of a fluorescent dextran [49].

The objective of this work is to examine and expand the breadth of applicability of thermal FFF to the separation of polysaccharides. The solvent chosen is DMSO, although similar separations are expected in other solvents except water for polysaccharides.

The separations of starch and cellulose are complicated by their poor solubility. A preferred solvent for starch is DMSO [32-36]. However, even in DMSO, starch polymers are difficult to dissolve; all the procedures reported in the literature involve vigorous heating, stirring, and filtering. These steps may cause both mechanical and thermal polymer degradation. The sample filtration step can be bypassed using thermal FFF.

THERMAL FFF PRINCIPLES

The separation of polymers in thermal FFF is realized by the coupling of the thermal diffusion (induced by a temperature gradient) and the nonuniform flow of the carrier along the channel axis. A schematic view of differential polymer retention in a thermal FFF channel is shown in Figure 1. After a polymer sample is injected into the FFF channel inlet, the thermal diffusion, driven by the temperature gradient, and the normal diffusion, driven by the concentration gradient, are usually balanced within a fraction of a minute. As a result, an exponential equilibrium concentration profile will be formed against the cold wall (designated as the accumulation wall) for each component. Because of the nonuniformity of the flow velocity profile in the FFF channel, components with different mean elevations (designated as ℓ_1 and ℓ_2 in Figure 1) above the accumulation wall will occupy different velocity regions and will thus be swept through the channel at different velocities and emerge at different times. Therefore, the degree of polymer retention in FFF is directly related to the mean elevation ℓ. For well-retained polymer samples, the FFF retention time t_r is given by the theoretical equation [51]

$$\frac{t_r}{t^0} \cong \frac{1}{6(\ell/w)} = \frac{1}{6\lambda} \tag{1}$$

where t^0 is the void time (the emergence time of a nonretained species), w is the channel thickness, and λ is the dimensionless mean elevation ℓ/w. An approximate relationship between the dimensionless mean elevation and the polymer's normal

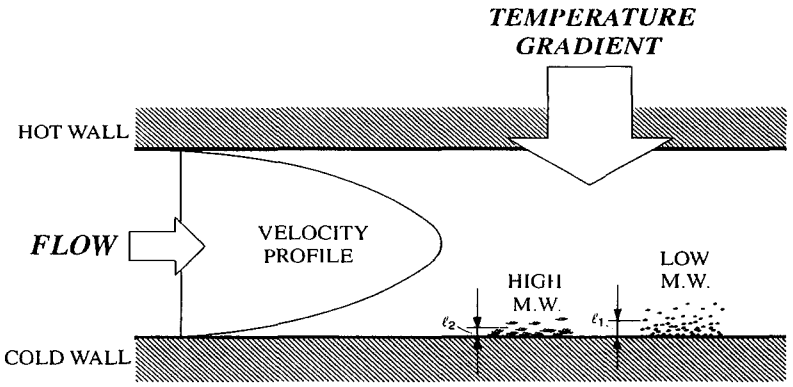

FIGURE 1. Schematic view of polymer components undergoing differential flow transport in the thermal FFF channel.

diffusion coefficient D, thermal diffusion coefficient D_T, and the temperature drop ΔT across the channel thickness is [51]

$$\lambda\Delta T = \frac{D}{D_T} \tag{2}$$

The polymer diffusion coefficient is found to obey the following scaling law [53, 54]

$$D = AM^{-b} \tag{3}$$

where M is the polymer molecular weight and A and b are constants for a given polymer-solvent system at a given temperature. For example, b approaches 0.6 for a linear flexible polymer in a good solvent [54]. Although no satisfactory theory has been developed to predict D_T, the thermal FFF results of Schimpf and Giddings for polystyrene and a few other polymer standards showed that D_T is essentially independent of the polymer molecular weight [50]. Since D_T may have a slight dependence on molecular weight for some polymer-solvent systems, we use the exponent n instead of b:

$$\lambda\Delta T = \phi M^{-n} \tag{4}$$

According to Equation 4, plotting the logarithm of $\lambda\Delta T$ against the logarithm of the polymer molecular weight M should yield a straight line whose slope is -n and intercept is $\log\phi$. This logarithmic linear relation has been confirmed by experiments on several synthetic polymers [50]. Therefore, Equation 4 provides a

basis for thermal FFF molecular weight calibration. Unlike the universal calibration parameters of SEC [30], the calibration parameters of Equation 4 are solely the properties of the polymer-solvent system and not dependent upon the characteristics of the individual separation system. By substituting Equation 4 into Equation 1, we get

$$\frac{t_r}{t^0} \cong \frac{\Delta T M^n}{6\phi} \tag{5}$$

This tells us that the retention in thermal FFF is controlled by the imposed temperature drop and the molecular weight of the polymer sample. The higher the molecular weight, the longer the retention time. However, a rigorous relationship between t_r and M requires a more sophisticated calibration procedure.

The thermal FFF calibration procedure will not be described in detail here. It should be noted that the flow velocity profile in the thermal FFF channel differs slightly from the well-known parabolic profile because the viscosity varies across the channel thickness with the temperature variation. This complicates the relationship between the mean elevation and the retention time t_r. More rigorous equations for retention as a function of dimensionless mean elevation have been derived by Gunderson, et al. [46] and amended more recently by Asten, et al. [52]. In these treatments the velocity profile is calculated using a temperature-dependent solvent viscosity. The reciprocal viscosity, called the fluidity, is approximated by a cubic polynomial expression in absolute temperature. The viscosity data for DMSO used in this work were obtained from Gaylord Chemical Corp. [55] The fluidity of DMSO can be described by the following equation

$$\frac{1}{\eta} = 1035 - 9.128\ T + 0.02536\ T^2 - 0.00001973\ T^3 \tag{6}$$

where η is the viscosity in poises and T is absolute temperature. This equation shows that there is a large variation of viscosity across the FFF channel. For example, the viscosity of the carrier near the cold wall held at 30 °C is about 2 centipoise whereas it is only about 0.74 centipoise near the hot wall at a temperature of 100 °C.

EXPERIMENTAL

Apparatus and procedures

The thermal FFF apparatus used in this work was of conventional design [47, 50]. The surfaces of the copper bars enclosing the channel were chrome plated and

finely polished. Two 1.5-kilowatt cartridge heaters were inserted into the hot bar. Passages were drilled in the cold bar to allow tap water to run through as a coolant. The temperature drop between the bars was maintained through the control of the power duty cycle of the inserted heaters with a single-board computer. A 127-μm thick Kapton polyimide spacer was clamped tightly between the bars by 20 evenly spaced bolts. The center of the spacer was cut out to leave a ribbon-like flow channel measuring 2 cm in breadth and 35.6 cm in tip-to-tip length.

In previous work, the channel inlet and outlet consisted of holes drilled directly into one of the copper bars [47, 50]. However, in the course of this study, we observed corrosion of the bared copper by DMSO. To avoid the exposure of copper to the solvent, we modified the inlet and outlet by inserting 1/16" (0.159 cm)-OD Teflon tubes with an inner diameter of 305 μm into the hot bar all the way to its surface. The tubes were mounted with Swagelog fittings.

A Kontron (London, England) Model 414 LC pump was used to deliver chromatography-grade DMSO solvent to a Rheodyne (Cotati, California) sample injector, which was connected to the inlet of the thermal FFF channel. The injection loop was 20 μL. The dead volume between the channel and the injector was 25 μL. This requires a minimum time delay of 13.5 s after injection to allow the sample to reach the channel at a flow rate of 0.2 mL/min. After arrival of the sample at the head of the channel, the solvent flow was switched to bypass the channel for 30 s to allow the polymer components to relax into their equilibrium exponential distributions under stop-flow conditions. Channel flow was then re-started to carry out the run. A detector was connected to the channel outlet using a 305 μm-ID Teflon tube. Both a Wyatt (Santa Barbara, California) Dawn F laser photometer and a Varex (Burtonsville, Maryland) Model A evaporative light scattering detector (ELSD) were used in this study.

Because the pump was not designed for working steadily for the flow rates under 0.1 mL/min, we used a circulatory loop, consisting of a 6-meter-long 254 μm-id stainless steel tube, an solvent filter, and a back pressure regulator, to split the carrier flow from the pump into two streams and send one of them back to the solvent container and the other to the injector. In this way, we were able to adjust the flow rate in the FFF channel to well below 0.1 mL/min while allowing the pump to run at a higher flow rate setting. The flow rate was always calibrated with a well-sealed burette and a stopwatch.

Materials

Model polysaccharides including pullulans, dextrans, and Ficolls were examined in this work. The characteristics and original source of each of these samples are shown in Table 1. Samples of corn starch, cationic corn starch, and isolated amylose and amylopectin, provided by H. D. Scobell of A. E. Staley Manufacturing Co. (Decatur, Illinois), were also subjected to the thermal FFF. A sample of potato starch purchased from Sigma Chemical (St. Louis, Missouri) was also studied. Most of these samples were supplied in the form of amorphous white powder. Some starch samples, however, were also supplied in solutions.

Chromatography-grade DMSO, identical to that used as the carrier, was employed as the solvent for preparing solutions of these polysaccharide samples. Reagent-grade lithium nitrate ($LiNO_3$) was used to enhance the thermal FFF retention of the cationic starch in DMSO.

Sample preparation

To prepare polysaccharide solutions from the solid powder form, samples were first weighed and then put in vials. DMSO was then added to the vials. While the samples of pullulan, dextran, and Ficoll were all readily dissolved in DMSO at room temperature, the starch samples required a much higher temperature (in the range 100 ° to 160 °C) to dissolve. A silicone oil bath and a Haake (Berlin, Germany) Model FE-2 water bath were thus used to heat the vials containing the mixture of the starch powder and DMSO. In addition, nitrogen was bubbled into the vials through an immersed 1/16"(0.15875 cm)-OD Teflon tube to help remove O_2 and mix the starch powder with DMSO. All the vials were mounted on a custom-built tilted rotor that rotated slowly until the polymers were completely dissolved. Once the solutions were made, they were all cooled to room temperature. The final concentration of the solutions for injection to the FFF channel was adjusted to 0.1 % (w/v). This concentration is below the overlap concentrations [54] of all these polysaccharides.

RESULTS AND DISCUSSION

Model polysaccharides (pullulans, dextrans, and Ficolls)

Figure 2 shows sets of thermal FFF fractograms (detector response versus time) of different molecular weight samples (see Table 1) of pullulans, dextrans,

TABLE 1. Model Polysaccharide Samples

Sample	Nominal M	M_w/M_n	[η], dl/g	Original Source
pullulan #1	100,000[a]	1.10	-	Polymer Laboratories, Ltd.
pullulan #2	186,000[a]	1.13	-	Polymer Laboratories, Ltd.
pullulan #3	853,000[a]	1.14	-	Polymer Laboratories, Ltd.
dextran #1	150,000[b]	-	0.350	Pharmacia Fine Chemicals
dextran #2	506,000[b]	-	0.530	Pharmacia Fine Chemicals
dextran #3	2,000,000[c]	-	0.700	Pharmacia Fine Chemicals
Ficoll #1	132,000	-	0.013	KABI Pharmacia Ophthalmics
Ficoll #2	321,000	-	0.172	KABI Pharmacia Ophthalmics
Ficoll #3	461,000	-	0.194	KABI Pharmacia Ophthalmics
Ficoll #4	741,000	-	0.237	KABI Pharmacia Ophthalmics
Ficoll #5	1,130,000	-	0.282	KABI Pharmacia Ophthalmics
Ficoll A	-	-	-	KABI Pharmacia Ophthalmics*

[a]From ultracentrifugal sedimentation equilibrium

[b]From light scattering

[c]From intrinsic viscosity

*Lot label 400-QC-113347

and Ficolls. For these particular FFF runs, the temperature drop ΔT of the system was set at 27.8 °C and the carrier flow rate was adjusted to 0.2 mL/min. The observation of differential retention beyond the void time t^0 confirms the applicability of thermal FFF to these three classes of polysaccharides. The relatively broad peaks (which are broader than those generated by SEC) are a result of the high selectivity of thermal FFF (much higher than SEC) and do not imply inferior resolution [51]. Rather, these broad peaks represent the broad molecular weight distributions of the polymers (see later).

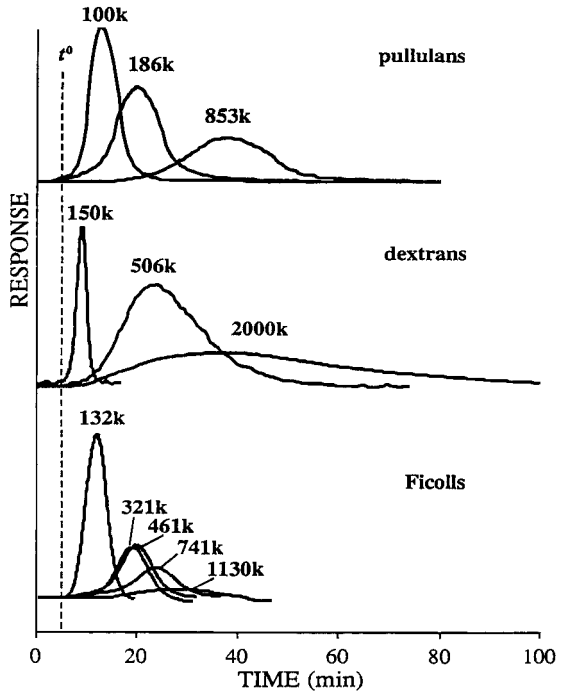

FIGURE 2. Thermal FFF fractograms of various model polysaccharides in DMSO. Conditions: sample concentration, 0.1% (w/v); flow rate, 0.2 mL/min; temperature drop, 27.8 °C; cold wall temperature, 30.0°C; detector, Varex ELSD Model A, used with 40 psi. helium carrier gas.

As described earlier, thermal FFF retention is dependent upon both the thermal diffusion coefficient D_T and the normal diffusion coefficient D. From Figure 2, it is clear that these polysaccharides, especially the pullulans, are well retained which demonstrates that the thermal diffusion effect for these polysaccharides in DMSO is quite strong, or, in other words, that the D_T values are quite high in DMSO. Kirkland and Yau reported a very weak retention (thermal diffusion) effect for the same type of polysaccharides in an aqueous carrier [48]. Thus we conclude that an organic solvent is a better choice for the carrier in the

separation of polysaccharides using thermal FFF. As mentioned above, we lack theoretical guidelines about the dependence of D_T on solvent characteristics and must rely on such empirical evidence.

According to the scaling law for D (see Equation 3), the diffusion coefficient is a function of both molecular weight M and conformation. A branched polymer assumes smaller geometric chain dimensions and hence greater values of the diffusion coefficient than a linear polymer [54]. The fact that dextrans have partially branched structures provides a tentative explanation for why dextrans are less retained than pullulans in thermal FFF for a given molecular weight (see Figure 2). Furthermore, among these three categories of model polysaccharides, highly branched Ficolls are the least retained in thermal FFF for a given molecular weight. These observations support the assumption that the diffusion coefficient D and not D_T is the parameter that dominates the changes in thermal FFF retention of these model polysaccharides. Further work is needed for verifications.

It is necessary in most FFF work to check the fractograms and retention data for any possibility of sample overloading. Once an FFF channel is overloaded with a polymer sample, the eluted polymer peak will change in position and shape with the sample amount and will thus no longer reflect properties of the polymer components such as the molecular weight. For this reason, FFF runs were carried out for several different injected sample amounts. Figure 3 shows such an "overloading" test for the sample dextran #2. For this particular sample and for the conditions used, the onset of sample overloading occurs at about 20-40 μg. The results reported below are all free from overloading effects.

In order to derive the MWD from the FFF retention data, several steps must be taken. First, the polynomial expression for DMSO fluidity shown in Equation 6 is used for determining the accurate velocity profile in the thermal FFF channel. Following this, the treatment developed by Gunderson et al. [46, 52] has been used to calculate the dimensionless mean elevation λ from measured t_rs. Thermal FFF molecular weight calibration plots are then established for each of the three kinds of polysaccharides according to Equation 4. Figure 4 shows a logarithmic plot of $\lambda\Delta T$ as a function of the molecular weight M for pullulans, dextrans, and Ficolls. Data for this plot were acquired at a fixed cold wall temperature but at several different temperature drops (27.8 °C, 37.0 °C, 44.2 °C, and 53.4 °C). The calibration parameters, n and logϕ, obtained from the least square fit are tabulated in Table 2.

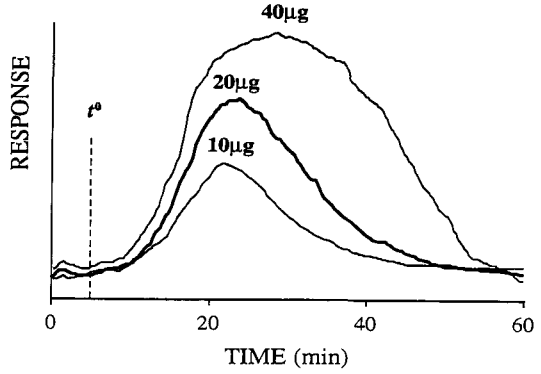

FIGURE 3. Investigation of overloading for dextran #2. Conditions: same as Figure 2.

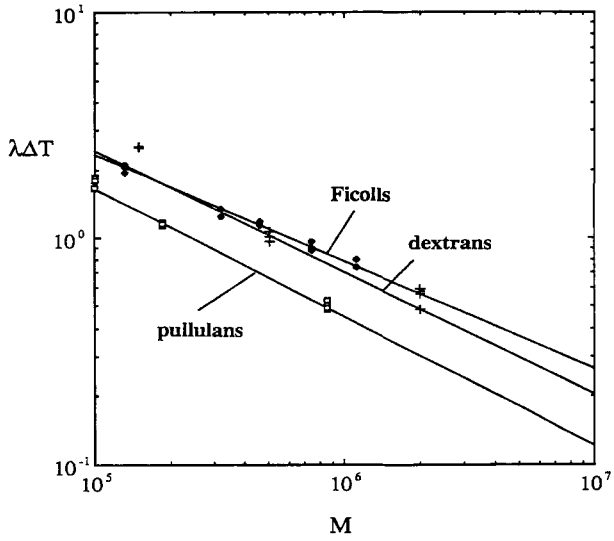

FIGURE 4. Thermal FFF molecular weight calibration plots: calculated λΔT values as a logarithmic function of the molecular weight M for pullulans, dextrans, and Ficolls at a fixed cold wall temperature of 30 °C but at several temperature drops (27.8 °C, 37.0 °C, 44.2 °C, and 53.4 °C).

TABLE 2. Molecular Weight Calibration Parameters*

Sample	Slope, -n	Intercept, logϕ
pullulans	-0.568	3.057
dextrans	-0.539	3.079
Ficolls	-0.475	2.746

*Refer to Equation 4

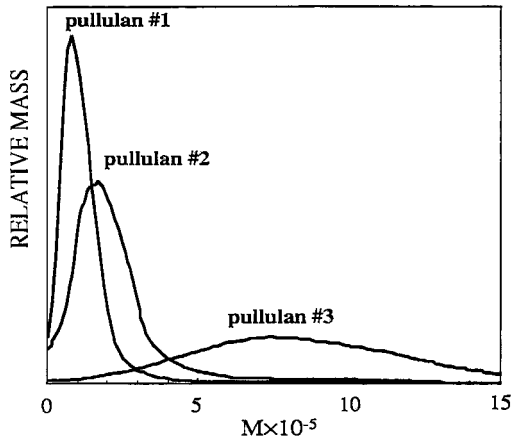

FIGURE 5. MWD curves calculated from the thermal FFF fractograms for pullulans #1, #2, and #3.

Using these calibration parameters, we have calculated the MWDs from the thermal FFF fractograms. Figures 5 to 9 show the MWD curves, the relative mass as a function of molecular weight, calculated from the fractograms using a computer program developed at our research center (the FFFRC).

Starch polymers

The cationic corn starch was well retained and fractionated in DMSO by thermal FFF, as shown in Figure 10. The amylose content is estimated from the

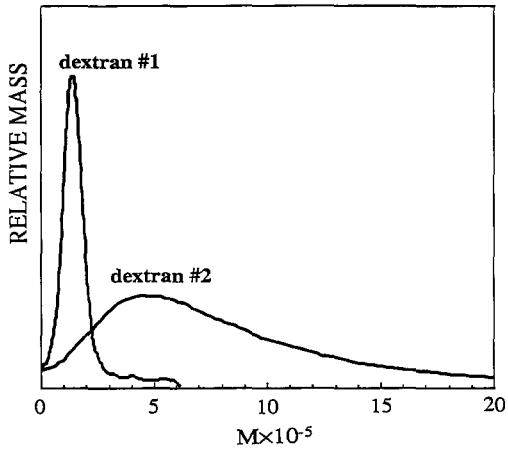

FIGURE 6. MWD curves calculated from the thermal FFF fractograms for dextrans #1 and #2.

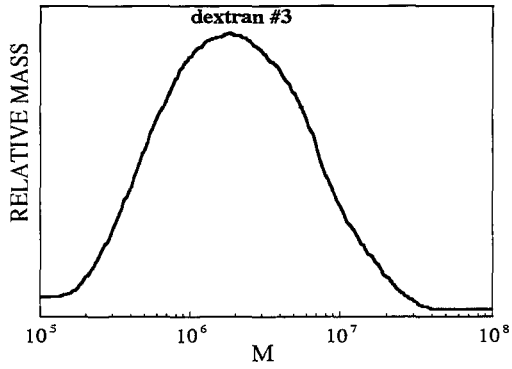

FIGURE 7. MWD curve obtained for dextran #3.

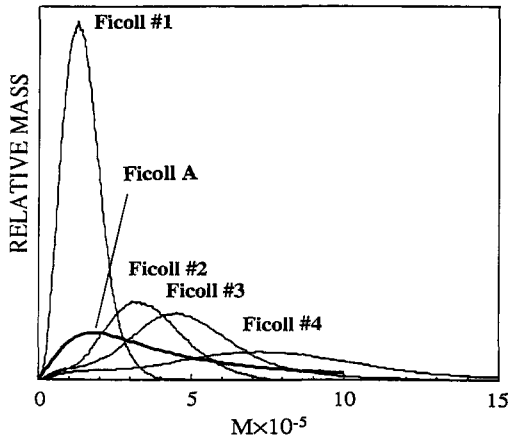

FIGURE 8. MWD curves obtained from the thermal FFF fractograms for Ficolls #1, #2, #3, #4, and A.

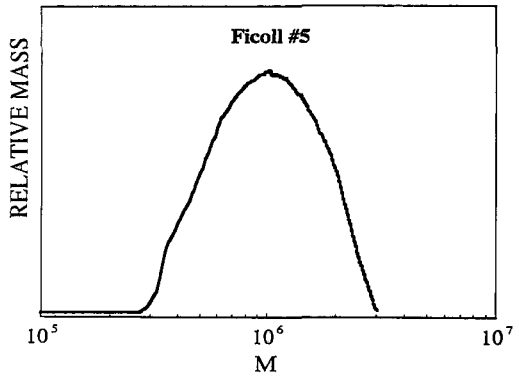

FIGURE 9. MWD curve calculated for Ficoll #5.

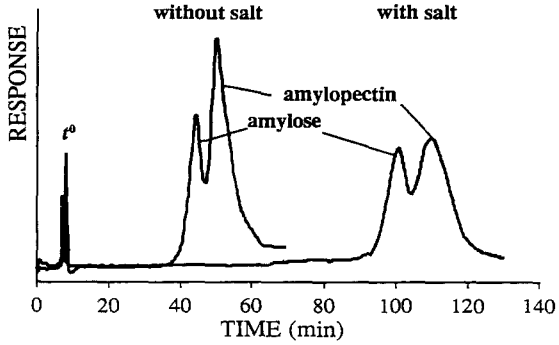

FIGURE 10. Separation of a cationic corn starch in DMSO (left) by thermal FFF. Conditions: sample concentration, 0.28 % (w/v); channel flow rate, 0.1 mL/min; temperature drop, 70 °C; detector, Wyatt Dawn F laser photometer, signal displayed at 90 °. At the right, separation in DMSO with addition of 1.0×10^{-4}M $LiNO_3$.

FFF fractogram peak areas to be about 30%, which is consistent with information from the supplier.

It was found that at an ionic strength of 10^{-4} M ($LiNO_3$ dissolved in DMSO), the thermal FFF retention was significantly enhanced, approximately doubled, as compared with that in pure DMSO (see Figure 10). Below this ionic strength, the enhancement of retention was also observed but to a lesser extent. At an even higher salt concentration, such as 10^{-2} M, we observed the reversible adsorption of cationic starch in the channel; the cationic starch peak did not elute out of the channel, even when run for a few hours, until the field (the temperature gradient) was removed. The explanation of the salt effect is not entirely clear due in part to the lack of knowledge on how D_T varies with the ionic strength. Three effects are expected to play a role. One is the unknown variation in D_T. Another is that the salt ions will reduce the thickness of the electrokinetic double layer on the accumulation wall, which tends to exclude the polymer molecules. Therefore, the addition of a salt will tend to lower the mean elevation and increase the retention time at a given external field strength (temperature gradient). The other change due to the addition of a salt is the well-known polyelectrolyte screening effect [56]. Here the added ions act as a screen to reduce the repulsion between the charged

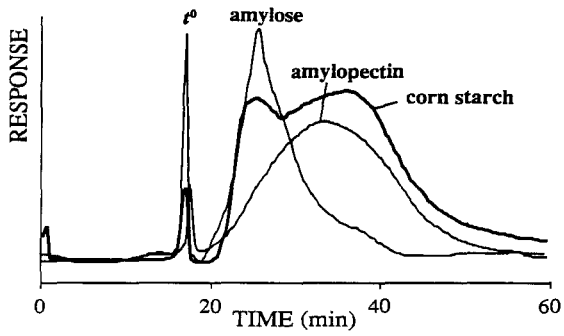

FIGURE 11. Separation of underivatized corn starch in DMSO by thermal FFF. Superimposed are the thermal FFF fractograms of corn starch and both an amylose and an amylopectin fraction isolated from corn starch. Conditions: sample concentration, 0.28 % (w/v); channel flow rate, 0.05 mL/min; temperature drop, 65 °C; detector, Wyatt Dawn F laser photometer, 90 ° angle.

chain segments. The geometric dimensions of the polyelectrolyte chain are thus reduced and the diffusion coefficient increased as salt is added. This will lead to a higher mean elevation and a shorter retention time. The salt effects shown in Figure 10 suggest that the former effect ("wall exclusion") dominates, assuming there is no large change in D_T. Such salt effects require further investigation, probably using better understood model polyelectrolytes.

Both corn and potato starches show relatively weak retention in DMSO. No observable salt effect was found on the retention of these starch samples. The partial separation of corn starch was achieved in DMSO as shown in Figure 11. The amylose and amylopectin components of the study can be identified with the first and second peaks, respectively, because isolated amylose and amylopectin samples have the same retention characteristics. The superimposed fractograms of Figure 11 illustrate this.

The thermal diffusion of starch in DMSO appears to be relatively weak. In order to achieve higher resolution in thermal FFF, a higher ΔT will be required. Another possibility includes the use of alternate solvents.

ACKNOWLEDGMENTS

This work was supported by Grant No. CHE-9102321 from the National Science Foundation.

We would like to thank the following people for their help in this work: Dr. G. Lai of Kellogg Co. (Battle Creek, Michigan) for technical discussions and the generous gift of some of the pullulan and dextran samples; Mr. H. D. Scobell of A. E. Staley Manufacturing Co. for technical discussions and the gift of various starch samples; Dr. K. Granath of Pharmacia AB (Uppsala, Sweden) for providing Ficoll samples.

The data analysis was done on a PC computer using a program that was developed by Dr. P. S. Williams of the FFFRC. We had very useful discussions with Dr. P. Shiundu of the FFFRC on salt effects.

REFERENCES

1. C. D. Melia, Critical Review on Therapeutic Drug Carrier Systems, 8, 395 (1991)
2. S. A. Barker, Endeavour, 15, 155(1991)
3. J. S. Laskowski, Q. Liu, N. J. Bolin, Int. J. Miner. Process., 33, 223 (1991)
4. T. Uryu, T. Yoshida, K. Hatanaka, Sen'i Gakkaishi, 48, 176 (1992)
5. A. LeDuy, L. Choplic, J. E. Zajic, J. H. T. Luong, in Encyclopedia of Polymer Science and Technology, 2nd Ed., H. F. Mark, N. M. Bikales, C. G. Overberger, G. Menges, eds., John Wiley & Sons, New York, 1985, Vol. 13, pp. 650-661.
6. J. F. Robyt, in Encyclopedia of Polymer Science and Technology, 2nd Ed., H. F. Mark, N. M. Bikales, C. G. Overberger, G. Menges, eds., John Wiley & Sons, New York, 1985, Vol. 4, pp. 752-767.
7. B. D. Davies, W. Hoss, J. P. Lin, F. J. Lionetti, Mol. Cell. Biochem., 44, 23 (1982)
8. T. C. Gerrish, L. E. Carosino, U.S. Patent 616,474 (1990)
9. K. Sato, G. Ishibashi, Y. Katsuki, H. Kaito, H. Muraki, Y. Yamaguchi, Eur. Patent 466,491 (1992)
10. K. T. Concannon, S. C. Haskins, B. F. Feldman, Am. J. Vet. Res., 53, 1369 (1992)

11. J. Rhodes, B. Zhang, M. R. Lifely, Immunology, 75, 626 (1992)

12. C. B. Thompson, K. A. Eaton, S. M. Princiotta, C. A. Rushin, C. R. Valeri, Report, BUSM-83-08, 1983, Order No. AD-A140382, Gov. Rep. Announce. Index (U.S.), 84(15), 72(1984)

13. V. A. Btunotts, L. R. Emerson, E. N. Rebis, A. J. Roy, in Natl. Conf. Manage. Uncontrolled Hazard. Waste Sites, 1983, pp. 209-216

14 N. L. Edwards, B. S. Mitchell, I. H. Fox, J. J. Mond, Adv. Exp. Med. Biol., 165, 129(1984)

15. S. Hussain, M. S. Mehta, J. I. Kaplan, P. L. Dubin, Anal. Chem., 63, 1132 (1991)

16. A. H. Young, in Starch: Chemistry and Technology, 2nd Ed., L. Whistler, J. L. BeMiller, E. F. Paschall, eds., Academic Press, New York, 1984, pp. 249-283.

17. J. R. Daniel, in Encyclopedia of Polymer Science and Technology, 2nd Ed., H. F. Mark, N. M. Bikales, C. G. Overberger, G. Menges, eds., John Wiley & Sons, New York, 1985, Vol. 3, pp. 90-123.

18. A. Heyraud, P. Salemis, Carbohydr. Research, 107, 123 (1982)

19. B. Chu, Q. Ying, C. Wu, J. R. Ford, M. S. Dhadal, Polymer, 26, 1408 (1985)

20. J. J. Magda, J. Lou, S. G. Baek, K. L. DeVries, Polymer, 32, 2000 (1991)

21. J. W. Hoyt, in Encyclopedia of Polymer Science and Technology, 2nd Ed., H. F. Mark, N. M. Bikales, C. G. Overberger, G. Menges, eds., John Wiley & Sons, New York, 1985, Vol. 5, pp. 129-151.

22. H. H. Kausch, Polymer Fracture, 2nd Ed., Springer-Verlag, Berlin, 1986

23. L. Soltes, D. Berek, S. Mikulsova, Colloid Polym. Sci., 258, 702 (1980)

24. W. Siebourg, R. D. Lundberg, R. W. Lenz, Macromolecules, 13, 1013 (1980)

25. R. Beckett, Z. Jue, J. C. Giddings, Environ. Sci. Technol., 21, 289 (1987)

26. R. S. Seright, J. M. Maerker, G. Holzwarth, Polym. Preprints (A. C. S. Div. Polym. Chem.), 22(2), 30 (1981)

27. A. MacArthur, D. McIntyre, Polym. Preprints (A. C. S. Div. Polym. Chem.), 24(2), 102 (1983)

28. H. G. Barth, J. Chromatogr. Sci., 18, 409(1980)

29. T. E. Eremeeva, T. O. Bykova, V. S. Gromov, J. Chromatogr., 522, 67 (1990)

30. P. L. Dubin, in Advances in Chromatography, J. C. Giddings, E. Grushka, P. R. Brown, eds., Marcel Dekker, New York, 1992, Vol. 31, pp. 119-151.

31. J. C. Giddings, in Advances in Chromatography, J. C. Giddings, E. Grushka, J. Cazes, P. R. Brown, eds., Marcel Dekker, New York, 1982, Vol. 20, pp. 217-258.

32. M. Vincendon, M. Rinaudo, Carbohydr. Polym., 2, 135 (1982)

33. J. G. Sargeant, H. Wycombe, Starch/Staerke, 34, 89 (1982)

34. P. Salemis, M. Rinaudo, Polym. Bull., 11, 397 (1984)

35. P. Salemis, M. Rinaudo, Polym. Bull., 12, 283 (1984)

36. T. Yamada, K. Suzuki, H. Katuzaki, M. Hisamatsu, K. Tsu, Starch/Staerke, 42, 217 (1990)

37. E. A. DiMarzio, C. M. Guttman, Macromolecules, 3, 131 (1970)

38. K. Kamide, S. Manabe, E. Osafune, Makromol. Chem., 168, 173 (1973)

39. K. A. Dill, B. H. Zimm, Nucleic Acids Res., 7, 735 (1979)

40. T. S. Young, X. Yan, T. E. Hogen, G. B. Butler, J. Macromol. Sci. Chem., A22, 437 (1985)

41. M. A. Langhorst, F. W. Stanley, S. S. Cutie, J. H. Sugarman, L. R. Wilson, D. A. Hoagland, R. K. Prud'homme, Anal. Chem., 58, 2242 (1986)

42. R. Tijssen, J. Bos, M. E. van Kreveld, Anal. Chem., 58, 3036 (1986)

43. G. Holzworth, L. Soni, D. N. Schultz, Macromolecules, 19, 422 (1986)

44. J. C. Giddings, Sep. Sci., 1, 123 (1966)

45. M. N. Myers, K. D. Caldwell, J. C. Giddings, Sep. Sci. , 9, 47 (1974)

46. J. J. Gunderson, K. D. Caldwell, J. C. Giddings, Sep. Sci. Technol., 19, 667 (1984)

47. Y. S. Gao, K. D. Caldwell, M. N. Myers, J. C. Giddings, Macromolecules, 18, 1272 (1985)

48. J. J. Kirkland, W. W. Yau, J. Chromatogr., 353, 95 (1986)

49. K.-G. Wahlund, A. Litzen, J. Chromatogr., 461, 73 (1989)

50. M. E. Schimpf, J. C. Giddings, J. Polym. Sci., Polym. Phys. Ed., 27, 1317 (1989)

51. J. C. Giddings, Science, 260, 1456 (1993)

52. A. C. van Asten, H. F. M. Boelens, W. Th. Kok, H. Poppe, P. S. Williams, J. C. Giddings, Sep. Sci. Technol., in press

53. P. Flory, Principles of Polymer Chemistry, Cornell University Press, Ithaca, New York, 1953

54. P.-G. de Gennes, Scaling Concepts in Polymer Physics, Cornell University Press, Ithaca, New York, 1979

55. Dimethyl sulfoxide product literature, Gaylord Chemical Corporation, 106 Galeria, Slidell, Louisiana 70459

56. M. Mandel, in Polyelectrolytes: Science and Technology, M. Hara, ed., Marcel Dekker, New York, 1993

Received: December 27, 1993
Accepted: January 20, 1994

JOURNAL OF LIQUID CHROMATOGRAPHY, 17(14&15), 3261-3283 (1994)

SOLUTION PROPERTIES OF POLYELECTROLYTES. XI. ADSORPTION EFFECTS IN AQUEOUS SIZE-EXCLUSION CHROMATOGRAPHY OF POLYANIONS

AGUSTÍN CAMPOS, ROSA GARCÍA, IOLANDA PORCAR, AND VICENTE SORIA
Departament de Química Física
Universitat de València
E-46100 Burjassot, Valencia, Spain

ABSTRACT

Elution profiles of a series of polymer standards such as sodium poly(styrene sulphonate), poly(acrylic acid) and poly(L-glutamic acid) have been obtained from size-exclusion chromatography experiments using separately two types of hydrophilic supports. A variety of mobile phase compositions have been performed to enhance adsorption effects in order to study how this phenomenon can affect to the chromatographic separation mechanism of polyanions. Distribution coefficient values, in general greater than unity, have served to quantify the adsorption effect, as well as to analyze their dependence on eluent ionic strength, on the ionic groups of the support and on the chemical nature and molar mass of the polyion. The physical basis of the weak polymer-gel attractive interaction have been attributed to hydrogen-bonding and to hydrophobic effects. We present basic equations derived from the Flory-Huggins theory of polymer solutions to explain the adsorption process in terms of preferential interaction, being this description consistent with the expected values assigned to the interaction parameters involved in the above theory.

INTRODUCTION

Aqueous size-exclusion chromatography (ASEC) of water soluble polymers and biopolymers has been an emerging field in the last decade due to the mild and non-destructive character as well as to the short-time consuming of this separation technique (1-4). In contrast with the elution mechanism of polymers in organic media (5,6), the understanding of the separation mechanisms of hydrophilic ionic polymers in aqueous media demands much more theoretical and experimental contributions, mainly due to the diverse nature of the so-called secondary effects referred to as polymer-gel interactions distorting pure ASEC (7-17).

Similarly to the elution of non-ionic polymers in organic media (18,19), polyelectrolytes in aqueous solutions can be early or retarded eluted relative to the elution of an equivalent uncharged polymer at the same experimental conditions. The early elution has been termed as ion-exclusion effect and it is generally assumed to be caused by electrostatic repulsion between the charges along the polyion and the residual charges of the gel packing. Recently, considerable efforts have been devoted to study this secondary effect, including chromatographic and physico-chemical parameters accounting for it, as well as practical recommendations for the total suppression in both rigid and soft gels, by means of the addition of a simple electrolyte to the eluent (8,10,14,20). Simultaneously, most chromatographers involved in biochemical separations have detected the same effect when peptides, proteins and complex macromolecular structures have been eluted using water-compatible porous packing materials (16,17,21).

The opposite effect leads to displacements towards elution volumes higher than those of the non-ionic polymers taken as reference, as a consequence of attractive solute-gel interactions. The nature of these interactions has been treated in depth, being classed as: i) electrostatic attraction, ii) hydrogen-bonding, and iii) hydrophobic interaction (22-24). It is a difficult task to elucidate what of these contributions is responsible for the adsorption effect because more than one type of forces can affect to the separation mechanism. The partial or total prevention of this secondary effect has been directed towards the addition of some components to the mobile phase, such as a few p.p.m. of neutral surfactants (25,26).

The abovementioned displacements of the elution volumes towards lower or higher values have been advantageously employed for separation of biological macromolecules (27). Moreover, it is well-known that one packing can be used for several types of liquid chromatography by a suitable selection of the eluent components. In this context, at present ion-exchange chromatography (IEC) (28) and hydrophobic interaction chromatography (HIC) (29-31) are two important branches of liquid chromatography, being both carried out on a given gel packing at low or high mobile phase ionic strength, respectively. To date, both IEC and HIC techniques are widely implanted in separation of peptides and proteins rather than in the characterization of ionic polymers.

This paper concerns to the adsorption secondary effect evidenced by means of the elution of synthetic polyelectrolytes which differ in chemical nature and molar mass. Two hydrophilic and organic-based conventional packings such as TSK PW4000 and Ultrahydrogel have been used separately, and the obtained results compared between them. The influence of eluent pH and ionic strength has also been considered in order to regulate adequately the intensity of the adsorptive effects. In addition, a semi-quantitative analysis of the SEC results of polyions, when a weak hydrophobic interaction takes place, is developed in the framework of the Flory-Huggins (FH) theory in terms of polymer-gel network compatibility.

MATERIALS AND METHODS

Chemical and Reagents

Sodium acetate, acetic acid, sodium monohydrogen phosphate and sodium dihydrogen phosphate involved in the preparation of buffer solutions were all analytical grade from Merck (Darmstadt, Germany). Water was distilled and deionized in a Milli-Q system (Millipore, Mildford, MA, USA) and its conductivity was daily tested. The non-ionic water-soluble polymers were dextran standards purchased from Pharmacia (Uppsala, Sweden) with molecular weights (MW) of

10, 17.7, 40, 66.9, 83.3, 170, 500 and 2000 (blue dextran) kg·mol^{-1}. The chromatographic low-molar-mass range was covered by poly(ethylene oxide) (PEO) from Fluka (Darmstadt, Germany) with MW of 2 and 4 kg·mol^{-1}. Used polyelectrolytes were narrow-distribution samples (polydispersities lower than 1.1 in all instances) of poly(L-glutamic acid) (PGA) from Sigma (St. Louis, MO, USA) with MW of 13.6, 43 and 77.8 kg·mol^{-1}; sodium poly(styrene sulphonate) (PSS) from Pressure Chemical (Pittsburgh, PA, USA) with MW of 1.6, 16, 31, 88 and 177 kg·mol^{-1}; and poly(acrylic acid) (PAA) from Aldrich (Milwaukee, WI, USA) with MW of 5, 90 and 250 kg·mol^{-1}.

Size-Exclusion Chromatography

All chromatographic measurements were performed on a Waters liquid chromatograph (Mildford, MA, USA) equipped with an M-45 solvent delivery system, a U6K universal injector and an R-401 refractive index detector, coupled to a Yokogawa Electric Works dual-channel recorder (Tokyo, Japan).

Two organic-based column were used in this work. A Spherogel TSK PW4000 (30 × 0.75 cm I.D.) packed with hydroxylated polyether copolymer of 500 Å nominal pore diameter from Beckman Instruments (Galway, Ireland) and an Ultrahydrogel 250 (30 × 0.78 cm I.D.) packed with hydroxylated poly(methacrylate)-based gel of 250 Å nominal pore diameter from Waters. Both columns will be hereinafter referred to as TSK and UHG, respectively. The interstitial packing volume and total volume were 5.15 and 10.40 mL for the TSK and 5.48 and 10.46 mL for the UHG column, as measured with blue dextran and ^2H_2O, respectively.

The mobile phase for non-ionic polymers was distilled and deionized water and for the polyelectrolytes it was made up from NaAc/HAc buffer (pH 5.0) and from Na_2HPO_4/NaH_2PO_4 buffer (pH 7.0) to the desired ionic strength ranging from 0.01 to 0.20 M. In all instances, mobile phases were filtered and degassed through regenerate cellulose 0.45-μm filters from Micro Filtration Systems (Dublin,

CA, USA). All pH measurements were made with a Crison pH-meter model MicropH 2000 (Barcelona, Spain).

All chromatographic measurementss were conducted at room temperature and the columns were equilibrated at least 12 h prior to starting any experiment. Chromatograms were obtained at a flow-rate of 1 $mL \cdot min^{-1}$ in isocratic mode, by injection of 100 μL of 0.1 % (w/v) solute solutions freshly prepared using the corresponding mobile phase as solvent. Flow-rates were measured and found to be constant within ±0.5% by weighting the collected effluent. Each sample was injected three times as a check on the reproducibility.

Viscometry

Measurements were made with an automatic Ubbelohde-type AVS 440 capillary viscometer from Schott Geräte (Hofheim, Germany) at 25.0±0.1 °C. Efflux times were obtained with precision of ±0.01 s as an average of five or six measures. At least five dilutions were obtained by adding the appropriate aliquots of solvent. Kinetic energy corrections were included in the calculation of specific viscosities. Intrinsic viscosity, [η], was determined by the usual extrapolation to zero solute concentration. For uncharged polymers, dextran and PEO, [η] was evaluated from their viscometric equations (32,33) in pure water because the influence of ionic strength and pH on the viscosity of non-ionic polymers may be neglected (11,13,20).

RESULTS AND DISCUSSION

Let us first present calibration curves $\log M[\eta]_I$ against elution volume (M, molar mass; $[\eta]_I$, intrinsic viscosity at a given ionic strength) for charged and uncharged standards as a function of eluent pH and ionic strength, I; chemical architecture of the macromolecules and some features of the gel packings. Figure 1

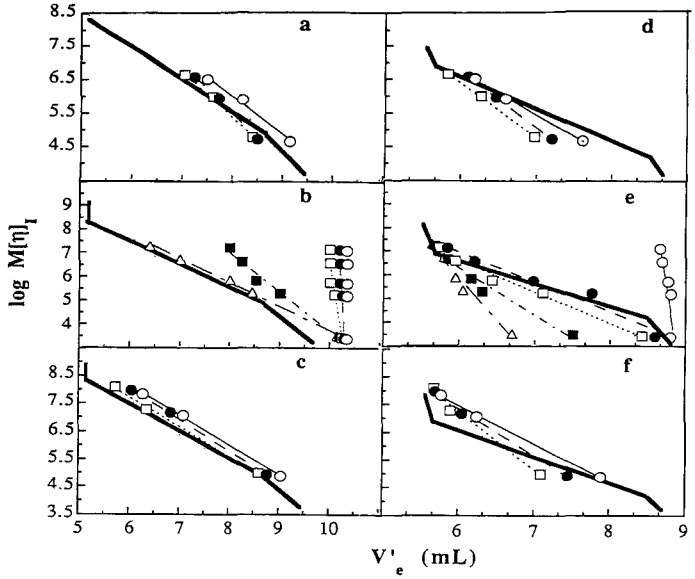

FIGURE 1. Calibration plots, $\log M[\eta]_I$ against retention volume in acetate buffer (pH 5.0) as eluent at diverse ionic strengths: (△) 0.01; (■) 0.02; (□) 0.05; (●) 0.1 and (○) 0.2 M. Solid lines refer to dextran calibrations in pure water. The following polyion/gel packing pairs are depicted: (a) PGA/TSK; (b) PSS/TSK; (c) PAA/TSK; (d) PGA/UHG; (e) PSS/UHG and (f) PAA/UHG.

compiles these calibration graphs for PGA, PSS and PAA (from top to bottom) using TSK and UHG (from left to right) as packing columns in acetate buffer (pH 5.0) with different ionic strength values ranging from 0.01 to 0.20 M. Because this paper is mainly concerned with solute adsorption as a non-exclusion effect in ASEC, in this Figure we have selected suitable experimental conditions that permits to emphasize this particular secondary effect. So that, other experimental conditions allowing an early elution of polyions relative to the non-ionic polymers have been omitted. We see that PGA and PAA calibration curves (parts a and c) follow a similar trend with respect to the reference one (dextran and PEO in the present

work), they are placed slightly on the right-hand side owing to a weak adsorption of the polyion by the gel. In contrast, the corresponding curves for PSS at I≥0.05 M show that all polymer samples are practically eluted at the same elution volume independent of their molar masses, reaching the column total pore volume. Notice that this anomalous behavior is caused by a strong adsorption of the PSS by the TSK gel under the assayed mobile phase compositions. The same measurements have been carried out using UHG column (Figures 1d-f). In general, calibration graphs approach to the reference one with increasing I, cross it, and then diverge on the other side. From the comparison between both sets of curves, for TSK and UHG, seems that the solute retention or adsorption effects are more pronounced when the former is used. However, at I=0.20 M, PSS shows a great retention irrespective the nature of the packing material. The same experiments have been carried out using phosphate buffer (pH 7.0) as mobile phase (not shown here). The results obtained in this case are similar but all curves were shifted to lower elution volumes denoting an increase in ion-exclusion secondary effects.

Basically, the retention volume of an ionic polymer depends on three major variables: mobile phase composition (pH and I), chemical nature of the stationary phase and chemical structure of the analyte, besides other chromatographic variables, not considered here, such as injected volume, sample concentration, flow-rate, etc. that can also interfere the separation process. The influence of the pH and I on the elution of a polyelectrolyte in aqueous media has been extensively studied in the past (11,13,34-36). For this reason, we next proceed to discuss the observed retention differences exclusively on the basis of the chemical nature of both polyion and gel. Figure 2 depicts calibration curves for PSS, PGA and PAA as well as the non-ionic polymers on TSK (part a) and on UHG (part b) in a common buffer solution at I=0.2 M (pH 5.0). In the light of the relative position of the calibration graphs respect to the reference one, it is easy to observe that the intensity of adsorptive effects increase according to the following order: PGA<PAA<PSS in both stationary phases.

Assuming that at pH 5.0, near to the $pK_{a(COOH)}$, the –COOH lateral functional groups of PGA and PAA are partially dissociated, c.a. 50%, both the protonated and dissociated forms will coexist. The protonated species will be

susceptible to bind to the –OH groups strategically located on the network of TSK or UHG via H-bonding, whereas the unprotonated forms will be fully screened by the counter-ions because of the high salt concentration (I=0.2 M) of the eluent. In the light of this argument, the adsorption forces will depend on the density of the –COOH groups by polymer chain. For instance, at a given molecular mass of the polymer, PAA posses twice as much carboxylic groups as PGA since their monomer molar masses are 72 and 147 $g \cdot mol^{-1}$, respectively. For this reason, it can be expected that PAA adsorbs onto the gel stronger than PGA. This behavior is corroborated by the calibration graphs depicted in Fig. 2. In addition, the divergence between both calibration curves is more pronounced in UHG than in TSK, denoting the existence of additional specific interactions between the carbonyl ester group of methacrylate (the monomer base of UHG gel) and the –COOH group of PGA and PAA samples.

Unfortunately, the above arguments cannot be invoked to explain the anomalous retention exhibited by PSS. Under the experimental conditions assayed (pH 5.0; I=0.2 M), the charges of the sulphonic groups are fully screened by the counter-ions, hence the observed adsorption can be exclusively caused by hydrophobic interaction between the hydrocarbon patterns of the PSS and those of the TSK or UHG gel packings. In this case,the polymer-gel attractive interaction becomes more intense due to the unlocated nature of the driving forces involved, which affects to the overall domain of the macromolecule.

In order to analyze more in-depth the influence of the chemical nature of the gel packing, Figure 3 depicts calibration graphs for PSS in both gels. For the sake of comparison, we have selected in the present example a mobile phase ionic strength of I=0.1 M. From the inspection of this figure, it is clearly evidenced that PSS samples are eluted very close to the uncharged polymers when UHG column is used, denoting that the macromolecular separation is carried out according to a pure size-exclusion mechanism. In contrast, PSS suffers a strong adsorption on the TSK column. In the light of this behavior, it can be inferred that UHG gel is innerter than TSK one. However, if one whishes employ advantageously the hydrophobic character of this gel for separation of biomacromolecules, proteins for instance, the TSK packing will be preferred. In conclusion, when the remaining variables (pH, I, type of solute) are fixed, the packing hydrophobicity observed will be TSK>UHG.

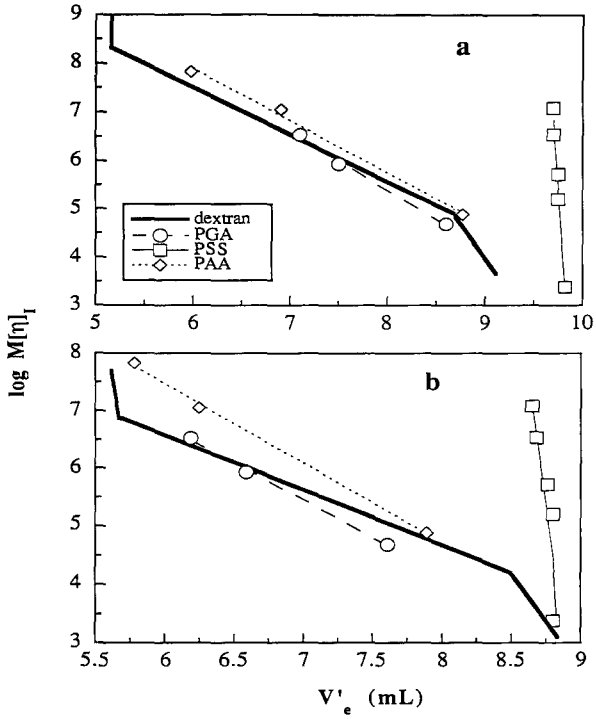

FIGURE 2. Comparison between the calibration plots obtained from charged (symbols) and uncharged (solid line) standards polymers in acetate buffer (pH 5.0) at 0.2 M, using TSK (part a) and UHG (part b) as gel packings.

To date, considerable efforts have been devoted to give a theoretical description of the secondary effects in SEC, including organic, aquoorganic and aqueous mobile phases (4,19,23). Most of them consider a unique force as the origin of the interactions between adsorbent (gel packing) and solute (polyelectrolyte). In this way, for instance, physico-chemical treatments accounting for electrostatic effects (8,12), solid-liquid adsorption and hydrophobic interaction (23,31) can be examples of the abovestated. However, in the particular case of the

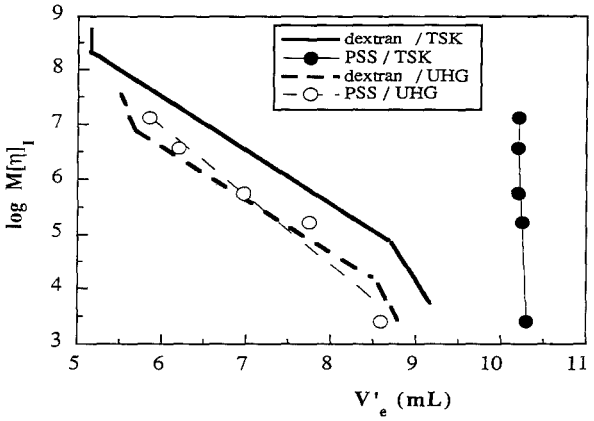

FIGURE 3. Comparison between the calibration curves for diverse polymer/gel packing pairs as specified in the legend plot, using acetate buffer (pH 5.0) at 0.1 M as eluent.

elution of polyanions through the gel packings used here, more than one force resembles to contribute to the overall adsorption effect, being more difficult to perform a theory predicting properly this effect. A temptative to explain, at least semiquantitatively, adsorption in ASEC has been developed in the frame of the Flory-Huggins theory of polymer solutions for multicomponent systems.

The first assumption deals with the fact that adsorption effects can be viewed as a reversible adsorption-desorption equilibrium between solute (S) and gel (G), expressed as follows:

$$S + G \leftrightarrow SG$$

if the activity coefficients corresponding to occupied (SG) and unoccupied (G) sites are supossed to be the same (37), the adsorption equilibrium constant can be defined as:

$$K_{ad} = \frac{[SG]}{[S][G]} \qquad (1)$$

where [G] and [SG] are the molar concentrations of the free and occupied gel active centers, respectively, in the volume of the stationary phase available to the solute, and [S] is the molar concentration of free solute. According to Laurent and Killander (38) and following the development proposed by Janado (23), the elution volume of a polymer can be expressed as:

$$V'_e = V_0 + K_{SEC}\left[1 + \frac{K_{ad}[G]_0}{1 + K_{ad}[S]}\right]V_p \qquad (2)$$

being V'_e, V_0 and V_p, the elution volume of a polyelectrolyte sample, the interstitial packing volume and the pore volume, respectively. $[G]_0$ refers to the total concentration of stationary phase accessible to the solute and K_{SEC} to the chromatographic distribution coefficient when the solute partition is due solely to steric exclusion effect.

On the other hand, when secondary effects in SEC become important, the elution volume of a polymer sample can be defined as (11,39):

$$V'_e = V_0 + K_{SEC}K_pV_p \qquad (3)$$

being K_p the partition coefficient accounting for secondary effects, adsorption in the present case. Comparison of eqns. 2 and 3 leads to:

$$K_p = 1 + \frac{K_{ad}[G]_0}{1 + K_{ad}[S]} \qquad (4)$$

Notice that K_p is a partition coefficient obtained by conventional elution chromatography, $K_p=(V'_e-V_0)/(V_e-V_0)$, whereas K_{ad} refers to an equilibrium constant. Moreover, the physical meaning of the former parameter corresponds to a ratio of polymer concentrations between the mobile and the stationary chromatographic phases, whereas K_{ad} denotes the ratio of molar concentrations of the species involved in a true chemical equilibrium. At this point, when the injected

polymer solution becomes highly diluted, it can be assumed that $[S] \rightarrow 0$, and then eqn. 4 transformed into:

$$K_p = 1 + K_{ad}[G]_0 = 1 + K'_{ad} \qquad (5)$$

since $[G]_0$ is a constant for a given chromatographic gel, $K'_{ad} = K_{ad}[G]_0$. Therefore, K'_{ad} or K_p can be used to quantitatively evaluate adsorption effects. Thus, positive values of K'_{ad} imply $K_p > 1$ (see eqn. 5) or $V'_e > V_e$, in other words, calibration curves for polyelectrolytes shifted towards the right-hand side of the reference one obtained for uncharged polymers.

In Table 1 we present K_p values extracted from calibration curves at pH 5.0 and 7.0 for PSS in both TSK and UHG columns. The eluent ionic strength was 0.1 M in both sets of experiments. In general, the K_p values increase as the molecular weight goes up and pH decreases, according to previous reported data for aqueous and organic SEC (11,18). From the comparison of K_p data obtained in both columns at pH 5.0, it can be observed strong adsorption in TSK whereas in UHG this effect vanishes, yielding K_p values close to unity which denotes that the elution occurs mainly according to a pure size-exclusion mechanism. In the light of this behavior, UHG packings will be more convenient for polymer characterization via conventional SEC, whereas TSK columns seem to be more appropriate to elute solutes according to hydrophobic interaction chromatography (HIC). Similar trends have been found for the remainder polyelectrolyte/gel systems studied here.

In order to investigate the quantitative variation of K_p values within each calibration curve, Figure 4 depicts its dependence on both sample molecular weight and eluent ionic strength, for PSS in TSK at pH 5.0 as an example. Lines connecting points have been drawn to guide the eye. On the one hand, at a given molecular weight, K_p shows a linear dependence on the inverse of the square root of ionic strength, $I^{-1/2}$, in accordance with the functionality exhibited by other variables such as the chromatographic radii of a macromolecule, R (14), the electrostatic repulsion barrier between the polyion and the charged pore, X_e (8), the ion-exclusion or repulsion volume (10), K_{SEC} (40), the persistence length, L_e (41) or the elution volume (36,42) among others. On the other hand, at a fixed ionic

TABLE 1

Values of the Distribution Coefficient, K_p, obtained from SEC Measurements as a Function of the PSS Molar Mass at Different Mobile Phase Compositions. The Ionic Strength of the Buffer Solutions used as Eluents was 0.1 M in all Experiments.

M_2 (kg·mol^{-1})	Column TSK		Column UHG	
	pH 5.0	pH 7.0	pH 5.0	pH 7.0
1.6	1.40	1.24	0.99	0.80
16	1.60	1.41	1.07	0.87
31	1.91	1.68	1.08	0.81
88	2.80	2.46	1.22	0.88
177	4.81	3.60	1.95	1.68

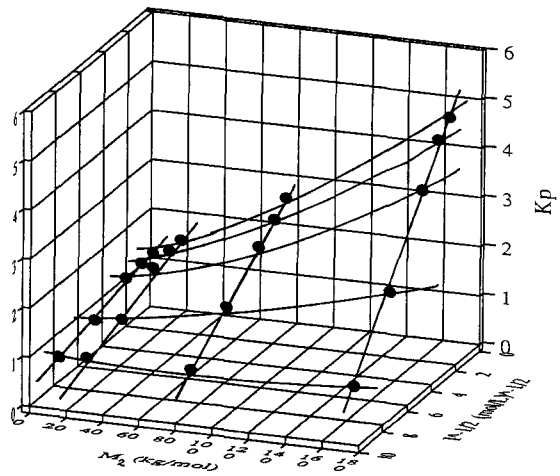

FIGURE 4. Plot of K_p dependence on both M_2 and $I^{-1/2}$ for PSS in a TSK PW4000 column using acetate buffer (pH 5.0) as eluent.

strength, K_p values seem to follow an exponential variation with the molecular weight, mainly at high K_p values. Theoretical prediction of this last dependency has been made in the framework of the Flory-Huggins (FH) polymer solutions theory (43-46). On this regard, some authors consider a ternary system formed by a solvent(1) (the eluent), a polymer(2) (the eluite) and a polymer(3) (the crosslinked polymeric network or gel chromatographic packing) yielding a master equation which correlates K_p with the polymer molecular weight, M_2, through:

$$-\ln K_p = \frac{\phi_3}{\rho_2 V_1}(1 + g_{23} - g_{12} - g_{13})M_2 \qquad (6)$$

being ρ_2 the density of the injected polymer solution, V_1 the molar volume of solvent, ϕ_3 the volume fraction of gel involved in the ternary phase, and g_{ij} the Flory-Huggins interaction parameters.

To date, the validity of the above equation has been exclusively tested for uncharged polymers in organic media (44). For ionic polymers such as polyelectrolytes and proteins in aqueous media, a non-unique dependence has been postulated. Thus, Hjerten (47) proposed the relationship $\log K_p \propto M$ for low molecular weight compounds, whereas for globular and flexible macromolecules the functionality $\log K_p \propto M^{2/3}$ worked better. In previous papers, our group has reported the accomplishment of $\ln K_p \propto M^{-1/2}$ for synthetic polyelectrolytes at low ionic strengths (see Figs.5 and 2 from refs.11 and 13, respectively). However, at moderate and high ionic strengths, we believe that eqn. 6 could be an appropriate functionality to quantitative analyze adsorption secondary effects in ASEC. This aseveration can be supported *a priori* by the fact that at high ionic strength, most charges on the polyion are screened by counterions increasing the chain flexibility and reaching the polymer a random-coil conformation similar to that for synthetic polymers in organic media.

Figure 5 depicts plots of eqn. 6 for: (a) PSS in TSK, (b) PSS in UHG and (c) PAA in TSK using acetate buffer (pH 5.0) at different ionic strengths. The horizontal line drawn on these plots at zero value in ordinates (K_p=1) denotes the

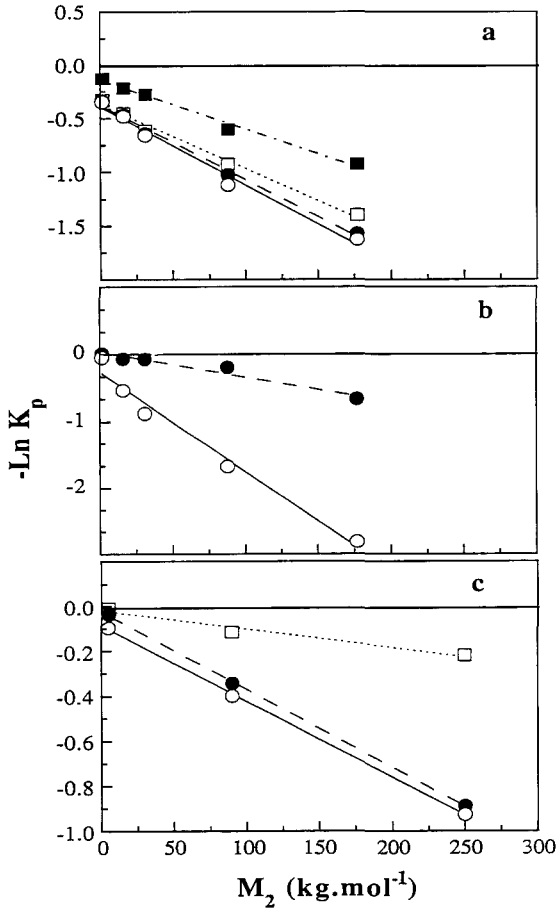

FIGURE 5. Plot of eqn. 6 for the following polyelectrolyte/gel systems: (a) PSS/TSK; (b) PSS/UHG and (c) PAA/TSK. Symbols stand for eluent ionic strength and have the same meaning as in Fig. 1.

location of the pure size-exclusion mechanism, corresponding upper and lower zones to electrostatic polymer-gel repulsion ($K_p<1$) and to polymer-gel adsorption ($K_p>1$), respectively. Firstly, it deserves to be remarked that experimental K_p values fit well to a straight line in all cases in spite of the marked structural differences of polyelectrolytes and gels used. These results support the validity of eqn. 6, at least under the chromatographic conditions and molecular weight range assayed here. Second, the absolute slope values increase as the mobile phase ionic strength does, in accordance with previously reported experiments, where $K_p>1$ were often obtained at high I values (9,48,49). Moreover, the slope values could be regarded as a quantitative measure of how intense becomes the driving forces involved in the adsorption phenomena between the network links on the gel packing and links of the eluted linear polyion.

Figure 6 shows similar plots of eqn. 6 for PSS (part a) and PGA (part b) in TSK using phosphate buffer (pH 7.0) and different I values, as mobile phase. Some comments supporting the selected experimental conditions on this Figure deserve to be made: (i) pH 7.0 was used because most biopolymers display a practical activity in biological fluids streamed in living tissues at a pH values close to neutrality; (ii) the selection of an appropriate I values becomes important in order to minimize secondary effects; (iii) the above experimental conditions can also serve to test the fulfillment of eqn. 6 when size-exclusion and electrostatic repulsion besides adsorption effects take place. From the inspection of Figure 6a, as expected, for $I \geq 0.1$ M the adsorption effects govern the chromatographic elution of PSS whereas at $I \approx 0.01$ M the ion-exclusion seems to be the predominant effect. Elution mechanisms in ASEC are not only controlled by ionic strength but also by the chemical nature and pK_a of the ionic group of the polyelectrolyte. To corroborate this argument, Figure 6b shows plots of eqn. 6 for PGA in the same range of I. In contrast with that displayed in part a, at $I \geq 0.1$ M neither adsorption nor electrostatic repulsion are evidenced, whereas at $I \approx 0.01$ M strong polymer-gel repulsions occur. Again, good linear fits are always obtained corroborating the validity of eqn. 6 for charged polymers in aqueous media.

Following our inspection of Figures 5 and 6, it seems that the slopes of the straight lines depicted are closely related to the binary g_{ij} interaction parameters. On

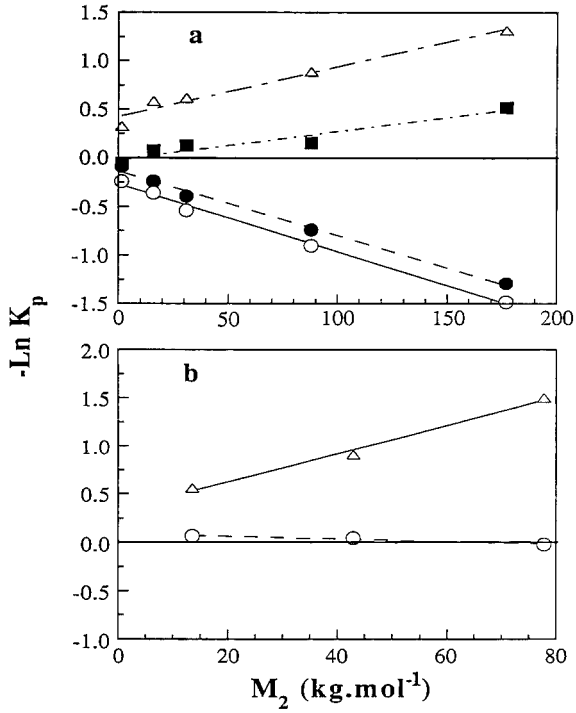

FIGURE 6. Plot of eqn. 6 for the systems: PSS/TSK (a) and PSS/UHG (b) in phosphate buffer (pH 7.0) as mobile phase. Symbols stand for eluent ionic strength and have the same meaning as in Fig. 1.

this regard, recent contributions (50,51) have also analyzed the swelling and collapse of soft gels in polymer solutions (charged or not) in terms of the interaction of components (compatibility) within the FH approximation. Note that for a quantitative interpretation of the elution mechanisms on the basis of polymer-gel compatibility through the slope values of eqn. 6, it is necessary the availability of the g_{ij} experimental values. Owing to the lack of g_{ij} data in the literature for polyions in buffer solutions, we can only speculate about the sign of the slope, directly related to the elution mechanism governing the SEC separation process. In

the particular case that polyelectrolytes are eluted according to the pure size-exclusion mechanism, the slope of eqn. 6 approaches to zero (see Figure 6b). From a thermodynamic viewpoint, this behaviour implies that the g_{23} parameter is close to zero because neither favorable ($g_{23}<0$) nor unfavorable ($g_{23}>0$) polymer-gel interactions are involved in the separation mechanism. However, a more plausible explanation could be given for ionic polymers in hydrophilic gels if one assumes that both favorable and unfavorable interactions exist but cancel each other. Therefore, under chromatographic conditions in which the elution data are slightly shifted from the pure SEC, $g_{23} \approx 0$, and the slope of the above plots will be proportional to $(1 - g_{12} - g_{13})$ and eqn. 6 for these cases can be transformed into:

$$-\ln K_p \cong \frac{\phi_3}{\rho_2 V_1}(1 - g_{12} - g_{13})M_2 \qquad (7)$$

For this particular situation, the entity $(1 - g_{12} - g_{13})$ is coincident with the numerator of the following expression (45):

$$\lambda = \bar{v}_3 \frac{1 - g_{12} - g_{13}}{1 - 2g_{12} - 2(dg_{12}/d\phi_1)} \qquad (8)$$

being λ the preferential solvation parameter, widely studied in polymer-mixed solvent systems (see eqn. 20 from ref.45), and $\bar{v}_3$ the partial specific volume of component 3. Assuming that the denominator of eqn. 8 is always positive (52), valid for random-coil conformations, the sign of the λ parameter and the sign of $(1 - g_{12} - g_{13})$ will be coincident, allowing us a more comprehensive analysis of the secondary effects in ASEC in terms of λ instead of the g_{ij} interaction parameters. First of all, it is important to understand the physical meaning of the sign of λ. On this regard, favorable or preferential eluent-gel interactions are represented by $\lambda>0$ and favorable polymer-gel interactions by $\lambda<0$. These statements can also be associated to the polymer-gel incompatibility and compatibility, respectively. Obviously, when both types of interactions are counterbalanced λ vanishes meaning that macromolecules are eluted according to a pure SEC mechanism. In the light of this formalism, $K_p>1$ corresponds to $\lambda<0$ denoting that the adsorption effect can be

viewed as a polymer-gel compatibility. In contrast, when the main secondary effec is the electrostatic repulsion, $K_p<1$ or $\lambda>0$ closely related to polymer-gel incompatibility.

CONCLUSIONS

It has been selected the partition coefficient, K_p, or its related equilibrium constant K'_{ad} (see eqn. 5), to quantify the intensity of the polymer-gel packing adsorption. The values of this parameter have been extracted from basic chromatographic equations dealing with elution of polyelectrolytes. In most of the experiments reported here, $K_p>1$ denoting that adsorptive effects take place. Some speculations about the driving forces involved in the polymer-gel packing interactions reveal that H-bonding can be the origin of this phenomenon when PAA and PGA are eluted. However, in the case of PSS the adsorption effect can be assigned to hydrophobic interaction between some regions on the surface of the polyelectrolyte and those on the stationary phase. This behavior has been confirmed in the two hydrophilic packings studied here, being the adsorption effects more intense on the TSK column than on the UHG one, for the same polymer eluted under fixed experimental conditions. Therefore, it seems that UHG gel packing is innerter than TSK for size-exclusion separation purposes.

Finally, we have presented in this contribution an attempt to explore adsorption secondary effects in ASEC by means of the Flory-Huggins theory of polymer solutions extended to the eluent(1)/polymer(2)/gel packing(3) ternary system. Some transformations of the original equations allow us to introduce the λ parameter (see eqn. 8) in order to justify the adsorption effects in terms of polymer-gel compatibility. Within the limits of the accuracy of the data, we conclude that linear plots depicted in Figures 5 and 6 support the validity of the functionality obtained in eqn. 6 through the FH theory.

Additional experimental and theoretical contributions, beyond the chromatographic scope, must be done, mainly to evaluate the g_{ij} parameters for ionic species.

ACKNOWLEDGEMENTS

Support from the Dirección General de Investigación Científica y Técnica (Spain) under Grant No. PB91-0808 is gratefully acknowledged. I. P. also thanks Ministerio de Educación y Ciencia (Spain) for a long-term predoctoral fellowship.

REFERENCES

1. C.G. Smith, P.B. Smith, A.J. Pasztor Jr., M.L. Mckelvy, D.M. Meunier, S.W. Froelicher and A.S. Ellaboudy, *Anal. Chem.*, 65: 217R-243R (1993).

2. P.L. Dubin, *Adv. Chromatogr.*, 31: 119-151 (1992).

3. H.G. Barth and B.E. Boyes, *Anal. Chem.*, 64: 428R-442R (1992).

4. P.L. Dubin, in *Aqueous Size-Exclusion Chromatography*, P.L. Dubin, ed., Elsevier, Amsterdam, 1988, Ch. 3.

5. R. Audebert, *Polymer*, 20: 1561-1566 (1979).

6. H.G. Barth and J.W. Mays, eds., *Modern Methods of Polymer Characterization*, Wiley Interscience, New York, 1991.

7. M. Potschka, *J. Chromatogr.*, 441: 239-260 (1988).

8. P.L. Dubin, C.M. Speck and J.I. Kaplan, *Anal. Chem.*, 60: 895-900 (1988).

9. S. Mori, *J. Chromatogr.*, 471: 367-374 (1989).

10. S. Mori, *Anal. Chem.*, 61: 530-534 (1989).

11. V. Soria, A. Campos, R. García, M.J. Parets, L. Braco and C. Abad, *J. Liq. Chromatogr.*, 13: 1785-1808 (1990).

12. P.L. Dubin, R.M. Larter, C.J. Wu and J.I. Kaplan, *J. Phys. Chem.*, 94: 7243-7250 (1990).

13. E. Pérez-Payá, L. Braco, C. Abad, V. Soria and A. Campos, *J. Chromatogr.*, 548: 93-104 (1991).

14. M. Potschka, *Macromolecules*, 24: 5023-5039 (1991).

15. M. Potschka, *J. Chromatogr.*, 648: 41-69 (1993).

16. S.L. Edwards and P.L. Dubin, *J. Chromatogr.*, 648: 3-7 (1993).

17. P.L. Dubin, S.L. Edwards, M.S. Mehta and D. Tomalia, *J. Chromatogr.*, 635: 51-60 (1993).

18. J.E. Figueruelo, V. Soria and A. Campos, in *Liquid Chromatography of Polymers and Related Materials II* (Chromatographic Science Series, Vol.13), J. Cazes and X. Delamare, eds., Marcel Dekker, Inc., New York, 1980, pp. 49-71.

19. S. Mori, in *Steric Exclusion Liquid Chromatography of Polymers* (Chromatographic Science Series, Vol.25), J. Janca, ed., Marcel Dekker, Inc., New York, 1984, pp. 161-211.

20. P.L. Dubin and M.M. Tecklenburg, *Anal. Chem.*, 57: 275-279 (1985).

21. R.C. Montelaro, in *Aqueous Size-Exclusion Chromatography*, P.L. Dubin, ed., Elsevier, Amsterdam, 1988, Ch. 10.

22. T. Hanai, *J. Chromatogr.*, 550: 313-324 (1991).

23. M. Janado, in *Aqueous Size-Exclusion Chromatography*, P.L. Dubin, ed., Elsevier, Amsterdam, 1988, Ch. 2.

24. A. Ben-Naim, *Hydrophobic Interaction*, Plenum Press, New York, 1980.

25. A.R. Cooper and D.S. van Derveer, *J. Liq. Chromatogr.*, 1: 693-726 (1978).

26. S.N.E. Omorodion, A.E. Hamielec and J.L. Brash, *J. Liq. Chromatogr.*, 4: 1903-1916 (1981).

27. P. Oroszlan, R. Blanco, X.M. Lu, D. Yarmush and B.L. Karger, *J. Chromatogr.*, 500: 481-502 (1990).

28. K. Gooding and F. Regnier, eds., *High Performance Liquid Chromatography of Biological Macromolecules: Methods and Applications*, Marcel Dekker, Inc., New York, 1988.

29. S. Shaltiel and Z. Er-el, *Proc. Natl. Acad. Sci. USA*, 70: 778 (1973).

30. C. Clothia and J. Janin, *Nature*, 256: 705 (1975).

31. X. Geng, L. Guo and J. Chang, *J. Chromatogr.*, 507: 1-23 (1990).

32. F. R. Senti, N.N. Hellmann, N.H. Ludwing, G.E. Babcock, R. Tobin, C.A. Class and B. Lamberts, *J. Polym. Sci.*, 17: 527 (1955).

33. H.G. Elias, *Kunst.-Plast.*, 4: 1 (1961).

34. R. García, I. Porcar, A. Campos, V. Soria and J.E. Figueruelo, *J. Chromatogr.*, 655: 3-9 (1993).

35. R. García, I. Porcar, A. Campos, V. Soria and J.E. Figueruelo, *J. Chromatogr.*, (in press).

36. R. García, I. Porcar, A. Campos, V. Soria and J.E. Figueruelo, *J. Chromatogr.*, (in press).

37. D. Graham, *J. Phys. Chem.*, 57: 665 (1953).

38. T.C. Laurent and J. Killander, *J. Chromatogr.*, 14: 317 (1964).

39. J.V. Dawkins and M. Hemming, *Makromol. Chem.*, 176: 1815 (1975).

40. M. Rinaudo and J. Desbrieres, *Eur. Polym. J.*, 16: 849 (1980).

41. M. Tricot, *Macromolecules*, 17: 1698-1704 (1984).

42. M.G. Styring, H.H. Teo, C. Price and C. Booth, *Eur. Polym. J.*, 24: 333-339 (1988).

43. J. Lecourtier, R. Audebert and C. Quivoron, *J. Chromatogr.*, 121: 173 (1976).

44. J.M. Barrales-Rienda, P.A. Galera-Gómez, A. Horta and E. Sáiz, *Macromolecules*, 18: 2572-2579 (1985).

45. R. Tejero, R. Gavara, C. Gómez, B. Celda and A. Campos, *Polymer*, 28: 1455-1461 (1987).

46. R. García, B. Celda, V. Soria, R. Tejero and A. Campos, *Polymer*, 31: 1694-1702 (1987).

47. S. Hjertén, *J. Chromatogr.*, 50: 189-208 (1970).

48. B. Stenlund, *Adv. Chromatogr.*, 14: 37-75 (1974).

49. M.S. Strege and P.L. Dubin, *J. Chromatogr.*, 463: 165-170 (1989).

50. sixth and seventh terms of eqn. 3 from T. Ikehara and T. Nishi, *Phys. Rev. Lett.*, 71: 2497-2500 (1993).

51. section 6 from V.V. Vasilevskaya and A.R. Khokhlov, *Macromolecules*, 25: 384-390 (1992).

52. Since $g_{12} + dg_{12}/d\phi_1 = g_{12} - dg_{12}/d\phi_2 = \chi_{12}$ and the χ_{12} values cannot exceed 0.5 according to the Flory-Huggins theory for random-coil polymers.

Received: December 17, 1993
Accepted: January 6, 1994

JOURNAL OF LIQUID CHROMATOGRAPHY, 17(14&15), 3285-3306 (1994)

INSIGHT INTO THE CHEMICAL HETEROGENEITY OF CATIONIC POLY-ELECTROLYTES BY GRADIENT-HPLC USING SALT GRADIENTS †

U. LEHMANN[1]‡, M. AUGENSTEIN[1]*, AND B. NEIDHART[2]
[1]*Röhm GmbH*
64275 Darmstadt, Germany
[2]*Fachbereich Chemie*
Phillips-Universität
35032 Marburg, Germany

ABSTRACT

The chromatographic behaviour of cationic poly(meth)acrylates was investigated in HPLC using salt gradients as the mobile phase. A quantitative correlation was found between retention time and number of charges per macromolecule. Information on the copolymerization behaviour of binary systems could be derived from the chromatograms. Insight into the chromatographic mechanism was gained by temperature dependent HPLC.
Thus the method is suitable for the characterisation of cationic polymethacrylates. The influence of parameters like ionic strength, pH-value, temperature, and poresize of the stationary phase corresponds widely with physico-chemical data and models of ionic macromolecules. The results offer a basis for setting up standard methods for the chromatographic characterisation of polyelectrolytes of similar structure.

---

* To whom correspondence should be addressed

† Part of diploma thesis of Ulrich Lehmann, Marburg (1992)

present address: Max-Planck-Institute for Polymer Research, 55128 Mainz, FRG

INTRODUCTION

Detailed knowledge about the correlation between molecular structure and properties of polymers is one of the main prerequisites for their preparation and technical production aiming at a tailor-made behaviour and an optimised process of synthesis. The properties of cationic copolymers e.g. depend on whether the charge distribution along the polymer chain is random or blocked. Therefore it is of major interest to get information on the molar mass and the heterogeneity of copolymers.

Up to now NMR-spectroscopy has been the method of choice for investigations on the chemical structure of copolymers [1]. In principle this method provides conclusions about the microstructure and the mean composition of polymers. However, it is not possible to discover details about the distribution of the chemical composition by NMR.

For some time past chromatographic methods like HPLC and SEC have gained increasing importance for the characterisation of polymers [2]. Gradient-HPLC of polyelectrolytes was performed by HUANG [3], who investigated copolymers of the cationic monomer diallyldimethylammoniumchloride with acrylamide with the aim of getting information on the structural heterogeneity of these copolymers of low charge density with not more than 10 per cent of charged comonomer. HUANG found after ultrasonic treatment that the polymers showed reduced retention times, a fact he attributed to a lower number of charges per molecule due to chain fragmentation. HUANG expected information about the chemical heterogeneity within single polymer chains based on the hypothesis that after fragmentation chains with a homogeneous charge distribution would give rise to a single sharp peak in the chromatogram whereas chains with a heterogeneous charge distribution would show two broad peaks, the first one relating to fragments with lower charge density and the second one covering fragments with higher charge density. HUANG, however, reported only very few results that were not able to give strong evidence for his hypothesis.

Regarding these interesting aspects it seemed worth to start a systematic investigation on the correlation between retention time and charge number of cationic polyelectrolytes. Using well characterised samples of cationic poly(meth)acrylates the chromatographic mechanism was to be investigated.

Another intention of the study was to test whether the method was suitable to get insight into the behaviour of copolymerization by characterising the chemical heterogeneity of the resulting copolymer samples. Because this group of polyelectrolytes proved easily soluble in water, aqueous solutions were used as mobile phase. Due to the

presence of ionic charges along the polyelectrolyte chaines it seemed consequent to count on the interactions of these groups with the stationary phase as the main separation mechanism [4]. Selecting the stationary phase, however, it had to be taken into account that strongly polar packings were likely to cause quasi irreversible adsorption originating from a cooperative action of multiple charges along the chain; in contrast on less suface active packings the polymers might not be retarded sufficiently.

MATERIALS

The chromatographic investigations were performed with four different types of polymers composed of the monomers trimethylammoniumethylmethacrylate-chloride (1), trimethylammoniumethylacrylate-chloride (2), and acrylamide (3). In the following the homopolymer poly-trimethylammoniumethylmethacrylate-chloride and the copolymers poly-trimethylammoniumethylacrylate-chloride-co-acrylamide and poly-trimethylammoniumethylmethacrylate-chloride-co-acrylamide are named poly-1, poly-2-co-3 and poly-1-co-3 respectively. For the experiments ten samples of poly-1 (A1 to A10), thirteen samples of poly-2-co-3 (B1 to B10 and D1 to D3) and one sample of poly-1-co-3 (E3) were used. The polymerization of samples B1 to B10 was not conducted to complete conversion, but interrupted at a small degree of conversion, G.

The molar masses were determined by size exclusion chromatography in aqueous solution using poly-1-calibrants. The maximum M_{Max} of the differential molar mass distribution W(lnM), was used for the calculation of the charge number Z; as this charge number is related to the maximum of the molar mass distribution it refers to the corresponding polymer fraction only and not to the whole sample. When correlating these Z-values with peak maximum retention times from gradient HPLC, it is assumed that it is the same polymer fraction eluting with the peak maximum in SEC and in HPLC. Furthermore, it has to be assumed that the copolymers, too, follow the calibration curve and that in HPLC the peak maximum fraction corresponds to the average composition of the sample. It is not claimed that these assumptions were close to correct, so that an error of up to about 10 percent has to be taken into account.

The charge number Z is calculated for homopolymers using eq.1 and for copolymers eq. 2, with M_1, M_2 and a_1, a_2 being the molar masses and mole fractions of the charged (1) and uncharged (2) comonomers respectively.

$$Z = \frac{M_{Max}}{M_1} \qquad (1)$$

$$Z = \frac{M_{Max}}{a_1 M_1 + a_2 M_2} a_1 \qquad (2)$$

Table 1 summarizes the SEC-results and the charge numbers for ten homopolymer samples poly-1, three samples of poly-2 and eleven copolymer samples investigated in this study.

Samples which were polymerized up to complete conversion normally show a broad distribution of their composition, especially if at the beginning of the reaction one of the monomers is consumed preferably; in any case the mean composition is identical to that of the monomers in the reaction mixture. For the high conversion binary copolymers (D1 to D3 and E3) it can be estimated from the copolymerization diagrams [5] how the composition of the resulting polymer chains changes during the course of the reaction. Samples B4 to B10, however, show a narrow distribution of their chemical composition because in this case the polymerization was interrupted at a small degree of conversion so that all polymer chains were formed under similar conditions. The composition of monomer units in the polymer, however, differs from the composition in the reaction mixture depending on the values of the copolymerization parameters. From the copolymerization parameters r_1 and r_2 the instantaneous mole fraction x_{1P} of the monomer 1 in the polymer can be calculated as a function of the mole fraction x_{1M} of the monomer 1 in the reaction mixture by using eq. 3 [6,7].

$$x_{1P} = \frac{r_1 x_{1M}^2 + x_{1M}(1-x_{1M})}{(r_1+r_2-2) x_{1M}^2 + 2(1-r_2) x_{1M} + r_2} \qquad (3)$$

For the copolymerization of monomer 2 with monomer 3, TANAKA [6] determined the copolymerization parameters to be $r_2 = 0.48$ and $r_3 = 0.64$ corresponding to a non-ideal azeotropic copolymerization. Other authors like BAADE et al. [7] determined values which

TABLE 1

Weight average molar mass M_w, peak maximum molar mass M_{Max}, charge number Z, polydispersity $U = (M_w/M_n) - 1$, degree of conversion G and mole fraction x_{3P} of acrylamide in the polymer calculated according to eq.3 for samples of poly-1 (A1-A10), poly-2 (B1-B3), poly-2-co-3 (B4-D3) and poly-1-co-3 (E3)

Sample	M_w /(10^3g/mol)	M_{Max} /(10^3g/mol)	U	G/%	Z/10^3	x_{3P}
A 1	6	5	0,9		0,02	
A 2	45	34	2,2		0,16	
A 3	44	39	1,5		0,19	
A 4	79	75	1,6		0,36	
A 5	137	93	2,0		0,45	
A 6	320	240	3,8		1,2	
A 7	765	570	3,1		2,8	
A 8	2.500	2.000	1,6		9,8	
A 9	6.350	5.400	2,0		26,0	
A10	8.300	7.600	1,5		37,0	
B 1	4.500	2.700	1,6	4,3	13,9	0,00
B 2	3.800	2.600	1,1	4,3	13,5	0,00
B 3	4.700	3.200	1,3	4,3	16,6	0,00
B 4	4.700	2.400	1,9	4,3	11,7	0,14
B 5	6.100	3.400	1,6	3,9	14,8	0,34
B 6	5.800	3.100	1,9	1,8	12,3	0,45
B 7	7.100	3.800	1,5	2,8	14,1	0,53
B 8	6.200	3.400	1,6	3,9	11,4	0,60
B 9	5.600	3.000	2,9	3,0	8,2	0,71
B10	4.200	2.200	2,0	3,0	2,9	0,89
D 1	5.000	3.400	8,1	100,0	15,3	0,30
D 2	4.300	3.000	7,9	100,0	11,2	0,50
D 3	6.100	4.100	3,1	100,0	11,4	0,70
E 3	7.700	5.800	2,1	100,0	20,8	0,50

differed only slightly from the former. In Tab. 1 the mole fractions of acrylamide x_{3P} for the B-samples are given as calculated from eq. 3.

Synthesis of Polyelectrolyte Samples

Poly-1:

An aqueous solution of 1 (c = 1.2 mol/L) is adjusted to pH 4 with dilute H_2SO_4. At a temperature of 60°C an aqueous solution of 2,2'-azobis(2-amidinopropane)dihydrochloride (c = 0.65 mol/L) is added under exclusion of oxigen, resulting in a concentration of the initiator in the reactor of $9.2*10^{-4}$ mol/L. After a reaction time of 30 min the reaction mixture is precipitated into acetone/ethanol (6/1 (v/v)) and dried at 50°C under vacuum.

Poly-2-co-3 (B1 to B10):

The monomers 2 and 3 are weighed in the desired amounts and dissolved in water, resulting in a solution with a total concentration of the monomers of 2 mol/L. At a temperature of 45°C and by excluding oxigen an aqueous solution of peroxidisulfate (c = 0.02 mol/L) is added to this solution, resulting in a concentration of the initiator of 0.005 mol/L. After a reaction time of 20 min the reaction mixture is precipitated into acetone/ethanol (6/1 (v/v)) and the precipitate dried at 50°C. The polymerization of these samples was stopped at low degree of conversion by pouring the reaction mixture quickly into the precipitation bath.

The samples poly-1-co-3, E3, and poly-2-co-3, D1 to D3, are standard products of Röhm GmbH, which are produced in technical amounts also by radical polymerization.

METHODS

All HPLC-columns contained a macroporous hydroxyethylmethacrylate-gel (HEMA) crosslinked with ethylenglycoldimethacrylate. Aqueous solutions of sodium chloride were applied as the mobile phase, the ionic strength of which steadily increased in the course of a gradient program. The pH-value of the mobile phase was kept constant at 7.4 by means of a phosphate buffer system. The gradient program described by HUANG [3] could not be used, as the salt concentration obviously was too low and not compatible with the highly charged polymers investigated in this study. Therefore new gradient programs had

to be developed which were based on the results of separations under isocratic conditions. A detailed description of the programs is given by Tab. 2. When applied to separations with the shorter column, the program P1 lead to peaks sufficiently sharp so that the maxima could be read from the chromatograms with good precision. Program P2 was used for runs with the two longer columns.

In order to achieve sufficient reproducibility of the retention times a buffered mobile phase turned out to be necessary. With unbuffered media the retention times became shorter with the number of runs; this effect was attributed to uneluted polyelectrolytes which reduced the activity of the stationary phase. Complete reconstitution of the column after each chromatographic run turned out to be indispensable for reproducible separations and was achieved by washing the column intensely with the solution of lowest salt concentration.

HPLC System

The chromatographic system consisted of a gradient HPLC-pump (L-6200), an autosampler (AS-6000), and a UV-detector (L-4000) from E.Merck (Darmstadt, F.R.G). The chromatogram s were registered by a recorder (Abimed Linear) from Linear Instruments Corp. (Irvine/California). For thermostatic control a kryostat (Lauda UKT 600) from Meßgerätewerk Lauda (Tauber, F.R.G.) and a waterbath (Julabo HC5) from Julabo Labortechnik GmbH (Seebach, F.R.G.) were applied. The detector signals were recorded digitally by the central computer of Röhm GmbH.

Separation columns were from Polymer Standard Service (Mainz, F.R.G.). The dead time/dead volume was determined by injection of an aqueous solution of sodium nitrate. Column 1 was PSS HEMA Bio 40 (dimensions: 8 x 50 mm; pore diameter 4 nm) with a dead time of 1.4 min. Columns 2 and 3 were PSW HEMA 40 and 1000 resp. (8 x 250 mm; pore diameters 4 nm and 100 nm resp.) with dead times of 9.0 and 9.3 min resp. The particle diameter of all columns was 10 µm.

Buffer-solution (ionic strength I = 0.1 mol/L; pH 7.4) :

In a 1 L measuring flask 1.18 g KH_2PO_4 p.a. (Fluka, Switzerland) and 10.85 g Na_2HPO_4 p.a. (Fluka) were dissolved and filled up to the mark with water Lichrosolv (Merck) [11].

Buffered solution of sodium chloride (I = 2.0 mol/L; pH 7.4) :

In a 1 L measuring flask 1.18 g KH_2PO_4 p.a., 10.85 g Na_2HPO_4 p.a., and 111.04 g NaCl p.a. (Merck) were dissolved and filled up to the mark with water Licrosolv.

TABLE 2

Course of ionic strength I with time for the gradient programs P1 and P2 (the delay time with respect to the detector amounted to approximately 5 min)

gradient program P1:		gradient program P2:	
time/min	I/(mol/L)	time/min	I/(mol/L)
0	0.1	0	0.1
2	0.1	20	1.1
22	1.1	21	0.1
24	0.1	50	0.1
40	0.1		

Samples for HPLC-separation:

About 100 mg of the polymer were weighed in a 20 mL measuring flask and filled up to the mark with a solution of sodium chloride (c = 0.2 mol/L) prepared with water Licrosolv (Merck). The resulting polyelectrolyt concentration was about 5 g/L.

Size Exclusion Chromatography

The apparatus consisted of an HPLC-pump from Bischoff Analysentechnik und -geräte GmbH (Leonberg, F.R.G.). Four separation columns (Ultrahydrogel) with pore sizes of 200, 100, 50, and 25 nm from Waters Chromatography Division (Eschborn, F.R.G.) were applied (dimensions: 7.8 x 300 mm). A differential refractometer from Knauer Wissenschaftliche Geräte KG (Oberursel, F.R.G.) was used, the signals of which were recorded by the central computer of Röhm GmbH. The separation columns were connected in series with decreasing pore sizes and run with an acetate buffer (acetic acid (c = 0.5 mol/L) / sodium acetate (c = 0.5 mol/L)) in water at a flowrate of 0.8 mL/min according to OTT [12]. The concentration of the polymers in the injected solution was 0.25 g/L; the injection volume was 300 µL at a temperature of 22°C.

Preparation of samples for SEC:

About 5 mg of the polymer were weighed in a 20 mL measuring flask and filled up to the mark with the above acetate buffer. The samples were kept for about 12 h and then

injected onto the column after addition of a small amount (spatula) of sodium acetate as an internal standard (dead time: 38.2 min).

The SEC system was calibrated using fifteen samples of poly-1 prepared by radical polymerization with molar mass from 6.000 to 10^7 g/mol and polydispersity $U = (M_w/M_n)-1$ varying from 1 to 5. The molar masses of these samples were determined by light scattering and ultracentrifuge measurements [13]. The calibration function was calculated by iterative optimization on the basis of the chromatogram and the M_w-value of all calibrants.

RESULTS

Peak Assignment

Fig.1 shows a typical chromatogram which was obtained with the gradient program P1 for the homopolymer sample A6. The positive baseline drift is caused by the increasing concentration of sodium chloride along the gradient when the UV-detector is set to 220 nm. Peak 1 appears with the dead volume (t_R = 1.5 min) and stems from the solvent of the sample. Peak 3 has a retention time of 16 min, is much broader and related to the polymer. Peak 2 is also found in the blank sample (deionised water); it might be suspected that with increasing salt content in the mobile phase impurities from the eluent are eluted, which before had been enriched in the stationary phase at low salt concentrations.

Fig. 2 shows a typical chromatogram for a sample of poly-2-co-3 with peak 3 corresponding to the copolymer. Peak 1 could be due to an elution of excluded polymer without or with only few charges because its retention time is shorter (1.2 min) than that of the solvent peak. As stated above, peak 2 possibly is caused by impurities from the eluent. Peaks 4 and 5 occur within the isocratic part of the chromatogram and may be attributed to polymer with low charge density, to low molar mass oligomers, or to residual monomer.

Problems with Column Overloading

Whereas in size exclusion chromatography the retention times decrease proportionally with the logarithm of the molar mass of the polymers, in gradient-HPLC of polyelectrolytes it can be expected that the retention times increase with the number of ionic charges. For

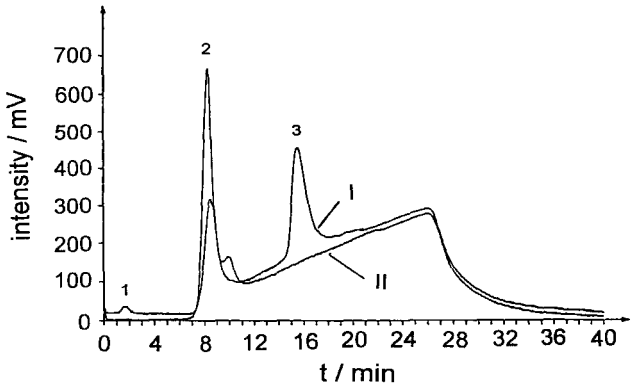

FIGURE 1 : Chromatogram for (I) the homopolymer poly-1 (sample A6; M_w = 320.000 g/mol) and for (II) a blank sample; column: PSS HEMA Bio 40; injection volume: 5 µL; analyte conc.: 5 g/L; flow rate: 1.0 mL/min; gradient P1; UV-detection: 220 nm.

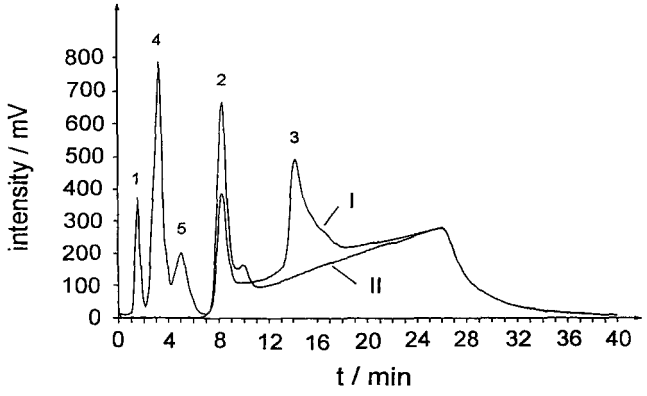

FIGURE 2 : Chromatogram for (I) the copolymer poly-2-co-3 (sample B9; M_w = 5.6 * 10^6 g/mol); and for (II) a blank sample; (for conditions see Fig.1)

homopolyelectrolytes the charge number is proportional to the molar mass, which means that under ideal conditions the chromatogram from HPLC, as an image of the charge distribution, should correlate with the distribution of the molar mass. However, such a comparison turned out to be difficult because the evaluation of the gradient-HPLC-chromatograms is complicated by the baseline drift. After subtraction of the baseline the chromatogram from HPLC (Fig.3a) of the sample A6 (poly-1) looks like a reflection of the respective distribution of the molar masses (Fig.3b) with a "tailing" for the first and a "fronting" for the latter. The asymmetric shape of the HPLC-peak may be due to an overloading of the column caused by an insufficient column capacity. Overloading of the separation column can easily occur because the large number of charges along each polymer chain will lead to an early occupation of the active sites of the gel surface even at low polymer concentrations.

The fact of increasing peak maximum retention times with decreasing analyte concentration supports the supposition of column overloading (Fig.4). The range of concentration independent retention times would be expected for concentration c below 0.2 g/L and could not be reached because of too low peak intensities. At constant analyt concentration decreasing injection volumes, too, lead to increasing retention times (Fig.5), an effect which also supports the hypothesis of column overloading.

These correlations make clear that in the following discussion it must be kept in mind that peakshapes and retention times may be effected by overloading of the column. Furthermore it has to be taken into account that multiple retention mechanisms and chromatographic effects from the polydispersity of the samples might be influencing the peakshape.

Retention Times of Homopolyelectrolytes and Copolyelectrolytes - Effect of Number and Density of Ionic Groups

Irrespective of their molar masses the homopolymer samples of poly-1 show similar retention times under isocratic conditions (at constant ionic strength). When the gradient P1 is applied, however, the retention time of peak 3 (Fig.1) increases from 13.2 min to 15.1 min with increasing molar mass (sample A2 to A10). From this a linear correlation between t_R and log M_{Max} can be derived (Fig.6): the more repetition units a polymer chain has, the longer is its retention time.

Furthermore, in Fig.6 the logarithms of the calculated charge numbers Z for the copolymers poly-2-co-3 (B-samples) from Tab.1 are plotted versus the corresponding

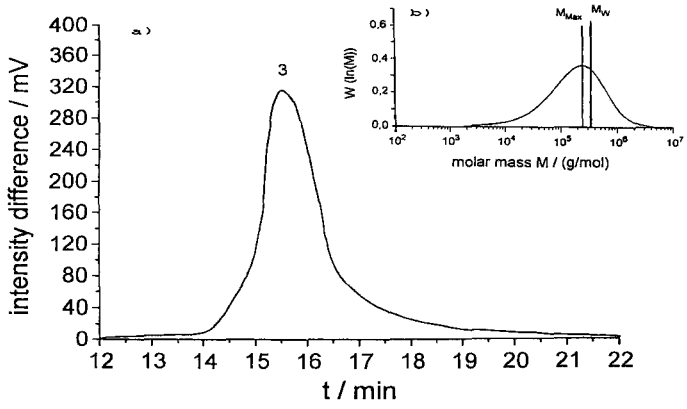

FIGURE 3 : Section-chromatogram (peak 3) of poly-**1**, sample A6, after subtraction of the baseline (a); (for conditions see Fig.1);
molar mass distribution (b)

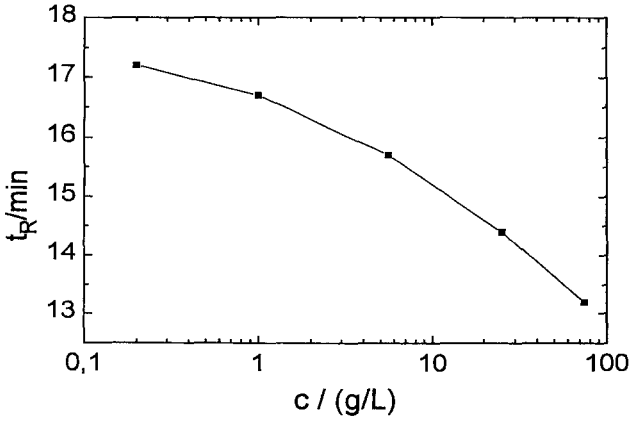

FIGURE 4 : Influence of the analyte concentration c on the retention time t_R for poly-**1**, sample A3 (M_W = 44.000 g/mol); injection volume: 10 µl (for other conditions see Fig.1)

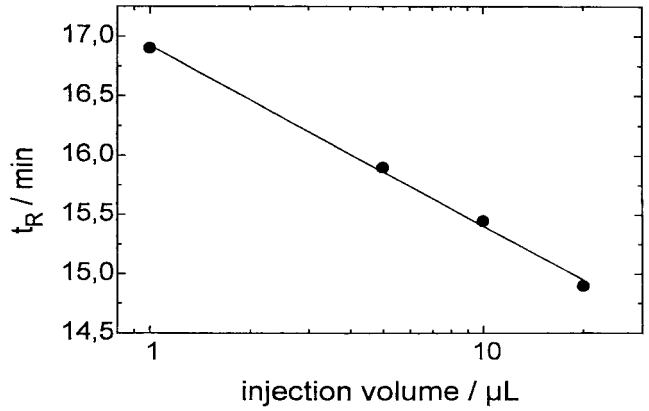

FIGURE 5 : Influence of the injection volume on the retention time t_R for poly-1, sample A2; (for conditions see Fig.1)

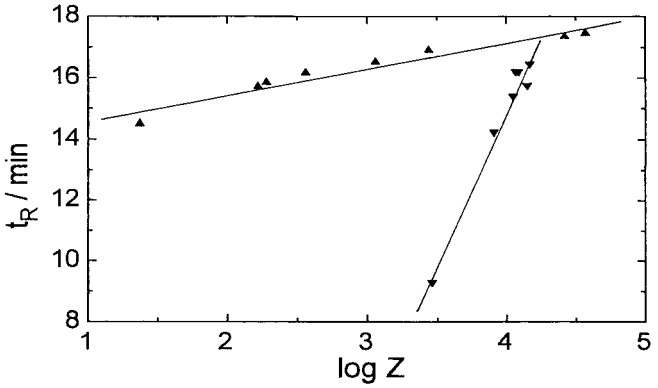

FIGURE 6 : Influence of the charge number Z on the retention time t_R for homopolymers and copolymers
(▲): poly-1; (▼): poly-2-co-3;
injection volume : 10 µL; (other conditions see Fig.1)

retention times of peak 3 (Fig.2). Due to similar charge numbers the data points for samples B4 to B7 cumulate within a small area, whereas for samples B8 to B10 the retention times show the expected dependency: t_R increases with increasing charge number. In this case the slope of the curve, however, is much steeper than that for the homopolymers. The reason for this may be that these samples of poly-2-co-3, in contrast to those of poly-1, not only have different charge numbers but also different charge densities. At a given charge number the homopolymers have longer retention times and the difference to the retention times of the copolymers is increasing with decreasing charge density of the latter.

As the M_W-values of these copolymer samples do not differ much from each other, it may be assumed that all copolymers approximately have the same chain length as far as the peak maximum fraction is concerned; it therefore can be expected that the retention times of the copolymers decrease with decreasing mole fraction x_{2P} of the charged comonomer. For low contents of the charged comonomer Fig.7 reveals a strong dependency of the retention time on the mole fraction of the comonomers; at high contents the curve flattens like a saturation function.

These results suggest that above a certain charge density the interaction of the chain with the stationary phase is at its optimum so that a further increase of the charge density cannot intensify the interactions. The following consideration may explain this: Polymer molecules with high charge density like poly-1 and the poly-2-co-3-samples B1 to B7 have many charged groups in close vicinity to each other which can interact cooperatively with the active centers of the stationary phase. Desorption of some of the groups is easily compensated for by the adsorption of adjacent groups which results in long retention times. However, excessive charges of the polyelectrolyte situated close to the active center of the stationary phase cannot intensify the binding of the analyte any more. In the case of polymer molecules with low charge density like the samples B8 to B10 (poly-2-co-3) less ionic groups can interact simultaneously with a particular binding site of the stationary phase with the result of a shorter retention time as compared to a macromolecule with the same number, but higher density of charges.

Information from the Chromatograms on the Copolymerization Behaviour

Fig.8 shows the chromatogram for sample D3 (poly-2-co-3). From the shape of peak 3 - also displayed in the insert after subtraction of the baseline - conclusions should be

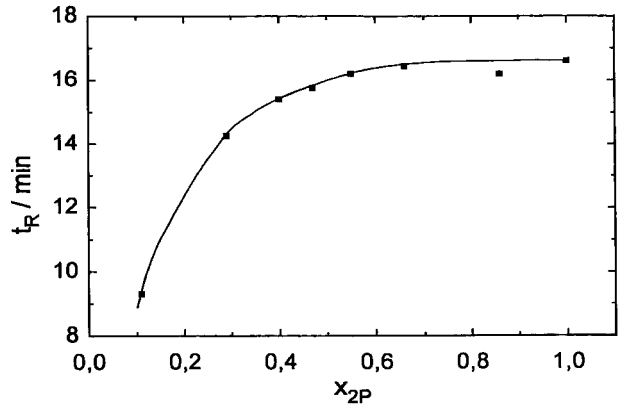

FIGURE 7 : Influence of the mole fraction x_{2P} of the charged comonomer according to Tab.2 on the retention time t_R (poly-2-co-3; B-samples); (for conditions see Fig.1)

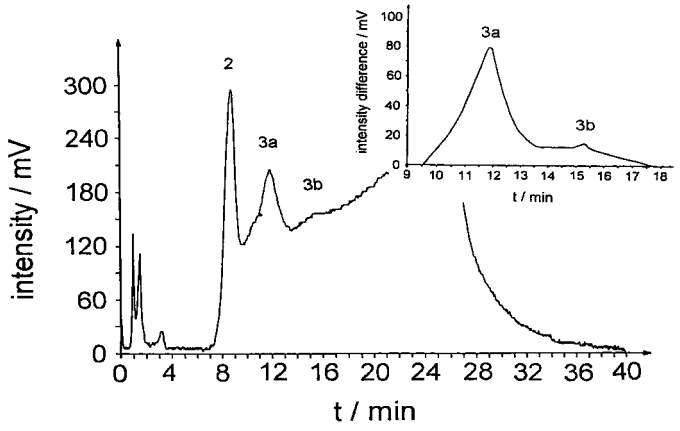

FIGURE 8 : Chromatogram of poly-2-co-3 (sample D3; x_{2P} = 0.3); insert: amplified section after substraction of the baseline (for conditions see Fig.1)

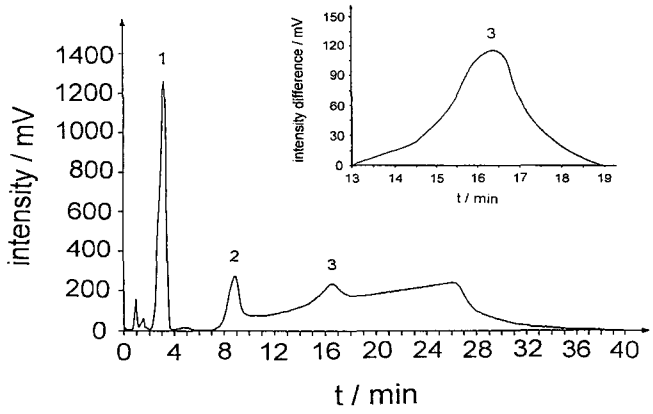

FIGURE 9 : Chromatogram of poly-1-co-3 (sample E3; x_{1P} = 0.5); insert: peak 3 after substraction of the baseline and amplification; (for conditions see Fig.1)

possible about the copolymerization behaviour of the monomers **2** and **3**. In agreement with the copolymerization parameters it is expected that a reaction mixture deficient in the charged monomer **2** leads to a polymer with relatively high contents of **2** and therefore a high charge density (peak 3b). During the course of the polymerization the decreasing concentration of monomer **2** supports the reaction of the uncharged comonomer giving rise to a fraction with lower charge density (peak 3a). It is unexpected however that the alleged distribution curve exhibits a distinct bimodality; this probably is related to overloading of the separation column resulting in a strongly pronounced peak 3a.

Similarly the chromatogram for sample E3 (Fig.9) provides information on the copolymerization behaviour of the monomers **1** and **3**. Again, peak 3 is shown in the insert after subtraction of the baseline and amplification and presents a distinctly flat slope despite of a possible overloading of the column. As to the copolymerization parameters (r_1 = 1.71 and r_3 = 0.25) according to TANAKA [6] it must be expected that during the polymerization of comonomers **1** and **3** the charged comonomer **1** polymerizes much faster than the uncharged comonomer **3**; consequently the production of polymer chains with high charge density - corresponding to long retention times - is favoured at the beginning of the reaction. In the course of the reaction the mixture becomes more and more deficient in the charged comonomer **1** resulting in polymer chains with decreasing

number of charged groups and decreasing retention times. At the end of the reaction the charged comonomer is totally consumed and pure polyacrylamide is formed; this may be the reason for the intensive peak 1 with t_R equal to about 3 min. These results lead to the conclusion that the peakshape in the chromatogram - with some reservations due to overloading effects - contains information on the copolymerization behaviour of the respective comonomers.

Temperature Dependency of the Retention Times

The kinetics and thermodynamics of chromatographic interactions are known to be influenced by temperature [8], which also influences the solubility of the polymers in the mobile phase. For the investigation of the influence of temperature on the separation of the polymers the column was placed in a water bath at seven different (8, 15, 22, 29, 36, 43, and 50°C) but constant temperatures. Whereas the retention times for polymers with low charge density (samples B9 and B10) did not vary significantly with temperature, its influence proved more and more pronounced with increasing charge density of the polymers (samples B8 and A10): retention times increased with increasing temperature (Fig.10). Obviously it is the charge density which controls the elution behaviour at different temperatures. This supports the assumption that the charged groups of the polymer molecules cause interactions between the polyelectrolyte molecules and the stationary phase. Within the temperature interval from 22 to 29°C the slope of the resulting curve is remarkably steeper compared to the other temperature intervals which suggests a change in the separation mechanism.

Influence of Column Length and Pore Size on the Chromatographic Separation

As to the homopolymer samples poly-1 application of the gradient program P2 results in a linear correlation between retention time and log Z both for short (50 mm) and long (250 mm) columns. However, on the longer column the net retention time starts at lower values (9.2 min) and increases more rapidly with the charge number (up to 12.8 min). Consequently, the resolution R_S calculated for the samples A2 and A9 (poly-1) is better for the long column (R_S = 0.82) than for the short column (R_S = 0.55). This result is in disagreement with investigations on the chromatographic separation of proteins by SNYDER et al.

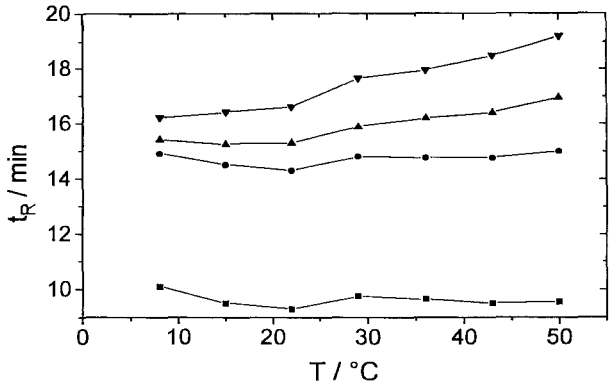

FIGURE 10 : Influence of temperature T on the retention time t_R for poly-1 and poly-2-co-3; samples (▼) A10;(▲) B8; (●) B9; (■) B10; (for conditions see Fig.1)

[9], who found the retention time influenced by the salt concentration of the mobile phase, but not by the column length. These differences in retention time and resolution observed for columns of different lengths in this study may be caused by a slightly different column packing material and they underline that - in contrast to proteins - polyelectrolytes interact intensely with the surface of the stationary phase.

For the experiments described so far column packings with a pore size of 4 nm were used in order to ensure the same separation conditions for all polymers by excluding the analytes from the pore volume. On packing materials with a pore size of 100 nm, however, the shorter chain molecules of A1 and A2 (poly-1; M_w = 6.000 and 45.000 g/mol resp.) had longer retention times than sample A10 (M_w = 8.300.000 g/mol) despite of their much lower charge number. This indicates that short chained polymer molecules can also interact within the pores of the stationary phase. The longer the polymer chains are the better they are excluded from the pores. Thus, for the high molar mass samples A6, A8, and A10 a linear correlation between retention time and log Z is found for these large pore materials as well as for the small pore materials discussed above.

From these results the conclusion is drawn that interactions of the ionic groups of the polymers with the surface of the stationary phase may occur in the pores as well as in the outer grain spheres. Therefore, it is recommended that for comparative investigations the pore size of the packing material has to be chosen in a way that either all sample constituents can get into the pores or all are excluded from the pores.

DISCUSSION

Concluding, it can be stated that moderately polar HPLC-separation columns of the type PSS HEMA are suitable for the characterization of cationic poly(meth)acrylates. The ionexchange capacity of this stationary phase is much lower than that of typical ionexchange materials of commercial standard; this helps to avoid irreversible sorption. The interactions of the polyelectrolytes with the stationary phase and their retention times depend on the ionic strength of the mobile phase. Therefore it turned out to be advantageous to vary the ionic strength by application of a gradient.

The retention time of the polymers depends on the number of charges per molecule and on the charge density along the polymer chain. A linear correlation between the retention time and the logarithm of the charge number was found.

The dependency of the retention time on the charge density of the polyelectrolytes can be explained by a qualitative model where in the case of macromolecules with high charge density the active centers of the stationary phase are attacked by many charges simultaneously; this makes the desorption of the macromolecule more difficult than in the case of molecules with lower charge density. Satisfactory reproducibility of the retention times was achieved by applying buffered media as mobile phases in order to prevent retention times from increasing with increasing pH. It may well be that the stationary phases contain anionic residues from initiator fragments which interact with the analyte molecules. Such anionic groups underlie an acid-base-equilibrium so that ionization is enhanced at higher pH-values. As a consequence of the presumably low consumption of initiator during the production process a very small number of active centers on the stationary phase would be expected - this could be the reason for the observed effects of column overloading.

Different separation mechanisms may be dominant in the chromatography of polyelectrolytes with moderately polar stationary phases. The total activation energy E_a of the interaction process can be estimated from the variation of the capacity factor k' with temperature by plotting the ln k'-values versus 1/T (eq.4) [10]. The order of magnitude of E_a allows conclusions about the predominant mechanism.

$$\ln k' = \ln k_o - \frac{E_a}{RT} \qquad (4)$$

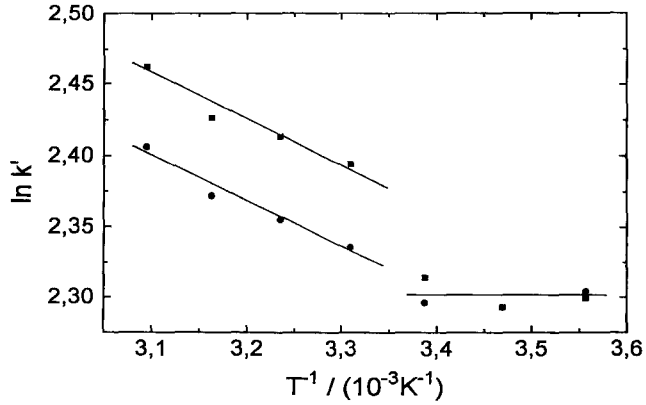

FIGURE 11 : Arrhenius plot for ln k' versus 1/T;
(■) poly-1 (sample A6); (●) poly-2-co-3 (sample B6)

As an example Fig.11 shows an Arrhenius plot for a homopolymer and a copolymer sample. Roughly, three areas can be distinguished: i) between 8 and 22°C k' is almost constant and happens to be identical for copolymer and homopolymer, ii) between 22 and 29°C the value of k' strongly increases, especially for the homopolymer sample, iii) within the temperature interval from 29 to 50°C k' steadily increases and a regression line can be drawn from which the activation energy is calculated equal to 1.8 kJ/mol and 2.1 kJ/mol for samples A6 (poly-1) and B6 (poly-2-co-3) respectively. From the fact that the activation energies for both samples were determined to be equal within the limits of error it can be concluded that in both cases the same chromatographic mechanism is predominant. The energy values lie in the lower range of what is expected for an adsorption mechanism. Although the properties of polyelectrolytes are known to be very complex it seems not inconsiderate to state that adsorption interactions play an important role in gradient chromatography of polyelectrolytes. However, the temperature dependency (Fig.11) is not as simple as to exclude the existence of other mechanisms and it seems very likely, indeed, that the predominant mechanism changes within the temperature interval investigated.

The chromatogram obtained by gradient-HPLC can be taken as an image of the charge distribution of the polymer given by the distribution of molar mass and chemical

composition. Moreover, the chromatograms contain information about the copolymerization behaviour of the different pairs of monomers. As far as the copolymerization parameters for the respective comonomers were known, qualitative agreement was found between experimental and expected results. Unfortunately, it cannot be ruled out that the chromatograms were influenced by overloading effects; from this point of view it would be appropriate to increase the relative detector sensitivity by applying salt solutions as mobile phases which are more transparent, whereby it would be possible to further decrease the absolute amounts injected. Even more information would be accessible by cross fractionation via coupling of SEC and HPLC so that the single SEC-fractions of a polyelectrolyte sample could be separated subsequently according to charge numbers by gradient-HPLC.

ACKNOWLEDGEMENTS

The authors kindly acknowledge the support given by Polymer Standards Service, Mainz, who gave two separation columns at their disposal. We thank Mrs. S. Seibert and Mr. N. Schulz (Röhm GmbH) for their help during the experiments and the sytheses of samples, and we are grateful to Mr. K. Spengler (Röhm GmbH) who supported the data aquisition. We kindly thank Professor Dr. G. Glöckner, Dresden, who gave the first impulse for this study.

REFERENCES

1. E. D. Becker, High Resolution NMR, Theory and Chemical Applications, Academic Press, New York, 2nd edition, 1980, p. 116

2. G. Glöckner, "Polymer Characterization by Liquid Chromatography", in Journal of Chromatography Library, vol.34, Elsevier Science Publishers, Amsterdam, 1986

3. S. S. Huang, J. Chromatogr., 536: 203 (1991)

4. G. Glöckner, H. G. Barth, J. Chromatogr., 499: 645 (1990)

5. H. G. Elias, Makromoleküle (Band 1, Grundlagen), 5.Auflage, Hüthig & Wepf Verlag, Basel, 1990, p. 632

6. H. Tanaka, J. Polym. Sci.: Polym. Chem. Ed., 24: 29 (1986)

7. W. Baade, D. Hunkeler, A. E. Hamielec, J. Appl. Polym. Sci., 38: 185 (1989)

8. H. Engelhardt, Hochdruck-Flüssigkeits-Chromatographie, Springer-Verlag, Berlin, 1975

9. L. R. Snyder, M. A. Stadalius, M. A. Quarry, Anal. Chem., 55: 1413A (1983)

10. K. P. Kringe, B. Neidhart, W. Brockmann, J. Liquid Chromatogr., 4(10): 1875 (1981)

11. Fa. E. Merck, Laborprodukte für die Praxis, 1988, p. 95

12. G. Ott, Dissertation, Technische Hochschule Darmstadt, 1991, p. 66

13. M. Stickler, Angew. Makromol. Chem., 123/124: 85 (1984)

Received: November 19, 1993
Accepted: February 10, 1994

JOURNAL OF LIQUID CHROMATOGRAPHY, 17(14&15), 3307-3313 (1994)

THE BOOK CORNER

ADVANCES IN CHROMATOGRAPHY, VOLUME 33, Edited by P. R. Brown and E. Grushka, Marcel Dekker, Inc., New York, NY, 283 pages, 1993. Price: $135.00.

The present volume of Advances in Chromatography comprises six chapters representing very interesting and timely topics. The editors should be commended on an excellent job in selecting both the topics and the authors. This volume is enjoyable reading and is recommended to all chromatographers and analytical chemists who deal with separation science.

Table of Contents:

HANDBOOK OF CAPILLARY ELECTROPHORESIS, Edited by J. P. Landers, CRC Press, Inc., Boca Raton, FL, 649 pages, 1994. Price: $99.50.

The Handbook of Capillary Electrophoresis contains twenty-three chapters which are grouped into 5 parts as shown in the Table of Contents below. The book is well written, well organized and reasonably priced at $99.50. The book lacks a special chapter on the theory of capillary electrophoresis and the chapter on pharmaceuticals, although well written, does not discuss chiral separations in detail and the material presented in the book on this topic is inadequate. The other chapters cover the material to date and are written by experts in their areas of expertise. The Forword is written by Professor B. Karger who asks, then answers, the question "why there is such interest in CE?" He ends his Forword by saying:

"The next few years should see a rapid expansion of capillary electrophoresis, particularly with respect to the number of users and the breadth of applications. In many respects the field is following the history of liquid chromatography. As more workers use capillary electrophoresis, those areas that need improvement are identified and the appropriate improvements developed.

It is thus clear that capillary electrophoresis is on its way to becoming a major analytical/separation tool. Further, it will likely emerge as a significant tool for biological measurements. By examining the chapters in this book, the reader will obtain a good understanding of the current status of capillary electrophoresis."

We agree with his assessment. The book is recommened to all those interested in separation science.

Table of Contents:

INTELLIGENT SOFTWARE FOR CHEMICAL ANALYSIS, Edited by L. M. C. Buydens and P. J. Schoenmakers, Data Handling in Science and Technology, Volume 13, Elsevier Science Publishers, Amsterdam, The Netherlands, 366 pages, 1993. Price: $200.00.

Various emerging techniques for automating intelligent functions in the laboratory are described in this book. Explanations on how systems work are given and possible application areas are suggested. The main part of the book is devoted to providing data which will enable the reader to develop and test his own systems. The emphasis is on expert systems; however, promising developments such as self-adaptive systems, neural networks and genetic algorithms are also described. The editors' goals can be summarized as follows:

(i) to demonstrate the applicability of expert systems and other "intelligent software" in analytical chemistry, and

(ii) to provide the reader with sufficient detailed information to initiate and conduct his or her own projects.

The editors identify four groups of scientists for whom the book has been written:

(i) Practicing analytical chemists, in industry or elsewhere, who wish to learn about the various exciting new types of software discussed in this book. They may want to find out more about possible applications, potential pitfalls and potential benefits. All of this they can find in this book.

(ii) Chemometricians or, in more down-to-earth terms, all chemists with an interest in developing software systems for use in the laboratory. The present

book will tell them a lot about what can be done and how. It will also give them numerous ideas for directing research and development efforts.

(iii) (Post-) graduate students in (analytical) chemistry or chemometrics can study this book to come to grips with one of the most promising areas of their science and can use the information provided here for their own projects.

(iv) Software engineers or scientists will find, in this book, many possible applications of technologies they may be familiar with. As will be explained in the book,
analytical chemistry offers a very fertile soil for turning abstract new technologies into systems of great practical value.

The book is well written by experts in their fields. Although the price of $200.00 is in the range of other scientific books, it is a little bit expensive for students.

Table of Contents:

CAPILLARY ELECTROPHORESIS THEORY AND PRACTICE, P. Camilleri, Editor, CRC Press, Boca Raton, FL, 495 pages, 1993. Price: $89.95.

Capillary Electrophoresis (CE) is unique among separation techniques since it combines the separation mechanisms of electrophoresis and chromatography, the

detection techniques of liquid chromatography and the column surface modification procedures of gas chromatography. Capillary electrophoresis is attracting the attention of an ever-broadening spectrum of scientists of diverse backgrounds. At present, capillary electrophoresis encompasses the widest scope of applications in comparison to other microseparation techniques.

Several books covering the subject have appeared in the last year, of which this book is one of the latest. The chapters have been written by experts who have been working in the field for some time, and were designed to be general in order to appeal to scientists of diverse backgrounds. Chapter 1 presents the history and development of capillary electrophoresis. Chapter 2 gives an excellent textbook-style discussion of instrumentation and detection systems, and Chapter 8 completes the presentation on detectors with interfacing capillary electrophoresis and mass spectrometry. Micellar electrokinetic capillary chromatography is discussed in Chapter 4. The other chapters cover applications as is outlined in the following Table of Contents.

The book is mainly about capillary zone electrophoresis and that is not clearly reflected in the title. Isoelectric focusing, isotachophoresis and other electrophoresis techniques are only briefly discussed in a few sections scattered across the various chapters. Furthermore, since theory is part of the book title, one would have hoped to see at least a chapter devoted to the systematic presentation of the theoretical basis of the technique.

One useful feature of the book is the compilation presented in Appendix II, which lists buffer constituents, additives and pH for different practical situations. The book is a useful addition to the libraries of laboratories that practice capillary zone electrophoresis.

Table of Contents:

Chapter 8 **Interfacing Capillary Electrophoresis with Mass Spectrometry,** S. Pleasance and P. Thibault, (311).

Chapter 9 **Capillary Electrophoresis in Biomedical and Pharmaceutical Research**, D. Perrett, (371).

Appendix I **Manufacturers and Suppliers of CE Equipment and Components,** D. Perrett, (409).

Appendix II **List of Buffers and Additives for Capillary Electrophoresis Separation**, G.N. Okafo, (413).

Appendix III **Examples of Capillary Electrophoresis Separations**, (445).

Reviewed by:

Dr. George M. Janini
Chemical Synthesis and Analysis Laboratory
Program Resources, Inc./DynCorp
NCI-Frederick Cancer Research and Development Center
Frederick, Maryland

JOURNAL OF LIQUID CHROMATOGRAPHY, 17(14&15), 3315-3321 (1994)

LIQUID CHROMATOGRAPHY CALENDAR

1994

AUGUST 14 - 17: Summer National Meeting & Particle Technology Forum, AIChE, Denver, Colorado. Contact: AIChE Express Service Center, 345 East 47 Street, New York, NY 10017, USA.

AUGUST 21 - 23: Australasian Plastics & Rubber Inst. 7th Technology Convention, Melbourne, Australia. Contact: APRI, P. O. Box 241, Mont Albert 3127, Australia.

AUGUST 21 - 26: 208th ACS National Meeting, Washington, DC. Contact: ACS Meetings, ACS, 1155 16th Street, NW, Washington, DC 20036-4899, USA.

AUGUST 29 - SEPTEMBER 2: Synthetic Membranes in Science & Industry, University of Tubingen, Germany. Contact: Dechema e.V., Exhibitions & Congresses, Theodor-Heuss-Allee 25, P. O. Box 150104, D-60486 Frankfurt am Main, Germany.

SEPTEMBER 4 - 9: 4th European Rheology Conference, Seville, Spain. Contact: C. Gallegos, Dept. de Ingenieria Quimica, Universidad de Seville, 41071 Seville, Spain.

SEPTEMBER 5 - 7: 25th International Symposium on Essential Oils, Grasse, France. Contact: Assoc. des Ingenieurs et Techniques de la Parfumerie (A.I.T.P.), 48 ave. Riou-Blanquet, 06130 Grasse, France.

SEPTEMBER 8 - 10: Surfaces in Biomaterials 1994, Scottsdale, Arizona. Contact: Surfaces in Biomaterials Foundation, c/o Ardel Management, P. O. Box 26111, Minneapolis, Minn, USA.

SEPTEMBER 12 - 15: 3rd International Conference on Separations in Biotechnology, University of Reading, U.K. Contact: SCI, Conference Office, 14/15 Belgrave Square, London SW1X 8PS, U.K.

SEPTEMBER 25 - 28: Future of Spectroscopy: From Astronomy to Biology, Ste.-Adele, Que., Canada. Contact: Doris Ruest, Conference Mgr., NRC Canada, Ottawa, Ont., Canada K1A 0R6.

SEPTEMBER 27 - 29: CCPC International Conference on Chemical Process Automation, Houston, Texas. Contact: AIChE Express Service Center, 345 East 47th Street, New York, NY 10017, USA.

OCTOBER 3 - 4: Course on Capillary Electrophoresis, Budapest, Hungary. Contact: Dr. F. Kilar, Central Research Laboratory, Medical School, University of Pecs, Szigeti ut 12, H-7643 Pecs, Hungary.

OCTOBER 5 - 7: 9th Inetrnational Symposium on Capillary Electrophoresis, Budapest, Hungary. Contact: Dr. F. Kilar, Central Research Laboratory, Medical School, University of Pecs, Szigeti ut 12, H-7643 Pecs, Hungary.

OCTOBER 9 - 14: 186th Meeting of the Electrochemical Society. Contact: Electrochem. Soc., 10 S. Main St., Pennington, NJ 08534-2896, USA.

OCTOBER 16 - 19: 46th Southeastern Regional Meeting, ACS, Birmingham, Alabama. Contact: L. Kispert, Chem Dept, Univ of Alabama, Box 870336, Tuscaloosa, AL 35115, USA.

OCTOBER 17 - 19: 3rd Int'l Symposium on Supercritical Fluids, Strasbourg, France. Contact: Int'l Soc for the Advancement of Supercritical Fluids, 1 rue Grandville, B. P. 451, F-54001 Nancy Cedex France.

OCTOBER 18 - 22: 30th ACS Western Regional Meeting, Sacramento, California. Contact: S. Shoemaker, Calif. Inst of Food & Agricultural Res., Univ. of Calif-Davis, 258 Cruss Hall, Davis, CA 95616-8598, USA.

OCTOBER 23 - 27: Annual Meeting of the American Association of Cereal Chemists, Nashville, Tennessee. Contact: J. M. Schimml, AACC, 3340 Pilot Knob Road, St. Paul, MN 55121-2097, USA.

OCTOBER 24 - 26: 2nd Internat'l Conference on Chemistry in Industry, Bahrain, Saudi Arabia. Contact: SAICSC-ACS, P. O. Box 1723, Dhahrain 31311, saudi Arabia.

NOVEMBER 2 - 5: 29th Midwestern Regional Meeting, ACS, Kansas City, Kansas. Contact: M. Wickham-St. Germain, Midwest Res. Inst, 425 Volker Blvd, Kansas City, MO 64110, USA.

NOVEMBER 3: Anachem Symposium, Dearborn, Michigan. Contact: Paul Beckwith, Program Chairman, Detroit Edison Co., 6100 W. warren, Detroit, MI 48210, USA.

NOVEMBER 7 - 10: 13th Int'l Conference on the Application opf Accelerators in Research & Industry, Denton, Texas. Contact: J. L. Duggan, Univ. of N. Texas, Dept. of Physics, P. O. Box 5368, Denton, TX 76203, USA.

NOVEMBER 10 - 11: 17th Int'l Conference on Chemistry, Biosciences, Pharmacy & Environmental Pollution, New Delhi, India. Contact: V. M. Bhatnagar, Alena Chem of Canada, P. O. Box 1779, Cornwall, Ont., Canada K6H 5V7.

NOVEMBER 11 - 12: 3rd Conference on Current Trends in Computational Chemistry, Jackson, Mississippi. Contact: J. Leszczynski, Jackson State University, Dept. of Chem., 1400 J. R. Lynch St., Jackson, MS 39217, USA.

NOVEMBER 13 - 16: 50th Southwest Regional Meeting, ACS, Fort Worth, Texas. Contact: H. C. Kelly, Texas Christian Univ, Chem Dept, Ft. Worth, TX 76129, USA.

NOVEMBER 13 - 18: Annual Meeting of the A.I.Ch.E., San Francisco, California. Contact: AIChE Express Service Center, 345 East 47th St., New York, NY 10017, USA.

NOVEMBER 14 - 17: 33rd Eastern Analytical Symposium, Somerset, New Jersey. Contact: Sheri Gold, EAS, P. O. Box 633, Montchanin, DE 19710, USA.

NOVEMBER 16 - 18: Envirosoft'94, 5th Int'l Conference on Development and Application of Computer Techniques to Environmental Studies, San Francisco, California. Contact: Computational Mechanics, Inc., 25 Bridge St., Billerica, MA 01821, USA.

DECEMBER 4 - 6: IBEX'94, International Biotechnology Expo & Scientific Conference, Moscone Center, San Francisco, California. Contact: Cartlidge & Associates, Inc., 1070 Sixth Avenue, Suite 307, Belmont, CA 94002, USA.

1995

MARCH 6 - 10: PittCon'95: Pittsburgh Conference on Analytical Chemistry & Applied Spectroscopy, New Orleans, Louisiana. Contact: Pittsburgh Conference, Suite 332, 300 Penn Center Blvd., Pittsburgh, PA 15235-9962, USA.

APRIL 2 - 7: 209th ACS National Meeting, Anaheim, Calif. Contact: ACS Meetings, ACS, 1155 16th Street, NW, Washington, DC 20036-4899, USA.

APRIL 25 - 28: Biochemische Analytik '95, Leipzig. Contact: Prof. Dr. H. feldmann, Inst. fur Physiologische Chemie der Universitat, Goethestrasse 33, D-80336 Munchen, Germany.

MAY 28 - JUNE 2: HPLC'95, 19th International Symposium on Column Liquid Chromatography, Convention Center, Innsbruck, Austria. Contact: HPLC'95 Secretariat, Tyrol Congress, Marktgraben 2, A-6020 Innsbruck, Austria.

MAY 31 - JUNE 2: 27th Central regional Meeting, ACS, Akron Section. Contact: J. Visintainer, Goodyear Research, D415A, 142 Goodyear Blvd, Akron, OH 44236, USA.

JUNE 6 - 8: 28th Great Lakes Regional ACS Meeting, LaCrosse-Winona Section. Contact: M. Collins, Chem. Dept., Viterbo College, La Crosse, WI 54601, USA.

JUNE 14 - 16: 50th Northwest/12th Rocky Mountain Regional Meeting, ACS, Park City, Utah. Contact: J. Boerio-Goates, Chem Dept, 139C-ESC, Brigham Young Univ, Provo, UT 84602, USA.

JULY 9 - 15: SAC'95, The University of Hull, UK, sponsored by the Analytical Division, The Royal Society of Chemistry. Contact: The Royal Society of Chemistry, Burlington House, Picadilly, London W1V 0BN, UK.

AUGUST 20 - 25: 210th ACS National Meeting, Chicago, Illinois. Contact: ACS Meetings, ACS, 1155 16th Street, NW, Washington, DC 20036-4899, USA.

SEPTEMBER 12 - 15: 5th International Symposium on Drug Analysis, Leuven, Belgium. Contact: Prof. J. Hoogmartens, Inst. of Pharmaceutical Sciences, Van Evenstraat 4, B-3000 Leuven, Belgium.

OCTOBER 18 - 21: 31st Western Regional Meeting, ACS, San Diego, Calif. Contact: S Blackburn, General Dynamics, P. O. Box 179094, San Diego, CA 92177-2094, USA.

OCTOBER 22 - 25: 25th Northeastern Regional Meeting, ACS, Rochester, New York. Contact: T. Smith, Xerox Corp, Webster Res Center, M/S 0128-28E, 800 Phillips Rd, Webster, NY 14580, USA.

NOVEMBER 1 - 3: 30th Midwestern Regional ACS Meeting, Joplin, Missouri. Contact: J. H. Adams, 1519 Washington Dr., Miami, OK 74354-3854, USA.

NOVEMBER 1 - 4: 31st Western Regional ACS Meeting, San Diego, California. Contact: T. Lobl, Tanabe Research Labs, 4450 Town Center Ct., San Diego, CA 92121, USA.

NOVEMBER 5 - 7: 30th Midwestern Regional Meeting, ACS, Joplin, Missouri. Contact: J. H. Adams, 1519 Washington Dr, Miami, OK 74354, USA.

NOVEMBER 29 - DECEMBER 1: Joint 51st Southwestern/47th Southeastern Regional Meeting, ACS, Peabody Hotel, Memphis, Tenn. Contact: P.K. Bridson, Chem Dept, Memphis State Univ, Memphis, TN 38152, USA.

DECEMBER 17 - 22: 1995 International Chemical Congress of Pacific Basin Societies, Honolulu, Hawaii. Contact: ACS Meetings, 1155 16th Street, NW, Washington, DC 20036-4899, USA.

1996

FEBRUARY 26 - MARCH 1: PittCon'96: Pittsburgh Conference on Analytical Chemistry & Applied Spectroscopy, Chicago, Illinois. Contact: Pittsburgh Conference, Suite 332, 300 Penn Center Blvd., Pittsburgh, PA 15235-9962, USA.

MARCH 24 - 29: 211th ACS National Meeting, New Orleans, LA. Contact: ACS Meetings, ACS, 1155 16th Street, NW, Washington, DC 20036-4899, USA.

JUNE 16 - 21: "HPLC '96: Twentieth International Symposium on High Performance Liquid Chromatography," San Francisco Marriott Hotel, San Francisco, California. Contact: Mrs. Janet Cunningham, Barr Enterprises, P. O. Box 279, Walkersville, MD 21793, USA.

AUGUST 18 - 23: 212th ACS National Meeting, Boston, Mass. Contact: ACS Meetings, 1155 16th Street, NW, Washington, DC 20036-4899, USA.

OCTOBER 16 - 19: 52nd Southwest Regional ACS Meeting, Houston, Texas. Contact: J. W. Hightower, Dept. Chem. Eng., Rice University, Houston, TX 77251, USA.

OCTOBER 24 - 26: 52nd Southwestern Regional Meeting, ACS, Houston, Texas. Contact: J. W. Hightower, Chem Eng Dept, Rice Univ, Houston, TX 77251, USA.

NOVEMBER 6 - 8: 31st Midwestern Regional Meeting, ACS, Sioux Falls, South Dakota. Contact: J. Rice, Chem Dept, S. Dakota State Univ, Shepard Hall Box 2202, Brookings, SD 57007-2202, USA.

NOVEMBER 9 - 12: 48th Southeast Regional ACS Meeting, Greenville, South Carolina. Contact: H. C. Ramsey, BASF Corp., P. O. Drawer 3025, Anderson, SC 29624-3025, USA.

1997

APRIL 6 - 11: 213th ACS National Meeting, San Antonio, Texas. Contact: ACS Meetings, ACS, 1155 16th Street, NW, Washington, DC 20036-4899, USA.

SEPTEMBER 7 - 12: 214th ACS National Meeting, Las Vegas, Nevada. Contact: ACS Meetings, 1155 16th Street, NW, Washington, DC 20036-4899, USA.

1998

MARCH 29 - APRIL 3: 215th ACS National Meeting, St. Louis, Missouri. Contact: ACS Meetings, 1155 16th Street, NW, Washington, DC 20036-4899, USA.

AUGUST 23 - 28: 216th ACS National Meeting, Orlando, Florida. Contact: ACS Meetings, 1155 16th Street, NW, Washington, DC 20036-4899, USA.

1999

MARCH 21 - 26: 217th ACS National Meeting, Anaheim, Calif. Contact: ACS Meetings, 1155 16th Street, NW, Washington, DC 20036-4899, USA.

AUGUST 22 - 27: 218th ACS National Meeting, New Orleans, Louisiana. Contact: ACS Meetings, 1155 16th Street, NW, Washington, DC 20036-4899, USA.

2000

MARCH 26 - 31: 219th ACS National Meeting, Las Vegas, Nevada. Contact: ACS Meetings, 1155 16th Street, NW, Washington, DC 20036-4899, USA.

AUGUST 20 - 25: 220th ACS National Meeting, Washington, DC. Contact: ACS Meetings, 1155 16th Street, NW, Washington, DC 20036-4899, USA.

2001

APRIL 1 - 6: 221st ACS National Meeting, San Francisco, Calif. Contact: ACS Meetings, 1155 16th Street, NW, Washington, DC 20036-4899, USA.

AUGUST 19 - 24: 222nd ACS National Meeting, Chicago, Illinois. Contact: ACS Meetings, 1155 16th Street, NW, Washington, DC 20036-4899, USA.

2002

APRIL 7 - 12: 223rd ACS National Meeting, Orlando, Florida. Contact: ACS Meetings, 1155 16th Street, NW, Washington, DC 20036-4899, USA.

SEPTEMBER 8 - 13: 224th ACS National Meeting, Boston, Mass. Contact: ACS Meetings, 1155 16th Street, NW, Washington, DC 20036-4899, USA.

The Journal of Liquid Chromatography will publish, **at no charge**, announcements of interest to liquid chromatographers in every issue of the Journal. To be listed in Meetings & Symposia, we will need to know: Name of the meeting or symposium, sponsoring organization, when and where it will be held, and whom to contact for additional details. Incomplete information will not be published. You are invited to send announcements to **Dr. Jack Cazes, Editor, Journal of Liquid Chromatography, P.O. Box 2180, Cherry Hill, NJ 08034-0162, USA.**

Give your students a solid foundation in analytical chemistry **and** *the ability to select the most appropriate techniques with the* **new edition** *of...*

Send for your free examination copy today! *(see coupon for details)*

Undergraduate Instrumental Analysis

Fifth Edition, Revised and Expanded

JAMES W. ROBINSON
Louisiana State University, Baton Rouge

August, 1994
872 pages, illustrated
$65.00

International praise for previous editions...

"The book will be of value not only for undergraduate students, but it can be recommended to every analytical chemist who wants to refresh his [or her] knowledge." ***—Analytica Chimica Acta***

"...provides a very solid basis for an undergraduate course....its modular chapters, comprehensive list of techniques, and good coverage of topics... make it useful as an undergraduate text."
—Journal of the American Chemical Society

"...The level of treatment and the writing style are particularly suited to introductory courses in this topic in chemistry and related areas."
—Chemistry in Australia

"...In a book of this type it is refreshing to find such a wide range of analytical techniques, each comprehensively described. All the needs, in terms of these techniques, of any undergraduate would easily be satisfied by this book."
—Chemistry and Industry

Marcel Dekker, Inc.

270 Madison Avenue
New York, NY 10016
(212) 696-9000

Hutgasse 4, Postfach 812
CH-4001 Basel, Switzerland
Tel. 061-261-8482

This thoroughly rewritten and enlarged **new edition** of an incomparable text provides detailed discussions of the major chemical analytical techniques—**including the latest innovations**—used in all phases of the field, shows how each technique relates to the others, **and** illustrates the benefits and limitations of each—demonstrating the specific information that individual techniques provide.

Contains helpful chapters devoted to general concepts such as Beer's law, the Boltzmann distribution, error analysis, single- and double-beam optics, signal-to-noise ratios, emission and absorption of radiation, calibration techniques, and semiconductors!

Maintaining the fluidity of style and quality of coverage that made the previous editions so successful, ***Undergraduate Instrumental Analysis, Fifth Edition, Revised and Expanded***, offers

- **updated chapters** on mass spectrometry chromatography, Fourier transform infrared spectroscopy, nuclear magnetic resonance, plasma emission, atomic absorption, and hyphenated techniques
- a **new section** on the spectral interpretation of infrared spectroscopy, MS, and NMR
- a host of **additional review questions** in each section (with all answers in the Solutions Manual)
- and much more!

Undergraduate Instrumental Analysis, Fifth Edition, Revised and Expanded is the text of choice for all second-semester courses on quantitative analysis and more advanced courses on instrumental analysis for students in chemistry; chemical engineering; biochemistry; agriculture; environmental, marine, food, and veterinary science; as well as premedical and predental students.

Here are just a few of the colleges and universities that have benefited from previous editions...

Alfred University
American International College
Auburn University
Bowling Green State University
Brock University, Canada
Carroll College
Chestnut Hill College
Claflin College
Corpus Christi State University
Drury College
Fayetteville Technical Institute
George Washington University
Johnson C. Smith University
Lafayette College
Louisiana State University
Loyola University
Luther College
Marist College
Medical College of Pennsylvania
Northwestern College
Ohio Northern University
University of Pittsburgh
Rice University
St. Francis Xavier University, Canada
St. Norbert College
College of St. Rose
Southern Arkansas University
Susquehanna University
Syracuse University
University of Tennessee at Chattanooga
University of Texas at Arlington
Texas State Technical Institute
Washington and Jefferson College
Williams College
University of Wisconsin—Madison
and many others!

See over for contents

Undergraduate Instrumental Analysis CONTENTS

Fifth Edition, Revised and Expanded

ISBN: 0—8247—9215—7

This book is printed on acid-free paper.

A Solutions Manual is available to instructors only. Requests must be made on official school stationery

Keep abreast of the **latest** *theoretical and applied research developments in the field with...*

Contains over **340** equations, tables, drawings, and photographs!

Advances in Chromatography

Volume 34

edited by
PHYLLIS R. BROWN, *University of Rhode Island, Kingston*
ELI GRUSHKA, *The Hebrew University of Jerusalem, Israel*

May, 1994 / 456 pages, illustrated / $165.00

Reviewer praise for this valuable series...

"...the articles [are] of high scientific standard, up to date, very well written, and interesting to read... well presented and edited."
—*Journal of Chromatography*

"...a valuable contribution to the chromatography literature...belongs in every library used by chromatographers." —*Liquid Chromatography*

"...maintains the high quality that chromatographers have come to expect from this invaluable series." —*Journal of Pharmaceutical Sciences*

The rapidly expanding growth of the literature on chromatography and capillary electrophoresis makes it difficult for any single individual to maintain a coherent view of progress in the field. Rather than attempt to read the avalanche of original research papers, investigators trying to preserve even a modest awareness of advances must rely upon **authoritative** surveys.

Featuring reliable, **up-to-the-minute** reviews of major developments in chromatography, this critically praised series separates the most important advances from an overabundance of supplementary materials.

Internationally acclaimed experts analyze the most* current *innovations in their areas of specialization!

Furnishing more than **800** literature citations, allowing for further, in-depth study of recent trends in research, **Volume 34** examines timely subjects such as

- high performance capillary electrophoresis—*of particular interest to engineers, chemists, biotechnologists, and environmental scientists*
- gas chromatography, matrix isolation, and infrared spectrometry—*geared toward the needs of food scientists, medical professionals, and agriculturalists*
- statistical theories of peak overlap in chromatography —*especially applicable to quality control engineers*
- capillary electrophoresis of carbohydrates and proteins —*expressly for pharmacologists, biochemists, biologists, and medical professionals*
- supercritical fluid chromatography—*essential for chemists, environmental scientists, engineers, and biologists*
- and much more!

Advances in Chromatography is an indispensable resource for all researchers who need to use separation methods effectively—especially analytical, organic, inorganic, clinical, and physical chemists; chromatographers; biochemists and biological chemists; agrochemists; chemical, materials, and quality control engineers; biotechnologists; toxicologists; pharmacologists; pharmacists; physiologists; zoologists; botanists; food, cosmetic, polymer, and environmental scientists; oceanographers; research and quality control scientists in academia, government, hospitals, and industry; and upper-level undergraduate and graduate students in these disciplines.

Contents

ISBN: 0—8247—9087—1

This book is printed on acid-free paper.

Marcel Dekker, Inc.

270 Madison Avenue, New York, NY 10016
(212) 696-9000

Hutgasse 4, Postfach 812, CH-4001 Basel, Switzerland
Tel. 061-261-8482

*Obtain the **best possible results** by understanding the essentials involved in the chromatographic process with...*

LIQUID CHROMATOGRAPHY FOR THE ANALYST

RAYMOND P. W. SCOTT
Georgetown University, Washington, D.C., and Birbeck College, University of London, United Kingdom

January, 1994
344 pages, illustrated
$75.00

This **practical guide** provides a clear presentation of the chromatographic process—demonstrating the functions of all associated instrumentation *and* the procedures necessary to obtain accurate qualitative and quantitative results.

Supplies a* host of applications *from a variety of sources to help identify the best equipment, the most appropriate columns, and the most suitable phase systems for specific samples!

Written by an international expert with over 45 years of industrial and academic experience, ***Liquid Chromatography for the Analyst***

- covers essential fundamental theory
- explains the chromatographic process using established physical chemical terminology
- illustrates chromatographic behavior with current practices
- gives **useful examples** to aid in applying principles to actual problems
- furnishes supporting experimental evidence for theoretical explanations
- and much more!

With its direct, jargon-free style that permits easy access to information, ***Liquid Chromatography for the Analyst*** is an invaluable resource for analytical chemists, laboratory technicians, and upper-level undergraduate, graduate, and continuing-education courses in analytical chemistry or separation science.

CONTENTS

ISBN: 0—8247—9184—3
This book is printed on acid-free paper.

MARCEL DEKKER, INC.

270 Madison Avenue
New York, NY 10016
(212) 696-9000

Hutgasse 4, Postfach 812
CH-4001 Basel, Switzerland
Tel. 061-261-8482

ELECTRONIC MANUSCRIPT SUBMISSION

Effective immediately, manuscripts will be accepted on computer diskettes. A printed manuscript must accompany the diskette. For approximately one year, the diskettes will be used, on an experimental basis, to produce typeset-quality papers for publication in the Journal of Liquid Chromatography. Diskettes must be in an IBM-compatible format with MS-DOS Version 3.0 or greater. The following word processing formats can be accommodated:

ASCII	DisplayWrite Native
EBCDIC	Enable 1.0, 2.0, 2.15
Framework III 1.0, 1.1	IBM Writing Assistant
Microsoft Word 3.0, 3.1, 4.0, 5.0	Multimate 3.3
Multimate Advantage 3.6	Multimate Advantage II 3.7
Navy DIF	Office Writer 4.0, 5.0, 6.0, 6.1
PeachText 5000 2.12	PFS:First Choice 1.0, 2.0
PFS:Write Ver C	Professional Write 1.0, 2.0, 2.1
Q&A Write 3.0	RapidFile (Memo Writer) 1.2
Samna Word IV & IV+ 1.0, 2.0	Total Word 1.2, 1.3
Volkswriter 3, 4	Volkswriter Deluxe 2.2
Wang PC Ver 3	WordPerfect 4.1, 4.2, 5.0, 5.1*
WordStar 3.3, 3.31, 3.45, 4.0, 5.0, 5.5, 6.0	XyWrite III XyWrite III+

* The **preferred** word processor is **WordPerfect 5.1.**

Manuscripts and diskettes should be prepared in accordance with the **Instructions for Authors** given at the back of this issue of the Journal. They should be sent to the Editor:

Dr. Jack Cazes
Journal of Liquid Chromatography
P. O. Box 2180
Cherry Hill, NJ 08034

INSTRUCTIONS TO AUTHORS

Journal of Liquid Chromatography is published in the English language for the rapid communication of research in liquid chromatography and its related sciences and technologies.

Directions for Submission

One typewritten manuscript, suitable for direct reproduction, and two (2) clear copies with figures must be submitted. Since the Journal is produced by direct photography of the manuscripts, typing and format instructions must be strictly followed. Non-compliance will result in return of the manuscript to the author and will delay its publication. To avoid creasing, manuscripts should be placed between heavy cardboards before mailing.

Manuscripts may also be submitted on **computer diskettes**. A printed manuscript must also be submitted with diskettes because, at the present time, we are experimenting with manuscripts on diskettes. Diskettes must be readable with an IBM-compatible computer (Macintosh or other type not acceptable) and must be formatted with MS-DOS 3.1 or greater. Be sure to indicate the word processing software that was used to prepare the manuscript diskette.

Manuscripts and computer diskettes should be mailed to the Editor:

Dr. Jack Cazes
Journal of Liquid Chromatography
P. O. Box 2180
Cherry Hill, NJ 08034

Reprints

Due to the short production time for papers in this journal, it is essential to order reprints immediately upon receiving notification of acceptance of the manuscript. A reprint order form will be sent to the author with the letter of acceptance for the manuscript. Reprints are available in quantities of 100 and multiples thereof. Twenty (20) free reprints will be included with orders of 100 or more reprints.

Format of the Manuscript

1. The general format of the manuscript should be:
   Title
   Author(s)' names and full addresses
   Abstract
   Text Discussion
   References

2. **Title & Authors:** The entire title should be in capital letters and centered within the width of the typing area, located at least 2 inches (5.1 cm) from the top of the page. This should be followed by 3 lines of space, then by the names and addresses of the authors, also centered, in the following manner:

A SEMI-AUTOMATIC TECHNIQUE FOR THE SEPARATION AND DETERMINATION OF BARIUM AND STRONTIUM IN WATER BY ION EXCHANGE CHROMATOGRAPHY AND ATOMIC EMISSION SPECTROMETRY

F. D. Pierce and H. R. Brown
Utah Biomedical Test Laboratory
520 Wakara Way
Salt Lake City, Utah 84108

3. **Abstract:** The title **ABSTRACT** should be typed, capitalized and centered, 3 lines below the addresses. This should be followed by a **single-spaced**, concise abstract. Allow 3 lines of space below the abstract before beginning the text of the manuscript.

4. **Text Discussion:** Whenever possible, the text discussion should be divided into major sections such as

INTRODUCTION
MATERIALS
METHODS
RESULTS
DISCUSSION
ACKNOWLEDGEMENTS
REFERENCES

These **major headings** should be separated from the text by two lines of space above and one line of space below. Each major heading should be typed in capital letters, centered and underlined.

Secondary headings, if any, should be placed flush with the left margin, underlined and have the first letter of main words capitalized. Leave two lines of space above and one line of space below secondary headings.

5. The first word of each **paragraph** within the body of the text should be indented five spaces.

6. **Acknowledgements**, sources of research funds and address changes for authors should be listed in a separate section at the end of the manuscript, immediately preceding the references.

7. **References** should be numbered consecutively and placed in a separate section at the end of the manuscript. They should be typed single-spaced, with one line space between each reference. Each reference should contain names of all authors (with initials of their first and middle names); do not use *et al.* for a list of authors. Abbreviations of journal titles will follow the American Chemical Society's Chemical Abstracts List of Periodicals. The word **REFERENCES** should be capitalized and centered above the reference list.

Following are acceptable reference formats:

Journal:

1. D. K. Morgan, N. D. Danielson, J. E. Katon, Anal. Lett., 18: 1979-1998 (1985)

Book:

1. L. R. Snyder, J. J. Kirkland, Introduction to Modern Liquid Chromatography, John Wiley & Sons, Inc., New York, 1979.

2. C. T. Mant, R. S. Hodges, "HPLC of Peptides," in HPLC of Biological Macromolecules, K. M.

Gooding, F. E. Regnier, eds., Marcel Dekker, Inc., New York, 1990, pp. 301-332.

8. Each page of manuscript should be numbered lightly, with a light blue pencil, at the bottom of the page.

9. Only standard symbols and nomenclature, approved by the International Union of Pure and Applied Chemistry (IUPAC) should be used.

10. Material that cannot be typed, such as Greek symbols, script letters and structural formulae, should be drawn carefully with dark black India ink. Do not use any other color ink.

Additional Typing Instructions

1. The manuscript must be prepared on good quality **white bond paper**, measuring approximately 8½ x 11 inches (21.6 cm x 27.9 cm). The typing area of the first page, including the title and authors, should be 5½ inches wide by 7 inches high (14 cm x 18 cm). The typing area of all other pages should be no more than 5½ inches wide by 8½ inches high (14 cm x 21.6 cm).

2. The **title, abstract, tables and references** are typed single-spaced. All other text should be typed 1½-line spaced or double line spaced.

3. It is essential to use **dark black** typewriter or printer ribbon so that clean, clear, **solid characters** are produced. Characters produced with a dot/matrix printer are not acceptable, even if they are "near letter quality" or "letter quality." Erasure marks, smudges, hand-drawn corrections and creases are not acceptable.

4. **Tables** should be typed on separate pages, one table to a page. A table may not be longer than one page. If a table is larger than one page, it should be divided into more than one table. The word **TABLE** (capitalized and followed by an Arabic number) should precede the table and should be centered above the table. The title of the table should have the first letters of all main words in capitals. Table titles should be typed single line spaced, across the full width of the table.

5. **Figures (drawings, graphs, etc.)** should be professionally drawn in **black** India ink on separate sheets of **white** paper, and should be placed at the end of the text. They should not be inserted in the body of the text. They should not be reduced to a small size. Preferred size for figures is from 5 inches x 7 inches (12.7 cm x 17.8 cm) to 8½ inches by 11 inches (21.6 cm x 27.9 cm). **Photographs** should be professionally prepared *glossy* prints. A typewriter or lettering set should be used for all labels on the figures or photographs; they may not be hand drawn.

Captions for figures should be typed single-spaced on a separate sheet of white paper, along the full width of the type page, and should be preceded with the word FIGURE and an Arabic numeral. All figures and lettering must be of a size that will remain legible after a 20% reduction from the original size. Figure numbers, name of senior author and an arrow indicating "top" should be written in light blue pencil on the back of the figure. Indicate the approximate placement for each figure in the text with a note written with a light blue pencil in the margin of the manuscript page.

6. The **reference list** should be typed single-spaced. A single line space should be inserted after each reference. The format for references should be as given above.

JOURNAL OF LIQUID CHROMATOGRAPHY, 17(14&15), (1994)

Contents Continued

JOURNAL OF LIQUID CHROMATOGRAPHY

Volume 17, Numbers 14 & 15, 1994

Special Issue on
Polymer Separation by
Non-exclusion Liquid Chromatography

CONTENTS

(continued on inside back cover)

MARCEL DEKKER, INC. New York, Basel, Hong Kong

Contributions to this journal are published free of charge